https://doi.org/10.15388/vu.thesis.131
https://orcid.org/0000-0003-3377-9447

VILNIUS UNIVERSITY

Agnė
GEDRIMIENĖ

Accuracy of Digital Implant Impressions and Implant-Supported Restorations: In Vitro and In Vivo Assessments

DOCTORAL DISSERTATION

Medicine and Health Science,
Odontology (M 002)

VILNIUS 2021

This dissertation was written between 2016 and 2020 at Vilnius Universtity, Faculty of Medicine, Institute of Odontology.

Academic supervisor
Prof. Dr. Vygandas Rutkūnas (Vilnius University, Medicine and Health Science, Odontololy, M 002).

Academic consultant
Assoc. Prof. Dr. Darius Jegelevičius (Kaunas University of Technology, Technology Science, Electrical and Electronics Engineering, T 001).

This doctoral dissertation will be defended in a public meeting of the Dissertation Defence Panel:
Chairman – **Prof. Dr. Vytautė Pečiulienė** (Vilnius University, Medicine and Health Science, Odontology, M 002).

Members:
Prof. Dr. Marco Ferrari (Siena University (Italy), Medicine and Health Science, Odontology, M 002);
Prof. Dr. Elena Jasiūnienė (Kaunas University of Technology, Technology Science, Measurement Engineering, T 010);
Doc. Dr. Laura Linkevičienė (Vilnius University, Medicine and Health Science, Medicine, M 001);
Prof. Dr. Gediminnas Žekonis (Lithuanian University of Health Sciencies, Medicine and Health Science, Odontology, M 002).

The dissertation shall be defended at a public meeting of the Dissertation Defence Panel at 13:00 on February 5, 2021 in the main hall of the Faculty of Medicine.
Address: 21 M.K. Čiurlionio Street, Vilnius, Lithuania
Phone No.: +370 686 12017; email: mf@mf.vu.lt

The text of this dissertation can be accessed through the libraries of (name of the institutions granted the right to conduct doctoral studies in alphabetical order), as well as on the website of Vilnius University: *www.vu.lt/lt/naujienos/ivykiu-kalendorius*

https://doi.org/10.15388/vu.thesis.131
https://orcid.org/0000-0003-3377-9447

VILNIAUS UNIVERSITETAS

Agnė
GEDRIMIENĖ

Skaitmeniniu būdu gautų atspaudų ir restauracijų ant dantų implantų tikslumo laboratorinis ir klinikinis vertinimas

DAKTARO DISERTACIJA

Medicinos ir sveikatos mokslai,
Odontologija (M 002)

VILNIUS, 2021

Disertacija rengta 2016–2020 metais Vilniaus universiteto Medicinos fakulteto Odontologijos institute.

Mokslinis vadovas
prof. dr. Vygandas Rutkūnas (Vilniaus universitetas, medicinos ir sveikatos mokslai, odontologija, M 002).
Mokslinis konsultantas
doc. dr. Darius Jegelevičius (Kauno technologijos universitetas, technologijos mokslai, elektros ir elektronikos inžinerija, T 001).

Gynimo taryba:
Pirmininkė – **prof. dr. Vytautė Pečiulienė** (Vilniaus universitetas, medicinos ir sveikatos mokslai, odontologija, M 002).
Nariai:
prof. dr. Marco Ferrari (Sienos universitetas (Italija), medicinos ir sveikatos mokslai, odontologija, M 002);
prof. dr. Elena Jasiūnienė (Kauno technologijos universitetas, technologijos mokslai, matavimų inžinerija, T 010);
doc. dr. Laura Linkevičienė (Vilniaus universitetas, medicinos ir sveikatos mokslai, medicina, M 001);
prof. dr. Gediminas Žekonis (Lietuvos sveikatos mokslų universitetas, medicinos ir sveikatos mokslai, odontologija, M 002).

Disertacija ginama viešame Gynimo tarybos posėdyje 2021 m. vasario 5 d. 13.00 val. Vilniaus universiteto Medicinos fakulteto Didžiojoje auditorijoje. Adresas – M. K. Čiurlionio g. 21, Vilnius, Lietuva, tel. 8 686 12 017; el. paštas mf@mf.vu.lt.

Disertaciją galima peržiūrėti bibliotekose ir VU interneto svetainėje adresu: *https://www.vu.lt/naujienos/ivykiu-kalendorius*

Acknowledgements

I would like sincerely thank everyone, who helped with the study, every research project, preparation of publications, and doctoral dissertation:

Prof. Dr. Vygandas Rutkūnas for the idea of the study and support during the whole process.

Prof. Dr. Rimas Adaškevičius for the consultations on the measurements of 3D images.

Dr. Sima Rekštytė and Dr. Mangirdas Malinauskas for the help and consultations teaching me to work with SEM and the time spent in the laboratory.

Dental technicians Tomas Simonaitis, Rugilė Jusrgaitytė, Silvija Skiudulaitė, researchers Justinas Pletkus, Liudas Auškalnis, Dainius Barauskis and Mykolas Akulauskas for the help collecting and analyzing the data.

Assoc. Prof. Dr. Darius Jegelevičius for the consultations and help preparing the dissertation.

Prof. Dr. Vytautė Pečiulienė for supporting me during the doctoral and residency studies.

My family, friends and co-workers for endless support and believing in me.

CONTENTS

LIST OF ABBREVIATIONS

CAD/CAM	Computer-aided design/computer-aided manufacturing
3D	Three-dimensional
FPD	Fixed partial denture
iFPD	Implant-supported fixed partial denture
DW	Digital workflow
CW	Conventional workflow
IOS	Intraoral scanner
SB	Scan body
SEM	Scanning electron microscopy
DII	Digital implant impression
CII	Conventional implant impression
CMM	Coordinate measurement machine
ICP	Iterative closest point
MSE	Mean square error
MB	Mesiobuccal
DB	Distobuccal
ML	Mesiolingual
DL	Distolingual
M	Mesial
D	Distal

Ti	Titanium base
D_{misfit}	The difference in distances between the passive and non-passive situation
$D_{passive}$	The distance from the top margin of the titanium base to the top margin of the passive implant analogue
$D_{non-passive}$	The distance from the top margin of the titanium base to the top margin of the non-passive implant analogue
D_{cement}	The shortest vertical distance from the inferior edge zirconia framework to the top edge of the titanium base
Δ	Difference between calculated measurements
STL	Standard tessellation language
SR	Screw resistance
RS	Reference scan
MIOS	Model scanning with intraoral scanner
ISO	International Organization for Standardization
SD	Standard deviation
NS	Not significant
IQR	Interquartile range
P	Passive
NP	Non-passive

1. INTRODUCTION

1.1. Relevance of the Study

Digital technologies have revolutionized clinical prosthodontics, extending diagnostic, treatment, and follow-up possibilities. CAD/CAM (computer-aided design/computer-aided manufacturing) changed the analogue sequence of prosthesis manufacturing, which for a long time served as the gold standard. The developed optical impressions, digital modeling of the restoration, and milling of the final prosthesis without waxing and casting today is a common practice.[1] The advantages of optical impressions, such as time and cost-saving efficiency, more comfortable procedure for the patient, better communication with laboratory, more convenient treatment planning, and simpler clinical steps have already been widely discussed in the literature.[2–6] Also, CAD/CAM and 3D (three-dimensional) printing capabilities helped to accelerate the manufacturing procedures, to apply new prosthetic materials, such as zirconia, lithium-disilicate or ceramic-reinforced composite.[7]

However, the main problem of digital workflow is that the accuracy of impressions and final restorations produced from digital impressions is not well investigated. As osseointegrated dental implants are virtually immobile, they are not able to compensate for any inaccuracies of the prosthesis. Due to a build-up of errors during clinical and laboratory steps, a certain amount of inaccuracies is, however, unavoidable. Unfortunately, the majority of the studies on the accuracy of implant impressions and fit of the restorations are performed in laboratory conditions and only very few *in vivo* studies have been published recently.[8–12] Laboratory conditions eliminate oral humidity, soft tissue movements, fogging of the intraoral scanner (IOS) optics, which could certainly affect the results of *in vitro* studies. The ambiguity still remains about methodological aspects when accuracy is evaluated in *in vitro* study and what accuracy thresholds to define as clinically significant ones. Different, not well standardized, and sophisticated study designs evaluating different clinical scenarios also make it difficult to interpret the results.[10]

The accurate transfer of spatial implant position in relation to neighboring implants and teeth is essential for the correct design and fit of the final implant-supported fixed partial dentures (iFPD), in order to avoid mechanical and biological complications.[13] Several methods are suggested for implant impression accuracy assessment in the literature, such as angulation and distance measuring between implants,[14–16] 3D surface superimposition[17]

or vertical implant position registration,[18,19] plaster, and digital model comparison.[18] Moreover, the usage of digital splint, when artificial landmarks of different materials have been attached to edentulous places, was presented in the literature as a method to improve digital implant impressions.[20–22] Laboratory and clinical methods of passive fit evaluation of bridge type iFPD are also discussed in the literature.[23–25] However, there is still a lack of information, particularly on how the angle and distance between implants could affect the accuracy of implant impressions in partial and in fully edentulous situations. Also, a quantitative evaluation of the passivity of iFPD in the clinical environment would help to evaluate and compare the fit in a more predictable way.

1.2. The aim of the Study

To evaluate and compare the accuracy of conventional and digital implant impressions and implant-supported fixed partial dentures, produced through conventional and digital workflow under *in vitro* and *in vivo* conditions.

1.3. Objectives of the Research

1. To compare the accuracy of digital implant impressions *in vitro* using partially and fully edentulous models with five different intraoral scanners.
2. To evaluate the effect of the digital splint technique on the accuracy of digital impressions in *in vitro* scanning with five different intraoral scanners.
3. To compare the accuracy of conventional and digital implant impressions with two intraoral scanners under clinical conditions, measuring distance and angulation between implants, rotation, vertical shift, and surface mismatch of the scan bodies.
4. To estimate the effect of distance and angle between implants on the accuracy of digital implant impression in clinical conditions.
5. To evaluate and compare the fit of two-implant-supported zirconia fixed partial dentures, manufactured according to conventional and digital workflows in clinical conditions (D_{misfit}).
6. To estimate the cement gap differences in digitally and conventionally produced implant-supported partial dentures (D_{cement}).

7. To evaluate and compare the screw resistance of the prosthetic screw of two-implant-supported zirconia fixed partial dentures clinically and under laboratory conditions.
8. To evaluate and compare *in vivo* and *in vitro* accuracy differences of intraoral scanner, when taking digital implant impressions in edentulous situations.

1.4. Significance of the Study

The data of this study would provide a broad range of new information about the accuracy of dental implant impressions and implant-supported restorations and allow us to estimate the influence of different clinical and laboratory parameters. Understanding the accuracy aspects of digital implant impressions under laboratory conditions could help optimizing it in clinical situations. Clinical and laboratory studies are needed to evaluate the fit difference of iFPDs fabricated through conventional and digital workflow. Factors influencing the clinical accuracy of digital implant impression and restoration might be identified.

Also, it would be evaluated how distance and angulation between implants can influence the accuracy of dental implant impressions. This information would help choosing the type of implant impressions that are the most suitable in partial or fully edentulous situations with parallel and tilted implants. As digital implant impression accuracy might be influenced by the type of the IOS, five different IOS will be compared.

Objective and subjective methods will be used to evaluate and compare the fit and cement gap of iFPDs fabricated using conventional or digital workflow. Clinical parameters, such as the distance between titanium (Ti) base and implant analogue, the distance between the margin of the restoration and Ti base (cement gap), the balance of restoration and screw resistance (SR) of the prosthetic screw will be investigated, which could affect the fit of the final restoration.

1.5. Statements to defend

1. Digital splint (additional reference objects) is a valuable tool for improving digital implant impressions' accuracy in both partially and fully edentulous models.

2. There is no clinically significant difference in the accuracy between conventional and digital implant impressions for two-implant supported fixed partial dentures.
3. The distance and angulation between implants have an impact on the accuracy differences between conventional and digital implant impressions.
4. Clinically the fit of conventionally and digitally manufactured zirconia implant-supported fixed partial dentures does not differ.
5. The accuracy of a digital implant impression does not differ when scanning under clinical and laboratory conditions.

1.6. Approbation of the Research

Publications (Clarivate Analytics Web of Science)

1. Rutkunas V., Geciauskaite A., Jegelevicius D., Vaitiekūnas M. Accuracy of digital implant impressions with intraoral scanners. A systematic review. *Eur J of Oral Implant* 2017;10 Suppl 1:101-120.
2. Gedrimiene A., Adaskevicius R., Rutkunas V. Accuracy of digital and conventional dental implant impressions for fixed partial dentures: A comparative clinical study. *J Adv Prosthodont* 2019;11:271–9. https://doi.org/10.4047/jap.2019.11.5.271.
3. Rutkunas V., Larsson C., Vult von Steyern P., Mangano F., Gedrimiene A. Clinical and laboratory passive fit assessment of implant-supported zirconia restorations fabricated using conventional and digital workflow. *Clin Implant Dent Relat Res* 2020;22:237–45. https://doi.org/10.1111/cid.12885.

Presentations

Oral

1. Pletkus J, Rutkunas V, Auskalnis A, Kubilius M, Kaktys J, Gendviliene I, Borusevicius R, Gedrimiene A. Complete digital workflow and immediate functional loading of implant-supported monolithic glass ceramic crowns. European Prosthodontic Association/ International College of Prosthodontists Meeting, the Netherlands, 2019. The 28th Annual Scientific Meeting of the European Association for Osseointegration. Portugal, 2019. Printed: *Clin Oral Impl Res*. 2019; 30 (19): 367-367. https://doi.org/10.1111/clr.323_13509

2. Rutkunas V, Gedrimiene A, Pletkus J, Jegelevicius D. Planning the accurate implant-supported restorations through the digital workflow. Digital Dentistry Society 2019 Global Conference. Germany, Oct 3–5, 2019.

Poster

1. Gedrimiene A, Rutkunas V, Jegelevicius D, Akulauskas M, Barauskis D, Auskalnis L, Dirse J, Bilius V. *In vitro* study on digital splint effect to the accuracy of digital dental implant impression. European Association for Osseointegration (EAO)'s 28th annual scientific meeting. Portugal, 2019; European Prosthodontic Association/ International College of Prosthodontists Meeting, Netherlands, 2019. Printed: *Clin Oral Impl Res*. 30: 365-365. doi:10.1111/clr.322_13509

2. LITERATURE REVIEW

Since the 1980s, IOS have been developed into multifunctioning devices, which nowadays contribute immensely to dentistry in various ways. The main object of intraoral scanners is to improve the daily procedures of dentistry and ensure the maximal comfort for the patient.

Very few studies in the literature discuss time, cost analysis, or patient- and dentist-related preferences between digital and conventional workflows. Despite the first investment into initial equipment of IOS is quite high, the digital workflow, clinical studies have revealed, statistically significantly helps in decreasing overall costs, such as active chair-time per patient, laboratory manufacturing time, and material expenses – about 18% in cases of one implant iFPD.[3] Moreover, as the impression procedure takes time and sometimes causes an unpleasant gagging reflex or suffocation hazard, less time-consuming and more comfortable procedures such as digital impressions instead of conventional ones became more preferable for the patients.[2] Dentists as well have evaluated the advantages of a digital workflow, but their preferences differ among the age groups. Younger dentists more often choose DW instead of CW because of their better adaptability to new technologies and lack of experience with CII.[4]

The main working principles of intraoral scanners can be based on active triangulation, confocal microscopy, active wavefront sampling, and photogrammetry.[26]

Active triangulation (Cerec Omnicam, Dentsply Sirona, Charlote, USA, Emerald, Planmeca OY, Helsinki, Finland) serves a non-contact optical data acquisition technique. Monochromatic or polychromatic light is projected on the target object and reflections are recorded with a detector. The distance information is obtained by measuring the angles of a triangular plane using the Pythagoras theorem.[27,28] This technique also requires a homogeneous reflective surface, so different surfaces have to be coated with a special powder in order to get an accurate digital data. Primescan IOS (Dentsply Sirona, Germany, USA) has huge improvements comparing to previous products of Dentsply, including a Smart Pixel sensor that immensely accelerates scanning workflow.[29]

The parallel confocal microscopy method (Trios, Trios 3, Trios 4, 3Shape, Copenhagen, Denmark) is based on moving the aspherical lens, which collects imaging data in all focal planes. Focused light is emitted on the target through a small hole and only a concentrated reflected beam reaches the sensor. Because of the irregularities of acquired data, a mathematical algorithm was invented to compensate for the distortions. This kind of system

topographically slices the object into many parts and stitches it back together, creating a 3D image ("point-and-stitch reconstruction").[30] Since these types of scanners do not need surface dusting, they can produce colorful images, but additional equipment increases the weight and size of the scanner.[26]

Active wavefront sampling (Medit i500, Medit Corp, Seongbuk-gu, Seoul, Korea, True Definition, 3M ESPE, St. Paul Minessota, USA) describes the method of rotating aperture for image capturing at several positions. This improves the accuracy of the scan and avoids image overlapping. Moreover, an increased number of samples enhances the spatial resolution and sensitivity of the data. Since active wavefront sampling devices function as video cameras, only light dusting of the scanned surfaces is needed.[26,27]

Other working principles of IOS include the LED light stream, such as Carestream 3600 (Carestream Dental, Atlanta, USA). In accordance with 3D active video technology, it can provide high-quality 3D color images without the dusting of the surface.[31]

Photogrammetry (Pic scanner, PIC Dental LLC, Miami, USA, iCam4d, Imetric 4D Imaging Sàrl, Courgenay, Switzerland) operates when photographs of the selected object are taken from at least two different locations. The 3D coordinates of the object are constructed mathematically, when the point of the object, image, and camera optical center are aligned together.[32] Despite the spatial position of a dental implant can be detected with high accuracy, these type of scanners are not used very often clinically, because they cannot provide bite registration, soft tissue capturing, or scan combined cases, such as implant and teeth preparations in one clinical case.

However, the accuracy of IOS is defined not only by its working principle but also by the software capabilities of creating 3D images and stitching them together, registering occlusal relations of the jaws, capturing only implant, only dental, or combined cases. Moreover, the popularity of the IOS in the market is also dependent on a combination of several selecting parameters, such as financial investment, scanning speed, user friendly software, integration with CBCT and the CAD programs of dental technicians, the weight of the IOS scanning wand, and regular costs of the software licenses and updates. In the present study, several of the best available IOS in the market at that time were selected, but the comparison of their working principle was not the main object.

Every IOS device has its manufacturers' recommendations on scanning strategy. Ender and Mehl[33] have discovered that the technique when the scanning tip is positioned occlusally than tilted 30 degrees buccally and orally has shown the best trueness (23.3 μm) of all measured techniques. Also, scanning protocol has an important influence on full-arch scanning accuracy.

However, other studies showed that the differences of the trueness and precision were not statistically significant between different scanners and scanning strategies. Moreover, an appropriate scanning technique can be applied to the required situation without any discrepancies.[34] Muller et al. have claimed that scanning the strategy on the maxillary model starting from occlusal surfaces, moving palatally, and finishing buccally showed the best results of accuracy.[35] However, 3Shape recommendations on maxilla scanning are different: to begin with the occlusal part, then proceed buccally, and finish on palatal surfaces. These findings contribute to the fact that accuracy of the IOS may not depend on the scanning strategy.

The scan body (SB) is a device for digital registration of implant position. Various manufacturers offer different types and shapes of scan bodies for almost every implant system. Scan body usually consists of the base (metal or non-metal), the body, and the scanning part, which varies in shapes and size. The unique shape of the scan body helps CAD software libraries to identify the view of a scanned scan body via an acquired surface geometry mechanism and incorporate the required digital implant analogue in the model for further CAD/CAM procedures. This superimposition mechanism is usually based on the iterative closest point algorithm (ICP), which calculates the minimum root-mean-square error between the CAD model and scanned view of the scan body.[36] Moreover, the most intraoral scanning software are designed to capture not only the position of an implant, but also the formed emerging profile of the prospect crown. Biomet 3i (Zimmer Biomet, USA) first launched an Encode technology to capture not only the position of the implant, but also the form of gingiva near the implant, the so-called emerging profile, with a standardized healing cap serving as a scan body as well. The main advantages of this method were to simplify the implant impression procedure and that the coded healing cup was replaced to final restoration without repeated trauma to the peri-implant tissues.[37] However, several *in vitro* studies have showed that this technique was less precise than open- and closed-tray conventional implant impressions for both parallel and tilted implant situations.[38–41]

Despite considerable improvement in intraoral scanners, their application is still limited in multiple implant or edentulous situations. The scanning of larger edentulous areas for fixed partial dentures, scanning strategy, number of implants, and properties of scan bodies are among the factors that can lead to clinically significant inaccuracies.[15,16,42] Errors tend to build-up during the process of taking impressions and fabricating models and restorations, and a certain degree of inaccuracy is unavoidable. Using conventional techniques, various aspects can influence the final fit of the restoration: dimensional

changes in elastomeric impressions, plaster models, wax-ups, cast frameworks, etc. Although the newest digital technologies can help to eliminate some steps and drawbacks in the conventional workflow, they also introduce specific types of errors during the digital impression, CAD/CAM, and 3D printing procedures. A conventional workflow combining analogue and digital techniques and involving analogue impressions, plaster models, and a CAD/CAM process for the framework fabrication is usually used. Based on the clinical situation, different combinations of analogue and digital techniques can be employed. Despite the workflow that is selected, inaccuracies can stem from porcelain firing processes, cementation techniques, and the manual skills of the operator.

An accurate implant impression is key to achieving long-lasting functional, passive, and aesthetic restorations. Since dental implants are virtually immobile, ill-fitting restorations can potentially cause mechanical complications (screw loosening, ceramic chipping) and biological complications (periimplantitis, mucositis), which are widely discussed in the literature.[43] The accuracy of screw-retained implant-supported restorations is one of the key aspects defining the success of dental implants and prostheses. The accuracy of the prosthesis is closely associated with the concept of passivity, which several authors have attempted to define.[23] Theoretically, the passivity of a screw-retained restoration is achieved when opposing surfaces of the implant and the prosthetic component are in maximal spatial congruency without strains in the components after the final tightening of all screws.[44] Controversial data regarding technical and biological complications originating from non-passive implant-supported prosthesis exists, but complete passivity is virtually impossible in clinical situations.[23–25] Various techniques of misfit evaluation are also widely discussed in the literature. Available laboratory tests include microscopic methods such as light microscopy or scanning electron microscopy (SEM) to measure the gap between abutment and implant. Misfit assessment also can be performed by measuring photoelastic stress and strain gauge, by conducting finite element analyses, or by making superimpositions of the framework and master model virtually.[45] In clinical conditions, misfit is usually evaluated by visual inspection, tactile sensation combined with alternate finger pressure, the one-screw (Sheffield) test, and other techniques. Radiography and screw-resistance measuring methods can also be used as additional methods.[23,44,45]

Data on the accuracy of digital implant impressions (DII) and restorations are of crucial importance for validating the procedure in implant prosthodontics.[46–48] Since a digital workflow is a relatively novel procedure and is becoming widely used, collecting evidence-based information is very

important. Unfortunately, the majority of studies evaluating DII accuracy are *in vitro* studies. Data vary from 1 implant[18,19] to multiple-[14,17,28,46,49–51] or full arch-[15,16,37,51–53] implant impression studies. Different protocols were used to compare the accuracy of conventional and digital implant impressions, but mostly distance, angulation,[37,51,52] and surface mismatch[17,49] parameters of scan bodies were calculated, the accuracy of model[18,19] and implant-supported restorations[16,54] was evaluated. Impression accuracy is usually assessed as a combination of trueness and precision under the ISO 5725-1:1994 standard, where the trueness describes the deviation of scans from the true dimensions of the object, while precision describes how much separate scans of the same object differ from each other. Several studies have analyzed the models from CII (conventional implant impression) and DII for a single-unit implant crown. One of them reported that the vertical distortion of an implant analogue in a milled model was 93 μm[19], while in another study the mean error was comparatively smaller – 14 ± 170 μm – but with a large standard deviation.[18] Moreover, comparing DII with a reference scan, the difference was -6 ± 40 μm. An analysis of accumulative errors in digital workflow showed that the largest source of inaccuracies was the milling process of the models and implant analogue positioning, but not the DII. In *in vitro* studies of multiple implant partially edentulous situations, linear deviations vary below 100 μm, when newer generation IOS were used (Trios 3, Trios Color, True Definition).[14,28,46,50,51,55] Some other *in vitro* studies were analyzing fully edentulous situations for implant-supported restorations on four,[37,56,57] five,[17,50,58] or six implants,[15,16,49,52] claiming that the accuracy of DII does not significantly differ from CII and could serve as a valid alternative. Some of the studies also explored the influence of angulated implants on the accuracy of DII. Reference models in these studies had the angulated implants from 10°[17] to 45°.[37] The clinically acceptable threshold for angle deviations generated during impression procedures is not defined in the literature. However, based on simple trigonometrical calculations (and assuming, that the maximal lateral apex movement of 50 μm is acceptable), Andressien et al.[59] have suggested that up to 0.4° in angle deviation between implants would be acceptable, with the total length of the implant being 14.8 μm. In the case of shorter implants, larger inter-implant angle deviations can possibly be accepted, as this angle can be calculated using the formula 2×arctan (0.5 L implant length in mm).

Besides the impression technique, master model fabrication, milling process, type of restoration material, and other factors can influence the final fit of the restoration.[45,48,60,61] A misfit is regarded as a potential risk factor for both cement- and screw-retained restorations. However, no widely accepted

clinical threshold of a marginal misfit has been determined, and values vary from 10[62] to 150[63] μm in the literature. According to Katsoulis et al., there is a biological and mechanical tolerance to the misfit of restorations on implants, and therefore no threshold for maximum gap size or strain levels (screw, framework, implant-bone complex) can be defined. Clinical methods used to assess misfit (visual, tactile, radiographic) are not sensitive enough to verify a gap of less than 50 μm, and misfit greater than 150 μm can easily be diagnosed without any sophisticated methods.[44] Furthermore, bone strains caused by non-passive implant prosthesis can decrease because of bone adaptation when implants are loaded statically and dynamically.[64]

Having a reference model is a straightforward procedure in an *in vitro* study, and it is usually obtained with industrial scanners or coordinate measurement machines (CMM). Applying an industrial-grade reference scanner in a human clinical study is also one of possible approaches, but can only be performed in the anterior region of the maxilla under special conditions.[65] Lack of reference data is the main problem, hence the very few published *in vivo* studies.[12,16,54,59,66] Andriessen et al. and Alsharbaty et al. have compared digital and conventional implant impressions for two implant-supported restorations, claiming that both linear and angular deviations were too large to produce a passive fit restoration.[12,59] Other randomized clinical trials have proven that there are no statistical differences between the accuracy of restorations on six implants, fabricated along the digital or conventional workflow, and bone loss after 12 or 24 months.[16,54,66] Despite different protocols and measurements were performed; inconsistent results of the existing literature show the need for further researches in the clinical field.

Another approach is to compare the accuracy of digital and conventional impressions performed under *in vitro* and *in vivo* conditions. In one study it was shown, that scanning the dental arch intraorally was twice less precise as scanning the model of the same dental arch.[67] However, newer research have presented different results.[68] The metal bar was attached to upper second molars intraorally and scanned with IOS. Then, an acrylic model of the same dental arch was manufactured with the same bar attached and also scanned with IOS. Despite the complexity of the protocol of the study, no statistically significant differences were found between the scanning accuracy *in vitro* and *in vivo* for both linear and angular measurements.

One of the latest systematic reviews on the accuracy of DII reported mean errors ranging from 6 to 337 μm,[8] but clinically acceptable thresholds for linear and angular measurements remain based on one clinical study.[59] The clinically acceptable values of implant-supported restorations passive fit also are documented in a very wide range. Moreover, since digital technology is

improving very fast, published data do not cover all arising questions about the clinical validity of the digital workflow, so further studies are recommended.

3. MATERIALS AND METHODS

This study is divided into several parts, including *in vitro* evaluation of dental implant impressions, *in vivo* evaluation of dental implant impressions and restorations, abd *in vitro – in vivo* evaluation of dental implant impressions. The clinical parts of the study were performed according to the standards of the Declaration of Helsinki and approved by the Vilnius Regional Ethics Committee for Biomedical Research (No 158 200-16-861-370). All patients filled out a consent form to participate in this study. The order of patients' randomization was performed using https://www.random.org/ software. The code numbers of patients were entered into the program and the order of impression taking was formed according to the results.

3.1. *In vitro* accuracy evaluation

Two types of maxilla models were printed using the Asiga Max UV (Asiga, Sydney, Australia, version 1.2.11) 3D printer according to the Frasaco model (Frasaco GmbH, Tettnang, Germany) design (the workflow chart is presented in figure 1).

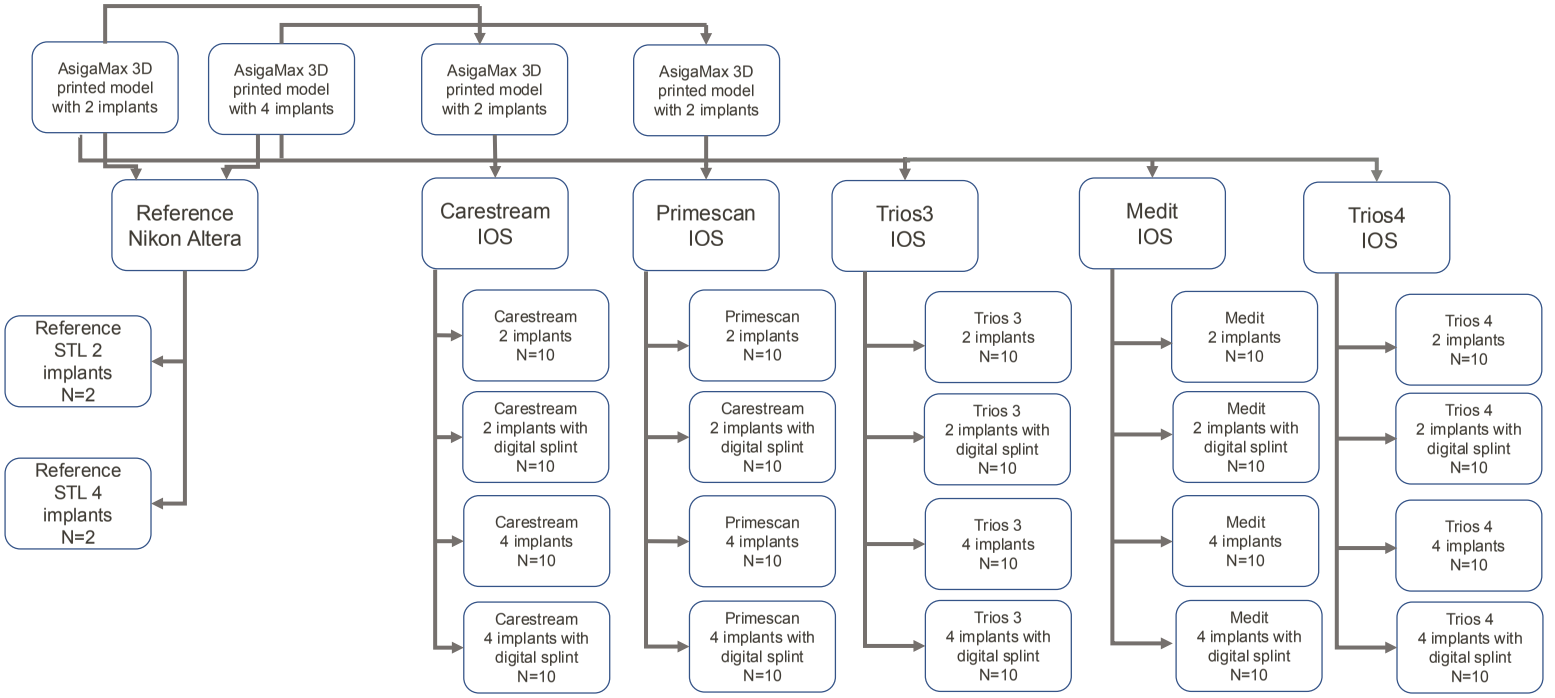

Figure 1. The workflow chart of an *in vitro* part of the study.

The first model was missing both premolars and molars on the right side, so Straumann BLT RC 4.1 mm diameter (Straumann, Basel, Switzerland) dental implants were inserted instead of first premolar (straight) and second molar (tilted 20° mesially) (Figures 2-3). Four implants were inserted in the second fully edentulous model symmetrically at second incisors (straight) and first molars (tilted 20° distally) areas (Figure 2-3). SB (CARES RC Mono scan body, Straumann, Basel, Switzerland) were attached with a 15 Ncm torque using a cordless electronical screwdriver (NSK iSD900, Tokyo, Japan) to the implants, and models were scanned using a Nicon Altera 10.7.6 (Nikon Metrology, Shinagawa, Tokyo, Japan) reference scanner to form reference scans. DII were taken with Primescan (Dentsply Sirona, Charlote, USA, version 5.0.1), Trios 3 (3Shape, version 1.18.2.10), Trios 4 (3Shape, version 19.2.2), CS3600 (Carestream dental, Atlanta, USA, version 3.1.0), Medit i500 (Medit, Seoul, South Korea, version 2.0.3) IOS ten times each (n=10) without digital splint. The scanning sequences were applied according to each manufacturer recommendations following IOS manuals. After this, tablets of hardened glass-ionomer cement (Fuji Plus, GC, Tokyo, Japan) were attached (glued with Super Moment glue (Henkel, Dusseldorf, Germany)) to edentulous areas to form the digital splint (additional object for scanning), and all models were scanned with five different IOS again. Scanning data were exported in standard tessellation language (STL) format for further analysis. All scans were aligned on the reference scan precisely by applying the best-fit alignment procedure using Geomagic Control X 2018 (3D Systems Corporation, North Caroline, USA) software. Distance, angulation, and vertical shift parameters between scan bodies were measured aligning CAD models of scan bodies to the scanned surfaces of scan bodies (Figures 4-5). The center point of the scan body was chosen as the intersection between a selected center axis and a top plane of the scan body. The distance between the center points of the two scan bodies was measured (Figures 4b and 5b). The angulation of the scan bodies was measured as the angle between two vectors representing the axes of the scan bodies in 3D space (Figures 4c and 5c). The shortest distance between a center point of one scan body and the top plane of another scan body was evaluated as the vertical shift of the scan body (Figures 4d and 5d). Trueness and precision were calculated of all the parameters measured and compared between the model groups with digital splint and without. Statistical analysis was performed with Matlab 2020a (The MathWorks Inc., Santa Clara, USA) statistical package. Testing for the data normality distribution, Shapiro–Wilk normality tests were carried out, and depending on the results, a Mann-Whitney Wilcoxon or Student two-sample t-test was applied for the estimation of statistically significant differences

between measurements. The level of significance was set at 0.05. GPower ver. 3.1.9.2 software (Dusseldorf University) served to calculate the power of statistical analysis.

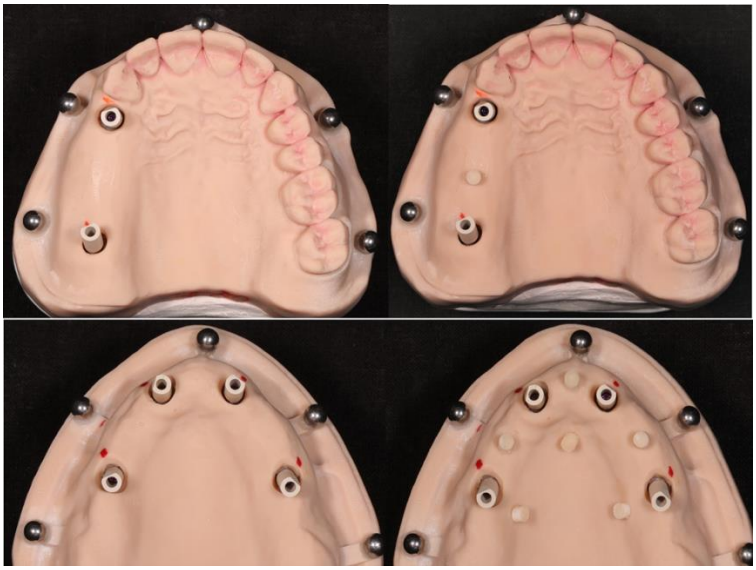

a) b)

Figure 2. The printed models, used for scanning: a) models without digital splint; b) models with digital splint.

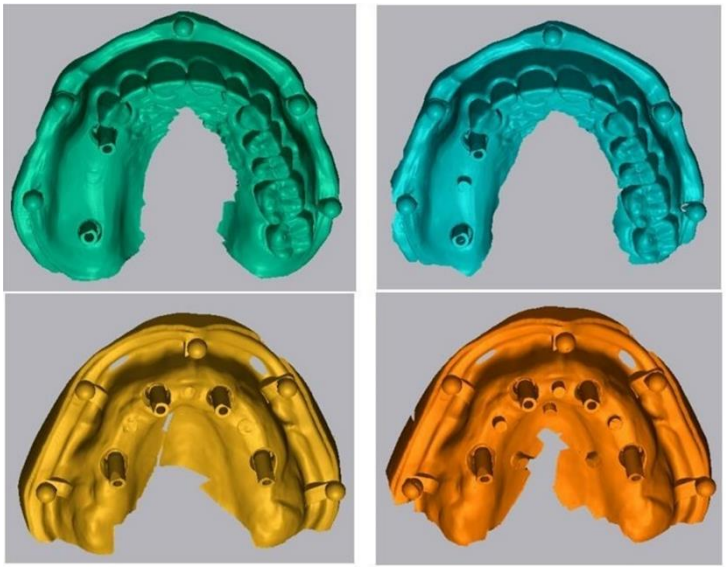

a) b)

Figure 3. The scanned models: a) without digital splint; b) with digital splint.

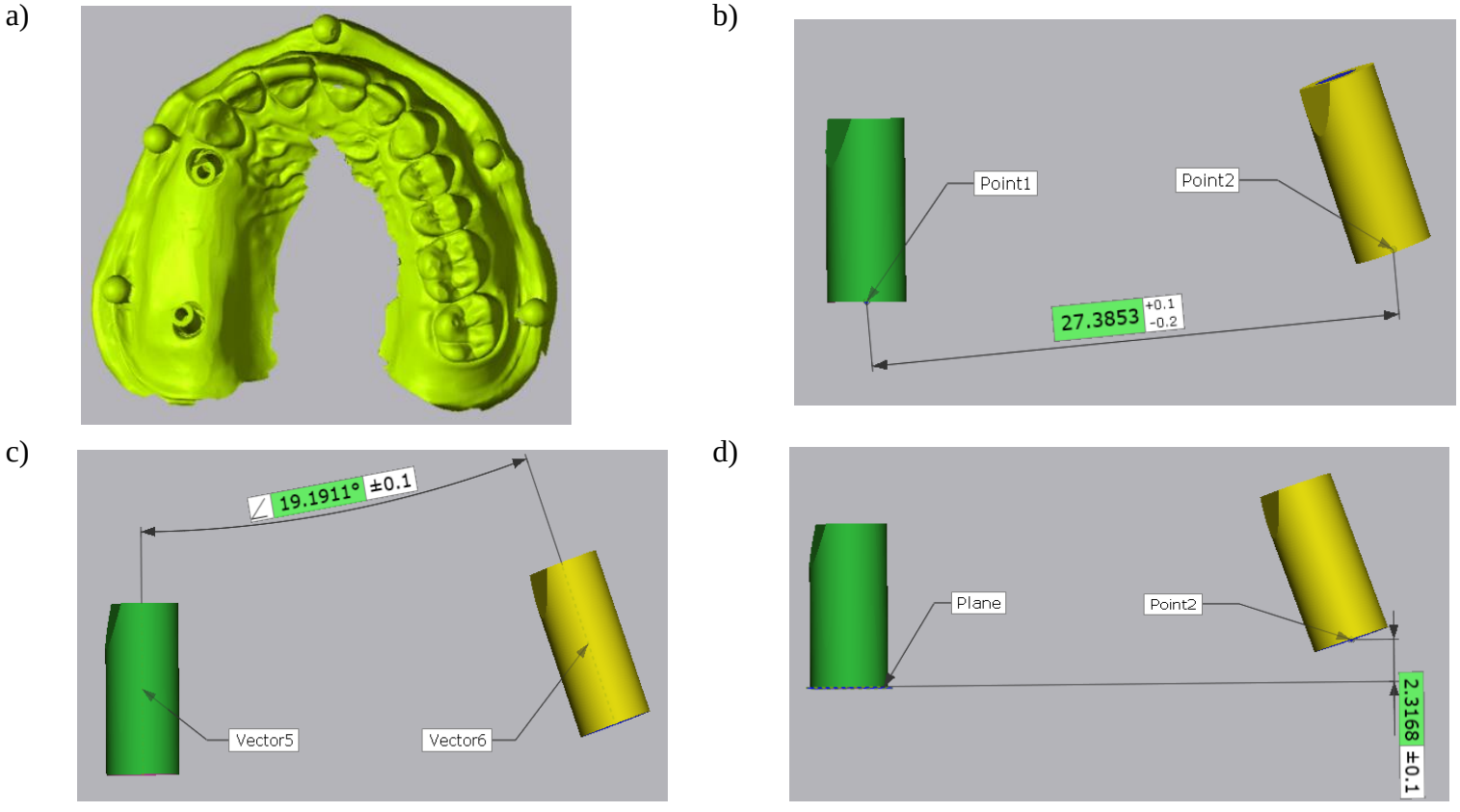

Figure 4 a) Partially edentulous model with scan bodies; b) Distance measurement between scan bodies; c) Angulation measurement between scan bodies; d) Vertical shift measurement of the scan bodies.

a)

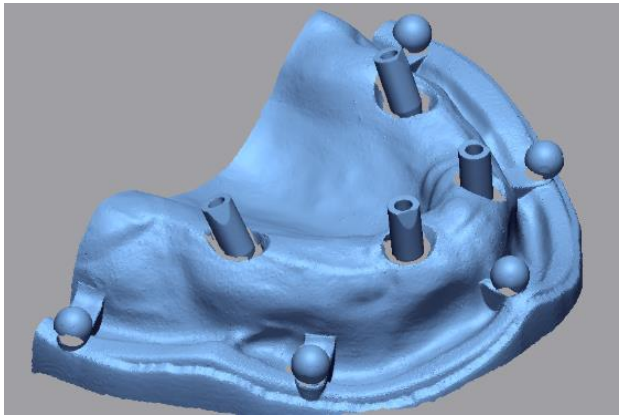

b)

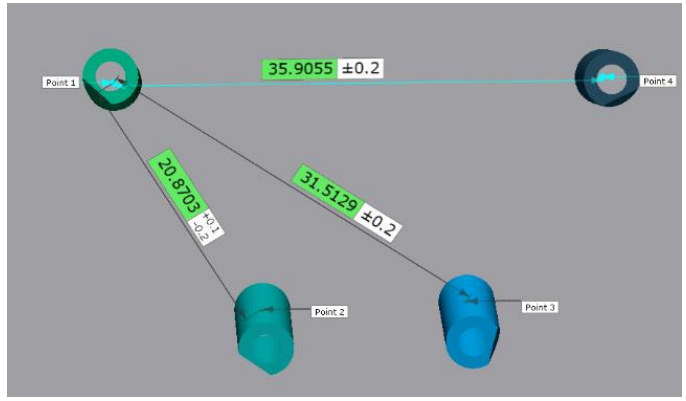

c)

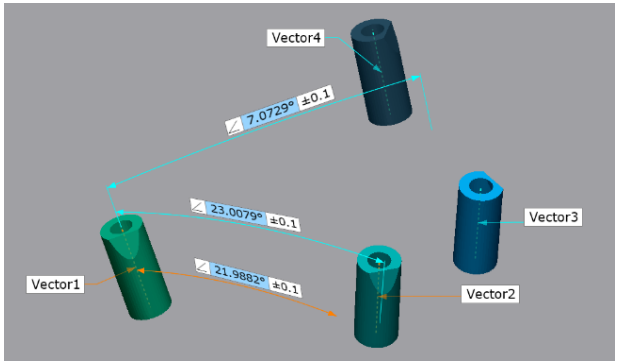

d)

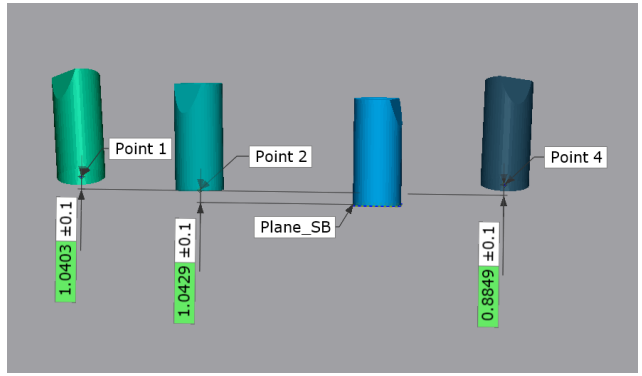

Figure 5 a) Fully edentulous model with scan bodies; b) Distance measurement between scan bodies; c) Angulation measurement between scan bodies; d) Vertical shift measurement of the scan bodies.

3.2. *In vivo* accuracy evaluation

3.2.1. Accuracy evaluation of dental implant impressions

The accuracy of dental implant impressions was analyzed in two separate experiments under the same protocol.

A) Comparison of conventional dental implant impression with Trios IOS digital dental implant impression.

Twenty patients requiring 27 fixed partial restorations on 2 implants AnyOne (Megagen, Daegu, Korea) participated in the clinical study using Trios IOS (3Shape, version 1.3.3.1). Two-unit (n=10), three-unit (n=11), and four-unit (n=6) zirconia (Katana Zirconia, Kuraray Noritake, Dental Inc., Osaka, Japan) restorations supported by two implants were evaluated. Three restorations were in the anterior area of the mouth and 24 were in the posterior area of the mouth. The average distance between implants was 14.3±7 mm.

B) Comparison of conventional dental implant impression with Trios 3 IOS digital dental implant impression.

Twenty-four fixed partial restorations in six patients and supported by 2 AnyOne implants (Megagen, Daegu, Korea) were included in the clinical study using Trios 3 IOS (3Shape; version 1.3.4.2). All implants were placed in the posterior area of the mouth. Two-unit (n = 7), three-unit (n = 11) and four-unit (n = 6) zirconia (Katana Zirconia, Kuraray Noritake) restorations were fabricated. The average inter-implant distance was 15.82 ± 5.66 mm.

For both experiments, two different types of implant impressions were performed for each case in a random order. A conventional open-tray impression technique with splinted transfers using vinyl-polysiloxane (Express, 3M, Mapplewood, USA) was used (CII group). A splinting procedure of the impression copings and their verification of passive-fit was applied.[69] When impression copings were fixated to implants, an approximately 5 mm wide strap of light- polymerizing acrylic resin (Individolux, VOCO, Cuxhaven, Germany) was wrapped around the copings and light cured on each side with a 1200 mW/cm light-intensity unit (Elipar Free light2, 3M/ESPE, USA). The splint was removed from the implants, examined and reattached again. A Sheffield 1-screw test was performed to ensure the passivity of the splint: one screw of the coping was tightened completely and the other was inspected for any fixating distortion or screwing

resistance.[24] Only after the verification of the splint, implant impressions were taken. Digital impressions were taken using original scan bodies (AnyOne Internal scan body, Megagen) torqued to the implants at 15 Ncm using a cordless electronical screwdriver (NSK iSD900, Tokyo, Japan) and a Trios IOS (3Shape, Copenhagen, Denmark; version 1.3.3.1) and Trios 3 IOS (3Shape; version 1.3.4.2) (DII group). The scanning technique making less than 1,000 images per arch was completed under the manufacturer's recommendations. In the maxilla, the scanning started from occlusal surface moving to buccal and palatal surfaces, while in the mandible after scanning the occlusal surfaces the lingual and buccal surfaces were captured (Figure 6). STL files were used for comparisons.

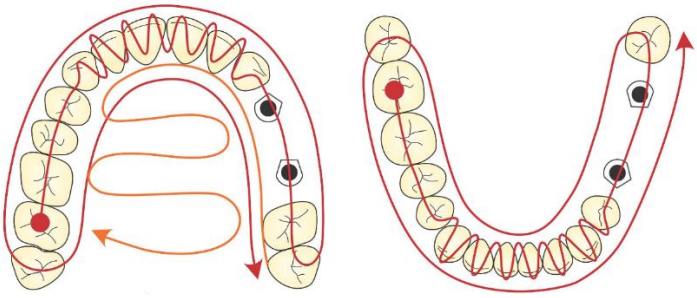

Figure 6. Scanning sequence with IOS: a) upper jaw, b) lower jaw.

Master models were fabricated from conventional impressions with type IV plaster (FujiRock, GC, Tokyo, Japan) under the manufacturer's instructions and allowed to set at room temperature for 24 hours. A verification jig, made according to the same technique used when joining the impression copings, was used to assess the accuracy of the position of the implant analogues in the master model. Passive-fit evaluation techniques, such as finger pressure, Sheffield, and screw-resistance tests[24] were used during the verification procedure. After verification of the master model, the same scan bodies at the same implant locations and in the same rotational positions were attached to the implant analogues using a 15 Ncm torque. Scanning of master models was completed using a D800 (3Shape, Copenhagen, Denmark) laboratory scanner and Dental System software (3Shape, version 2.9.9.3). After the exportation of the STL files, the 3D models were compared with the 3D models obtained from the DII procedure. Implant-supported zirconia restorations were fabricated from the conventional impressions. During all steps of the manufacture and final delivery of the restoration, the passive-fit

was additionally evaluated using the same techniques as were used with the verification jig. As all the restorations were clinically acceptable, master models were additionally confirmed as accurate. They were regarded as the best available reference representing conventional workflow due to the multiple verification procedures of the master model and final restorations.

The high-resolution and highly accurate 3D CAD models were imported into Rapidform 2006 (INUS Technology Inc, Seoul, Korea) reverse engineering software. 3D models produced from data captured by the IOS and laboratory scanner were compared with 3D CAD models of scan bodies. Each imported 3D model was checked for the presence of any non-manifold, redundant, crossing, and unstable faces in the imported shell. The positions of reference points were imported for calculations by using data analysis software in Matlab R2014b (The MathWorks, Inc.).

Each 3D model had its own position in space and own rotation. For the alignment of 3D models, a coarse alignment was applied, and then a fine alignment was performed using iterative closest point (ICP). The coarse alignment approximates the rigid transformation between models. This is a manual step in which a researcher must select three corresponding 3D points on the captured image and original 3D model of the scan body (Figure 7 a). Each pair of corresponding points is represented by a small square in a different color.

The fine alignment algorithm is an iterative procedure minimizing the mean square error (*MSE*) between points of the first model surface and the closest points, respectively, on the other surface. At each iteration of the algorithm, the geometric transformation that best aligns the original model and the closest points, respectively, on the scan body surface was chosen. The alignment procedure was repeated with other models of the scan bodies.

In the next steps, all processing and measurements were performed using only the high precision 3D CAD models of the scan body. To identify the scan body axis, the section plane was created on the scan body shell. This section plane is perpendicular to the cylinder part direction, while the reference vector normal to this reference plane is the axis of the scan body. The center point of the scan body is at the intersection between this axis and the top plane, which can be found by picking three reference points on the top surface of the scan body model (Figure 7 b)). A similar method of horizontal plane detection was discussed by Flugge et al.;[50] however, they did not use original 3D CAD files of the scan body for data analysis. In case the 3D model of the scan body was developed from a solid model, the top plane can be described as one flat polygon. So, in this study it is necessary only to define the position of this plane, passing through points $P_1(x_1,y_1,z_1)$, $P_2(x_2,y_2,z_2)$, and $P_3(x_3,y_3,z_3)$:

$$A \cdot x + B \cdot y + C \cdot z + D = 0 \quad (1)$$

here

$$A = \begin{vmatrix} y_2 - y_1 & z_2 - z_1 \\ y_3 - y_1 & z_3 - z_1 \end{vmatrix}$$
$$B = \begin{vmatrix} x_2 - x_1 & z_2 - z_1 \\ x_3 - x_1 & z_3 - z_1 \end{vmatrix}$$
$$C = \begin{vmatrix} x_2 - y_1 & y_2 - y_1 \\ x_3 - y_1 & y_3 - y_1 \end{vmatrix}. \quad (2)$$
$$D = -\begin{vmatrix} x_1 & y_1 & z_1 \\ x_2 & y_2 & z_2 \\ x_3 & y_3 & z_3 \end{vmatrix}$$

The Euclidean distance between center points $P_1(x_1, y_1, z_1)$ and $P_2(x_2, y_2, z_2)$ of two scan bodies was measured as the length of the straight line that connects these two points (Figure 7 c)) and can be expressed as:

$$d = \sqrt{(x_2 - x_1)^2 + (y_2 - y_1)^2 + (z_2 - z_1)^2}. \quad (3)$$

The angulation of scan bodies was measured as the angle between two vectors representing the axes of scan bodies in 3D space (Figure 7 d)). The angle between the two lines *u* and *v* was calculated using the expression:

$$\theta = \cos^{-1}\left(\frac{\vec{u} \cdot \vec{v}}{|\vec{u}| \cdot |\vec{v}|}\right), \quad (4)$$

where $\vec{u}$ and $\vec{v}$ are direction vectors of the lines *u* and *v*.

For the evaluation of the rotation between two scan bodies, the vertical edges of the scan body can be used. For the identification of the vector representing the top edge, the parameters of the side front plane and top plane of a flat surface of the scan body were calculated by picking three points on each wall. The result of the intersection of two selected front and top planes is the edge vector (Figure 7 e)). The angle between the top edges of two scan body models was calculated using formula (4). This angle is the rotation of one scan body in relation to the other one (Figure 7 f)).

The shortest distance between a center point of one scan body and the top plane of another scan body was calculated as:

$$d = \frac{A \cdot x + B \cdot y + C \cdot z + D}{\sqrt{A^2 + B^2 + C^2}}, \quad (5)$$

where *A*, *B*, *C*, and *D* are coefficients of the top plane of the scan body, and *x*, *y*, and *z* are coordinates of the center point of another scan body. This was evaluated as the vertical shift of the scan body (Figure 7 g)).

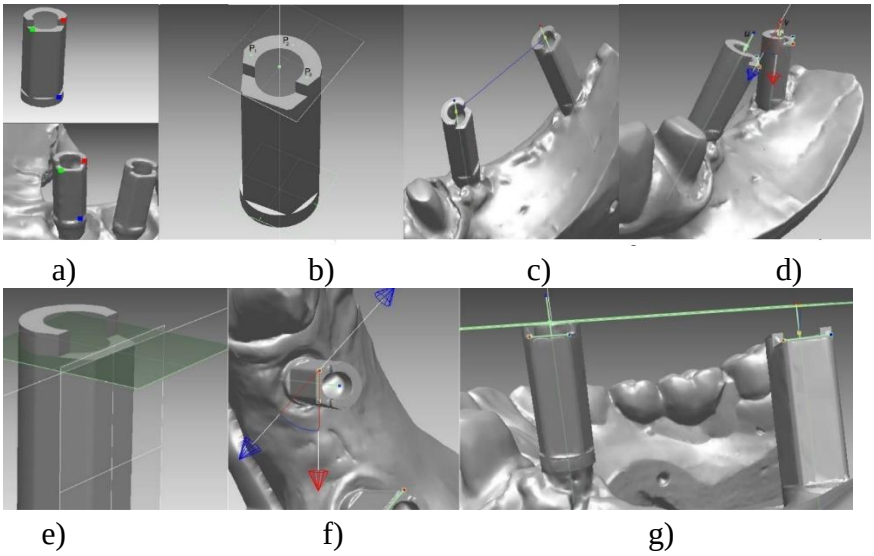

Figure 7. a) 3D computer models obtained using different scanning techniques. For coarse alignment, three corresponding points on the surface of each model are marked; b) The center point of the scan body is at the intersection between its axis and top plane; c) The Euclidean distance between the center points of two scan bodies; d) The angulation of scan bodies; e) Detecting the edge of the scan body; f) The rotation of one scan body in relation to the other one; g) The vertical shift of the scan body.

To evaluate the mismatch between the original model and the 3D model of the scan body, average distances between these given surfaces were measured. The Euclidean distance was calculated for each pair of corresponding points obtained by ICP algorithm. Five measurements for each parameter were done for each case.

To compare variables of conventional and digital groups, the average values and standard deviations of all parameters examined were calculated. New parameters of average distance between scan bodies and angulation were calculated by the formula (D800 data + IOS data)/2. They were used in order to evaluate the effect of the distance between scan bodies and angulation on the differences measured between conventional and digital impressions.

R software (Lucent Technologies, Auckland, New Zealand) package 2.3 – version 2 was used for statistical analysis. A Shapiro–Wilk test of normality revealed that not all data were distributed normally, and the Wilcoxon signed-rank test for paired data was therefore applied for the comparison of medians. Association between measured differences and distance between the scan bodies or angulation between implants was evaluated using the Spearman correlation coefficient and linear regression models. The power of statistical criteria was calculated using GPower (Dusseldorf University, Dusseldorf, Germany) version 3.1.9.2 software. Statistical significance was set at $p<0.05$.

3.2.2. Accuracy evaluation of dental implant restorations

3.2.2.1. Fit evaluation of dental implant restorations

Twenty-four two implant-supported iFPD AnyOne implants (Megagen) were included in this crossover type clinical study. Six patients participated in the study, requiring two implant-supported restorations: two-unit (n = 7), three-unit (n = 11) and four-unit (n = 6). Fourteen restorations were in the maxilla and ten were in the mandible, all of them were in the posterior area of the mouth. The workflow chart of the study is presented in Figure 8.

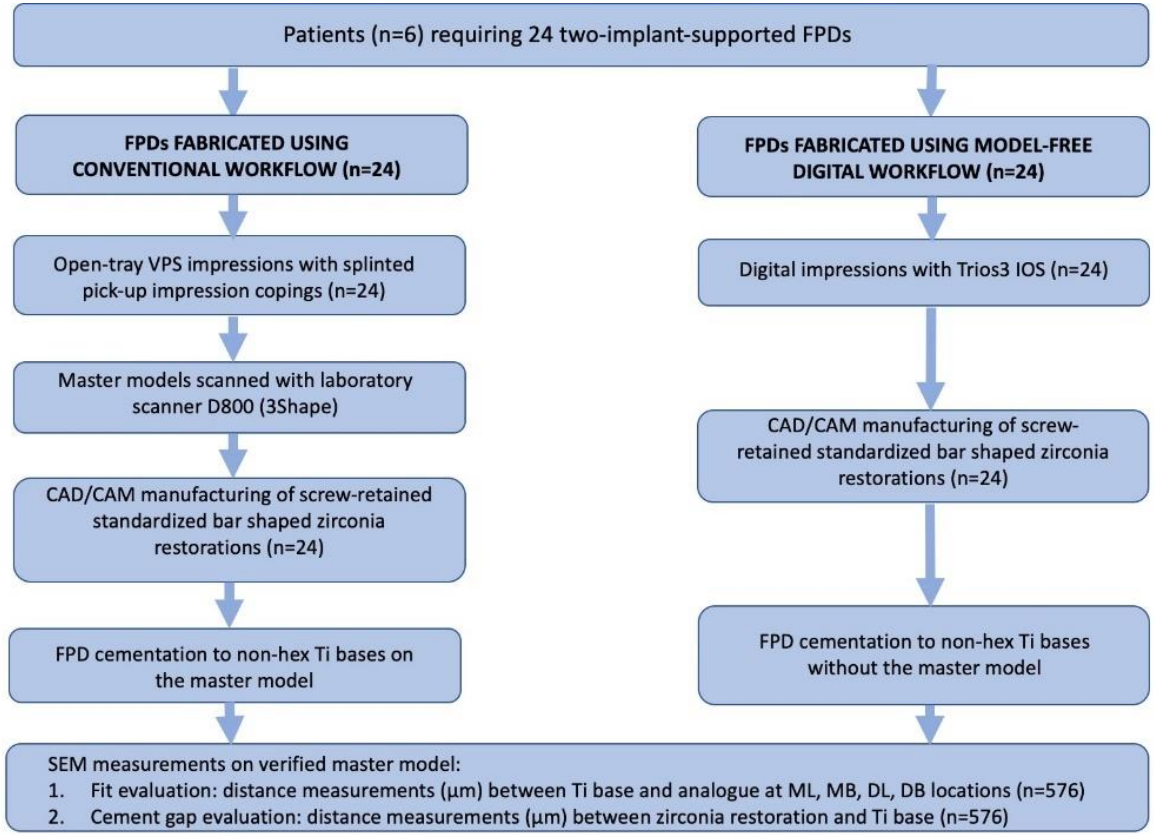

Figure 8. The workflow chart of fit evaluation of dental implant restorations.

Two zirconia restorations were fabricated for each case: one using a conventional workflow (group C) and another using a digital (group D) workflow. A total of 48 restorations were made. For the conventional workflow, open-tray impressions with splinted (using light-polymerizing (Individolux, VOCO, Cuxhaven, Germany) and auto-polymerizing acrylic resin (Pattern Resin, GC, Tokyo, Japan)) pick-up impression copings using vinyl–polysiloxane material (Express, 3M) were made.

The splinting procedure of the impression copings and verification of their passive-fit was done as described before.[69] Master models were poured from conventional impressions using type IV plaster (Fuji Rock, GC) according to the manufacturer's instructions and allowed to set at room temperature for 24 hours. After the fabrication of the master model, scanning with a laboratory scanner (D800, 3Shape, Denmark) was done. An experienced dental technician designed the screw-retained bar-shaped restorations (Dental System, 3Shape). They consisted of two cylinders connected with a bar and had a minimal diameter at the gingival level and no contacts to adjacent or opposing teeth. This was done in order to avoid any additional interference, except contact at the implant-abutment connection during the evaluation of the fit (Figure 9).

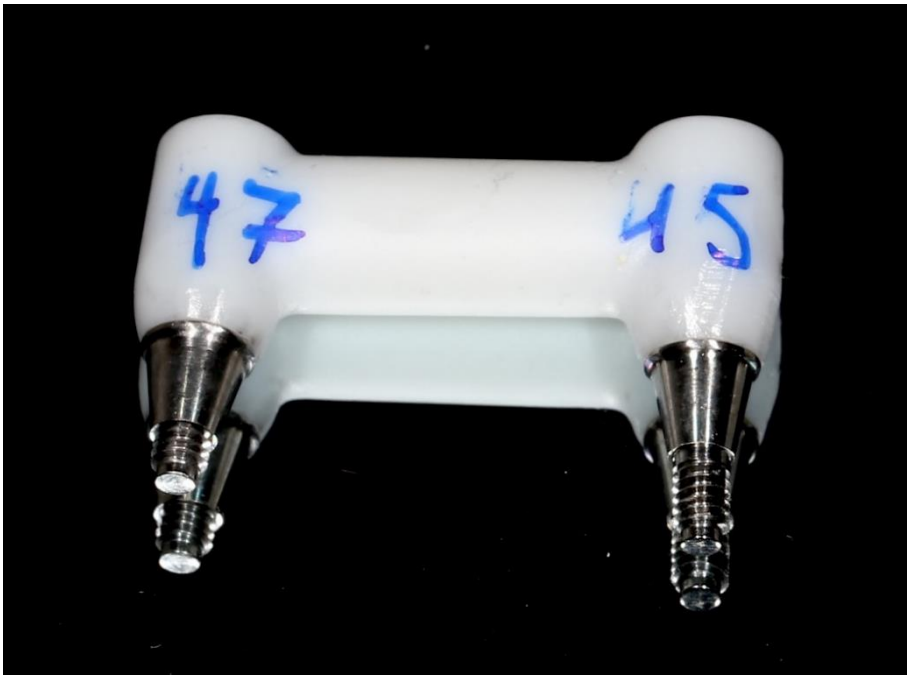

Figure 9. Two-implant-supported screw-retained zirconia restoration after cementation to titanium bases.

Restorations were milled from zirconia (Katana Zirconia, Kuraray Noritake, Dental Inc., Osaka, Japan) using a 5-axis milling machine (VHF Impression S1, VHF Camfacture AG, Ammerbuch, Germany). After milling, they were cemented (Multilink Hybrid, Ivoclar Vivadent, Schaan, Liechtenstein) on the original non-hex Ti (titanium) bases (AnyOne Internal AS20, Megagen, Korea), which were first screwed to implant analogues (Lab Analog LA350H, LA400H, Megagen) embedded in the master model. Twenty-four screw-retained restorations were made according to this conventional workflow and formed group C.

As for the digital group (D), intraoral scanning was performed using the original scan bodies torqued to the implants at 15 Ncm (using cordless electronical screwdriver (NSK iSD900, Tokyo, Japan)) and a Trios 3 (3Shape, version 1.3.4.2) intraoral scanner. The same scan bodies used for master cast scanning were used in the same implant locations and same rotational positions. A standardized scanning technique making less than 1,000 images per arch was used. The recommended scanning sequence was started from the occlusal surface and led buccally and palatally in the upper jaw. After scanning the occlusal surface in the lower jaw, it was continued on lingual and buccal surfaces. This data was used for the CAD design of the zirconia restorations by applying a standardized approach as in the conventional workflow group. The same milling strategies and parameters were used for the D group as for the C group. After the good fit of the zirconia restorations to the non-hex titanium bases (AnyOne Internal Non-Hexed, Megagen, Korea) was confirmed by a dental technician using a microscope, they were cemented together without the use of any model, and complete seating was assured. This group of specimens (n = 24) formed group D. Following cementation, the cement access was carefully removed and the abutment surface was polished and cleaned with alcohol.

All zirconia restorations in groups C and D were screwed on the corresponding master model and evaluated using SEM (Hitachi TM-1000, Hitachi High-Technologies Corporation, Tokyo, Japan) in random order. Measurements were performed in four selected areas on each implant analogue: mesiobuccal (MB), distobuccal (DB), mesiolingual (ML), and distolingual (DL). To standardize the measurement locations, they were marked on the implant analogues with a scratch, made with a sharp scalpel (Disposable scalpel, Huaian Medical Instruments, Huaian, China). It was assured that the implant analogue position was parallel to the measurement table during the measurements.

The screw of only the mesial implant was tightened to 35 Ncm and considered as passive, while the screw of the distal implant was not tightened

at all. The distance ($D_{passive}$) from the top margin of the Ti base to the top margin of the mesial implant analogue was measured three times at selected MB, DB, ML and DL locations by SEM at 150x magnification (Figure 10).

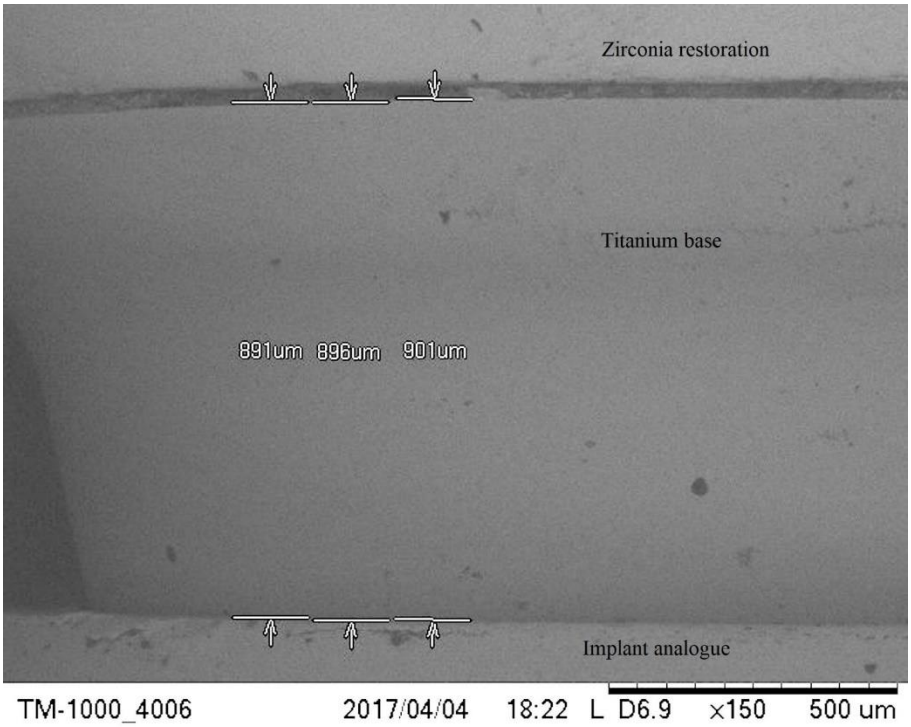

Figure 10. Measurement of distance from Ti base to implant analogue (D_{misfit}) at a standardized location marked with a scratch (x150 magnification).

The restoration was subsequently removed from the model, replaced again, and the screw on the distal implant abutment tightened to 20 Ncm. The distance ($D_{non-passive}$) on the mesial implant analogue was measured in an identical way. The same measurements were completed on the distal implant analogue as well. A total of 576 measurements were made. Because of inaccuracies in the SEM images, three measurements were rejected from the final evaluation. The difference in distances (D_{misfit}) between the passive and non-passive situation was calculated according to this formula:

$$D_{misfit} = D_{non-passive} - D_{passive}$$

As the difference between D_{misfit} in groups C and D, ΔD_{misfit} was calculated and used later to assess the possible associations of it with inter-implant distance and angulation:

$\Delta D_{misfit} = D_{misfit}$ (group C) – D_{misfit} (group D).

Root mean squares of D_{misfit} and ΔD_{misfit} were used for further analysis.

The cement gap in groups C and D was evaluated using SEM measurements. It was measured as the shortest vertical distance (D_{cement}) from the inferior edge zirconia framework to the top edge of the titanium base (Figure 11).

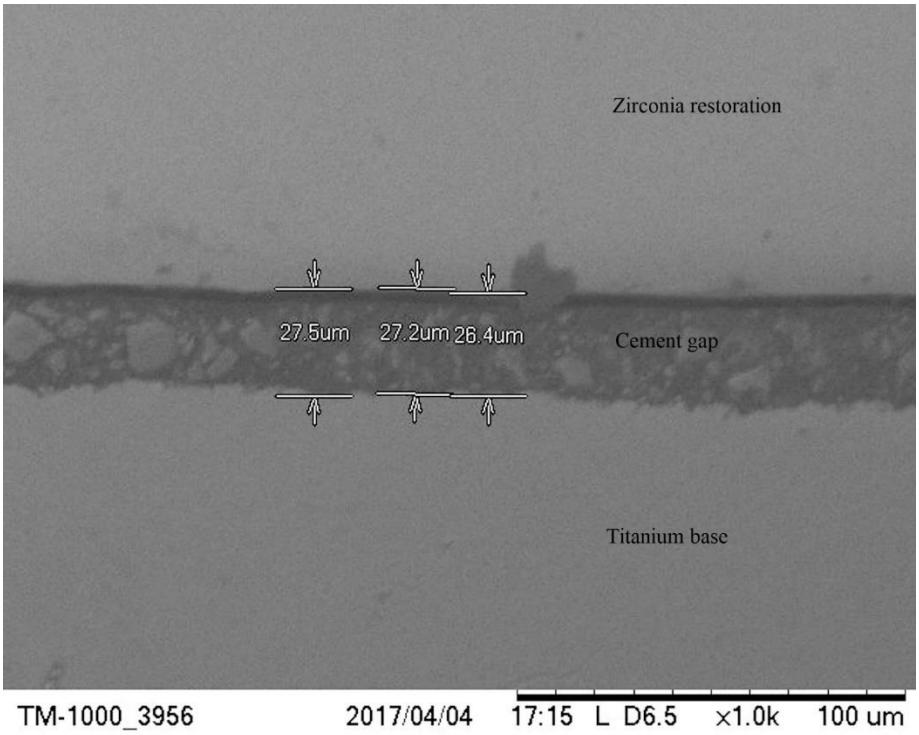

Figure 11. Measurement of D cement using SEM (x1000 magnification).

D_{cement} was evaluated at the same MB, DB, ML and DL locations using 1,000x magnification. Three measurements were made at each location. Overall, 576 measurements of cement gap were made, as three measurements were rejected because of inaccurate SEM images.

As the difference in D_{cement} between groups C and D, ΔD_{cement} was calculated in order to assess the possible associations of it with inter-implant distance and angulation:

$\Delta D_{cement} = D_{cement}$ (group C) – D_{cement} (group D).

Root mean squares of D_{cement} and ΔD_{cement} were used for further analysis.

There was an attempt to estimate the effect of the distance and angulation between the implants on the fit of the restorations. For this purpose, means of distances and angulations between the scan bodies were calculated using STL files produced from digital impressions (group D) and scanned master models (group C). Selected STL files and CAD models of scan bodies were imported and registered using a modified ICP algorithm in the reverse engineering software Rapidform 2006 (INUS Technology Inc., Seoul, Korea). The distance and angulation between scan bodies were measured for groups C and D. The center point of the scan body was chosen as the intersection between a selected center axis and a top plane of the scan body. The distance between the center points of the two scan bodies was measured. The angulation of the scan bodies was measured as the angle between two vectors representing the axes of the scan bodies in 3D space (Figure 12).

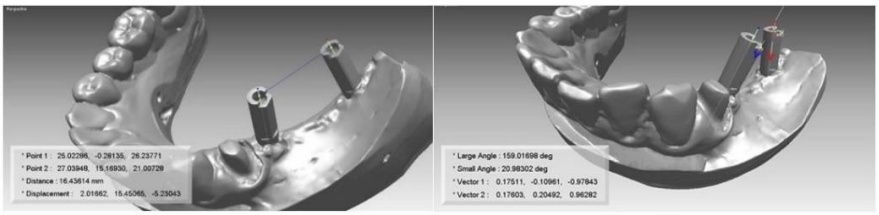

a) b)

Figure 12. a) Measurement of distance between scan bodies; b) measurement of inter-implant angulation between scan bodies using reverse engineering software.

Average linear and angular parameters were calculated using this formula: (D800 data + Trios 3 data)/2. These parameters were used to assess their possible effect on D_{misfit} and D_{cement}, as well as ΔD_{misfit} and ΔD_{cement}.

Statistical analysis was completed with R software ver. 2.3-2 (Lucent Technologies). In order to analyze the distribution of the data, the Shapiro–Wilk test of normality was applied. Since the data were not normally distributed, non-parametric tests were used. The Wilcoxon signed rank test for paired data and Friedman rank-sum test was applied to compare the medians of the distances in the groups and subgroups of C and D. The Spearmen correlation test was used to evaluate associations between D_{misfit}, ΔD_{misfit}, D_{cement}, and ΔD_{cement} of restorations in groups C and D and the average values of angulation and distance between the scan bodies.

GPower ver. 3.1.9.2 software (Dusseldorf University) served to calculate the power of statistical analysis. Statistical significance was defined at $p< 0.05$.

3.2.2.2. Passive fit evaluation of dental implant restorations

The clinical study involved 24 cases of two-implant-supported (AnyOne, Megagen) fixed partial restorations. The restorations that were investigated were distributed as follows with regards to length: two-unit (n = 7), three-unit (n = 11) and four-unit (n = 6) bridges. Ten of them were in the mandible and 14 in the maxilla.

Forty-eight zirconia restorations were fabricated according to the conventional (group C, n=24) and digital workflow (group D, n=24). For the conventional group vinyl–polysiloxane (Express, 3M) open-tray dental implant impressions were made with splinted pick-up impression copings using light-polymerizing acrylic resin (Individolux, VOCO, Germany) and auto-polymerizing acrylic resin (Pattern Resin, GC, Tokyo, Japan) with passivity verification after splinting under the technique mentioned before.[69] Master casts were poured using type IV plaster (Japan-Stone, Siladent, Goslar, Germany) according to the manufacturer's instructions and allowed to set at room temperature for 24 hours. The fabricated master casts were scanned with a D800 laboratory scanner (3Shape) using the original scan bodies (attached to the implant analogues, and 24 bar-shaped, screw-retained restorations were designed by an experienced dental technician using CAD software (Dental System, 3Shape). The restorations were of simplified shape, consisting of two cylinders connected with a bar. To avoid any interference with peri-implant tissues and neighboring teeth during seating, the restoration had a minimal diameter at the gingiva level and there were no contacts with adjacent or opposing teeth. Twenty-four restorations were milled from zirconia (Katana Zirconia, Kuraray Noritake, Dental Inc.) using a 5-axis milling machine with 5 μm drill compensation (VHF Impression S1, VHF Camfacture AG). After zirconia sintering procedures, the restorations were cemented (Multilink Hybrid, Ivoclar Vivadent) to original non-hexed titanium interfaces, which were screwed to the implant analogues embedded in the master casts. Twenty-four screw-retained zirconia restorations were made according to conventional workflow and formed study group C.

As for the digital (D) group of specimens, intraoral scanning with a Trios 3 (3Shape, version 1.3.4.2) intraoral scanner (IOS) was performed using original scan bodies torqued to the implants at 15 Ncm. Digital impressions were taken according to the recommendations of the Trios 3 manufacturer. In the upper jaw, scanning began with the occlusal surface to buccal and palatal surfaces, while in the lower jaw scanning began with the occlusal surface to lingual and buccal surfaces. The data obtained were used for the fabrication of another 24 zirconia restorations, replicating the CAD/CAM process that

was used for the conventional workflow. This resulted in zirconia restorations of identical shape for both groups. Since master casts produced using CAM or 3D printing technology are less accurate, cementation was done without the use of the master cast.

Having a reference in a clinical study concerning impression or restoration accuracy is always a very important objective. Traditional in-vitro techniques, such as when the reference cast is used to evaluate the fit of the restoration and when the registration of 3D implant positions is done with an industrial scanner or coordinate measuring machines could not be applied, however. Assuming the evidence that for the most extensive cases conventional impressions with splinted impression copings and plaster casts are still considered the most reliable technique, group C was taken as the reference and group D was compared to it.[70,71]

An alternate way of acquiring the best available reference by making an additional control cast from the splinted impression copings is reported in the literature.[12] This approach was used for 10 randomly selected cases. Using this technique, additional registration of implant positions was achieved with extra pick-up impression copings splinted intraorally with light-polymerizing acrylic resin (Individolux, VOCO, Germany). Immediately after the removal of the splints from the mouth, implant analogues were carefully attached to the copings, and control casts were fabricated using type IV plaster (Japan-Stone, Siladent). These control casts were used as the best available reference, which helped to compare the accuracy of conventional and digital restorations.

Measurements

The passive fit of restorations C and D was evaluated on three occasions: intraorally, on the master casts, and on the control casts. Restorations were checked intraorally for any major misfit or imbalance. After the application of the Sheffield test, they were rated as passively fitting or having a clinically detectable non-passive fit. During clinical evaluation, it was confirmed that specimens were not interfering with the gingiva, neighboring or opposing teeth, or restorations.

Afterward, the prosthetic screw only on the mesial implant was torqued to 5 Ncm using an implant surgery unit and a handpiece (W&H Implantmed, W&H Dentalwerk, Bürmoos, Austria) (Figure 13).

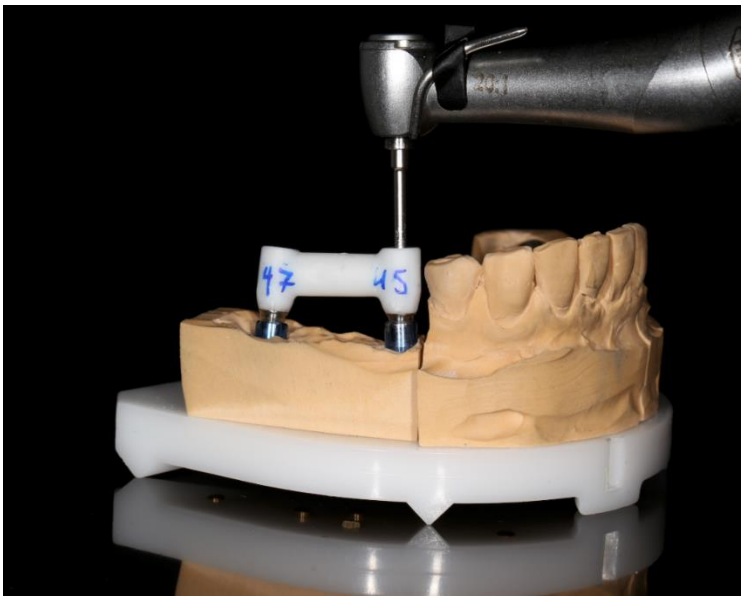

Figure 13. Initial torque of 5 Ncm was achieved with an implant surgery unit and a handpiece.

It was then tightened to 35 Ncm with the original prosthetic ratchet adapted with a goniometer (Saehan, Saehan Corporation, Bongamgongdan, Korea), which allowed measuring the rotation angle needed to achieve torque from 5 to 35 Ncm (Figure 14).

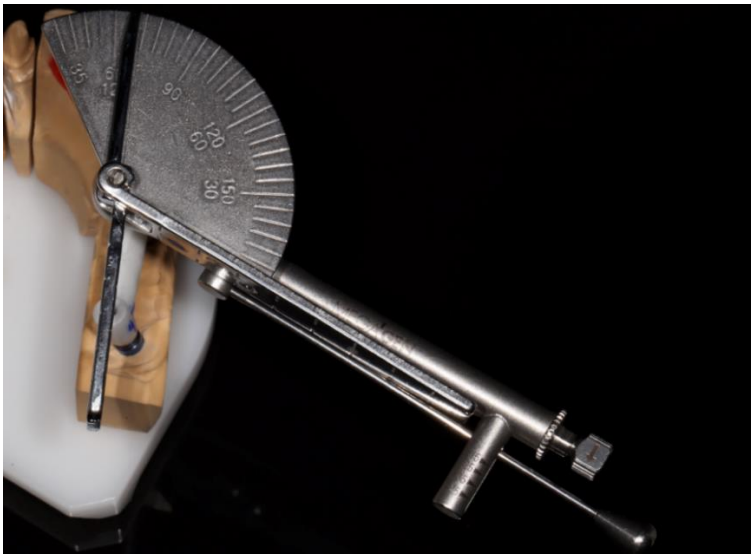

Figure 14. A prosthetic ratchet equipped with a goniometer was used to estimate the rotation angle needed to achieve torque from 5 Ncm to 35 Ncm.

This value was recorded as a rotation angle representing the screw resistance of a passive situation (SR passive). The screw was then untightened, the restoration was removed and repositioned, and the prosthetic screw on the distal implant was tightened to 15 Ncm. Then, the same technique was again applied to the prosthetic screw of the mesial implant, and rotation angle representing screw resistance of a potentially non-passive situation (SR non-passive) was registered. Rotation angles of the prosthetic screw of the distal implant were evaluated in an identical way.

The screw resistance (SR) parameter was calculated as the difference of rotation angles in passive and non-passive situations by the formula:

$$SR = SR_{passive} - SR_{non\text{-}passive}.$$

SR represented the level of non-passive fit of the restoration. Root mean squares of SR were used for further analysis. Ninety-six SR measurements were done with the frameworks of groups C and D intraorally. In addition, 96 SR measurements were performed on the master casts, and 40 SR measurements were performed on the control models in an identical manner by the two calibrated operators.

To identify the average angle of rotation of the completely passive situation, a titanium base without a crown was tightened on the master cast from 5 Ncm to 35 Ncm with a ratchet and goniometer 10 times, each time measuring the angle. The average tightening angle was calculated (87±5°) and used as a reference.

To find associations between measurements of screw resistance and inter-implant distance and inter-implant angulation, the distance and angulation between the scan bodies were measured for specimens of groups C and D. Selected STL files of groups C and D were analyzed in reverse engineering software Rapidform 2006 (INUS Technology Inc.) according to the ICP algorithm (Figure 7a)).

The center point of the scan body was chosen as the intersection between a selected center axis and the top plane of the scan body. The distance between the center points of two scan bodies was measured. The angulation of the scan bodies was measured as the angle between two vectors representing the axes of the scan bodies in 3D space. Average linear and angular parameters were calculated by the formula (D800 data + Trios 3 data)/2 and were used for further analysis.

Statistical analysis

Statistical analysis was performed using R software ver. 2.3-2 (Lucent Technologies). The Shapiro–Wilk test of normality was applied to the data. As most of the variables were not distributed normally, non-parametric tests were used.

The Wilcoxon signed-rank test for paired data was used to compare medians of SR between groups C and D when measured intraorally on the master and the control cast. A comparison was also made between the overall SR measurements obtained intraorally and on the master cast.

All cases were also divided into two groups, depending on whether inter-implant angulation was below or above 10 degrees. Differences in SR measurements were obtained intraorally and on the master, and control casts were compared between those groups.

To assess the associations between the SR measurements and distance or angle between the implants, the Spearman correlation test was applied. GPower ver. 3.1.9.2 software (Dusseldorf University) served to calculate the power of statistical analysis. Statistical significance was defined at $p< 0.05$.

3.3. *In vitro* and *in vivo* accuracy evaluation

Eight patients with at least one edentulous arch with 4 healed dental implants have participated in this study (n=10 edentulous jaws, 40 implants). For each patient, a conventional open-tray, vinyl-polysiloxane impression (Express, 3M ESPE) was taken to fabricate a screw-retained titanium bar with four holes in the area of second incisors and second premolar teeth. Four scan bodies (CARES RC Mono scan body, Straumann, Basel, Switzerland), were attached to the bar with auto-polymerizing resin (Pattern-resin, GC, Tokyo, Japan) perpendicular to the top surface of the bar and parallel to each other. Various types of implants were used for the patients, but only the position of scan bodies was important in the present part of the study.

The bar containing the scan bodies was screw-retained to the implants in the edentulous jaw and the situation was scanned with an intraoral scanner (IOS) (Trios 3, 3Shape) 8 times following the scanning strategy recommended by the manufacturer (IOS group). Then the bar was carefully removed from the mouth and attached to the master cast and scanned again 8 times using the same scanning strategy (MIOS group) (Fig. 15). All the files were inspected additionally for the absence of any scanning insufficiencies. Then, the master cast was scanned 8 times with a laboratory scanner (D800, 3Shape) and this

data was considered as the reference (RS group). Thus, 24 scans were done per one edentulous arch and 240 scans in total.

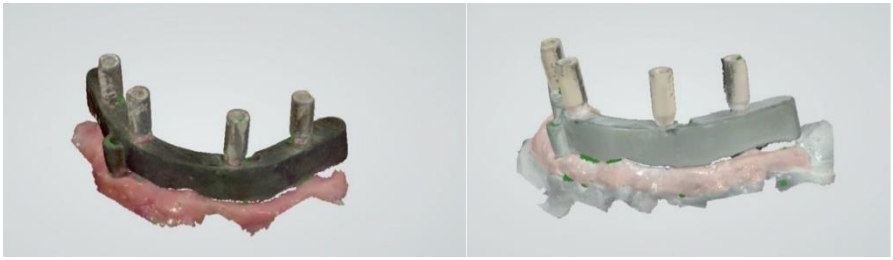

a) b)

Figure 15. The same titanium bar with 4 scan bodies was scanned intraorally (a) and extraorally on the master cast (b) using Trios 3 scanner.

All scans were exported in STL file format. All scans were aligned, and the bar area was cut using the same cutting plane by Geomagic Control X 2018 (3D Systems Corporation) software, leaving mainly scan body surfaces for further analysis. Figure 16 shows the data acquisition workflow and the example of the scan result. Surface alignment and measurements were performed using Geomagic Control X 2018 (3D Systems Corporation) software.

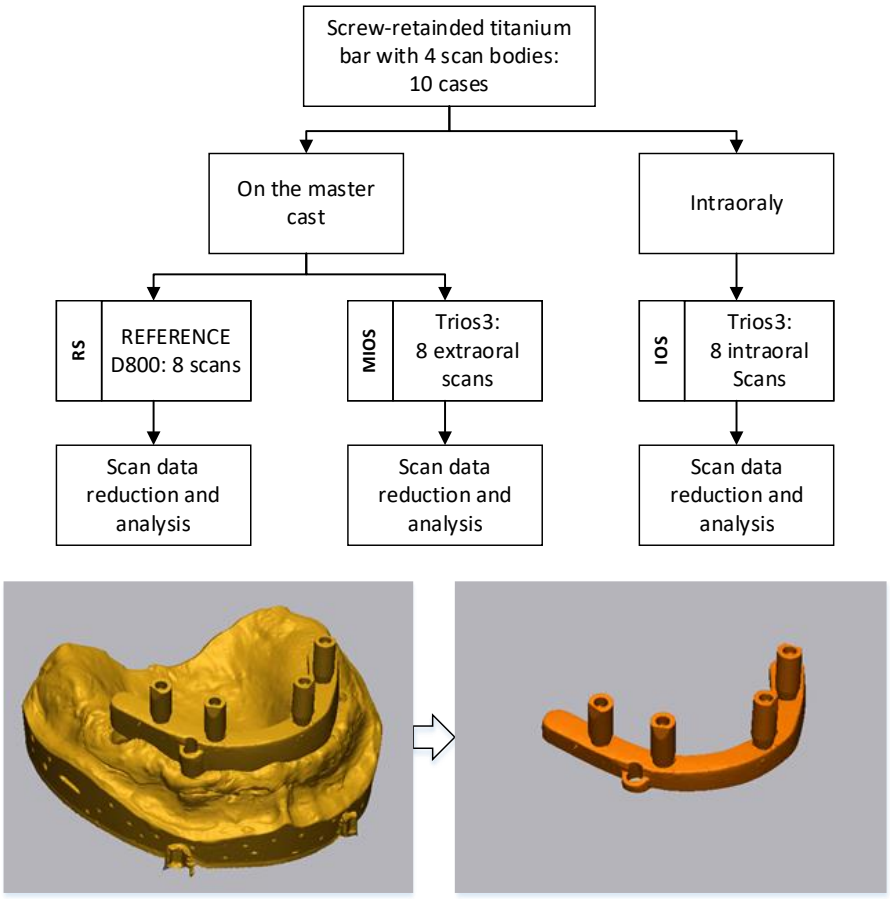

Figure 16. Data acquisition workflow. At the bottom, the example of the impression model with mounted implant bridge scanned with D800 (on the left) and cropped part of the implant bridge (on the right) is presented.

Accuracy, according to ISO 5725-1, consists of precision and trueness.[72] Precision describes the closeness of repeated measurements to each other. Higher precision means a better predictable result of the measurement. Trueness shows the measurement discrepancy to the true value. Accuracy for intraoral digital impressions assessment can be calculated using different measures – the literature presents examples of distance,[51,59,73] angulation,[51,59] or surface[51,74,75] measurements. There are also different approaches to the choice of measurement parameter for the trueness and precision estimation assessing the accuracy of the scanned surfaces. Mean[73] or root mean squared values of the distances could be used between surfaces[75] for trueness and precision calculation.

In this study, accuracy was computed for three types of measurements: the distance between scan bodies, angulation between scan bodies and intersurface distance between aligned scans. Distance and angulation accuracy was based on calculating mean values of the unsigned deviations and the surface accuracy was evaluated using root mean squared values of the deviation. The workflow of the data analysis is presented in Figure 17.

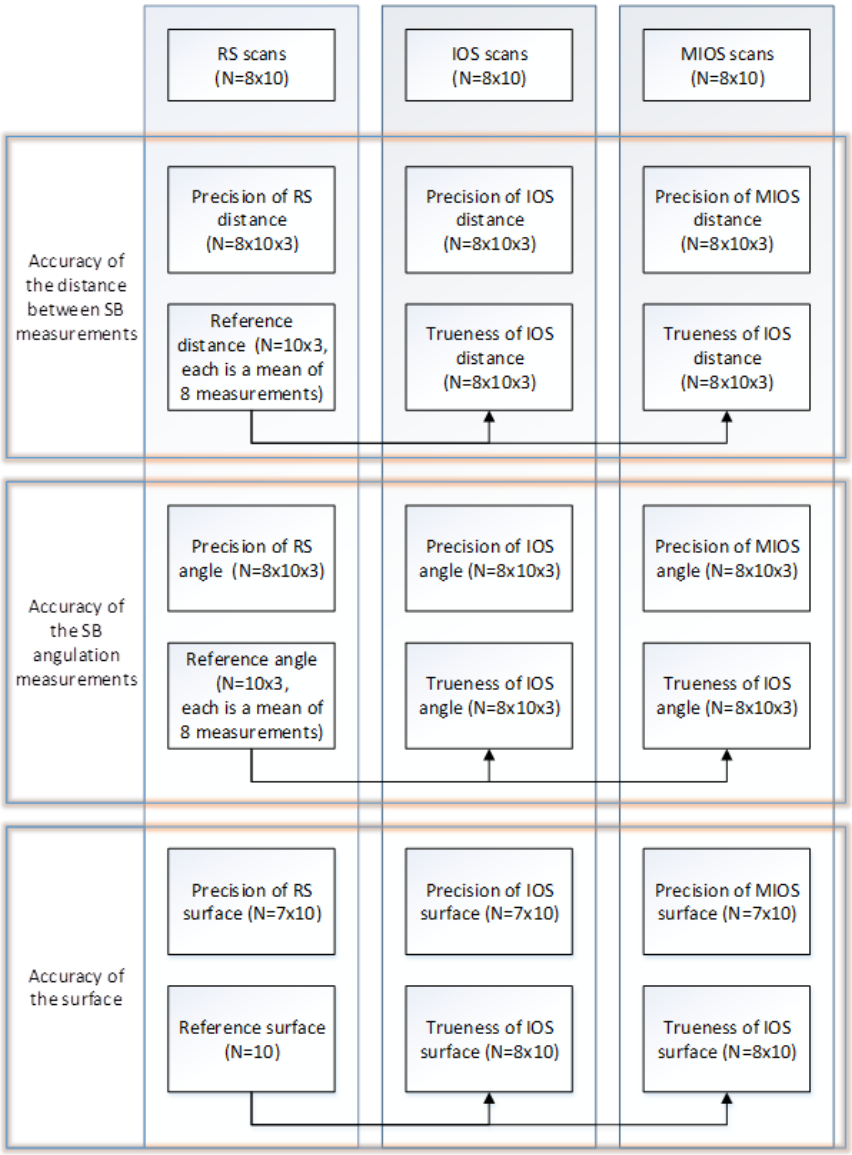

Figure 17. Data analysis workflow.

Distance measurements were done between the left scan body upper surface plane center (1) to the other scan bodies the same points (distances 1-2, 1-3, 1-4) (Figure 18).

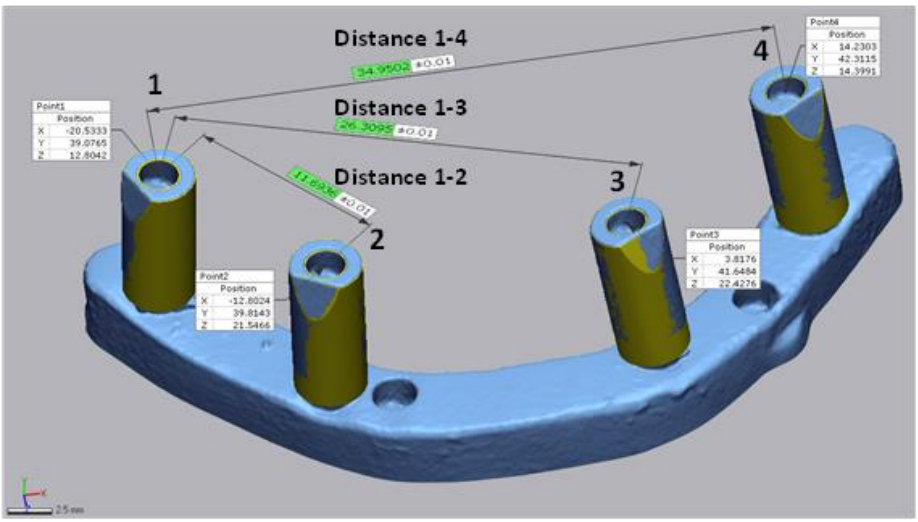

Figure 18. Distance measurement setup for intraoral and extraoral scanning comparison.

To find the scan body upper surface plane center, cylinders of CAD digital scan bodies were superimposed on the scan surface using an initial transform alignment followed by a precise alignment using the best-fit algorithm. Then the top plane centers of the digital scan bodies were identified using software tools. The three distances were measured for each scan composing 24 measurements for each case with every scanning modality (total 72 measurements per case) and all ten cases; 720 measurements were collected. At each distance, the mean was calculated using eight measurements on different scans of the same object. This mean then was used for the precision estimation. Distances measured with D800 were averaged for each distance at each case and used as a reference value for the estimation of trueness. Afterward, the differences between reference distances and measured distances using intraoral and extraoral Trios scanning were calculated. These differences (8 for each distance and 80 total for the 10 cases) in three separate distance classes (distance 1-2, distance 1-3, distance 1-4) formed the final data array for the statistical analysis of trueness.

Angles between the reference scan body axis (Figure 19) and the other scan bodies' axis were other measures of *in vivo* and *in vitro* scanning with IOS accuracy evaluation. Angles in 3D space were measured between the vectors

extracted from aligned CAD scan bodies' surfaces. The three angles were measured for each scan composing 24 measurements for each case with every scanning modality (total 80 measurements per case) and all ten cases, 720 measurements were collected. At each angle, the mean was calculated using eight measurements on different scans of the same object. This mean was then used for precision estimation. Angles measured with D800 were averaged for each distance and at each case and then used as a reference ground true in trueness calculations. Afterward, the differences between reference angles and measured angles using intraoral and extraoral IOS scanning were calculated. These differences (8 for each distance and 80 totally for each of the 10 cases) in three separate angle classes (angle at a distance 1-2, angle at a distance 1-3, angle at a distance 1-4) formed the final data array for the statistical analysis of trueness.

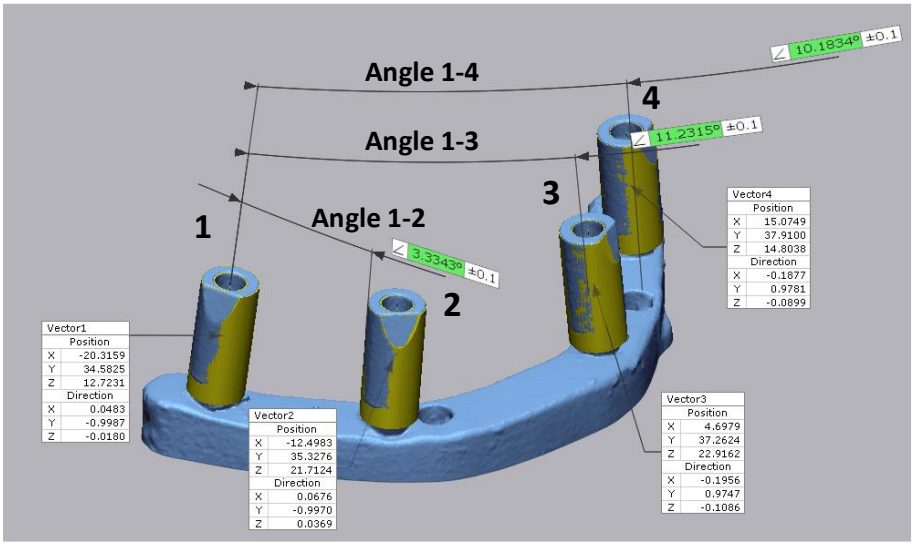

Figure 19. Angle measurement setup for intraoral and extraoral scanning comparison.

Scan surface accuracy was evaluated calculating the intersurface distance between the scans using 3D compare tool of Geomagic Control X software. Initially, for each of the scanners, surfaces under comparison were imported in Geomagic Control X software, aligned using transform alignment using manually selected reference points and, on the next step, aligned precisely by applying best-fit alignment procedure. Then the shortest 3D distance between surface points was calculated. For the precision estimation, for each of the scans' groups (MIOS, RS, and IOS), in each patient case the surface merge (for 8 surfaces of each patient case) was done using the volume merge tool.

Then a 3D comparison of each of the surfaces to this new surface was done. The surface with the smallest average distance from the merged surface was selected and marked as a reference for the precision estimation. On the next step, the rest seven surfaces were 3D compared and results (root mean squared values) were exported for the precision analysis. To assess the trueness, the RS scans at each of the ten cases were processed with volume merge and, following the same procedure as described in reference scans selection for the precision, the reference scans for the trueness analysis were selected. After this, the surfaces of IOS and MIOS were 3D compared to the reference surfaces and deviation results (root mean squared values) were exported for the precision analysis. Also, a comparison between IOS and MIOS surfaces was done. Here as a reference MIOS surface was taken (reference was selected by the same procedure as for the reference RS surface).

A statistical analysis was performed with Matlab (The MathWorks, Inc., USA) software. Testing for the differences, Shapiro–Wilk normality tests were carried out, and depending on the results, a Mann-Whitney U or Student two-sample t-test was applied for the estimation of statistically significant differences between measurements. GPower ver. 3.1.9.2 software (Dusseldorf University) served to calculate the power of statistical analysis. The level of significance was set at 0.05.

4. RESULTS

4.1. *In vitro* accuracy evaluation

In partially edentulous models, trueness results varied according to measured parameters. The results are presented in figures 20–27 and tables 1–6. For distance measurements, trueness mean values were from -46.74±15.37 μm of Trios 3 scanner to 392.07±314.28 μm of Medit i500 scanner in models without a digital splint, while in models with digital splint, the trueness of distance mean values were from -34.39±13.01 μm of Trios 4 IOS to 117.7±232.28 μm in CS3600 IOS. Trueness mean values of angulation varied from -0.03±0.52° of CS3600 IOS to 0.22±0.04° of Primescan IOS in models without digital splint, while in models with splint trueness, the mean values of angulation resulted from 0.02±0.18° of Trios 3 IOS to 0.44±0.49° of CS3600 IOS. For vertical shift measurements in models without digital splint, trueness varied from -107.97±47.06 μm of Trios 4 IOS to 107.16±103.47 μm for Medit i500. Trueness mean values of vertical shift in models with digital splint ranged from -14.99±45.00 μm of CS3600 IOS to -86.91±42.05 μm. Despite the digital splint having improved the trueness of all measured parameters for five tested IOS, there were no statistically significant differences between the measurements of models with digital splint or without, except for Medit i500 IOS in all parameters and Primescan in angle measurements ($p<0.05$). The best results in the precision of partially edentulous model demonstrated Trios 3 IOS in distance (12.82±7.18 μm), Primescan in angulation (0.03±0.03°), and vertical shift parameters (9.04±7.43 μm). However, there were also no statistically significant difference between the scans with and without digital splint ($p>0.05$) of any IOS tested, except for Medit i500 in the distance and vertical shift parameters and CS3600 in vertical shift.

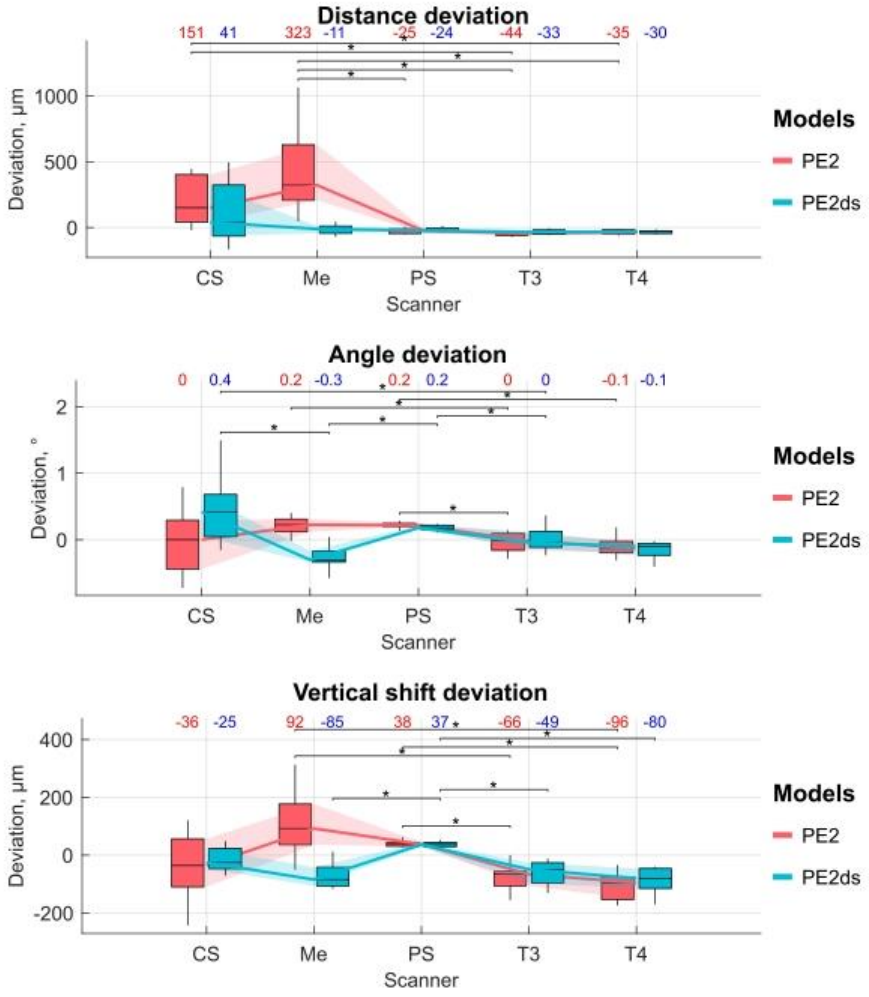

Figure 20. Trueness comparison of distance, angle and vertical shift measurements in partially edentulous models between different IOS. PE2 – partially edentulous model with 2 implants, ds – digital splint. Black lines with a star indicate groups that differed statistically significantly.

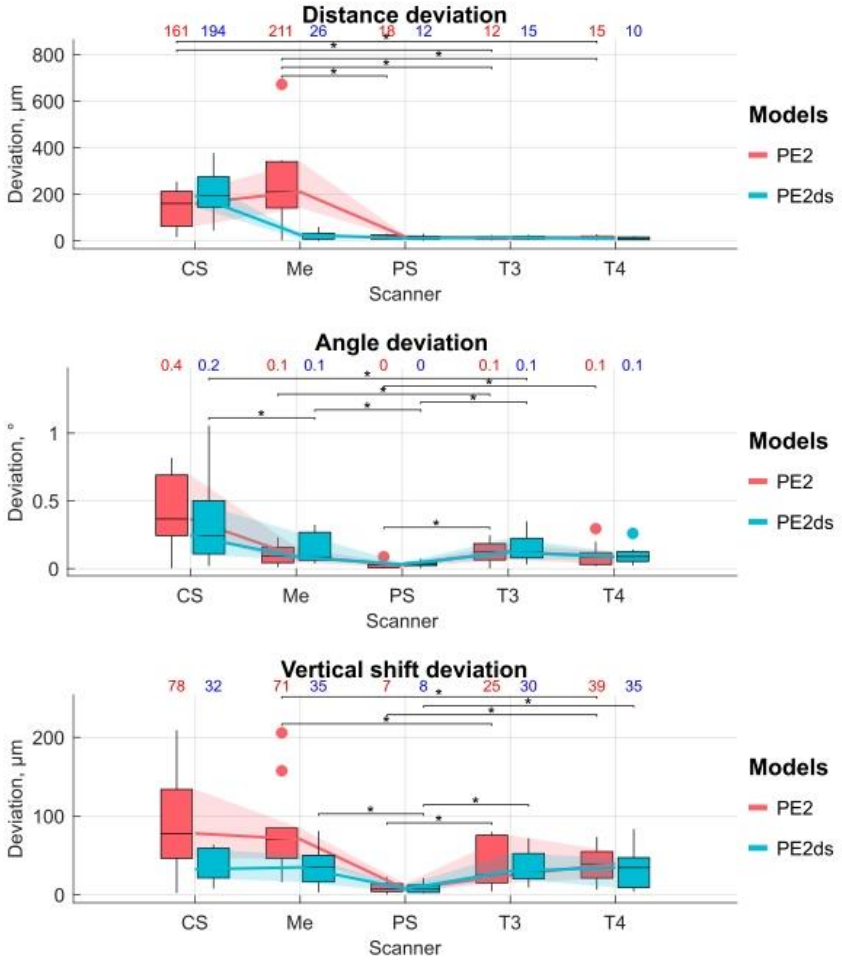

Figure 21. Precision comparison of distance, angle, and vertical shift measurements in partially edentulous models between different IOS. PE2 – partially edentulous model with 2 implants, ds – digital splint. Black lines with a star indicate groups that differed statistically significantly.

In fully edentulous models, a digital splint did not improve the trueness of the scanners in the distance, angle, and vertical shift parameters, but differences were statistically significant ($p<0.05$). However, the longer the distance between scan bodies was evaluated, the more deviations in distance, angle, and vertical shift parameters were detected. The usage of digital splint also did not improve the scanners' precision of the tested parameters, though there were no statistically significant differences ($p>0.05$). However, Primescan showed the best results of the precision of both distance, angle, and vertical shift parameters in all three measured distances, followed by Trios 4 IOS ($p<0.05$).

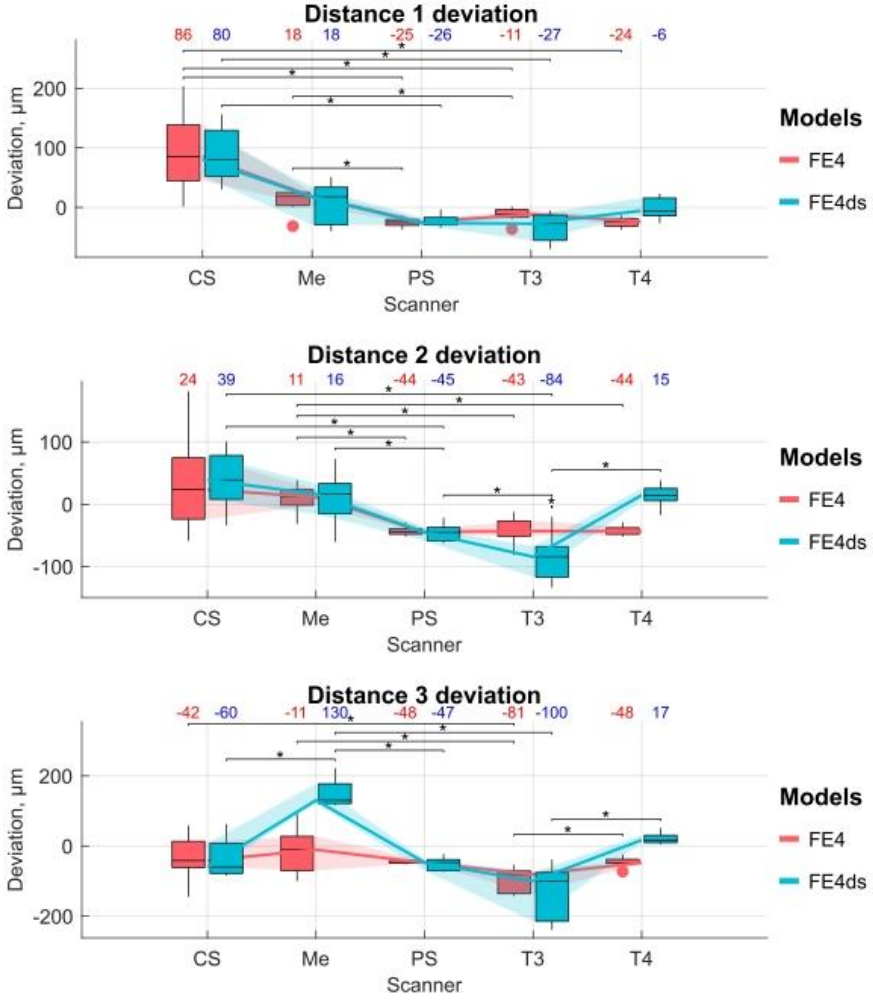

Figure 22. Trueness comparison of distances between scan bodies on fully edentulous models between different IOS. FE4 – fully edentulous model with 4 implants, ds – digital splint. Black lines with a star indicate groups which differed statistically significantly.

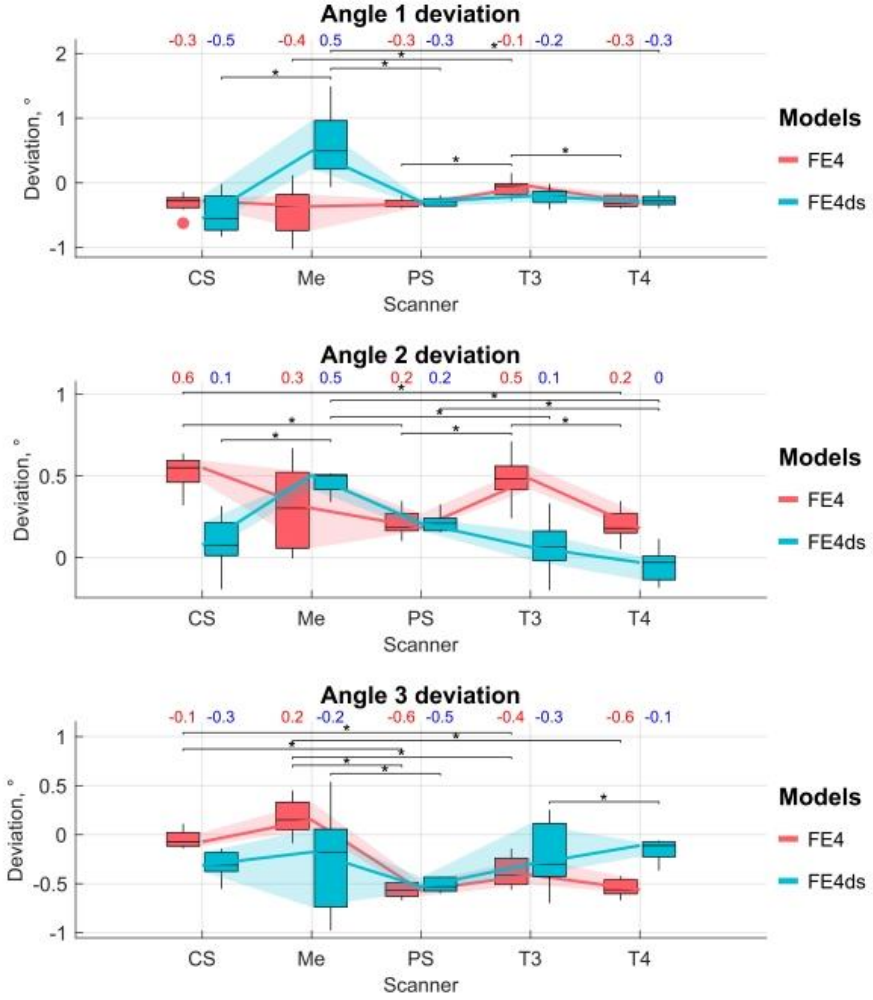

Figure 23. Trueness comparison of angles between scan bodies on fully edentulous models between different IOS. FE4 – fully edentulous model with 4 implants, ds – digital splint. Black lines with a star indicate groups that differed statistically significantly.

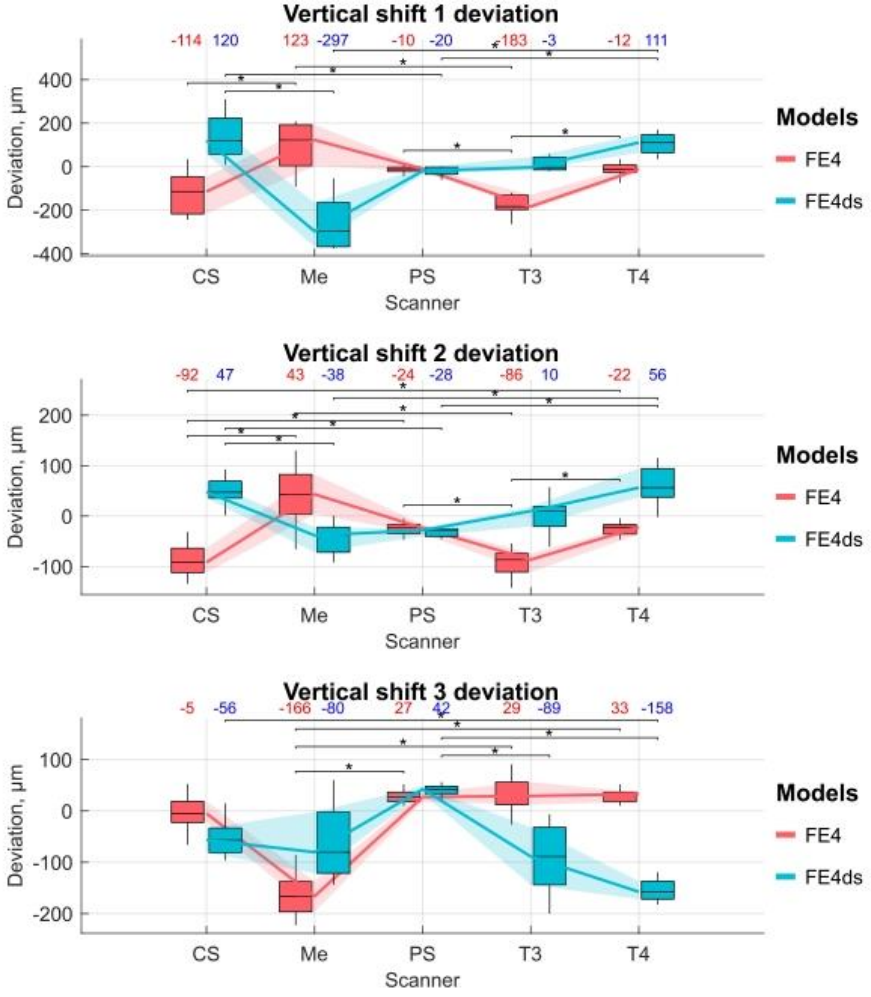

Figure 24. Trueness comparison of vertical shift between scan bodies on fully edentulous models between different IOS. FE4 – fully edentulous model with 4 implants, ds – digital splint. Black lines with a star indicate groups which differed statistically significantly.

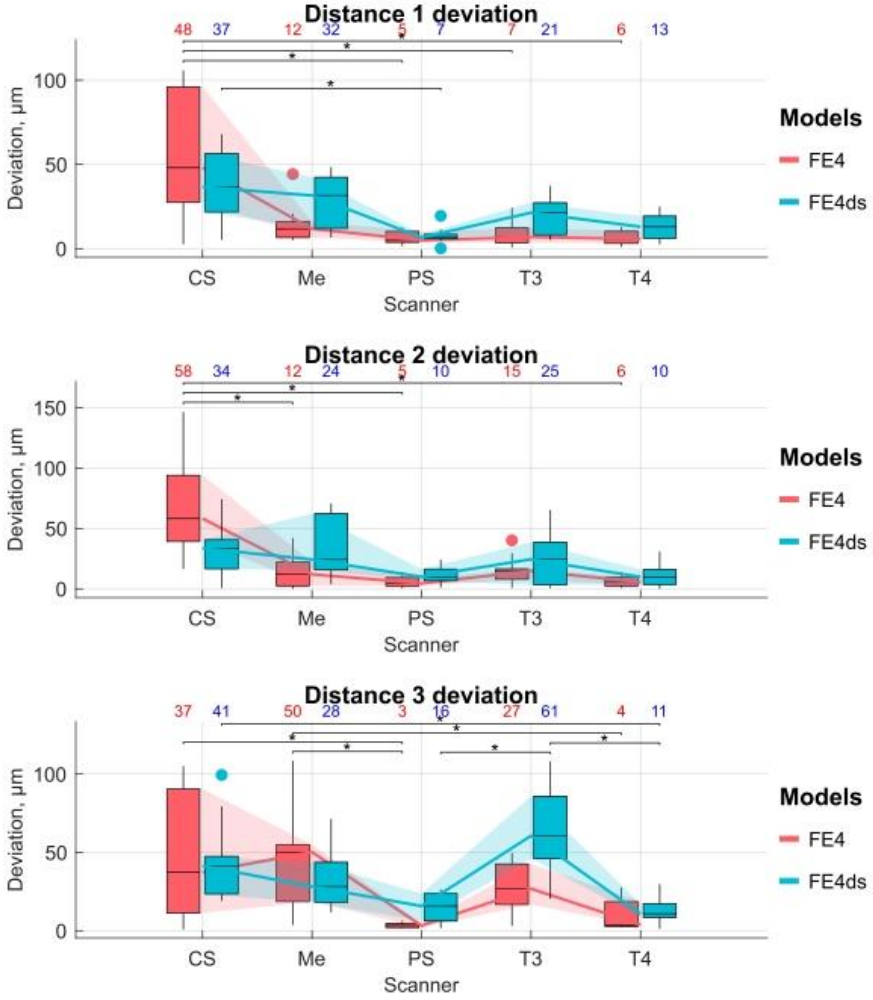

Figure 25. Precision comparison of distances between scan bodies on fully edentulous models between different IOS. FE4 – fully edentulous model with 4 implants, ds – digital splint. Black lines with a star indicate groups that differed statistically significantly.

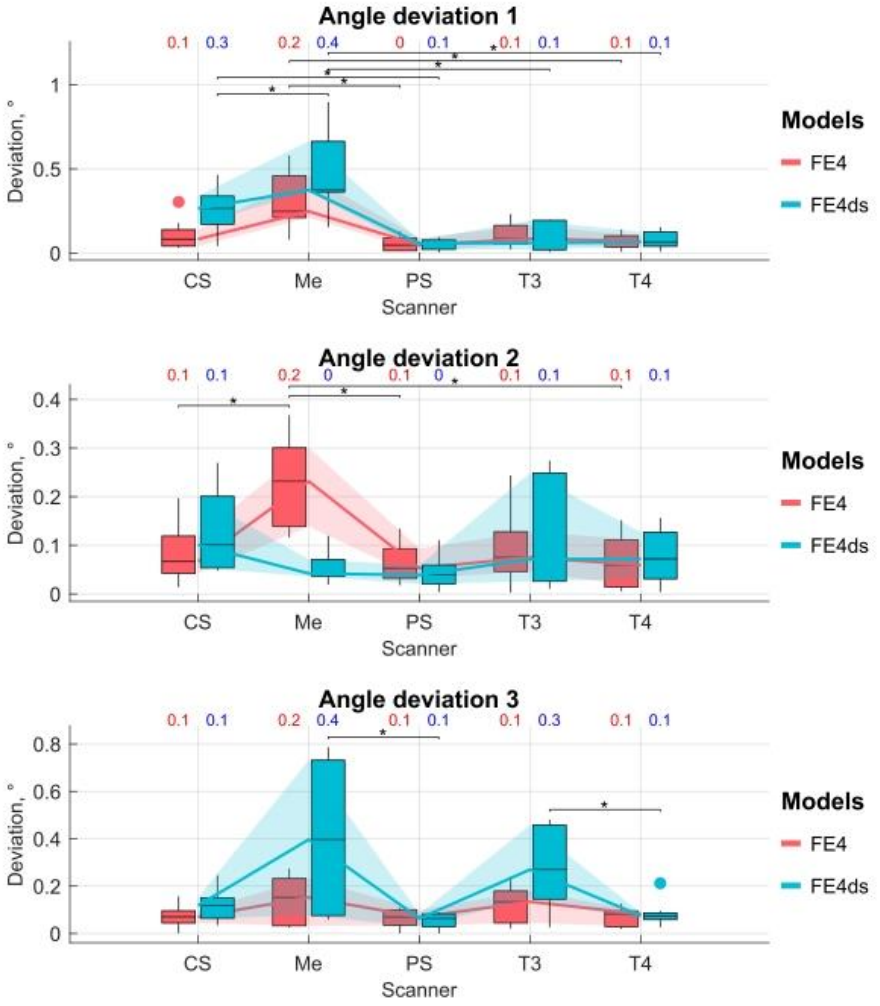

Figure 26. Precision comparison of angles between scan bodies on fully edentulous models between different IOS. FE4 – fully edentulous model with 4 implants, ds – digital splint. Black lines with a star indicate groups that differed statistically significantly.

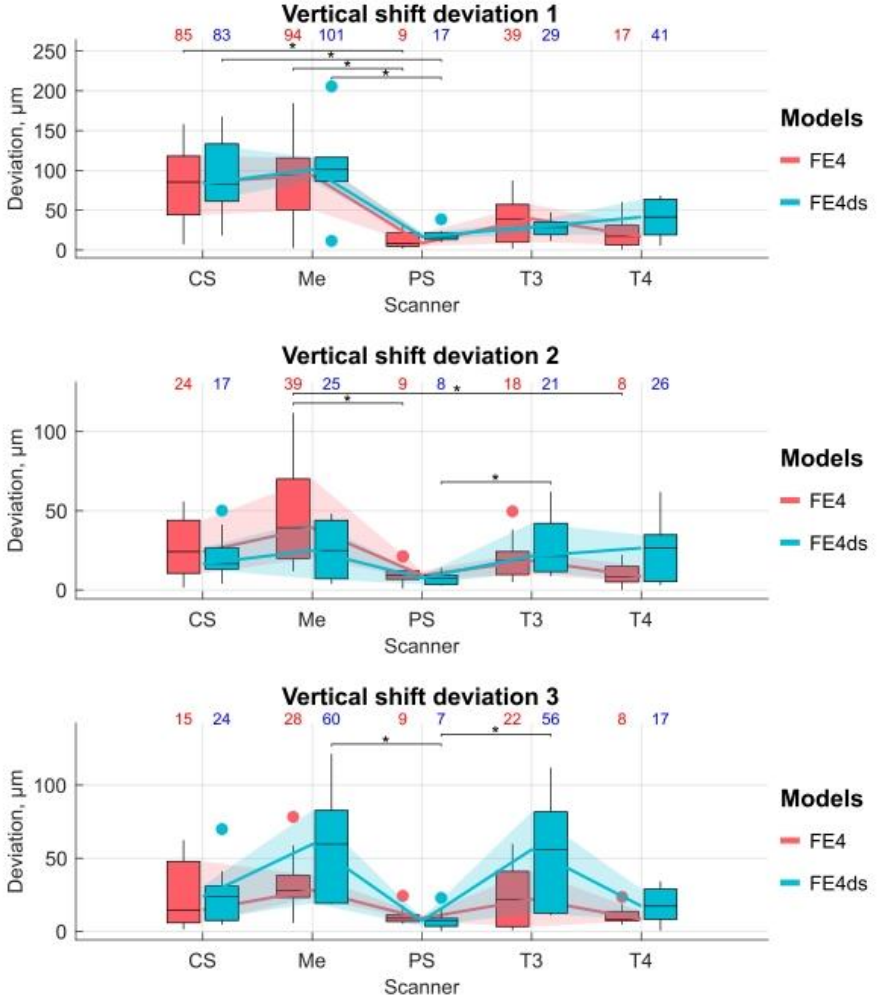

Figure 27. Precision comparison of vertical shift between scan bodies on fully edentulous models between different IOS. FE4 – fully edentulous model with 4 implants, ds – digital splint. Black lines with a star indicate groups that differed statistically significantly.

Table 1. Trueness of partially edentulous models in distance, angle, and vertical shift parameters. SD – standard deviation, CS – Carestream 3600 IOS, Me – Medit i500 IOS, PS – Primescan IOS, T3 – Trios 3 IOS, T4 – Trios 4 IOS. DS – digital splint. The bolded numbers represent statistically significant differences between the scans with and without digital splint.

	Distance	**Angle**	**Vertical shift**
	Mean±SD µm	Mean±SD°	Mean±SD µm
CS	190.76±172.57	-0.03±0.52	-33.68±115.13
CS_ds	117.70±232.28	0.44±0.49	-14.99±45.00
Me	**392.07±314.88**	**0.21±0.13**	**107.16±103.47**
Me_ds	**-12.17±34.55**	**-0.25±0.19**	**-69.12±45.20**
PS	-25.13±20.77	**0.22±0.04**	40.26±12.08
PS_ds	-17.45±16.11	**0.18±0.04**	36.73±10.82
T3	-46.74±15.37	-0.04±0.15	-75.60±50.41
T3_ds	-31.99±18.00	0.02±0.18	-59.48±44.86
T4	-33.36±18.10	-0.11±0.14	-107.97±47.06
T4_ds	-34.39±13.01	-0.15±0.13	-86.91±42.05

Table 2. Trueness of fully edentulous models in distance, angle, and vertical shift parameters. SD – standard deviation, CS – Carestream 3600 IOS, Me – Medit i500 IOS, PS – Primescaner IOS, T3 – Trios 3 IOS, T4 – Trios 4 IOS. DS – digital splint. The bolded numbers represent statistically significant differences between the scans with and without digital splint.

	Distance_1	Distance_2	Distance_3	Angle_1	Angle_2	Angle_3	Vertical shift_1	Vertical shift_2	Vertical shift_3
	Mean±SD µm	Mean±SD µm	Mean±SD µm	Mean±SD °	Mean±SD °	Mean±SD °	Mean±SD µm	Mean±SD µm	Mean±SD µm
CS	97.72±68.74	35.29±84.17	-39.30±64.46	-0.32±0.15	**0.52±0.10**	**-0.05±0.09**	**-124.25±95.87**	**-87.22±33.39**	**-3.58±37.20**
CS_ds	88.45±43.81	40.36±41.22	-37.14±53.84	-0.48±0.29	**0.08±0.16**	**-0.31±0.14**	**141.71±111.73**	**51.44±27.16**	**-55.00±33.17**
Me	12.78±19.59	10.50±19.79	**-17.07±59.74**	**-0.44±0.38**	**0.30±0.25**	**0.18±0.18**	**93.02±111.00**	**46.07±58.91**	**-163.85±40.73**
Me_ds	8.54±35.75	10.51±45.46	**150.82±43.69**	**0.60±0.58**	**0.46±0.07**	**-0.25±0.55**	**-259.15±129.62**	**-43.70±33.40**	**-61.32±76.66**
PS_	-24.93±8.01	-42.84±7.24	-46.05±4.32	-0.32±0.08	0.21±0.08	-0.56±0.08	-11.70±17.69	-25.80±12.63	**27.79±12.66**
PS_ds	-22.85±9.55	-45.72±13.36	-48.81±18.60	-0.28±0.07	0.22±0.05	-0.52±0.07	-21.50±21.33	-31.47±8.64	**40.81±10.85**
T3	**-12.17±11.50**	**-41.49±19.95**	-93.21±33.46	-0.08±0.13	**0.49±0.13**	-0.38±0.15	**-175.86±47.37**	**-92.45±25.78**	**31.20±34.71**
T3_ds	**-32.76±23.38**	**-85.10±34.78**	-130.77±73.46	-0.21±0.14	**0.08±0.17**	-0.22±0.34	**11.37±32.27**	**1.01±35.49**	**-88.33±64.70**
T4	**-24.51±8.39**	**-42.39±7.53**	**-45.02±14.20**	-0.29±0.08	**0.19±0.09**	**-0.54±0.08**	**-14.01±30.65**	**-24.85±13.05**	**28.57±13.20**
T4_ds	**-1.80±16.34**	**13.59±15.72**	**22.15±16.34**	-0.27±0.09	**-0.04±0.10**	**-0.15±0.10**	**103.05±47.33**	**59.80±34.74**	**-153.68±22.73**

Table 3. Significant differences of trueness between five IOS. CS – Carestream 3600 IOS, Me – Medit i500 IOS, PS – Primescaner IOS, T3 – Trios 3 IOS, T4 – Trios 4 IOS.

Type of model	Parameter	Significant differences between IOS
Partially edentulous	Distance	Me differ from PS, T3 and T4 CS differ from T3 and T4
Partially edentulous	Angle	PS differ from T3, T4 Me differ from T4
Partially edentulous	Vertical shift	Me, PS differ from T3, T4
Partially edentulous with digital splint	Distance	No significant differences
Partially edentulous with digital splint	Angle	Cs differ from Me, T4 PS differ from Me, T4
Partially edentulous with digital splint	Vertical shift	PS differ from Me, T3, T4
Fully edentulous	Distance 1	Cs differ from PS, T3, T4 Me differ from PS, T4
Fully edentulous	Distance 2	Me differ from PS, T3, T4
Fully edentulous	Distance 3	Cs, Me, T4 differ from T3
Fully edentulous	Angle 1	T3 differ from PS, T4, Me
Fully edentulous	Angle 2	CS, T3 differ from T4, PS
Fully edentulous	Angle 3	Me differ from PS, T4, T3 CS differ from PS, T4
Fully edentulous	Vertical shift 1	Me differ from T3, CS PS differ from T3 T3 differ from T4
Fully edentulous	Vertical shift 2	Me differ from CS, T3 T4 differ from CS, T3 PS differ from CS, T3
Fully edentulous	Vertical shift 3	T4 differ from Me PS differ from Me T3 differ from Me
Fully edentulous with digital splint	Distance 1	Cs differ from PS, T3
Fully edentulous with digital splint	Distance 2	CS differ from PS, T3 T3 differ from T4 Me differ from T3
Fully edentulous with digital splint	Distance 3	Me differ from CS, T3, PS T3 differ from T4
Fully edentulous with digital splint	Angle 1	Me differ from CS, PS, T4

Fully edentulous with digital splint	Angle 2	Me differ from T4, T3, CS PS differ from T4
Fully edentulous with digital splint	Angle 3	Me differ from PS T3 differ from T4
Fully edentulous with digital splint	Vertical shift 1	CS differ from Me, PS T4 differ from Me, PS
Fully edentulous with digital splint	Vertical shift 2	T4 differ from Me, PS CS differ from Me, PS
Fully edentulous with digital splint	Vertical shift 3	PS differ from T3, T4 CS differ from T4

Table 4. Precision of partially edentulous models in distance, angle, and vertical shift parameters. SD – standard deviation, CS – Carestream 3600 IOS, Me – Medit i500 IOS, PS – Primescaner IOS, T3 – Trios 3 IOS, T4 – Trios 4 IOS. DS – digital splint. The bolded numbers represent statistically significant differences between the scans with and without digital splint.

	Distance	**Angle**	**Vertical shift**
	Mean±SD	Mean±SD	Mean±SD
CS	143.39±83.28	0.41±0.28	**90.62±63.37**
CS_ds	200.48±96.42	0.35±0.33	**37.06±21.33**
Me	**238.48±189.63**	0.10±0.08	**81.76±57.25**
Me_ds	**26.49±20.34**	0.14±0.11	**35.53±24.95**
PS	17.49±9.57	0.03±0.03	9.04±7.43
PS_ds	12.88±8.66	0.03±0.02	8.30±6.37
T3	12.82±7.18	0.13±0.07	37.69±31.03
T3_ds	15.47±7.63	0.14±0.10	36.59±22.50
T4	15.33±8.14	0.10±0.09	39.71±21.50
T4_ds	10.96±5.84	0.10±0.07	32.35±24.61

Table 5. Precision of fully edentulous models in distance, angle, and vertical shift parameters. SD – standard deviation, CS – Carestream 3600 IOS, Me – Medit i500 IOS, PS – Primescaner IOS, T3 – Trios 3 IOS, T4 – Trios 4 IOS. DS – digital splint. The bolded numbers represent statistically significant differences between the scans with and without digital splint.

	Distance_1	Distance_2	Distance_3	Angle_1	Angle_2	Angle_3	Vertical shift_1	Vertical shift_2	Vertical shift_3
	Mean±SD	Mean±SD	Mean±SD	Mean±SD	Mean±SD	Mean±SD	Mean±SD	Mean±SD	Mean±SD
CS	55.57±35.97	**68.56±43.15**	46.80±41.49	**0.11±0.09**	0.08±0.06	0.07±0.05	78.64±48.15	26.38±18.48	26.94±23.81
CS_ds	36.99±19.98	**32.09±23.55**	44.68±26.07	**0.25±0.12**	0.13±0.09	0.11±0.06	94.45±50.70	21.34±15.01	25.34±19.66
Me	14.44±12.21	13.73±13.50	48.31±31.23	0.31±0.17	**0.22±0.09**	**0.14±0.10**	88.78±59.69	46.82±32.15	32.69±21.71
Me_ds	28.73±16.97	33.53±26.79	33.26±22.93	0.47±0.26	**0.06±0.04**	**0.41±0.32**	103.72±62.39	25.44±18.41	60.18±39.11
PS	6.47±4.20	5.49±4.35	3.63±1.80	0.06±0.04	0.06±0.04	0.06±0.04	13.06±10.99	10.22±6.60	10.56±6.04
PS_ds	7.71±5.00	10.75±7.08	15.27±9.32	0.05±0.03	0.04±0.03	0.06±0.03	18.68±8.20	7.37±3.79	8.08±6.73
T3	**8.41±7.25**	15.14±11.97	**27.81±16.13**	0.11±0.07	0.10±0.08	**0.12±0.07**	35.35±28.95	20.46±14.13	25.66±21.76
T3_ds	**19.53±11.08**	25.36±22.25	**64.73±27.22**	0.10±0.09	0.12±0.11	**0.28±0.16**	28.17±11.60	27.81±19.74	51.55±35.12
T4	**6.73±4.40**	5.81±4.34	9.89±9.58	0.07±0.04	0.07±0.05	0.07±0.04	22.06±19.96	**10.12±7.42**	10.92±6.34
T4_ds	**13.54±7.96**	11.61±9.87	12.99±8.92	0.08±0.05	0.08±0.05	0.08±0.05	38.96±23.55	**26.01±21.34**	18.18±12.21

Table 6. Significant differences in precision between five IOS. CS – Carestream 3600 IOS, Me – Medit i500 IOS, PS – Primescaner IOS, T3 – Trios 3 IOS, T4 – Trios 4 IOS.

Type of model	Parameter	Significant differences between IOS
Partially edentulous	Distance	Cs and Me differ from PS, T3 and T4
Partially edentulous	Angle	Cs differ from PS
Partially edentulous	Vertical shift	Cs, Me differ from PS
Partially edentulous with digital splint	Distance	Cs differ from Me, PS, T3, and T4
Partially edentulous with digital splint	Angle	Cs, Me differ from PS T3 differ from T4
Partially edentulous with digital splint	Vertical shift	Cs, Me, T3 differ from PS
Fully edentulous	Distance 1	Cs differ from PS, T3, T4
Fully edentulous	Distance 2	Cs differ from Me, PS, T4
Fully edentulous	Distance 3	Me differ from PS, T4 CS differ from PS
Fully edentulous	Angle 1	Me differ from PS, T4
Fully edentulous	Angle 2	Me differ from PS, T4, CS
Fully edentulous	Angle 3	No significant differences
Fully edentulous	Vertical shift 1	Me, CS differ from PS
Fully edentulous	Vertical shift 2	Me differ from PS, T4
Fully edentulous	Vertical shift 3	No significant differences
Fully edentulous with digital splint	Distance 1	Cs differs from PS
Fully edentulous with digital splint	Distance 2	No significant differences
Fully edentulous with digital splint	Distance 3	T3 differs from PS, T4 CS differ from T4
Fully edentulous with digital splint	Angle 1	Me differ from PS, T3, T4 CS differ from PS
Fully edentulous with digital splint	Angle 2	No significant differences
Fully edentulous with digital splint	Angle 3	Me differ from PS T3 differ from T4
Fully edentulous with digital splint	Vertical shift 1	Me, CS differ from PS
Fully edentulous with digital splint	Vertical shift 2	T3 differ from PS
Fully edentulous with digital splint	Vertical shift 3	Me, T3 differ from PS

4.2. *In vivo* accuracy evaluation

4.2.1. Accuracy evaluation of dental implant impressions

4.2.1.1. Comparison of conventional dental implant impression with Trios IOS digital dental implant impression

Statistically significant differences were found between digital and conventional impression measurements: inter-implant distance, angulation variables, and surface mismatch of scan bodies ($p<0.05$). Surface mismatch between mesially and distally located scan bodies were not statistically significantly different in the Trios group or the D800 group (Table 7).

Table 7. Differences between digital and conventional workflow measurements in distance between scan bodies, angulation, rotation, vertical shift, and surface mismatch near mesial and distal implants.

Variable	Conventional impression		Digital impression		Mean of differences (SD)	*p*-value	Wilcoxon signed-rank test power
	Mean (SD)	Median	Mean (SD)	Median			
Distance between scan bodies	14.28 (6.75) mm	14.99	14.33 (6.77) mm	15.00	73.7 (75) µm	0.00	6 %
Angulation	14.17 (9.54)°	10.16	14.38 (9.8)°	10.74	0.42 (0.3)°	0.00	10 %
Rotation	33.58 (23.19)°	28.40	33.27 (22.61)°	29.07	0.72 (0.55)°	0.098	8 %
Vertical shift	1.58 (2.15) mm	0.85	1.57 °(2.2) mm	0.83	98.9 (96.33) µm	0.63	6 %
Mismatch M implant	14.27 (21.5) µm	14.32	31.8 (25.6) µm	19.68	-	0.00	100 %
Mismatch D implant	14.65 (19.7) µm	14.32	30.68 (28.7) µm	22.67	-	0.00	100 %

Measurements of surface mismatch show that the D800 scanner is twice as accurate as IOS in this regard. Surface mismatch measurements for the Trios and D800 were 31.8±25.6 µm and 14.27±21.5 µm for mesial implant scan

bodies, and 30.68±28.7 μm and 14.65±19.7 μm for distal implant scan bodies (Table 7).

Statistically significant Spearman correlation coefficients showed that angulation and distance between scan bodies positively correlated to measured differences in distance between scanbodies, angulation, and vertical shift between both groups. The values of coefficients varied from 0.19 to 0.53, showing weak to medium correlation between variables (Table 8). According to linear regression results, all these associations were statistically significant (p<0.05) except for the association of the actual mean of distance between scan bodies with differences in the angulation between scan bodies.

Table 8. Results of the linear regression model (NS – not significant correlation). The results indicate, how inter-implant distance, angulation, and vertical shift correlate with actual means of inter-implant distance and angulation.

Dependent Variables (Differences between DII and CII)	Independent variables					
	Actual mean of distance between scan bodies			Actual mean of angulation		
	Spearmen coefficient	Linear regression model		Spearmen coefficient	Linear regression model	
		p-value	Model power		*p*-value	Model power
Distance between scan bodies	0.19	0.35	27 %	0.3	0.02	91 %
Angulation	0.08 (NS)	0.02	93 %	0.53	0.0	100 %
Vertical shift	0.53	0.0	99.9 %	0.52	0.0	100 %

The clinically acceptable threshold of linear and angular misfits is not well-defined in the literature yet. In order to have tentative threshold values, simplified calculations from the clinical study for linear (100 μm) and angular (0.4°) measurements by Andriessen et al. were taken as a reference.[59] The means and standard deviations of all measured parameters in all cases are presented in Figures 28–31.

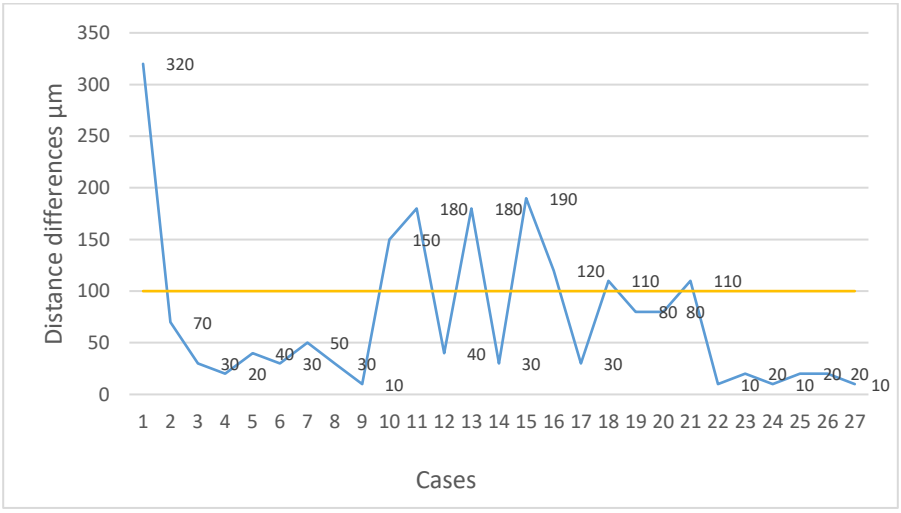

Figure 28. Differences of distance between scan bodies measurements of conventional and digital impression measurements (Mean 73.7±75 µm). The yellow line represents the tentative clinical threshold of 100-µm misfit.

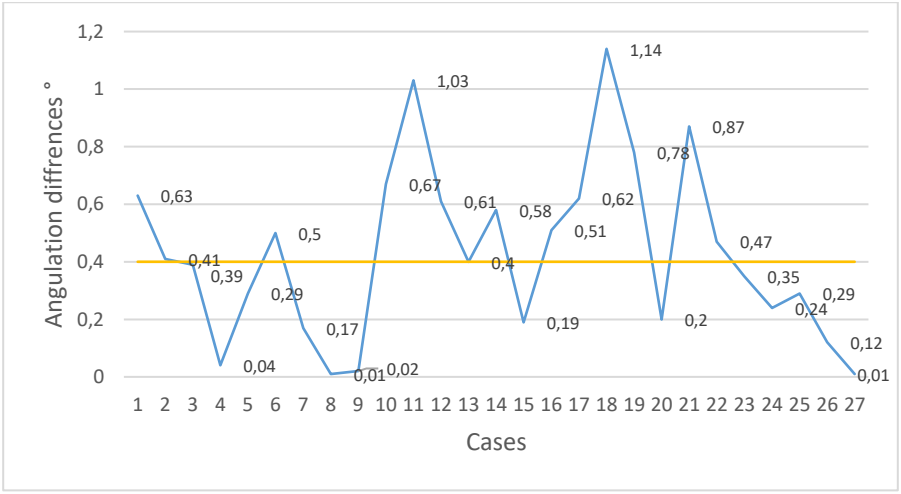

Figure 29. Differences in angulation between digital and conventional impression measurements (Mean 0.42±0.3°). The yellow line represents the tentative clinical threshold of angular misfit, 0.4°.

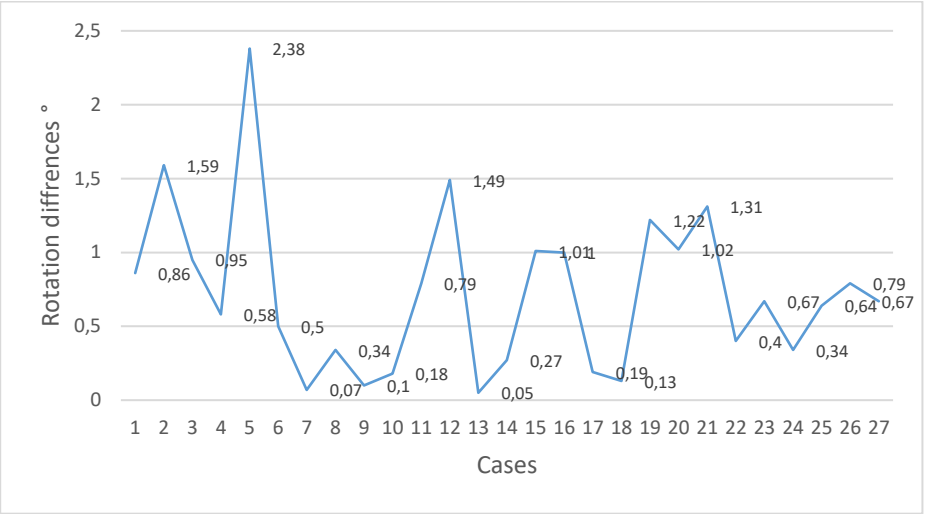

Figure 30. Differences in rotation between digital and conventional impression measurements (Mean 0.72±0.55°).

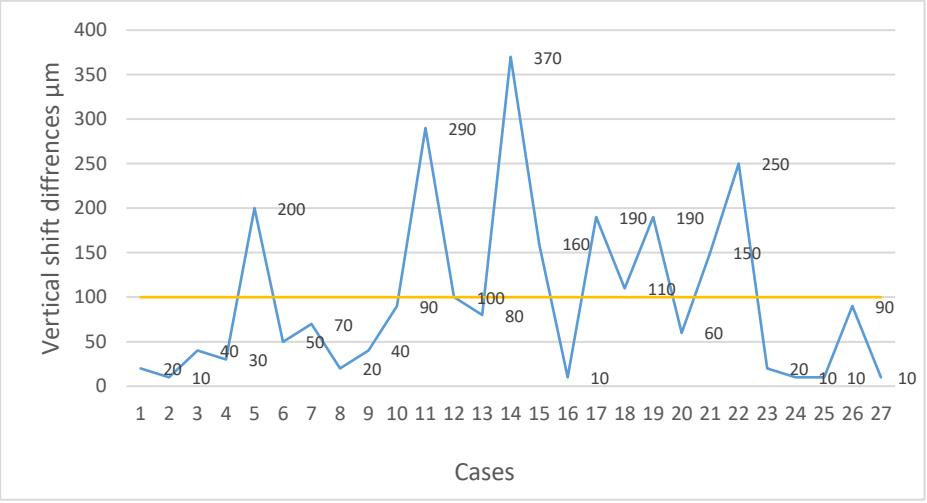

Figure 31. Differences in vertical shift between the D800 and Trios measurements (Mean 98.9±96.33 µm). The yellow line represents the tentative clinical threshold of 100 µm misfit.

4.2.2.2. Comparison of conventional dental implant impression with Trios 3 IOS digital dental implant impression

Mean differences between CII and DII groups for the distance between the scan bodies were found to be 70.8 ± 59 µm. Mean of differences for angulation were 0.37 ± 0.3°; for the rotation – 2.0 ± 1.37°, and for the vertical shift – 82.2 ± 61.7 µm. Except for the angulation variable, differences were found as

statistically significant between all digital and conventional impression measurements (Table 9).

Table 9. Differences between digital (and conventional workflow measurements in distance between scan bodies, angulation, rotation, vertical shift and surface mismatch near mesial and distal implants.

Variable	Conventional impression		Digital impression		Mean of differences (SD)	*p-value*	Wilcoxon signed-rank test power
	Mean (SD)	Median	Mean (SD)	Median			
Distance between scan bodies	15.80 (5.65) mm	16.19	15.83 (5.67) mm	16.16	70.8 (59) µm	<0.001	5 %
Angulation	9.99 (5.57) °	9.37	9.97 (5.65) °	9.66	0.37 (0.3) °	0.79	5 %
Rotation	35.65 (23.45) °	34.48	35.05 (23.42) °	34.8	2.0 (1.37) °	0.013	6.4 %
Vertical shift	1.54 (1.91) mm	1.2	1.57 (1.92) mm	1.1	82.2 (61.7) µm	0.001	5.8 %
Mismatch M implant	14.19 (3.22) µm	14.28	34.14 (36.69) µm	29.28	-	<0.001	98 %
Mismatch D implant	14.19 (2.29) µm	14.72	34.24 (14.64) µm	33.52	-	<0.001	100 %

Surface mismatch measurements comparing DII and CII were 34.14 ± 36.69 µm and 14.19 ± 3.22 µm for the mesial implant scan body and 34.24 ± 14.64 µm and 14.19 ± 2.29 µm for the distal implant scan body. Surface mismatch between mesially and distally located scan bodies in the DII group was statistically significantly different – contrary to the CII group, where no differences were detected. Distance between the scan bodies did not significantly correlate with any measured differences in distance between scan bodies, angulation, or vertical shift according to Spearman correlation coefficients. Angulation between implants statistically significantly correlated with the detected distance between scan bodies, angulation, and vertical shift differences, but this correlation was weak (Table 10). According to linear regression results, the association of inter-implant angulation with measured differences between DII and CII was statistically significant in all variables ($p<0.05$).

Means and standard deviations of all measured parameters are presented in figures 32–35. Differences of 100 µm for linear and 0.4 ° for angular variables were taken as tentative threshold values.[59]

Table 10. Results of the linear regression model (NS – not significant correlation). The results indicate, how the distance between scan bodies, angulation, and vertical shift correlate with actual means of distance between scan bodies and inter-implant angulation.

Dependent variables (Differences between DII and CII)	Independent variables					
	Actual mean of distance between scan bodies			Actual mean of inter-implant angulation		
	Spearmen coefficient	Linear regression model		Spearmen coefficient	Linear regression model	
		p-value	Model power		*p-value*	Model power
Distance between scan bodies	-0.036 (NS)	0.078	19.8 %	0.24	<0.001	64 %
Angulation	0.13 (NS)	0.08	19.6 %	0.35	0.013	35.1 %
Vertical shift	0.11 (NS)	0.219	8.3 %	0.36	0.0006	33.1 %

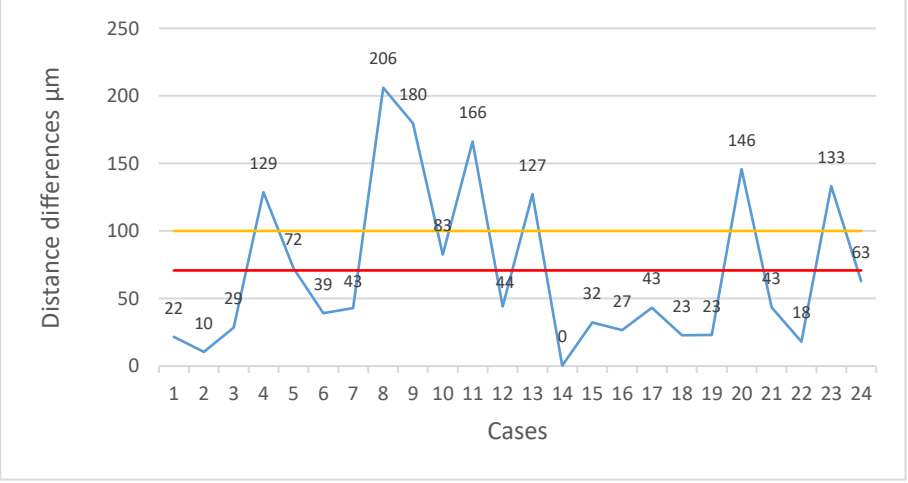

Figure 32. Differences of distance between scan bodies measurements of conventional and digital impressions (mean 70.8 ± 59 µm). The yellow line represents the tentative clinical threshold of 100 µm misfit, and the red line represents the mean of the differences measured.

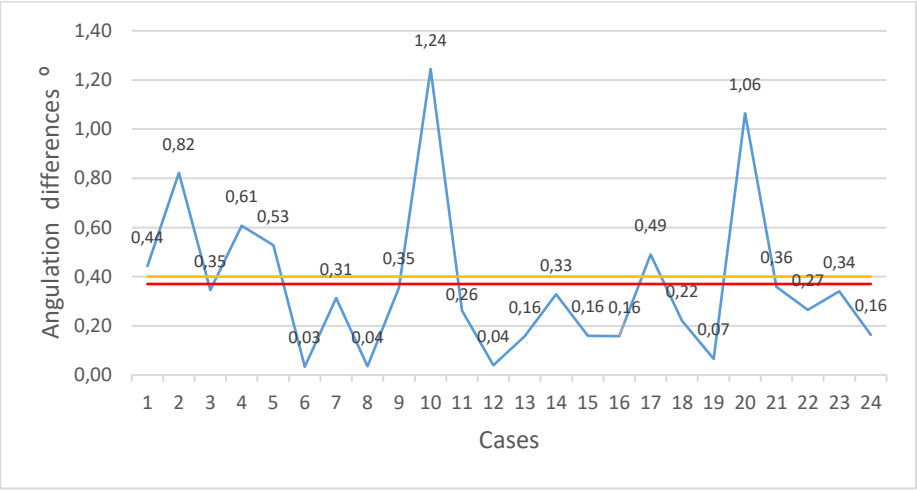

Figure 33. Differences in angulation between the measurements of digital and conventional impressions (mean 0.37 ± 0.3 º). The yellow line represents the tentative clinical threshold of angular misfit 0.4 °, and the red line represents the mean of differences measured.

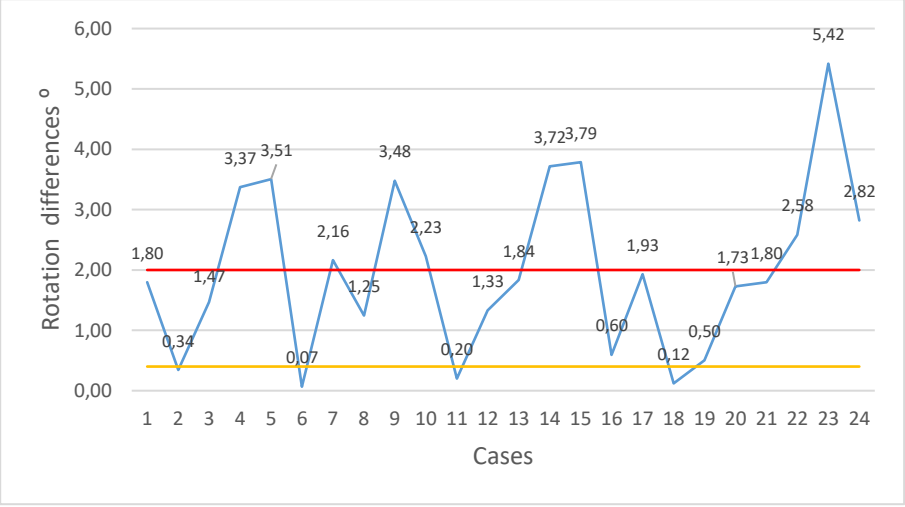

Figure 34. Differences in rotation between the measurements of digital and conventional impressions (mean 2.0 ± 1.37 º). The yellow line represents the tentative clinical threshold of angular misfit 0.4º, and the red line represents the mean of the differences measured.

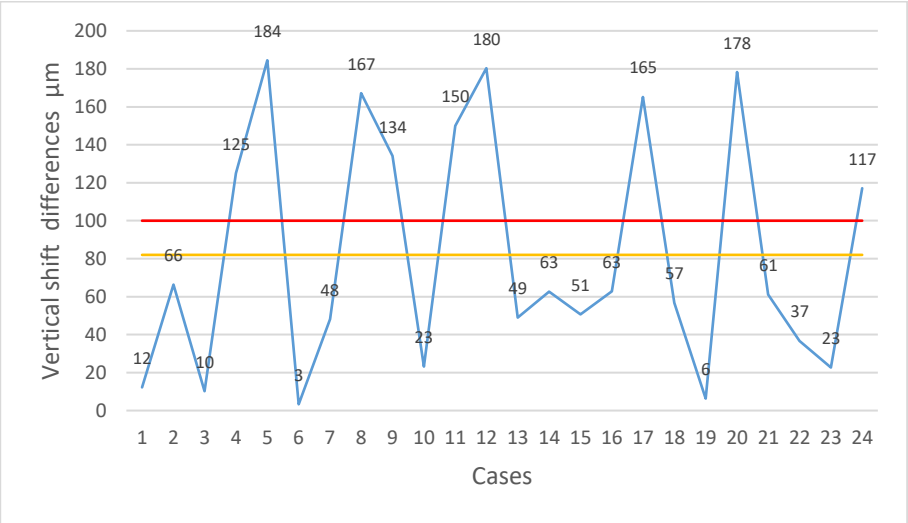

Figure 35. Differences in vertical shift between digital and conventional groups (mean 82.2 ± 61.7 µm). The red line represents the tentative clinical threshold of 100 µm misfit, and the grey line represents the mean of the differences measured.

4.2.2. Accuracy evaluation of dental implant restorations

4.2.2.3. Fit evaluation of dental implant restorations

According to Wilcoxon signed-rank test results, D_{misfit} was higher in group D than in C ($p < 0.05$) (Table 11). D_{misfit} measurements between groups C and D were statistically significantly different for all surfaces ($p < 0.05$) (Table 12). The cement gap (D_{cement}) between the zirconia restoration and the edge of the Ti base was found to be higher in group C. According to the Friedman rank-sum test, D_{cement} measurements of different surfaces were not significantly different ($p = 0.785$) (Table 13). Comparisons of ΔD_{misfit} values between the specimens from the maxilla and mandible showed that the differences were not statistically significant; however, ($p = 0.575$). Also, ΔD_{misfit} was not significantly different between two-, three- and four-unit cases ($p = 0.47$). ΔD_{cement} was however statistically significantly different between specimens from the maxilla and mandible ($p=0.0005$). This was not the case when restorations of different lengths were compared ($p = 0.052$) (Table 14).

Table 11. Medians and interquartile ranges [IQR] of D_{misfit} and D_{cement} in two-implant-supported zirconia FPDs fabricated through the digital (group D) and conventional (group C) workflows.

	C group	D group	Wilcoxon signed-rank test *p-value*
D_{misfit} [IQR] (μm)	59.00 [60.00]	78.00 [88.00]	0.00
D_{cement} [IQR] (μm)	38.90 [23.20]	34.90 [25.70]	0.00

Table 12. Comparison of D_{misfit} measurements in MB, ML, DB, and DL locations in digital (D) and conventional (C) groups.

Measurement location	D_{misfit}		Wilcoxon signed-rank test p-value	Friedman rank sum test p-value
	C group	D group		
	Median [IQR] (μm)	Median [IQR] (μm)		
MB	51.50 [55.25]	65.00 [67.50]	0.00	0.01
ML	62.00 [58.50]	96.00 [93.00]	0.00	
DB	67.00 [61.75]	78.00 [73.75]	0.00	
DL	68.00 [72.00]	71.00 [101.25]	0.01	

Table 13. Comparison of D_{cement} measurements in MB, ML, DB, and DL locations in digital (D) and conventional (C) groups.

Measurement location	D_{cement}		Wilcoxon signed-rank test p-value	Friedman rank sum test p-value
	C group	D group		
	Median [IQR] (μm)	Median [IQR] (μm)		
MB	36.40 [20.70]	40.05 [29.48]	0.51	0.79
ML	40.00 [23.50]	35.30 [26.80]	0.00	
DB	41.85 [21.50]	35.8 [23.68]	0.00	
DL	35.65 [26.28]	31.75 [22.50]	0.00	

A weak negative correlation between D_{misfit} and inter-implant distance was found in group C (Table 15). D_{cement} in both groups was not significantly correlating with inter-implant distance or inter-implant angulation. The

medians, interquartile ranges (IQR), minimum and maximum measurement values in both groups are presented in Figures 36 and 37.

Table 14. Comparison of ΔD_{misfit} and ΔD_{cement} between different subgroups: maxilla vs. mandible and two-unit vs. three-unit vs. four-unit FPDs.

Subgroups	ΔD_{misfit}	Wilcoxon signed-rank test *p-value*	Friedman rank sum test p-value	ΔD_{cement}	Wilcoxon signed-rank test *p-value*	Friedman rank sum test *p-value*
	Median [IQR] (μm)			Median [IQR] (μm)		
Maxilla	44.00 [64.00]	0.58	-	18.00 [17.60]	0.00	-
Mandible	42.50 [66.00]			13.70 [19.60]		
Two-unit	36.50 [47.25]	-	0.47	14.70 [21.09]	-	0.05
Three-unit	53.00 [72.00]			17.60 [17.70]		
Four-unit	42.50 [81.00]			14.65 [19.27]		

Table 15. Spearmen correlation coefficients between D_{misfit} (C), D_{misfit} (D), ΔD_{misfit}, and ΔD_{cement} and average measurements of inter-implant distance and angulation.

Variable	Inter-implant distance	Inter-implant angulation
D_{misfit} (C)	-0.199	-0.04 (NS)
D_{misfit} (D)	-0.094 (NS)	0.05 (NS)
D_{cement} (C)	0.12 (NS)	0.09 (NS)
D_{cement} (D)	0.11 (NS)	0.22 (NS)
ΔD_{misfit}	-0.034 (NS)	0.15 (NS)
ΔD_{cement}	-0.0136 (NS)	-0.036 (NS)

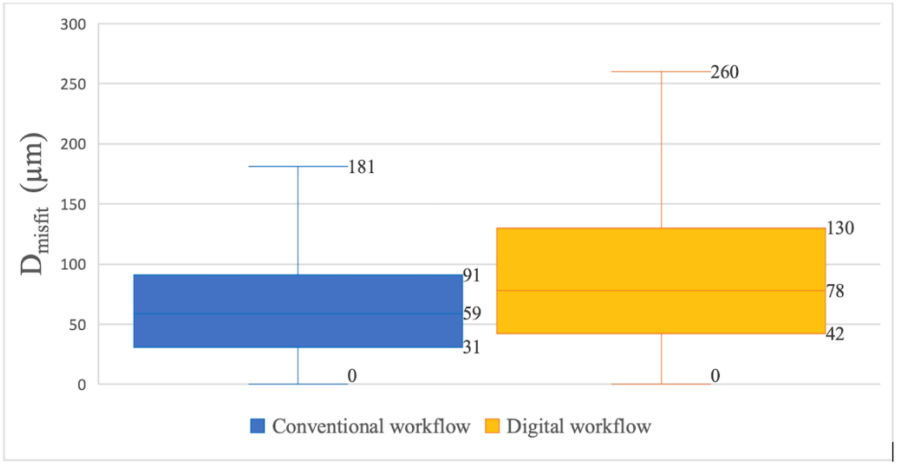

Figure 36. Medians, IQR, minimum and maximum values of D_{misfit} measurements in groups of conventional and digital workflows.

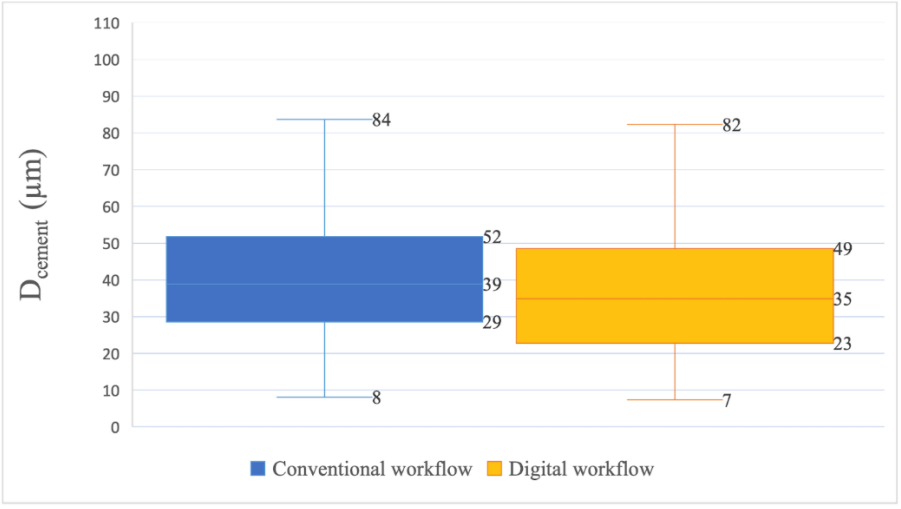

Figure 37. Medians, IQR, minimum and maximum values of D_{cement} measurements in groups of conventional and digital workflows.

4.2.2.4. Passive fit evaluation of dental implant restorations

Based on the intraoral evaluation, all restorations were considered clinically acceptable. Six restorations of group C and five restorations of group D were considered to have less than optimal passive fit. Evaluation on the master cast revealed that two restorations of group C and four restorations of group D were rated as having suboptimal fit (Table 16). Rotation angle

measurements obtained in passive and non-passive situations are presented in Table 17.

Table 16. Number of restorations that were rated as not having optimal passive fit during the evaluation intraorally and on the master and control cast.

Intraorally		Master cast		Control cast	
Group C	Group D	Group C	Group D	Group C	Group D
6	5	2	4	2	1

Table 17. Rotation angles (from 5 Ncm to 35 Ncm) of prosthetic screws in passive (P) and non-passive (NP) situations.

Intraorally				Master cast				Control cast			
Group C		Group D		Group C		Group D		Group C		Group D	
P	NP	P	NP	P	NP	P	NP	P	NP	P	NP
88± 17°	102 ±25°	84± 15°	95± 15°	84± 13°	86± 20°	83± 15°	85± 17°	87± 14°	90± 16°	85± 13°	87± 14°

Graphical representation and comparisons of screw resistance (SR) values in different groups are represented in Figure 38. SR of C restorations measured intraorally (16.25 ± 15.52°) were higher than of D restorations (13.85 ± 10.78°) (Table 18), but the difference was not statistically significant (p=0.557). While measuring SR on the master cast, group C SR (6.04 ± 7.43°) had lower values than group D (13.12 ± 13.86°), and the difference between them was statistically significant (p=0.0039). Overall SR measurements intraorally (13.22 ±13.06°) were found to be slightly higher than SR on the master cast (12.08 ± 11.79°), but the difference was not statistically significant (p=0.81).

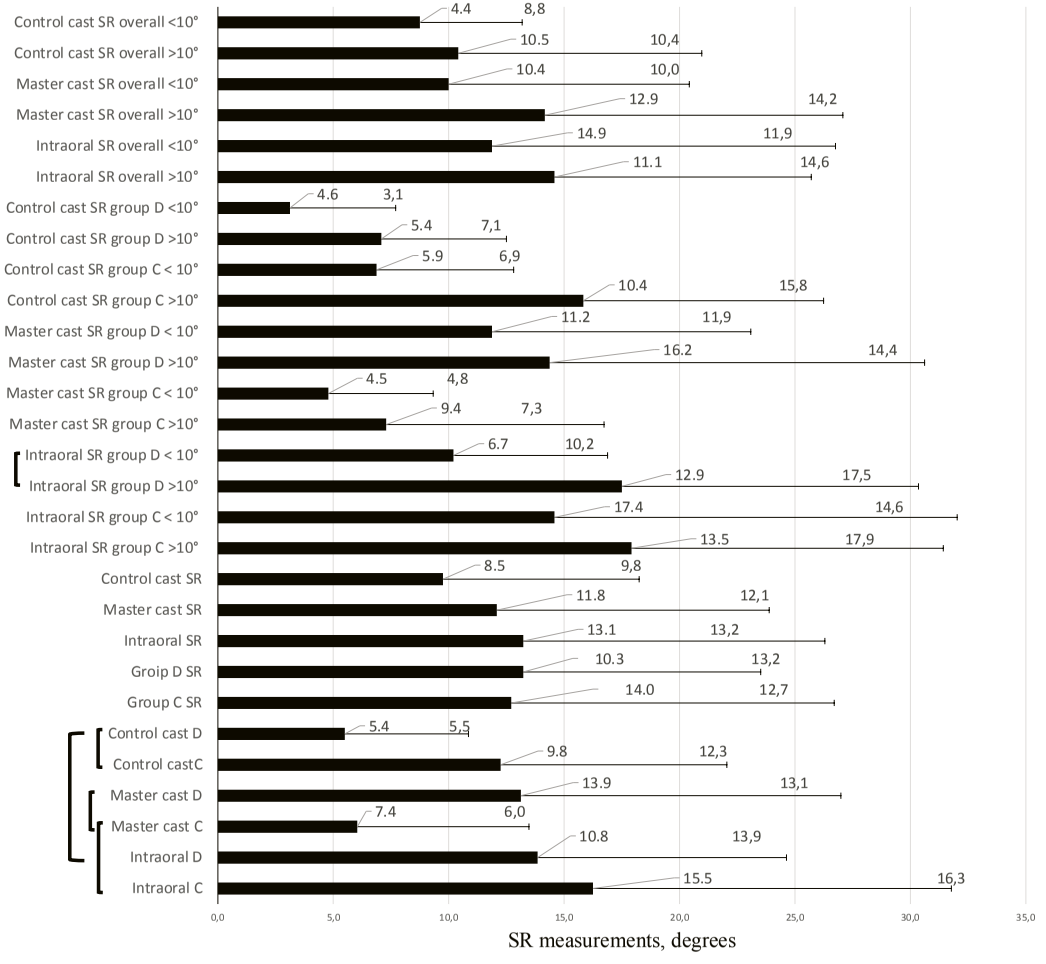

Figure 38. Screw resistance (SR) measurements of different groups of the specimens. Black arches indicate statistically significant differences.

Table 18. Screw resistance (SR) measurements of different groups of specimens.

Variable	Mean ± SD	Median (IQR)°
Group C SR intraoral	16.25 ± 15.52°	10 (10)°
Group D SR intraoral	13.85 ± 10.78°	10 (10)°
Group C SR on the master cast	6.04 ± 7.43°	5 (10)°
Group D SR on the master cast	13.12 ± 13.86°	10 (15)°
Group C SR on the control cast	12.5 ± 9.79°	10 (10)°
Group D SR on the control cast	5.5 ± 5.35°	5 (10)°
Group C SR overall	12.7 ± 13.98°	10 (15)°
Group D SR overall	13.22 ± 10.28°	10 (15)°
Intraoral SR overall	13.22 ±13.06°	10 (15)°
Master cast SR overall	12.08 ± 11.79°	10 (15)°
Control cast SR overall	9.75 ± 8.5°	5 (8.75)°

Table 19. Comparison of subgroups with inter-implant angulation higher and lower than 10 degrees.

Comparison groups	Wilcoxon signed-rank test p-value
Intraoral SR group C >10° vs. Intraoral SR group C < 10°	0.227
Intraoral SR group D >10° vs. Intraoral SR group D < 10°	0.037
Master cast SR group C >10° vs. Master cast SR group C < 10°	0.169
Master cast SR group D >10° vs. Master cast SR group D < 10°	0.336
Control cast SR group C >10° vs. Control cast SR group C < 10°	0.156
Control cast SR group D >10° vs. Control cast SR group D < 10°	0.103
Intraoral SR overall >10° vs. Intraoral SR overall < 10°	0.288
Master cast SR overall >10° vs. Master cast SR overall < 10°	0.145
Control cast SR overall >10° vs. Control cast SR overall < 10°	0.73

Table 20. Correlation of SR measurements to inter-implant distance and angulation. NS indicates not significant.

Variables	Inter-implant distance	Inter-implant angulation
Intraoral SR group C	0.1(NS)	0.18 (NS)
Intraoral SR group D	-0.19 (NS)	0.27 (NS)
Master cast SR group C	0.02 (NS)	0.05 (NS)
Master cast SR group D	0.17 (NS)	0.26 (NS)
Control cast SR group C	-0.03 (NS)	0.08 (NS)
Control cast SR group D	-0.15 (NS)	0.12 (NS)
Intraoral SR	-0.085 (NS)	0.22(NS)
Master cast SR	-0.041(NS)	0.31(NS)
Control cast SR	-0.51	-0.2(NS)
Group D SR	-0.14(NS)	0.145(NS)
Group C SR	0.067(NS)	0.21(NS)

Intraoral SR measurements of the group D restorations with inter-implant angle higher than 10° were statistically significantly different from the SR measurements of the ones with an angle smaller than 10° between the implants (p=0.037) (Table 19). Also, no statistically significant associations between measurements of SR and inter-implant distance or angulation were found according to Spearman correlation coefficients (Table 20). The average distance between implants measured 15.8±5.76 mm and the average angle between implants was 9.98±5.7°.

4.3. *In vitro in vivo* accuracy evaluation

Results of distance precision measurements for all three scanning setups and at different distances are shown in Figure 39 (here and thereafter the data are shown as boxplots with median, 25^{th}–75^{th} percentiles and whiskers).[76] The precision of the IOS scanner decreases with increased distance between SB. Also, it can be noted that *in vitro* scanning has better precision than *in vivo* scanning. A statistically significant difference between IOS and MIOS cases is seen only in the case of the largest distance (1-4).

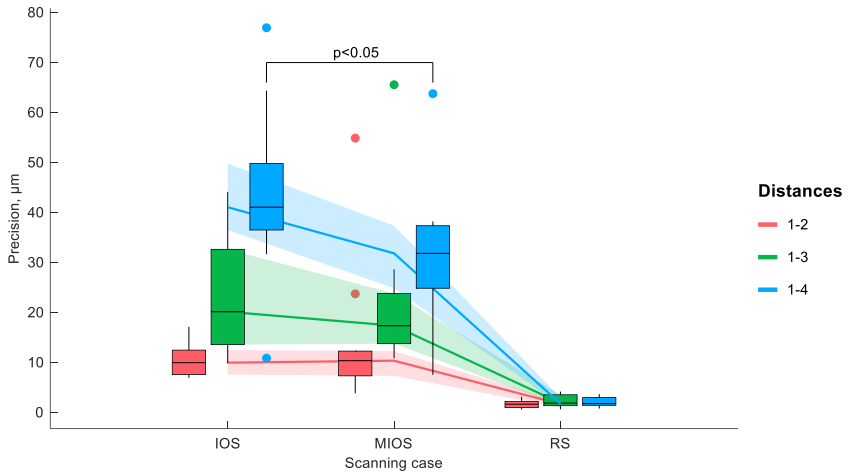

Figure 39. Precisions at each distance and for each scanning case, later measuring the distance between scan bodies. Color areas represent quartiles change, horizontal lines – median change, dots – outliers. IOS and MIOS differ significantly at distance 1-4.

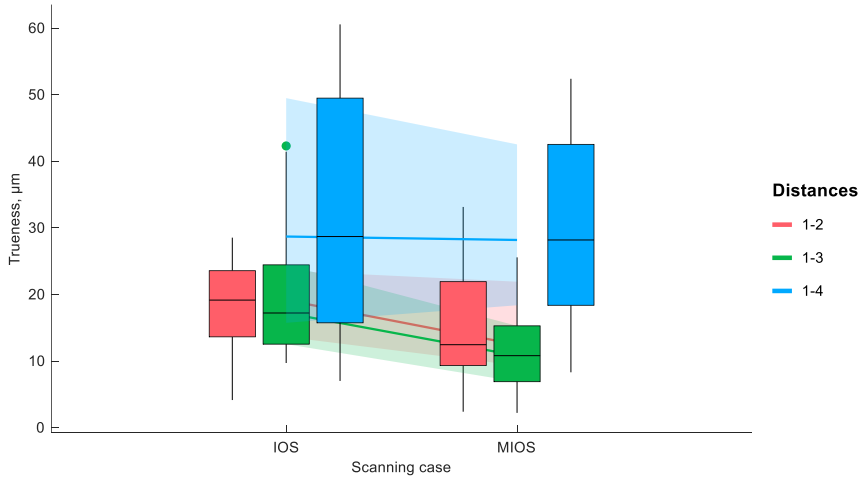

Figure 40. Trueness for each scanning condition measuring distance between scan bodies. Color areas represent quartiles change, horizontal lines – median change, dots – outliers.

Results for *in vivo* and *in vitro* scanning trueness in each distance and at each scanning condition are presented in Figure 40. Results show that trueness is comparable for both intraoral and extraoral scanning. Also, the bigger distances, the bigger deviation were found with intraoral scanning.

Results for accuracy of the distance measurements are summarized in Table 21.

Table 21. Mean with standard deviation precision and trueness of intraoral and extraoral scanning measuring distances between scan bodies

Data	Precision, µm	Trueness, µm
	mean±SD	mean±SD
IOS 1-2	10±3	18±7
MIOS 1-2	15±15	16±10
RS 1-2	2±0.8	----
IOS 1-3	24±13	21±12
MIOS 1-3	23±16	12±7
RS 1-3	2±1	----
IOS 1-4	44±18*	32±19
MIOS 1-4	31±16*	30±14
RS 1-4	2±1	----
IOS	26±19	24±14
MIOS	23±17	19±13
RS	2±1	----
*** indicates statistically significant difference, p<0.05**		

Results of angle deviations between scan bodies obtained with intraoral and extraoral scanning using Trios scanner are presented in figures 41–42. Figure 41 shows the precision of angle measurement in each distance and each scanning condition. Scanning *in vitro* seems to slightly less deviate than scanning *in vivo*. Also, slightly bigger deviations can be noticed with increased distance between SB. No statistically significant differences are observed between IOS and MIOS. Trueness of angulation is presented in figure 42. A statistically significant difference between angulation measurements is seen only at the 1-4 distance between SB. Table 22 summarizes the accuracy measurements of angulation.

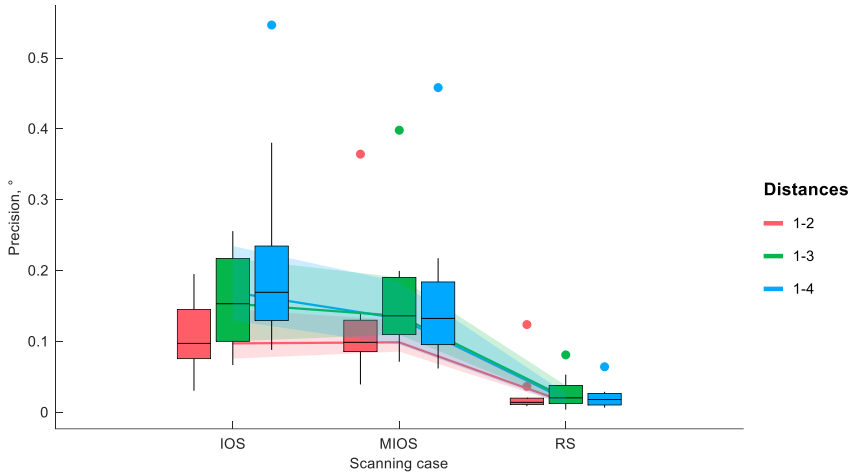

Figure 41. Precisions at each distance and for each scanning case, later measuring the angulation between scan bodies. Color areas represent quartiles change, horizontal lines – median change, dots – outliers.

Table 22. Mean with standard deviation precision and trueness of intraoral and extraoral scanning measuring angulation of scan bodies.

Data	Precision	Trueness
	mean±SD	mean±SD
IOS 1-2	0.11±0.05	0.07±0.05
MIOS 1-2	0.12±0.09	0.09±0.06
RS 1-2	0.02±0.04	----
IOS 1-3	0.16±0.07	0.07±0.05
MIOS 1-3	0.16±0.09	0.09±0.06
RS 1-3	0.03±0.02	----
IOS 1-4	0.22±0.14	0.18±0.10*
MIOS 1-4	0.16±0.11	0.07±0.05*
RS 1-4	0.02±0.02	----
IOS	0.16±0.10	0.11±0.08
MIOS	0.15±0.10	0.08±0.05
RS	0.03±0.03	----
*** indicates statistically significant difference, p<0.05**		

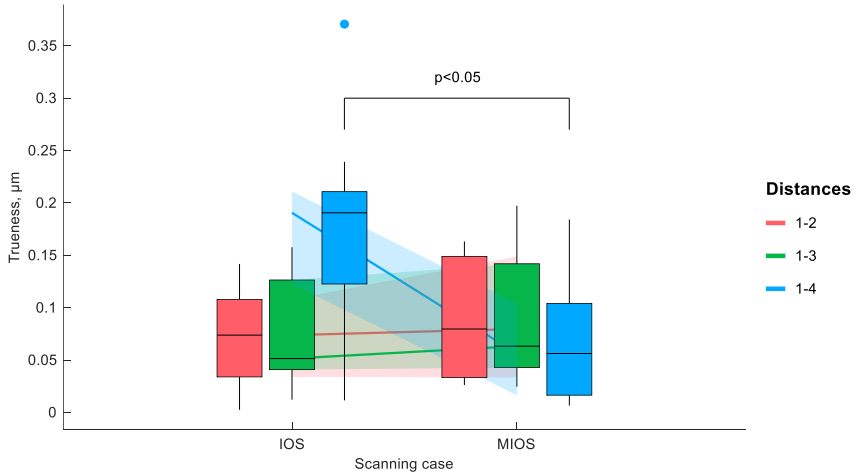

Figure 42. Trueness at each distance and for each scanning condition, later measuring the angulation of scan bodies. Color areas represent quartiles change, horizontal lines – median change, dots – outliers. IOS and MIOS differ significantly at distance 1-4.

Scan surface deviations showing differences of intraoral and extraoral scanning are presented in figures 43 and 44, and summarized in table 23. Precision results show no statistically significant differences between IOS and MIOS scans. As for trueness, a statistically significant difference between IOS and MIOS was found.

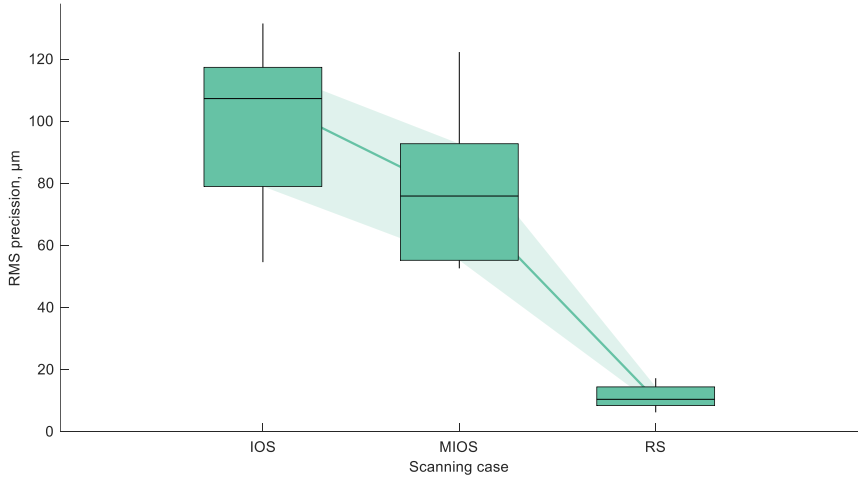

Figure 43 Root mean squared 3D surface deviations for each scanning condition for precision estimation. Color areas represent quartiles change, horizontal lines – median change.

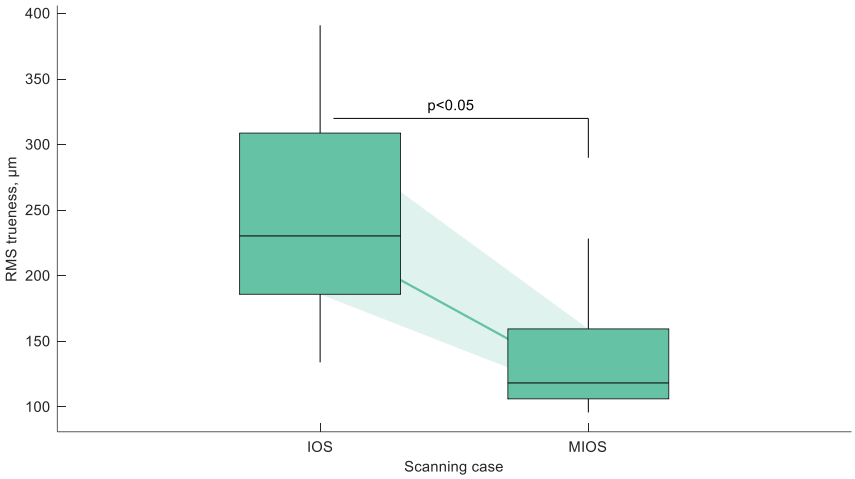

Figure 44. Root mean squared 3D surface deviations for each scanning condition for trueness estimation. Color areas represent quartiles change, horizontal lines – median change. IOS and MIOS surface deviation differ significantly.

Table 23. Trueness and precision of intraoral and extraoral scanning measuring RMS distance between surfaces

Data	**Trueness, µm**		**Precision, µm**	
	mean±SD	median	mean±SD	median
IOS	249±87	230	97±27	107
MIOS	137±45	118	78±25	76
RS	----	---	11±4	10

A comparison of the IOS surface to MIOS is shown in figure 45 and table 24. The results are comparable to results in figure 44, showing directly the difference between *in vivo* and *in vitro* scanning surfaces.

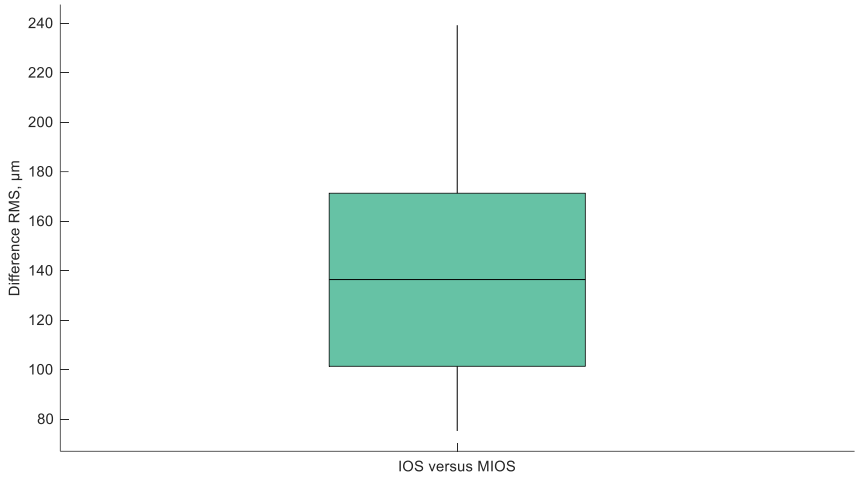

Figure 45. Root mean squared 3D surface deviation comparing IOS to MIOS. Circle represents the mean of the deviations.

Table 24. Comparison of IOS surface distance versus MIOS, in µm.

Difference RMS, µm	
mean±SD	median
143±51	136

5. DISCUSSION

DII are reported in the literature to be a viable alternative to conventional techniques; however, these statements are based mostly on *in vitro* study results and subjective clinical experience.[8] Several studies were designed and performed to evaluate and compare the accuracy of DII and CII as well as the impact of digital and conventional workflow to the passivity of implant-supported zirconia restorations *in vitro* and *in vivo*.

5.1. *In vitro* accuracy evaluation

The majority of published studies are *in vitro* because it is possible to obtain the true reference positions of scan bodies or implants using industrial measuring equipment. Applying industrial-grade reference scanner in a clinical study is one of the approaches, but can only be performed in the anterior region of the maxilla and under special conditions.[65] Moreover, using artificial landmarks in edentulous areas was suggested as a solution for better image suturing of IOS, where the amount of reference points is limited. In the first part of the study, hardened tabs of glass-ionomer cement were used as artificial landmarks forming the digital splint to test its impact on the trueness and precision of different IOS in partially and fully edentulous situations on 3D printed models. For partially edentulous cases, digital splint had a positive effect on scanning trueness and precision of distance, angulation, and vertical shift of scan bodies, especially for newer generation IOS. However, there were no statistically significant differences between the scans with and without digital splint ($p>0.05$).

In fully edentulous cases, digital splint made no statistically significant influence on trueness and precision as well, but the longer was the distance between scan bodies, the more deviations in distance, angulation, and vertical shift occurred. Moreover, for both partially and fully edentulous situations, Primescan, Trios 3 and Trios 4 scanners demonstrated results of trueness mostly with negative values comparing to Medit i500 and CS 3600, showing that the scanned object was smaller than the true reference. Several published studies also analyzed the impact of the digital splint on the scanning trueness and precision for teeth- and implant-supported restorations.[20–22] For fully edentulous models with embedded four implants and different scan bodies attached, dental floss, glass beads, and pressure-indicating paste were used as artificial landmarks in edentulous areas. However, none of those had any significant impact on scanning trueness and precision. The splinting of scan bodies with dental floss compromised the image capturing of the scan body

the most, compared to other artificial landmarks.[20] In the other study, the model with prepared teeth for bridge type restorations was scanned using the alumina tab-form marker as a digital splint. However, the digital splint had also no significant influence on the scanning trueness, and the procedure required more time and images for suturing than usual for some scanners tested. Precision, on the contrary, was statistically significantly improved by using the digital splint.[21] For a fully edentulous metal model with four implants and attached scan bodies, teeth-shaped artificial landmarks statistically significantly improved the trueness and precision of distance measurements for all IOS tested in the other published study.[22] Measuring the distances between scan bodies, it was also noticed, as in the present study, that deviations tend to accumulate when the distance increased. Still despite the IOS used, additional landmarks improved the scanning accuracy. Moreover, the form of the digital splint might have more influence on scanning speed than the type of IOS.[21,22] However, all the results of *in vitro* studies have to be evaluated with caution, because the patient-related issues, such as saliva, tongue and soft tissue movement were eliminated, but could have a significant impact on scanning accuracy. Moreover, despite the digital splint did not have a statistically significant effect on DII accuracy in the present study, for some scanners it improved scanning speed and 3D image formation.

5.2. *In vivo* accuracy evaluation

5.2.1. Accuracy evaluation of dental implant impressions

Very few *in vivo* studies evaluating the accuracy of digital implant impressions and restorations on implants have been published in the literature because of a lack of true reference scans for the data comparison.[8] Since in this study mostly all restorations were in the posterior region, using CMM for reference scanning could not be adapted.[65] Another approach was applied by Alsharbaty et al., where 36 patients with two implant-supported restorations were included. The accuracy of three impression techniques (DII using a Trios IOS, open-tray, and closed-tray CII) was evaluated by comparing them to reference models fabricated from splinted impression copings. Reference models were measured by a coordinate measuring machine. Conventional implant impressions made using the pick-up technique were found to be the most accurate. The accuracy of digital impressions showed the poorest results, and they were rendered clinically unacceptable to fabricate well-fitting restorations on implants. Angular mean deviation was found to be 6.77 ±

0.91°; mean linear displacement was 360 ± 46 μm, and the deviation of 3D distance was 220 ± 30 μm. However, this method of obtaining reference data in the clinical study still has to be validated.[12]

Since there are no reliable techniques to obtain a true reference in the clinical circumstances, master models fabricated from conventional impressions were used as the best available reference in this study. Also, validation of the master model was employed according to strict protocol. A fit assessment of the final restoration also served as additional criteria to confirm the accuracy of conventional impressions. In this way, digital impression accuracy was compared to the conventional one. However, considering general practice, more variability in the accuracy of conventional implant impressions could be expected.

The clinically relevant threshold for the distortions of impressions and restorations is still unknown. Based on the recent study, the threshold for horizontal/vertical misfit and angulation errors of two implant-supported restorations were taken as 100 μm and 0.4º, respectively.[59] Despite the complexity of evaluating misfit and its clinical significance,[44] these values were taken for the sake of comparison and in order to have a tentative threshold. In the part of the study, where Trios IOS was used for DII, differences in the means of inter-implant distance (73.7±75 μm) and vertical shift (98.9±96.33 μm) were lower than 100 μm. However, given that the means approached the tentative threshold and the high standard deviations, these differences could be regarded as potentially having clinical significance. Differences in mean angulation were above 0.4° (0.42±0.3°). In the part of the study, where Trios 3 IOS was used, statistically significant differences between scan bodies' distances were found between the conventional and digital groups; the resulting mean (70.8 ± 59 μm) was below 100 μm. Vertical shift differences were lower than 100 μm (82.2 ± 61.7 μm), and a statistically significant difference was found between CII and DII. Mean angulation differences were below 0.4° (0.37 ± 0.3 º). Considering these thresholds, the measured means can be regarded as having minimal clinical relevance. These results are in line with in-vitro studies concluding that DII can be as accurate as conventional impressions.[17,37] Also, the resulting differences were much lower as those recorded in the study by Alsharbaty et al.[12]

Dental implant abutment rotational misfit could be of clinical significance[77]; therefore, the rotation of scan bodies was evaluated. No statistically significant differences concerning rotation were found between conventional impressions and DII in the part of the study with Trios IOS, mean difference was found to be 0.72±0.55°. Using Trios 3 IOS mean rotation difference was found to be 2.0±1.37º, and a statistically significant difference

was detected between DII and CII. The clinical significance of these findings is limited considering given that non-hexed abutments or abutments without other anti-rotational features are generally recommended for multiple-unit implant-supported reconstructions. It should also be noted that rotational differences represent cumulative errors in scanning and scan body repositioning as well.[42] In cases when titanium interfaces without anti-rotational features are not available in the CAD/CAM workflow, rotational misfit could be clinically relevant depending on the rotational freedom of the abutments.[78]

Comparing surface mismatch data between mesial and distal scan body images obtained by Trios and Trios3 IOS, no statistically significant differences were found. Other authors claimed that scanning location considerably affects DII accuracy because this leads to cumulative errors in the image suturing process, especially in long-span situations.[15,16,53] These aspects could be very relevant for posterior cases were scanning procedure could be more challenging (in the study with Trios, 24 out of 27 restorations were in the posterior area and in the study with Trios 3, all 24 restorations in the posterior area).

Surface mismatch data of the laboratory scanner for mesial and distal scan bodies were two times better than IOSs. This could have clinical implications, since due to the higher surface mismatch, discrepancies in the position of the original CAD image of the scan body can appear, affecting estimated implant positions and resulting in the misfit of the restoration.

An analysis of linear regression models showed that the actual mean of distance between scan bodies does not significantly correlate with distance between scan bodies, angulation detected in both groups analyzing Trios and Trios 3 IOS. Vertical shift differences were affected by the actual mean of distance only in the study with Trios IOS. However, angulation between scan bodies significantly ($p<0.05$) affects the differences of all parameters assessed, although Spearman correlation coefficients were weak, ranging from 0.24 to 0.52. Flugge et al. and Papaspyridakos et al. have reported that increasing angulation and distance between scan bodies negatively affected scanning precision.[50,79] Nonetheless, other authors have claimed the opposite.[37,80] Limit values for inter-implant distance and angulation causing clinically significant errors should be defined for the different IOS in the future.

In the clinical part of the CII and DII comparison, a very robust protocol for verifying the accuracy of splints of master casts and restorations was used for the validation of the conventional technique. It could be expected that in daily clinical practice, the open-tray technique could produce less accurate

results. Furthermore, based on the systematic reviews, closed-tray impression procedures are considered to be less accurate than open-tray ones for multiple implant cases.[47,48,70] Therefore, the accuracy of digital impressions and closed-tray techniques should be compared by further research.

The accuracy of conventional implant impressions could be affected by many factors, including inter-implant distance, implant angulation, implant placement depth.[70] Besides these factors, the accuracy of digital impressions can also be influenced by scanner type,[28] software, scanning strategy,[35] and other factors specific to the digital workflow. The machining tolerance of scan bodies and repositioning accuracy could also affect the accuracy of DII,[42] although another study has not supported this.[81] Implant location could influence DII accuracy, as in posterior cases limited mouth opening, salivary flow, tongue movements, and a shallow vestibule in the mandible could interfere with the capturing and stitching of the images. Moreover, different types of implant-abutment connections could have an impact on the results, when the accuracy and precision of the impression techniques are evaluated.[82] As for digital scanning, the scan bodies are not removed, and during tray removal of conventional implant impression distortions can arise because of angulated implants especially with the internal type of connection.[57,83] External type of connection implant impressions do not face that problem because impression copings are of different design. The implant system used in the study employs an 11° internal hex connection. Therefore, the results of other studies with implants of different types of connections or different geometries of prosthetic components could be different.

5.2.2. Accuracy evaluation of dental implant restorations

A very limited number of clinical studies have reported accuracy outcomes with implant-supported prostheses fabricated using the digital workflow. In these studies, however, the fit was evaluated using mainly subjective and not standardized criteria.[66] In the current part of the study, the fit and cement gap were evaluated and compared between conventionally and digitally fabricated two-implant-supported FPDs using SEM measurements.

Accuracy of the digital impression also can be affected by many factors, including the type of the scan body and its manufacturing accuracy.[84,85] In the present study, the same scan bodies, in the same implant locations, and same rotational positions were used for taking digital impressions (group D) and for master model scanning (group C).

Linear deviations between splinted conventional implant impressions and digital impressions may vary from 11 μm[17] in laboratory studies, and to 130 μm[12] in clinical studies. Some of the studies have reported better accuracy with digital impressions than with conventional ones.[56] Thus, hypothetically, it is possible that the fit of FPD produced using the digital workflow could be better as compared to conventionally fabricated FPD.[86] However, the evidence is still lacking to support the selection of digital impressions for multiple-unit implant prosthodontics. Therefore, conventional impressions are still considered as the standard technique, especially for the more complex cases.

Impression taking is just the first step in the workflow. Therefore, the accuracy of the final prosthesis could be influenced by the distortions that are generated during CAD/CAM and other subsequent fabrications steps. Distortions pertinent to the specific workflow can lead to the incomplete seating of the prosthetic component. The design of the bar eliminated possible interferences with proximal contacts and soft tissues. Due to this, the perception of the clinician was not affected by these factors.

An analysis of SEM measurements has shown that the median values of D_{misfit} in D group (78μm) were significantly different from the C group (59μm). To avoid the influence of cofounding factors, CAD design, milling, sintering, and other parameters and procedures were standardized. Further on, all clinical procedures were completed by one investigator, while lab procedures – by another.

As misfit of 150 μm is widely reported as a clinical threshold,[63] the 19 μm difference in median values of D_{misfit} between groups C and D could be considered to have limited clinical significance. However, this clinical threshold was exceeded considering maximum values in C and D groups – 181μm and 250 μm, respectively. It must be noted again that measurements were done on a verified master cast which can, albeit minimally, deviate from the intraoral situation. Therefore, these results cannot be directly associated with the fit intraorally. Study designs that would be capable of obtaining a reference data representing intraoral situation are needed.

Considering different D_{misfit} measurement locations, significant differences were found between the groups and different locations. Up to 34 μm higher D_{misfit} values were detected in the group D, considering different locations. Increased marginal discrepancy could lead to less passive restoration and less precise fit between the Ti base and the implant. Increase of the bacterial contamination due to the misfit of the implant-abutment can cause inflammatory complications.[87] Also, detrimental effects on the implant

and marginal bone stability can be generated.[88] The ability of the clinician to detect these misfits clinically is still questionable.

Using a conventional workflow, milled restorations are usually cemented to Ti bases by finger pressure using the master model. Although this is a standard procedure, the cementation of multiple-unit cases with angulated implants can be more challenging and can lead to less reliable cementation. Cementation on the master model allows us to adjust contours of the restorations, as well as proximal and occlusal contacts. However, there is a possibility that discrepancies caused by various factors such as time-dependent model distortion and the repositioning accuracy of prosthetic components can lead to an incomplete seating of the restoration on the Ti base and less uniform cement gap.

3D printed models are still regarded as less accurate than conventional ones and can introduce significant deviations to the workflow.[89–91] If full-contour restorations are planned, a model-free fully digital workflow can be selected. In this case, the restorations are cemented to Ti bases without the 3D printed model. For this reason, a model free-approach was chosen in the current study. The original non-hex Ti bases were cemented with widely documented resin cement according to the manufacturer's instructions.[92,93]

Zirconia abutments bonded to Ti bases show similar mechanical stability compared with customized titanium abutments.[94] The size of the cement gap is important for the FPD's retention on both natural teeth and implant abutments or Ti bases. Mehl et al. have reported that the resulting cement space should be tested before a workflow is established, and a cement space of about 60 μm is preferred over a cement space of 100 μm.[95] Though D_{cement} was measured only on the marginal edge of the Ti base, it did not exceed 100 μm in both groups (41.68 μm in group C and 36.45 μm in group D). However, maximum D_{cement} values in both groups were slightly over 80 μm. A higher number of outliers in the C groups implies that the cementation technique on the master cast was less predictable in this regard.

Titanium abutment centering in the zirconia coping during cementation is important to the retentiveness of the restorations. To achieve an even distribution of the cement, a proper fit of the restoration on the master model with Ti bases attached to the implant analogues must be accomplished before the cementation. In this study, no statistically significant differences in D_{cement} were found between the measurements at different locations ($p = 0.79$) in both groups. Therefore, it can be claimed that cement distribution between the restoration and Ti base was even at the margins circumferentially. However,

the present study did not evaluate the cement thickness on the axial walls of the Ti bases.

A more complete seating of the restoration on a Ti base was found in group D, since the Ti base could adapt a position of maximum congruency to the zirconia framework without any restrictions. However, this has led to the decrease of the fit, as D_{misfit} was higher by 19 μm in group D. Further studies should answer the question whether an increase of the cement gap or the misfit would have a larger effect on the long-term prognosis of the implant-supported FPDs. It was also shown by other studies that besides the cement gap, cementation reliability was also affected by the type of cement, surface preparation, thermocycling, fatigue simulation, and material of prosthesis.[95,93]

The fit of a restoration can be influenced by the clinical situation, with distance, angulation, and depth of the implant placement is considered important factors. The length of the prosthesis or its curvature along the jaw can also affect the final fit.[44,45] In this study, two-, three-, and four-unit restorations were made all in the posterior region. However, neither ΔD_{misfit} ($p = 0.47$) nor ΔD_{cement} ($p = 0.05$) showed statistically significant differences between the different lengths of the restorations. Also, ΔD_{misfit} of maxillary and mandibular restorations was not statistically significant ($p = 0.58$), which implies that the vertical fit of the restorations was not influenced by the length or the location of the two-implant-supported FPDs. However, a significant difference was found considering ΔD_{cement} measured in maxilla and mandible. This difference (4 μm) might have resulted from the tendency of higher angulations of implants in the premolar region, however, the clinical significance of this is very questionable.

Cement gap parameters did not correlate with the distance or angulation between the implants. However, the weak negative correlation of D_{misfit} with inter-implant distance was detected in group C. This could suggest that with increased distance between implants, a less marginal misfit was observed. This can be attributed to a better ability to detect the misfit, when a one-screw test is applied during verification procedures in cases with larger inter-implant distance.

The limitations that could affect the results of the present study should be discussed. Repositioning errors of the impression copings or scan bodies could affect the accuracy of the implant impression and master model.[96,97] Stimmelmayr et al. have reported that the repositioning of the scan body significantly decreases the accuracy of the digital master model (discrepancies in scan body misfit 39 μm on the implant and 11 μm on implant analog).[98] However, other authors state that the precision of the scans after detachment and repositioning of the scan body do not significantly affect the digital

impression accuracy.[81] Also, the torque level of the scan body or the impression coping could influence the repositioning accuracy.[8] In the current study, a 15 Ncm torque was used for all impression components.

The type of implant-abutment connection also has an impact on the accuracy of the dental implant prosthesis. As an external type of abutment connection is more able to prevent vertical displacement during screw tightening, greater vertical displacement occurs with internal types of implant-abutment connections.[99] Also, the use of non-original Ti bases is associated with lower internal accuracy, which could affect the results.[100]

The lead of the titanium prosthetic screw of the Ti base (the distance along the axis of the screw that is covered by one complete rotation of it) used in the study was 400 μm. The gold prosthetic screw used in the Jemt et al. study had a lead of 300 μm.[63] Thus, to achieve 15 Ncm of torque and close a 150-μm marginal gap of the prosthesis, the screw had to be turned by 180°. In the current study, torque from 5 to 35 Ncm was achieved with an approximately 90° (exact value 87±5°) angle of rotation, when a single Ti base was placed on the implant analogue. Therefore, 100-μm vertical displacement between implant and abutment is expected during final tightening with a completely passive fit. The average intraoral angle of rotation with group C restorations was 88±17° in a passive situation and 102±25° in a non-passive situation. For group D, the average intraoral angle of rotation angle was 84±15° in a passive situation and 95±14° in a non-passive situation (Table 17). SR differences measured intraorally between groups C and D were not statistically significant ($p>0.05$), however. The difference in angle of rotation intraorally was 16° for group C and 14° for group D. This could lead to a 17.7-μm and 15.5-μm vertical displacement of the restoration respectively and clinically translate to a supra- or infra-occlusion situation. Any occlusal discrepancies higher than 8 μm of Shimstock foil can be sensed as an occlusion irregularity or affect proximal contacts.[101] The differences in SR measurements between groups C and D on the control cast were statistically significant ($p<0.017$). Since the control casts served as the best available reference, it can be assumed that restorations produced using a digital workflow had a better passive fit than ones fabricated with a conventional workflow. Also, angles of rotation of passive and non-passive screws in groups C and D had similar measurements in an intraoral situation and on the control cast, suggesting that a control cast represented the intraoral situation better than the master cast.

Previous studies investigated the effect of angulation between implants on the accuracy of impressions and restorations.[17,37,53,55,102,103] Several authors have researched the impact of implant angulation on impression accuracy. Lin et al. have investigated parallel, 15°, 30°, and 45° divergence between dental

implants situations and claimed that the divergence between implants significantly affected the accuracy of impressions and that the conventional method was more accurate than the digital one.[102] Similarly, Flugge et al. found that increased inter-implant distance and angulation negatively affected the accuracy of dental implant impressions.[50] Other studies, however, investigated the effect of angulations between the implants from 10 to 45 degrees but were not able to find any effect on implant impression accuracy.[17,37,53] No statistically significant difference was found in group C when restorations with higher and lower than 10-degree inter-implant angulation were compared. This was also the case intraorally as well as on the master and control cast. As for the group D restorations, SR mean in the group with more than 10 degrees of inter-implant angulation was statistically significantly higher than for restorations with less than 10 degrees of angulation ($p=0.037$) intraorally. In group D, however, SR measured on the master and control casts was not significantly different between the angulation groups.

In this study, all correlations of SR intraorally and on the master cast and control cast to inter-implant distance or angulation were not statistically significant. Therefore, these factors had no impact on the passive fit of the restorations. Similarly, no statistically significant differences in axial displacement were detected between restorations on parallel and angulated implants after final fixation and cyclic loading in another study.[104]

The limitation of the study is that different SR measurements can be achieved with distinct implant-abutment connection types. An internal implant-abutment 11° conical connection was used in this study that is less able to prevent vertical displacement of the abutment during the tightening of the screw than external ones.[99,104] SR measurements could also be affected by various types of prosthetic components that might or might not employ anti-rotational features.

Though the use of prosthetic ratchets is considered a reliable method to tighten a prosthetic screw,[105] the angle of rotation had to be evaluated using the goniometer, which is not documented well in the literature. One measuring unit on the scale of the goniometer is 5 degrees, which could limit the accuracy. As an alternative for measuring SR, an OsseoCare (Nobel Biocare) device, is described in the literature.[106] This device is not able to record angles of rotation, however.

5.3. *In vitro* in vivo accuracy evaluation

Several *in vitro* studies have evaluated trueness and precision of distance, angle, and 3D surface match parameters.[15,22,29,37,51] Iturrate et al. assessed the trueness and precision of distance, analyzing Trios 3, True Definition, and iTero intraoral scanners on a full-arch model with 4 implants.[22] Three different distances in length were compared. Precision varied from 14±15 μm in short distance (Trios 3) to 118±97 μm in the longest distance (iTero). Trueness of the same intraoral scanners and distances varied from 17±15 μm to 189±70 μm alternatively. Also, the precision and trueness of the longest distance with Trios 3 were reported as 55±47 μm and 101±75 μm. Comparing the data of the present study, the precision of the shortest and the longest distances in IOS group showed better results (10±3 μm and 44±18 μm alternatively). Moreover, trueness results of IOS and MIOS groups were also better than in the mentioned study. Despite the differences in study design (different lengths of the measurement distances and scanned jaws), the precision and trueness of the distance measurements in the present study demonstrated high accuracy. In the other *in vitro* study,[51] local trueness of distance and angulation in fully edentulous jaw scanned with Trios, CS3500, ZFx Intrascan, and Planscan IOS showed poorer results than in the present study. Moreover, other *in vitro* studies report 0.21±0.17°[15] and 0.17±0.14°[37] trueness of angulation, which is poorer than the IOS and MIOS data of angulation trueness gathered in the present study (0.11±0.08° and 0.08±0.05° alternatively). Despite overall trueness and precision of distance and angulation demonstrate very accurate results in the present study, there are statistically significant differences between the first and fourth scan body both in distance and angulation parameters. The data confirms the statements of other studies – that deviations accumulate in longer scanning distances or when the scanning area is located more posterior in the mouth.[15,22,49] The general precision and trueness of 3D surface analysis demonstrated different results than local precision and trueness measurements. Several laboratory studies[22,29,51] scanned fully edentulous models with six implants with different IOS. General precision data varied from 31.5±9.8 μm (Trios 3)[22] to 204.2±22.7 μm (Planscan),[51] while trueness varied from 44.9±8.9 μm (CS3600) [29] to 253.4±13.6 μm (Planscan).[51] In the present study, the precision and trueness of 3D surface analysis in groups, IOS, and MIOS showed poorer results than in the aforementioned studies. Such differences could arise because of the close layout of the scan bodies on the bar. Narrow proximal areas between scan bodies could compromise the access of the scanning tip and the appropriate scanning of SB, especially *in vivo*. Other *in vivo – in vitro* studies compared

full arch scanning accuracy intraorally and extraorally of the model of the same arch.[67,68] Since in one study model the scanning was twice as accurate than in the *in vivo* circumstances, [67] the newer data claimed different results.[68] The metal bar was attached to the second upper premolars intraorally and scanned with iTero IOS. Also, an acrylic model was manufactured from the conventional impression of intraoral situation and the same bar attached on the same teeth and scanned with IOS. Despite the fact that the scans were performed only in the upper jaw and the bar was constantly removed from the mouth, and including any possible errors of model manufacturing, the differences of scanning accuracy *in vivo* and *in vitro* were not statistically significant both in linear and angular parameters.[68]

The limitations that could affect the results of the present study also should be discussed. The bar with scan bodies formed a large construction, which could compromise the mouth opening of the patient and access to the area between the tongue and the bar. When the tip of the IOS is rotating in the limited space area, more images are usually accumulated and the scanning becomes more prone to errors.[15,53] Moreover, despite that Trios 3 is powder-free IOS, light reflections from the humid metal surface could negatively influence the scanning workflow.[107] To minimize the possible inaccuracies, the bar was sandblasted before scanning both intraorally and on the master model and the matted surface was constantly renewed.

Constantly improving technologies in digital dentistry increase the demand of high validity *in vitro* and especially *in vivo* studies. Updates in IOS software and hardware show promising results not only in trueness and precision,[29,51] but also in scanning speed, better data processing, and further analysis.[108] Additional functions of IOS, such as caries detector, 3D motion recording also increase the usage of digital technologies, which helps improving operators' skills and scanning precision.[15] Further research is needed on how these improvements can increase the accuracy of the digital workflow.

6. CONCLUSIONS

1. In partially and fully edentulous models, the Medit i500 and CS3600 IOS demonstrated the lowest accuracy of all five intraoral scanners tested. Primescan, Trios 3, and Trios 4 showed similar results of accuracy that were statistically significantly better than those performed using Medit i500 and CS3600 IOS.
2. The digital splint improved the accuracy of the scanning for partially edentulous models, but a statistically significant difference was detected only using the Medit i500 intraoral scanner. For fully edentulous models, the digital splint had a predominantly positive effect on trueness but did not improve the precision.
3. Conventional implant impressions clinically performed statistically significantly more accurately than digital implant impressions in selected parameters. The Trios 3 intraoral scanner demonstrated better accuracy than the Trios intraoral scanner, while the positional differences of the scan bodies, obtained with a conventional and Trios 3 intraoral scanner, were of limited clinical significance.
4. Both distance and angle between implants negatively affected the scanning accuracy of the Trios intraoral scanner, while only the angle between implants had a statistically significant effect on the accuracy of the Trios 3 intraoral scanner.
5. The fit (D_{misfit}) of two-implant-supported zirconia fixed partial dentures made with the conventional workflow was statistically significantly lower than the one made with the digital workflow, but the reported differences are minor and could be considered of limited clinical significance.
6. The cement gap of conventionally manufactured implant-supported fixed partial dentures was found to be significantly larger than in implant-supported fixed partial dentures produced through the model-free digital workflow.
7. There were no significant differences in screw resistance between conventionally and digitally manufactured implant-supported fixed partial dentures as measured intraorally. However, significant differences were found when measuring on master and control models.
8. Trueness and the precision of edentulous jaw digital implant impressions demonstrated statistically insignificant differences when scanned under clinical and laboratory conditions.

7. PRACTICAL RECOMMENDATIONS

1. A digital splint (additional reference objects) might be a useful tool for improving the accuracy of digital implant impressions in partially edentulous situations, when long-span, bridge-type, implant-supported fixed partial dentures are planned. For fully edentulous dental implant cases, a digital splint can improve the scanning trueness but has no impact on precision.
2. An angulation of more than 10° degrees between the implants could negatively affect the passive fit of digitally fabricated implant-supported fixed partial dentures. Using digital workflow in those cases, thorough evaluation of angle between the implants is recommended.
3. Digital workflow could be used as a valid alternative to the conventional one for manufacturing bridge-type, implant-supported fixed partial dentures, from two- to four-unit variants.
4. Passive-fit evaluation methods still lack objectivity; therefore, several evaluating methods have to be used clinically. Also, clinical evalutaion methods have to be continuosly objectified.

CURRICULUM VITAE

Name	Agnė
Surname	Gedrimienė
Date of birth	1990 06 09
Place of birth	Panevėžys
E-mail	geciauskaite.agne@gmail.com
Research activities website	https://www.researchgate.net/profile/Agne_Gedrimiene

Education

2009	Juozas Balčikonis gymnasium (with honors)
2014	Vilnius University, Faculty of Medicine, Institute of Odontology, *Master's Diploma*
2018	Vilnius University, Faculty of Medicine, Institute of Odontology, *Certificate of Specialist in Dental Prosthodontics*

Work experience

2014 – 2018	Dentist General Practitioner, Private practice
2018 – current	Dental Prosthodontist, Private practice
2019 – current	Member of a scientific group DIGITORUM

BIBLIOGRAPHY

1. Fasbinder, D. J. Computerized technology for restorative dentistry. *Am. J. Dent.* **26**, 115–120 (2013).
2. Joda, T. & Brägger, U. Patient-centered outcomes comparing digital and conventional implant impression procedures: a randomized crossover trial. *Clin. Oral Implants Res.* (2015) doi:10.1111/clr.12600.
3. Joda, T. & Bragger, U. Digital vs. conventional implant prosthetic workflows: a cost/time analysis. *Clin. Oral Implants Res.* **26**, 1430–1435 (2015).
4. Joda, T., Lenherr, P., Dedem, P., Kovaltschuk, I., Bragger, U. & Zitzmann, N. U. Time efficiency, difficulty, and operator's preference comparing digital and conventional implant impressions: a randomized controlled trial. *Clin. Oral Implants Res.* (2016) doi:10.1111/clr.12982.
5. Joda, T., Katsoulis, J. & Brägger, U. Clinical Fitting and Adjustment Time for Implant-Supported Crowns Comparing Digital and Conventional Workflows. *Clin. Implant Dent. Relat. Res.* (2015) doi:10.1111/cid.12377.
6. Zimmermann, M., Mehl, A., Mörmann, W. H. & Reich, S. Intraoral scanning systems - a current overview. *Int. J. Comput. Dent.* **18**, 101–129 (2015).
7. Spitznagel, F. A., Boldt, J. & Gierthmuehlen, P. C. CAD/CAM Ceramic Restorative Materials for Natural Teeth. *J. Dent. Res.* **97**, 1082–1091 (2018).
8. Rutkūnas, V., Gečiauskaitė, A., Jegelevičius, D. & Vaitiekūnas, M. Accuracy of digital implant impressions with intraoral scanners. A systematic review. *Eur. J. Oral Implantol.* **10 Suppl 1**, 101–120 (2017).
9. Wulfman, C., Naveau, A. & Rignon-Bret, C. Digital scanning for complete-arch implant-supported restorations: A systematic review. *J. Prosthet. Dent.* (2019) doi:10.1016/j.prosdent.2019.06.014.
10. Flügge, T. van der Meer, W. J., Gonzalez, B. G, Vach, K., Wismeijer, D. & Wang, P. The accuracy of different dental impression techniques for implant-supported dental prostheses: A systematic review and meta-analysis. *Clin. Oral Implants Res.* **29 Suppl 16**, 374–392 (2018).
11. Ahlholm, P., Sipilä, K., Vallittu, P., Jakonen, M. & Kotiranta, U. Digital Versus Conventional Impressions in Fixed Prosthodontics: A Review. *J. Prosthodont. Off. J. Am. Coll. Prosthodont.* (2016) doi:10.1111/jopr.12527.

12. Alsharbaty, M. H. M., Alikhasi, M., Zarrati, S. & Shamshiri, A. R. A Clinical Comparative Study of 3-Dimensional Accuracy between Digital and Conventional Implant Impression Techniques. *J. Prosthodont. Off. J. Am. Coll. Prosthodont.* (2018) doi:10.1111/jopr.12764.
13. Jung, R. E., Pjetursson, B. E., Glauser, R., Zembic, A., Zwahlen, M. & Lang, N. P. A systematic review of the 5-year survival and complication rates of implant-supported single crowns. *Clin. Oral Implants Res.* **19**, 119–130 (2008).
14. Lin, W.-S., Harris, B. T., Elathamna, E. N., Abdel-Azim, T. & Morton, D. Effect of implant divergence on the accuracy of definitive casts created from traditional and digital implant-level impressions: an in vitro comparative study. *Int. J. Oral Maxillofac. Implants* **30**, 102–109 (2015).
15. Gimenez-Gonzalez, B., Hassan, B., Özcan, M. & Pradíes, G. An In Vitro Study of Factors Influencing the Performance of Digital Intraoral Impressions Operating on Active Wavefront Sampling Technology with Multiple Implants in the Edentulous Maxilla. *J. Prosthodont. Off. J. Am. Coll. Prosthodont.* (2016) doi:10.1111/jopr.12457.
16. Gherlone, E., Capparé, P.,Vinci, R., Ferrini, F., Gastaldi, G. & Crespi, R. Conventional Versus Digital Impressions for 'All-on-Four' Restorations. *Int. J. Oral Maxillofac. Implants* **31**, 324–330 (2016).
17. Papaspyridakos, P., Gallucci, G. O., Chen, CJ., Hanssen, S., Naert, I. & Vandenberghe, B. Digital versus conventional implant impressions for edentulous patients: accuracy outcomes. *Clin. Oral Implants Res.* **27**, 465–472 (2016).
18. Koch, G. K., Gallucci, G. O. & Lee, S. J. Accuracy in the digital workflow: From data acquisition to the digitally milled cast. *J. Prosthet. Dent.* **115**, 749–754 (2016).
19. Lee, S. J., Betensky, R. A., Gianneschi, G. E. & Gallucci, G. O. Accuracy of digital versus conventional implant impressions. *Clin. Oral Implants Res.* **26**, 715–719 (2015).
20. Mizumoto, R. M., Yilmaz, B., McGlumphy, E. A., Seidt, J. & Johnston, W. M. Accuracy of different digital scanning techniques and scan bodies for complete-arch implant-supported prostheses. *J. Prosthet. Dent.* **123**, 96–104 (2020).
21. Kim, J.-E., Amelya, A., Shin, Y. & Shim, J.-S. Accuracy of intraoral digital impressions using an artificial landmark. *J. Prosthet. Dent.* **117**, 755–761 (2017).

22. Iturrate, M., Eguiraun, H. & Solaberrieta, E. Accuracy of digital impressions for implant-supported complete-arch prosthesis, using an auxiliary geometry part—An in vitro study. *Clin. Oral Implants Res.* **30**, 1250–1258 (2019).
23. Abduo, J., Bennani, V., Waddell, N., Lyons, K. & Swain, M. Assessing the fit of implant fixed prostheses: a critical review. *Int. J. Oral Maxillofac. Implants* **25**, 506–515 (2010).
24. Kan, J. Y., Rungcharassaeng, K., Bohsali, K., Goodacre, C. J. & Lang, B. R. Clinical methods for evaluating implant framework fit. *J. Prosthet. Dent.* **81**, 7–13 (1999).
25. Sahin, S. & Cehreli, M. C. The significance of passive framework fit in implant prosthodontics: current status. *Implant Dent.* **10**, 85–92 (2001).
26. Logozzo S, Franceschini G, Kilpella A, Caponi M. (PDF) A Comparative Analysis of Intraoral 3d Digital Scanners for Restorative Dentistry. https://www.researchgate.net/publication/284284335_A_Comparative_Analysis_of_Intraoral_3d_Digital_Scanners_for_Restorative_Dentistry .
27. Patzelt, S. B. M., Emmanouilidi, A., Stampf, S., Strub, J. R. & Att, W. Accuracy of full-arch scans using intraoral scanners. *Clin. Oral Investig.* **18**, 1687–1694 (2014).
28. van der Meer, W. J., Andriessen, F. S., Wismeijer, D. & Ren, Y. Application of intra-oral dental scanners in the digital workflow of implantology. *PloS One* **7**, e43312 (2012).
29. Manganao F. G., Hauschild, U., Veronesi, G., Imburgia, M., Mangano, C. & Admakin, O. Trueness and precision of 5 intraoral scanners in the impressions of single and multiple implants: a comparative in vitro study. - PubMed - NCBI. https://www.ncbi.nlm.nih.gov/pubmed/?term=Trueness+and+precision+of+5+intraoral+scanners+in+the+impressions+of+single+and+multiple+implants%3A+A+comparative+in+vitro+study (2019).
30. Kravitz, N. D., Groth, C., Jones, P. E., Graham, J. W. & Redmond, W. R. Intraoral digital scanners. *J. Clin. Orthod. JCO* **48**, 337–347 (2014).
31. Imburgia, M., Logozzo, S., Hauschild, U., Veronesi, G., Mangano, C. & Mangano, F. G. Accuracy of four intraoral scanners in oral implantology: a comparative in vitro study. *BMC Oral Health* **17**, (2017).
32. Rivara, F., Lumetti, S., Calciolari, E., Toffoli, A., Forlani, G. & Manfredi, E. Photogrammetric method to measure the discrepancy

between clinical and software-designed positions of implants. *J. Prosthet. Dent.* **115**, 703–711 (2016).
33. Ender, A. & Mehl, A. Influence of scanning strategies on the accuracy of digital intraoral scanning systems. *Int. J. Comput. Dent.* **16**, 11–21 (2013).
34. Medina-Sotomayor, P., Pascual M., A. & Camps A., I. Accuracy of four digital scanners according to scanning strategy in complete-arch impressions. *PLoS ONE* **13**, (2018).
35. Muller, P., Ender, A., Joda, T. & Katsoulis, J. Impact of digital intraoral scan strategies on the impression accuracy using the TRIOS Pod scanner. *Quintessence Int.* **47**, 343–349 (2016).
36. Mizumoto, R. M. & Yilmaz, B. Intraoral scan bodies in implant dentistry: A systematic review. *J. Prosthet. Dent.* **120**, 343–352 (2018).
37. Gintaute, Aiste. Accuracy of computerized and conventional impression-making procedures of straight and tilted dental implants. (Albert-Ludwigs-Universität, 2015).
38. Howell, K. J., McGlumphy, E. A., Drago, C. & Knapik, G. Comparison of the accuracy of Biomet 3i Encode Robocast Technology and conventional implant impression techniques. *Int. J. Oral Maxillofac. Implants* **28**, 228–240 (2013).
39. Eliasson, A. & Örtorp, A. The Accuracy of an Implant Impression Technique Using Digitally Coded Healing Abutments. *Clin. Implant Dent. Relat. Res.* **14**, e30–e38 (2012).
40. Ng, S., Tan, K., Teoh, K. H., Cheng, A. & Nicholls, J. Three-Dimensional Accuracy of a Digitally Coded Healing Abutment Implant Impression System. *Int. J. Oral Maxillofac. Implants* **29**, 927–936 (2014).
41. Al-Abdullah, K., Zandparsa, R., Finkelman, M. & Hirayama, H. An in vitro comparison of the accuracy of implant impressions with coded healing abutments and different implant angulations. *J. Prosthet. Dent.* **110**, 90–100 (2013).
42. Stimmelmayr, M., Güth, J.-F., Erdelt, K., Edelhoff, D. & Beuer, F. Digital evaluation of the reproducibility of implant scanbody fit--an in vitro study. *Clin. Oral Investig.* **16**, 851–856 (2012).
43. Moreira, A. H. J., Rodrigues, N. F., Pinho, A. C. M., Fonseca, J. C. & Vilaça, J. L. Accuracy Comparison of Implant Impression Techniques: A Systematic Review. *Clin. Implant Dent. Relat. Res.* **17 Suppl 2**, e751-764 (2015).

44. Katsoulis, J., Takeichi, T., Sol Gaviria, A., Peter, L. & Katsoulis, K. Misfit of implant prostheses and its impact on clinical outcomes. Definition, assessment and a systematic review of the literature. *Eur. J. Oral Implantol.* **10 Suppl 1**, 121–138 (2017).
45. Abduo, J. Fit of CAD/CAM implant frameworks: a comprehensive review. *J. Oral Implantol.* **40**, 758–766 (2014).
46. Chew, A. A., Esguerra, R. J., Teoh, K. H., Wong, K. M., Ng, S. D. & Tan, K. B. Three-Dimensional Accuracy of Digital Implant Impressions: Effects of Different Scanners and Implant Level. *Int. J. Oral Maxillofac. Implants* (2016) doi:10.11607/jomi.4942.
47. Kim, J.-H. D., Kim, K. R. D. & Kim, S. D. Critical appraisal of implant impression accuracies: A systematic review. [Review]. *J. Prosthet. Dent.* **114**, 185–192 (2015).
48. Papaspyridakos, P. Chen, C. J., Gallucci, G. O., Doukoudakis, A., Weber, H. P. & Chronopoulos, V. Accuracy of implant impressions for partially and completely edentulous patients: a systematic review. *Int. J. Oral Maxillofac. Implants* **29**, 836–845 (2014).
49. Vandeweghe, S., Vervack, V., Dierens, M. & De Bruyn, H. Accuracy of digital impressions of multiple dental implants: an in vitro study. *Clin. Oral Implants Res.* (2016) doi:10.1111/clr.12853.
50. Flugge, T. V., Att, W., Metzger, M. C. & Nelson, K. Precision of Dental Implant Digitization Using Intraoral Scanners. *J. Prosthodont.* **29**, 277–283 (2016).
51. Mangano, F. G., Veronesi, G., Hauschild, U., Mijiritsky, E. & Mangano, C. Trueness and Precision of Four Intraoral Scanners in Oral Implantology: A Comparative in Vitro Study. *PloS One* **11**, e0163107 (2016).
52. Gimenez, B. D., Ozcan, M. D., Martinez-Rus, F. D. & Pradies, G. D. Accuracy of a Digital Impression System Based on Active Triangulation Technology With Blue Light for Implants: Effect of Clinically Relevant Parameters. *Implant Dent.* **24**, 498–504 (2015).
53. Gimenez, B., Ozcan, M., Martinez-Rus, F. & Pradies, G. Accuracy of a digital impression system based on parallel confocal laser technology for implants with consideration of operator experience and implant angulation and depth. *J. Oral* **29**, 853–862 (2014).
54. Gherlone, E. F., Ferrini, F., Crespi, R., Gastaldi, G. & Capparé, P. Digital impressions for fabrication of definitive ‘all-on-four’ restorations. *Implant Dent.* **24**, 125–129 (2015).
55. Marghalani, A. Weber, H. P., Finkelman, M., Kudara, Y., El Rafie, K. & Papaspyridakos, P. Digital versus conventional implant impressions

for partially edentulous arches: An evaluation of accuracy. *J. Prosthet. Dent.* **119**, 574–579 (2018).
56. Menini, M., Setti, P., Pera, F., Pera, P. & Pesce, P. Accuracy of multi-unit implant impression: traditional techniques versus a digital procedure. *Clin. Oral Investig.* **22**, 1253–1262 (2018).
57. Alikhasi, M., Siadat, H., Nasirpour, A. & Hasanzade, M. Three-Dimensional Accuracy of Digital Impression versus Conventional Method: Effect of Implant Angulation and Connection Type. *Int. J. Dent.* **2018**, 1–9 (2018).
58. Amin, S., Weber, H. P., Finkelman, M., El Rafie K., Kudara, Y. & Papaspyridakos, P. Digital vs. conventional full-arch implant impressions: a comparative study. *Clin. Oral Implants Res.* **28**, 1360–1367 (2017).
59. Andriessen, F. S., Rijkens, D. R., van der Meer, W. J. & Wismeijer, D. W. Applicability and accuracy of an intraoral scanner for scanning multiple implants in edentulous mandibles: a pilot study. *J. Prosthet. Dent.* **111**, 186–194 (2014).
60. Beuer, F., Schweiger, J. & Edelhoff, D. Digital dentistry: an overview of recent developments for CAD/CAM generated restorations. *Br. Dent. J.* **204**, 505–511 (2008).
61. Kohorst, P., Brinkmann, H., Li, J., Borchers, L. & Stiesch, M. Marginal accuracy of four-unit zirconia fixed dental prostheses fabricated using different computer-aided design/computer-aided manufacturing systems. *Eur. J. Oral Sci.* **117**, 319–325 (2009).
62. Brånemark, P. I. Osseointegration and its experimental background. *J. Prosthet. Dent.* **50**, 399–410 (1983).
63. Jemt, T. Failures and complications in 391 consecutively inserted fixed prostheses supported by Brånemark implants in edentulous jaws: a study of treatment from the time of prosthesis placement to the first annual checkup. *Int. J. Oral Maxillofac. Implants* **6**, 270–276 (1991).
64. Karl, M. & Taylor, T. D. Bone Adaptation Induced by Non-Passively Fitting Implant Superstructures: A Randomized Clinical Trial. *Int. J. Oral Maxillofac. Implants* **31**, 369–375 (2016).
65. Nedelcu, R., Olsson, P., Nyström, I., Rydén, J. & Thor, A. Accuracy and precision of 3 intraoral scanners and accuracy of conventional impressions: A novel in vivo analysis method. *J. Dent.* **69**, 110–118 (2018).
66. Cappare, P., Sannino, G., Minoli, M., Montemezzi, P. & Ferrini, F. Conventional versus Digital Impressions for Full Arch Screw-Retained

Maxillary Rehabilitations: A Randomized Clinical Trial. *Int. J. Environ. Res. Public. Health* **16**, (2019).
67. Flugge, T. V. a, Schlager, S. b, Nelson, K. c, Nahles, S. d & Metzger, M. C. e. Precision of intraoral digital dental impressions with iTero and extraoral digitization with the iTero and a model scanner. [Miscellaneous Article]. *J. Orthod. Dentofac. Orthop.* **144**, 471–478 (2013).
68. Keul, C. & Güth, J.-F. Accuracy of full-arch digital impressions: an in vitro and in vivo comparison. *Clin. Oral Investig.* **24**, 735–745 (2020).
69. Rutkunas, V. & Ignatovic, J. A technique to splint and verify the accuracy of implant impression copings with light-polymerizing acrylic resin. *J. Prosthet. Dent.* **111**, 254–256 (2014).
70. Lee, H., So, J. S., Hochstedler, J. L. & Ercoli, C. The accuracy of implant impressions: A systematic review. *J. Prosthet. Dent.* **100**, 285–291 (2008).
71. Moreira, A. H. J., Rodrigues, N. F., Pinho, A. C. M., Fonseca, J. C. & Vilaça, J. L. Accuracy Comparison of Implant Impression Techniques: A Systematic Review. *Clin. Implant Dent. Relat. Res.* **17 Suppl 2**, e751-764 (2015).
72. https://www.iso.org/obp/ui/#iso:std:iso:5725:-1:ed-1:v1:en. ISO 5725-1:1994(en) Accuracy (trueness and precision) of measurement methods and results — Part 1: General principles and definitions.
73. Mutwalli H, Braian M, Mahmood D & Larsson C. Trueness and Precision of Three-Dimensional Digitizing Intraoral Devices. - PubMed - NCBI. https://www.ncbi.nlm.nih.gov/pubmed/30598665 (2018).
74. Ender, A. D. med dent a & Mehl, A. P. D. Accuracy of complete-arch dental impressions: A new method of measuring trueness and precision. *J. Prosthet. Dent.* **109**, 121–128 (2013).
75. Hayama H, Fueki K, Wadachi J & Wakabayashi N. Trueness and precision of digital impressions obtained using an intraoral scanner with different head size in the partially edentulous mandible. - PubMed - NCBI. https://www.ncbi.nlm.nih.gov/pubmed/?term=Trueness+and+precision+of+digital+impressions+obtained+using+an+intraoral+scanner+with+different+head+size+in+the+partially+edentulous+mandible. (2018).
76. Morel, P. Gramm: grammar of graphics plotting in Matlab. *J. Open Source Softw.* **3**, 568 (2018).

77. Abduo, J. & Swain, M. Influence of vertical misfit of titanium and zirconia frameworks on peri-implant strain. *Int. J. Oral Maxillofac. Implants* **27**, 529–536 (2012).
78. Alikhasi, M., Bassir, S. H. & Naini, R. B. Effect of multiple use of impression copings on the accuracy of implant transfer. *Int. J. Oral Maxillofac. Implants* **28**, 408–414 (2013).
79. Papaspyridakos, P., Benic, G. I., Hogsett, V. L., White, G. S., Lal, K. & Gallucci, G. O. Accuracy of implant casts generated with splinted and non-splinted impression techniques for edentulous patients: an optical scanning study. *Clin. Oral Implants Res.* **23**, 676–681 (2012).
80. Tan, M. Y., Yee, S. H. X., Wong, K. M., Tan, Y. H. & Tan, K. B. C. Comparison of Three-Dimensional Accuracy of Digital and Conventional Implant Impressions: Effect of Interimplant Distance in an Edentulous Arch. *Int. J. Oral Maxillofac. Implants* (2018) doi:10.11607/jomi.6855.
81. Fluegge, T., Att, W., Metzger, M. & Nelson, K. A Novel Method to Evaluate Precision of Optical Implant Impressions with Commercial Scan Bodies-An Experimental Approach. *J. Prosthodont. Off. J. Am. Coll. Prosthodont.* (2015) doi:10.1111/jopr.12362.
82. Gracis, S., Michalakis, K., Vigolo, P., Vult von Steyern, P., Zwahlen, M. & Sailer I. Internal vs. external connections for abutments/reconstructions: a systematic review. *Clin. Oral Implants Res.* **23 Suppl 6**, 202–216 (2012).
83. Papaspyridakos, P., Hirayama, H., Chen, C. J., Ho, C. H., Chronopoulos, V. & Weber, H. P. Full-arch implant fixed prostheses: a comparative study on the effect of connection type and impression technique on accuracy of fit. *Clin. Oral Implants Res.* **27**, 1099–1105 (2016).
84. Schmidt, A., Billig, J.-W., Schlenz, M. A., Rehmann, P. & Wöstmann, B. Influence of the Accuracy of Intraoral Scanbodies on Implant Position: Differences in Manufacturing Tolerances. *Int. J. Prosthodont.* **32**, 430–432 (2019).
85. Arcuri, L., Pozzi, A., Lio, F., Rompen, E., Zechner, W. & Nardi A. Influence of implant scanbody material, position and operator on the accuracy of digital impression for complete-arch: A randomized in vitro trial. *J. Prosthodont. Res.* **64**, 128–136 (2020).
86. Nedelcu, R., Olsson, P., Nyström, I. & Thor, A. Finish line distinctness and accuracy in 7 intraoral scanners versus conventional impression: an in vitro descriptive comparison. *BMC Oral Health* **18**, (2018).

87. Zekiy, A. O., Makurdumyan, D. A., Matveeva, E. A., Bogatov, E. A. & Kaliiants, T. V. Antiseptic sealant and a nanocoated implant-abutment interface improve the results of dental implantation. *Clin. Implant Dent. Relat. Res.* **21**, 938–945 (2019).
88. Toia, M., Stocchero, M., Jinno, Y., Wennerberg, A., Becktor, J. P., Jimbo, R. & Halldin A. Effect of Misfit at Implant-Level Framework and Supporting Bone on Internal Connection Implants: Mechanical and Finite Element Analysis. *Int. J. Oral Maxillofac. Implants* **34**, 320–328 (2019).
89. Cho SH, Schaefer O, Thompson GA, Guentsch A. Comparison of accuracy and reproducibility of casts made by digital and conventional methods. - PubMed - NCBI. https://www.ncbi.nlm.nih.gov/pubmed/25682531?dopt=Abstract (2015).
90. Jang Y, Sim Y, Park JK, Kim WC, Kim HY, Kim JH. Evaluation of the marginal and internal fit of a single crown fabricated based on a three-dimensional printed model. https://www.ncbi.nlm.nih.gov/pmc/articles/PMC6202428/ (2018).
91. Revilla-León, M., Gonzalez-Martín, Ó., Pérez López, J., Sánchez-Rubio, J. L. & Özcan, M. Position Accuracy of Implant Analogs on 3D Printed Polymer versus Conventional Dental Stone Casts Measured Using a Coordinate Measuring Machine. *J. Prosthodont. Off. J. Am. Coll. Prosthodont.* **27**, 560–567 (2018).
92. Arce, C., Lawson, N. C., Liu, P.-R., Lin, C. P. & Givan, D. A. Retentive Force of Zirconia Implant Crowns on Titanium Bases Following Different Surface Treatments. *Int. J. Oral Maxillofac. Implants* **33**, 530–535 (2018).
93. Lopes, A. C. de O., Machado, C. M., Bonjardim, L. R., Bergamo, E. T. P., Ramalho, I. S., Witek, L., Coelho, P. G. & Bonfante, E. A. The Effect of CAD/CAM Crown Material and Cement Type on Retention to Implant Abutments. *J. Prosthodont.* **0**,.
94. Pitta, J., Hicklin, S. P., Fehmer, V., Boldt, J., Gierthmuehlen, P. C. & Sailer, I. Mechanical stability of zirconia meso-abutments bonded to titanium bases restored with different monolithic all-ceramic crowns. *Int. J. Oral Maxillofac. Implants* **34**, 1091–1097 (2019).
95. Mehl, C., Zhang, Q., Lehmann, F. & Kern, M. Retention of zirconia on titanium in two-piece abutments with self-adhesive resin cements. *J. Prosthet. Dent.* **120**, 214–219 (2018).

96. Dellinges, M. A. & Tebrock, O. C. A measurement of torque values obtained with hand-held drivers in a simulated clinical setting. *J. Prosthodont. Off. J. Am. Coll. Prosthodont.* **2**, 212–214 (1993).
97. Tan, K. B. & Nicholls, J. I. The effect of 3 torque delivery systems on gold screw preload at the gold cylinder-abutment screw joint. *Int. J. Oral Maxillofac. Implants* **17**, 175–183 (2002).
98. Stimmelmayr, M., Güth, J.-F., Erdelt, K., Edelhoff, D. & Beuer, F. Digital evaluation of the reproducibility of implant scanbody fit—an in vitro study. *Clin. Oral Investig.* **16**, 851–856 (2012).
99. Kim, S.-J., Son, K. & Lee, K.-B. Digital evaluation of axial displacement by implant-abutment connection type: An in vitro study. *J. Adv. Prosthodont.* **10**, 388–394 (2018).
100. Alonso-Pérez, R., Bartolomé, J. F., Ferreiroa, A., Salido, M. P. & Pradíes, G. Original vs. non-original abutments for screw-retained single implant crowns: An in vitro evaluation of internal fit, mechanical behaviour and screw loosening. *Clin. Oral Implants Res.* **29**, 1230–1238 (2018).
101. Harper, K. A. & Setchell, D. J. The use of shimstock to assess occlusal contacts: a laboratory study. *Int. J. Prosthodont.* **15**, 347–352 (2002).
102. Lin, W.-S., Harris, B. T., Elathamna, E. N., Abdel-Azim, T. & Morton, D. Effect of implant divergence on the accuracy of definitive casts created from traditional and digital implant-level impressions: an in vitro comparative study. *Int. J. Oral Maxillofac. Implants* **30**, 102–109 (2015).
103. Rutkunas, V., Sveikata, K. & Savickas, R. Effects of implant angulation, material selection, and impression technique on impression accuracy: a preliminary laboratory study. *Int. J. Prosthodont.* **25**, 512–515 (2012).
104. Lee, J.-H., Kim, D.-G., Park, C.-J. & Cho, L.-R. Axial displacements in external and internal implant-abutment connection. *Clin. Oral Implants Res.* **25**, e83-89 (2014).
105. Neugebauer J. Comparison of design and torque measurements of various manual wrenches. - PubMed - NCBI. https://www.ncbi.nlm.nih.gov/pubmed/26009903.
106. Calderini, A., Maiorana, C., Garlini, G. & Abbondanza, T. A simplified method to assess precision of fit between framework and supporting implants: a preliminary study. *Int. J. Oral Maxillofac. Implants* **22**, 831–838 (2007).

107. Kurz, M., Attin, T. & Mehl, A. Influence of material surface on the scanning error of a powder-free 3D measuring system. *Clin. Oral Investig.* **19**, 2035–2043 (2015).
108. Ender, A., Zimmermann, M. & Mehl, A. Accuracy of complete- and partial-arch impressions of actual intraoral scanning systems in vitro. *Int. J. Comput. Dent.* **22**, 11–19 (2019).

SANTRAUKA

SANTRUMPŲ SĄRAŠAS

CAD/CAM – kompiuterinis modeliavimo ir gamybos metodas

3D – trimatis

DW – skaitmeninis gamybos būdas

CW – analoginis gamybos būdas

IOS – intraoralinis skeneris

SB – skenavimo kūnas

SEM – skenuojantis elektroninis mikroskopas

DII – implantų skaitmeninis atspaudas

CII – implantų analoginis atspaudas

CMM – koordinacinė matavimų mašina

MB – meziobukalinis

DB – distobukalinis

ML – meziolingvalinis

DL – distolingvalinis

M – mezialinis

D – distalinis

Ti – titaninė bazė

$\mathbf{D_{netikslumas}}$ – atstumo matavimų skirtumas, esant pasyviai ir nepasyviai situacijai

$\mathbf{D_{pasyvus}}$ – atstumas nuo viršutinio titaninės bazės krašto iki viršutinio implanto analogo krašto, esant pasyviai situacijai

$\mathbf{D_{nepasyvus}}$ – atstumas nuo viršutinio titaninės bazės krašto iki viršutinio implanto analogo krašto, esant nepasyviai situacijai

$D_{cemento}$ – trumpiausias atstumas nuo apatinio cirkonio oksido restauracijos krašto iki viršutinio titaninės bazės krašto

Δ – skirtumas tarp apskaičiuotų parametrų

STL – standartinė teselacijos kalba

SR – protezinio varžtelio pasipriešinimas

RS – atskaitinis skenavimas

MIOS – modelio skenavimas intraoraliniu skeneriu

ISO – Tarptautinė standartizacijos organizacija

SD – standartinis nuokrypis

NS – statistiškai nereikšmingas

IQR – tarpkvartilinis skirtumas

P – pasyvus

NP – nepasyvus

1. ĮVADAS

1.1. Tyrimo aktualumas

Skaitmeninės technologijos reikšmingai pakeitė klinikines ortopedinės odontologijos procedūras, praplėtė pacientų diagnostikos ir tolesnės priežiūros galimybes. CAD/CAM (angl. *computer-aided design/computer-aided manufacturing*) technologija leido pagreitinti protezų gamybos eigą, o optiniai atspaudai, skaitmeninis protezų modeliavimas, frezavimas, nenaudojant vaškavimo ir modelių, tapo kasdienė praktika[1]. Palyginti su analogais, optinių atspaudų privalumai, pavyzdžiui, laiko ir finansinių išteklių taupymas, malonesnės procedūros pacientui, greitesnis bendravimas su dantų technikų laboratorija, patogesnis gydymo planavimas, mokslinėje literatūroje aptariami gana plačiai[2–6]. Be to, CAD/CAM ir 3D (angl. *three-dimmensional*) spausdinimo galimybės leido pagreitinti protezų gamybą ir naudoti naujas medžiagas, tokias kaip cirkonio oksidas, ličio disilikatas ir keramikos dalelėmis sustiprintas kompozitas[7].

Vis dėlto pagrindinė problema išlieka tai, jog skaitmeninių atspaudų ir pagal juos pagamintų restauracijų ant dantų bei implantų tikslumas vis dar nepakankamai ištirtas. Kaupiantis paklaidoms klinikiniuose ir laboratoriniuose protezų gamybos etapuose, tam tikras protezų netikslumas yra neišvengiamas. Kauliniame audinyje integruoti implantai nejuda, todėl nelieka galimybės kompensuoti protezų ant implantų netikslumų. Deja, daugelis šias problemas analizuojančių publikuotų mokslinių tyrimų atlikti laboratorinėmis sąlygomis ir tik keli *in vivo*[8–10, 12, 110]. Laboratoriniuose eksperimentuose eliminuojama drėgmė, minkštieji audiniai, optinių prietaisų rasojimas, o tai gali reikšmingai paveikti tyrimo rezultatus. Be to, sudėtingi eksperimentų dizainai ir metodologijos apsunkina rezultatų interpretacijas, laboratorinėmis sąlygomis gautos rezultatų reikšmės sunkiai pritaikomos klinikinėje praktikoje[10].

Tikslus implanto erdvinės padėties ir santykio su greta esančiais implantais ar dantimis perkėlimas yra esminis atspaudo tikslas, siekiant pagaminti bedančio ar dalinai bedančio žandikaulio tikslų protezą ant implantų ir išvengti biologinių ar techninių komplikacijų[13]. Mokslinėje literatūroje aprašomi įvairūs metodai implantų atspaudų tikslumui nustatyti: kampo ir atstumo tarp implantų matavimas[14, 15, 111], skenavimo kūnų trimatis sutapdinimas[17], vertikalios implanto pozicijos registravimas[18, 19] bei gipsinių ir spausdintų modelių palyginimas[18]. Papildomų atskaitos taškų pritvirtinimas ilgose bedantėse zonose taip pat aprašomas kaip patikimas metodas atspaudų tikslumui pagerinti[20–22]. Laboratoriniai ir klinikiniai metodai dalinių ir pilnųjų protezų ant implantų

pasyvumui įvertinti taip pat aptariami mokslinėse publikacijose[23–25], tačiau vis dar trūksta informacijos, kaip dalinių ir pilnųjų protezų tikslumą veikia kampas ir atstumas tarp implantų. Be to, kiekybinė klinikinių tyrimų informacija leistų tiksliau įvertinti protezo tikimą burnoje.

1.2. Literatūros apžvalga

Nuo 1980 m. ištobulėjus intraoraliniams skeneriams ir jų programinei įrangai, vis dar išliko tikslumo apribojimų klinikinėse situacijose, kai protezuojama didesnė restauracija ant kelių implantų ar bedančiai žandikauliai. Tokie veiksniai, kaip skenavimo strategija, implantų skaičius, didelės bedantės zonos tarp implantų bei skenavimo kūnų ypatybės, yra vieni pagrindinių, lemiančių kliniškai reikšmingus atspaudų ir restauracijų netikslumus[15, 16, 42]. Be to, imant atspaudus, gaminant modelius ir restauracijas, smulkios paklaidos kaupiasi, todėl, kaip jau minėta, tam tikras galutinis protezų netikslumas yra neišvengiamas. Naudojant analoginį restauracijų gamybos būdą, daugelis veiksnių, tokių kaip dimensiniai atspaudinių medžiagų, gipsinių modelių pokyčiai, vaškavimas, liejimo procesai, daro neigiamą įtaką galutiniam protezo tikslumui. Skaitmeninės technologijos gelbėja eliminuojant kai kuriuos analoginio būdo trūkumus, tačiau atsiranda specifinių intraoralinio skenavimo, CAD/CAM, 3D spausdinimo paklaidų, todėl šiandienėje praktikoje daugiausia taikomas kombinuotas analoginis ir skaitmeninis protezų gamybos būdas.

Tikslus implantų atspaudas yra pagrindinis veiksnys, siekiant pagaminti ilgai tarnaujančią, pasyvią ir estetišką restauraciją. Kauliniame audinyje integruoti implantai yra stabilūs, todėl netikslios restauracijos gali išprovokuoti mechanines (protezinio varžtelio atsipalaidavimas, apdailos nuskilimas) arba biologines (periimplantitas, perimukozitas) komplikacijas[43]. Pasyvumas yra vienas iš svarbiausių prisukamo ant implantų protezo sėkmę lemiančių veiksnių. Prisukamos ant implantų restauracijos pasyvumas mokslinėje literatūroje apibrėžiamas kaip maksimalus implanto ir protezavimo komponento tarpusavio atitikimas be jokių įtampos jėgų, kai fiksacinis varžtelis yra priveržtas iki galo[23, 44]. Nors duomenys apie nepasyvios restauracijos ant implantų sukeltas biologines ir technines komplikacijas yra kontroversiški, vis dėlto visiškas restauracijų pasyvumas kliniškai yra neįmanomas[23–25]. Aprašomos įvairios metodikos restauracijų ant implantų tikslumui nustatyti. Laboratorinėmis sąlygomis dažniausiai naudojamas optinis arba skenuojantis elektroninis mikroskopas (SEM) atstumui nuo atramos iki implanto krašto išmatuoti. Taikant baigtinių elementų analizę, matuojama fotoelastinė įtampa modeliuose arba atliekamas paviršiaus sutapimo vertinimas, lyginant fizines restauracijas ar modelius su

skaitmeniniais[45]. Klinikinėje praktikoje restauracijų netikslumai dažniausiai aptinkami zonduojant, atliekant balansavimo testą, vieno varžtelio prisukimo (Šefildo) testą. Rentgenografija ir protezinio varžtelio pasipriešinimo testas naudojami kaip papildomi metodai[23, 44, 45].

Kasdienėje praktikoje sparčiai diegiamos skaitmeninės technologijos, todėl įrodymais pagrįsta informacija apie skaitmeninių atspaudų ir skaitmeniniu būdu pagamintų restauracijų ant implantų tikslumą yra labai svarbi[46–48]. Deja, dauguma tyrimų, vertinančių skaitmeninių atspaudų tikslumą, atlikti *in vitro* sąlygomis. Apžvelgiami duomenys varijuoja nuo vieno implanto atspaudo[18, 19] iki kelių atspaudų[14, 28, 46, 49–51, 84] ar viso bedančio žandikaulio lanko[15, 16, 51–53]. Siekiant palyginti analoginius ir skaitmeninius implantų atspaudus, naudoti skirtingi tyrimų protokolai, tačiau dažniausiai matuotas atstumas, kampas[37, 51, 52] tarp skenavimo kūnų ar jų paviršiaus sutapimo laipsnis[17, 49], vertintas modelių[18, 19] ir restauracijų ant implantų[54, 55] tikslumas. Atspaudo tikslumas dažniausiai vertinamas kaip tikrumo ir preciziškumo kombinacija pagal ISO 5725-1:1994 standartą. Tikrumas apibūdinamas kaip skenuoto objekto nuokrypis nuo tikrųjų objekto dimensijų. Preciziškumas išreiškia, kaip atskiri skenavimai skyrėsi vienas nuo kito (skenavimo atkartojamumas).

Mokslinėje literatūroje aprašyta keletas tyrimų, kuriais buvo lyginami modeliai iš analoginių ir skaitmeninių atspaudų restauracijai ant vieno implanto. Vienu iš šių tyrimų nustatyta, kad vertikalus implanto analogo poslinkis frezuotame modelyje buvo 93 µm[19], kitame tyrime nurodoma vidutinė paklaida daug mažesnė – 14±170 µm, bet turinti didelį standartinį nuokrypį[18]. Lyginant skaitmeninį atspaudą su analoginiu, nustatytas skirtumas –6±40 µm. Skaitmeninio protezų gamybos būdo paklaidų analizė rodo, jog didžiausias netikslumų šaltinis yra frezavimo procesas ir implantų analogų pozicionavimas, bet ne pats skaitmeninis atspaudas. Laboratorinėse studijose taip pat nustatyta, jog naudojant naujesnės kartos intraoralinius skenerius, tiesinių matavimų paklaidos neviršija 100 µm, kai skenuojama fiksuotoms dalinėms restauracijoms ant kelių implantų[14, 28, 46, 50, 51, 56].

Kitų *in vitro* tyrimų metu analizuoti visiškai bedančių žandikaulių keturių[37, 57, 58], penkių[17, 50, 59] ar šešių[15, 16, 49, 52] implantų skaitmeniniai atspaudai. Teigiama, jog skaitmeninių atspaudų tikslumas statistiškai reikšmingai nesiskiria nuo analoginių atspaudų, todėl skaitmeniniai atspaudai klinikinėje praktikoje gali būti naudojami kaip patikrinta alternatyva.

Minėtini tyrimai, kuriais analizuota kampo tarp implantų įtaka skaitmeninių atspaudų tikslumui. Šiuose tyrimuose atskaitos modeliai buvo implantai, kurių pasvirimo kampas varijavo nuo 10[17] iki 45[37] laipsnių. Kliniškai priimtinas atskaitos taškas, kai kampo tarp implantų skenavimo

paklaida neigiamai veikia skaitmeninio atspaudo tikslumą, mokslinėje literatūroje nėra apibrėžtas, tačiau, remdamiesi trigonometriniais skaičiavimais (ir priėmę, kad galimas maksimalus šoninis implanto judesys yra iki 50 µm, o implanto ilgis – 14,8 mm), Andriessenas ir bendraautoriai[60] teigia, kad 0,4° kampo skenavimo paklaida skaitmeninio atspaudo netikslumų nelemia.

Protezo tinkamumui[45, 48, 61, 62] gali turėti įtakos ne tik implantų atspaudo metodika, bet ir darbinio modelio gamyba, frezavimo procesas, restauracijų medžiagos tipas. Mokslinėje literatūroje protezo netikslumas apibrėžiamas kaip rizikos veiksnys, lemiantis cementuojamos ar prisukamos restauracijos ant implantų ilgalaikę sėkmę. Vis dėlto kliniškai reikšminga kraštinio netikslumo riba nėra patvirtinta įrodymais – aprašyti duomenys varijuoja nuo 10[63] iki 150[64] µm. Remiantis Katsoulis ir bendraautorių[44] nuomone, egzistuoja biologinė ir mechaninė tolerancija restauracijų ant implantų netikslumams, todėl didžiausias kraštinio tarpo netikslumas ar įtampos jėgų ve»tės (proteziniam varžteliui, implantui ar implanto ir kaulo kompleksui) iš viso negali būti apibrėžtos. Klinikinėje praktikoje naudojami metodai, pavyzdžiui, vizualinis taktilinis, rentgenografija, nėra pakankamai jautrūs diagnozuojant mažesnį negu 50 µm tarpelį ties kraštine restauracijos riba, o didesniems negu 150 µm netikslumams aptikti sudėtingų metodų nereikia. Be to, kauliniame audinyje aptinkamos įtampos jėgos ties nepasyviomis restauracijomis linkusios mažėti, nes pastebima kaulo remodeliacija, kai restauracijos ant implantų apkraunamos statiškai ir dinamiškai[65].

1.3. Tyrimo tikslas

Tyrimo tikslas – įvertinti ir palyginti implantų analoginių ir skaitmeninių atspaudų bei dalinių protezų ant implantų, gamintų naudojant skaitmeninį ir analoginį būdą *in vivo* ir *in vitro* sąlygomis, tikslumą.

1.4. Tyrimo uždaviniai

1. Palyginti implantų skaitmeninių atspaudų tikslumą, bedančių ir dalinai bedančių žandikaulių modelius skenuojant penkiais intraoraliniais skeneriais.
2. Įvertinti papildomų atskaitos taškų įtaką implantų atspaudų tikslumui, skenuojant penkiais intraoraliniais skeneriais laboratorinėmis sąlygomis.
3. Palyginti implantų skaitmeninių atspaudų tikslumą, skenuojant dviem skirtingais intraoraliniais skeneriais *in vivo* ir atliekant atstumo tarp

skenavimo kūnų, kampo tarp implantų, skenavimo kūnų rotacijos, vertikalaus poslinkio ir paviršiaus sutapimo matavimus.

4. Įvertinti atstumo ir kampo tarp implantų įtaką implantų skaitmeninių atspaudų tikslumui *in vivo*.

5. Įvertinti ir palyginti skaitmeniniu ir analoginiu būdu gamintų cirkonio oksido restauracijų, fiksuotų ant dviejų implantų, tinkamumą klinikinėmis sąlygomis ($D_{netikslumas}$).

6. Palyginti cemento tarpelio skirtumus skaitmeniniu ir analoginiu būdu gamintose cirkonio oksido restauracijose, fiksuotose ant dviejų implantų ($D_{cemento}$).

7. Įvertinti ir palyginti protezinio varžtelio prisukimo pasipriešinimą klinikinėmis ir laboratorinėmis sąlygomis ant dviejų implantų fiksuotose cirkonio oksido restauracijose, gamintose skaitmeniniu ir analoginiu būdu.

8. Palyginti ir įvertinti intraoralinio skenerio tikslumą skenuojant bedančius žandikaulius restauracijoms ant implantų *in vivo* ir *in vitro*.

1.5. Ginamieji teiginiai

1. Vertingas įrankis dalinių ir pilnųjų protezų ant implantų skaitmeninių atspaudų tikslumui gerinti yra skenuojant naudojami papildomi atskaitos taškai.

2. Kliniškai nėra statistiškai reikšmingo skirtumo tarp skaitmeninių ir analoginių atspaudų tikslumo, kai skenuojami fiksuoti tiltiniai protezai ant dviejų implantų.

3. Atstumas ir kampas tarp implantų turi įtakos skaitmeninių ir analoginių atspaudų tikslumo skirtumams.

4. Cirkonio oksido protezų ant dviejų implantų, gamintų skaitmeniniu ir analoginiu būdu, tinkamumas kliniškai nesiskiria.

5. Implantų skaitmeninio atspaudo tikslumas, skenuojant klinikinėmis ir laboratorinėmis sąlygomis, nesiskiria.

1.6. Medžiaga ir metodai

Tyrimas apima implantų skaitmeninių atspaudų tikslumo *in vitro* įvertinimą, skaitmeninių, analoginių atspaudų ir cirkonio oksido restauracijų, gamintų skaitmeniniu ir analoginiu būdu, *in vivo* įvertinimą ir implantų skaitmeninių atspaudų *in vivo* ir *in vitro* sąlygomis palyginimą. Klinikinė tyrimo dalis atlikta remiantis Helsinkio deklaracijos standartais, gautas Vilniaus regioninio skyriaus bioetikos leidimas (Nr. 158 200-16-861-370).

Visi tyrime dalyvavę pacientai prieš tyrimą užpildė ir pasirašė sutikimo dalyvauti tyrime formas. Pacientų tyrimo eiga sudaryta remiantis <https://www.random.org/> programa.

2. TIKSLUMO VERTINIMAS *IN VITRO*

3D spausdintuvu *Asiga Max* UV (*Asiga*, Australija) atspausdinti dviejų tipų viršutinio žandikaulio modeliai. Pirmajame modelyje trūksta dviejų kaplių ir dviejų krūminių dantų dešinėje pusėje, todėl buvo įsukti du *Straumann* BLT RC 4,1 mm diametro (*Straumann*, Šveicarija) implantai (pirmojo kaplio vietoje tiesus, o antrojo krūminio danties vietoje – pasviręs mezialiai 20° kampu). Antrajame bedančiame modelyje tokie pat implantai įsukti simetriškai: antrųjų kandžių vietoje tiesūs, o pirmųjų krūminių dantų vietoje – pasvirę distaliai 20° kampu. Skenavimo kūnus (CARES RC *Mono scan body*, *Straumann*, Šveicarija) priveržus 15 Ncm jėga, modeliai nuskenuoti *Nicon Altera* 10.7.6 (*Nikon Metrology*, Japonija) skeneriu ir suformuoti atskaitiniai virtualūs modeliai. Vėliau modeliai skenuoti skirtingais intraoraliniais skeneriais *Primescan* (*Dentsply Sirona*, JAV, 5.0.1 versija), *Trios* 3 (3*Shape*, Danija, 1.18.2.10 versija), *Trios* 4 (3*Shape*, Danija, 19.2.2 versija), CS3600 (*Carestream dental*, JAV, 3.1.0 versija), *Medit* i500 (*Medit*, Pietų Korėja, 2.0.3 versija) po 10 kartų (n = 10) be papildomų atskaitos taškų. Skenavimas atliktas pagal kiekvieno skenerio gamintojo rekomendacijas. Vėliau abiejų modelių bedantėse zonose priklijuotos stiklojonomerinio cemento tabletės, kaip papildomas atskaitos taškas skenuojant. Modeliai dar kartą skenuoti po 10 kartų (n = 10) penkiais skirtingais skeneriais. Gauta informacija išsaugota STL (angl. *Standard tessellation language*) formatu tolesnei analizei. Atskaitinių, be papildomų skenavimo atskaitos taškų ir su jais modelių palyginimas atliktas matuojant atstumą tarp skenavimo kūnų, kampą tarp implantų ir vertikalų skenavimo kūnų poslinkį. Skenavimo tikslumas vertintas kaip tikrumo ir preciziškumo kombinacija. Statistinė analizė atlikta *Matlab* 2020a (*The MathWorks Inc*., JAV) statistikos programa. Siekiant nustatyti, ar duomenys pasiskirstę pagal normalųjį skirstinį, taikytas Šapiro ir Vilko testas. Gautiems duomenims palyginti taikytas Stjudento t kriterijus priklausomoms imtims arba Mano ir Vitnio Vilkoksono kriterijus. Reikšmingumo lygmuo – 0,05. Kriterijų galiai apskaičiuoti taikyta *GPower* (*Dusseldorf University*, Vokietija, 3.1.9.2 versija) programa.

3. TIKSLUMO VERTINIMAS *IN VIVO*

3.1. Implantų atspaudų tikslumo vertinimas

Implantų atspaudų tikslumo vertinimas atliktas dviem eksperimentais pagal tą patį protokolą.

A. Implantų analoginių ir skaitmeninių atspaudų palyginimas, naudojant *Trios* intraoralinį skenerį

Tyrime dalyvavo 20 pacientų, kuriems buvo reikalingos 27 fiksuotos dalinės restauracijos ant dviejų implantų (*AnyOne, Megagen*, Pietų Korėja). Skaitmeniniams atspaudams naudotas *Trios* (3*Shape*, Danija, 1.3.3.1 versija) intraoralinis skeneris. Atspaudai imti dviejų (n = 10), trijų (n = 11) ir keturių (n = 6) vienetų cirkonio oksido restauracijoms ant dviejų implantų. Trys restauracijos buvo priekinių dantų srityje, o dvidešimt keturios – galinių dantų srityje. Vidutinis atstumas tarp implantų – 14,3±7 mm.

B. Implantų analoginių ir skaitmeninių atspaudų palyginimas, naudojant *Trios* 3 intraoralinį skenerį

Antrame eksperimente dalyvavo šeši pacientai, kuriems pagamintos 24 fiksuotos dalinės cirkonio oksido restauracijos ant dviejų implantų galinių dantų srityje (*AnyOne, Megagen*, Pietų Korėja): dviejų (n = 7), trijų (n = 11) ir keturių (n = 6) vienetų. Skaitmeniniams atspaudams naudota *Trios* 3 IOS (3*Shape*, Danija, 1.3.4.2 versija). Vidutinis atstumas tarp implantų – 15,82±5,66 mm.

Abiejų tyrimų metu analoginiai atspaudai imti naudojant vinil-polisiloksaninę atspaudinę masę (*Express*, 3M, JAV), suformuota duomenų grupė (CII). Atspaudinės detalės sujungtos kietėjančiomis šviesoje (*Individolux*, VOCO, Vokietija) ir savaime kietėjančiomis (*Pattern Resin*, GC, Japonija) plastmasėmis, patikrinta, ar sujungta konstrukcija tinka, ir tik įsitikinus, kad konstrukcija prie implantų prisisuka tinkamai, ji naudota atspaudams. Implantų skaitmeniniams atspaudams taikyti originalūs skenavimo kūnai (*AnyOne Internal scan body, Megagen*), prisukti 15 Ncm jėga, skenuota *Trios* ir *Trios* 3 intraoraliniais skeneriais pagal gamintojo rekomenduotą skenavimo eigą (DII duomenų grupė). Darbiniai modeliai pagal gamintojo instrukciją pagaminti iš IV klasės gipso (*FujiRock*, GC, Japonija) ir palikti stabilioje temperatūroje 24 val. sustingti. Modelių tikslumas patikrintas naudojant sujungtas atspaudines detales pagal jau

aprašytą metodiką, atliktas konstrukcijos balansavimo, vieno varžtelio ir protezinio varžto pasipriešinimo Šefildo testai. Vėliau prie modelių tokia pat kryptimi 15 Ncm jėga pritvirtinti tie patys skenavimo kūnai, modeliai skenuoti laboratoriniu D800 (3*Shape*, Danija) skeneriu, gauti duomenys išsaugoti STL formatu. Trimačiai skaitmeniniai modeliai palyginti su modeliais, gautais skenuojant intraoraliniais skeneriais burnoje, ir aukštos rezoliucijos CAD trimačiais skaitmeniniais modeliais, naudojant atvirkštinės inžinerijos programą. Duomenims lyginti išmatuoti parametrai: atstumas tarp skenavimo kūnų, kampas tarp implantų, skenavimo kūnų rotacija, vertikalus poslinkis ir skenavimo kūno paviršiaus sutapimas. Siekiant įvertinti atstumo tarp skenavimo kūnų ir kampo tarp implantų įtaką analoginių ir skaitmeninių atspaudų pasirinktų matavimų skirtumams, buvo apskaičiuotas išvestinis dydis – vidutinis atstumas tarp skenavimo kūnų ir vidutinis kampas tarp implantų pagal formulę:

(D800 duomenys + IOS duomenys)/2.

Statistinei analizei naudota R programa (*Lucent Technologies*, Naujoji Zelandija, 2.3–2 versija). Norint nustatyti, ar duomenys pasiskirstę pagal normalųjį skirstinį, atliktas Šapiro ir Vilko testas. Gautiems duomenims palyginti taikytas Stjudento t kriterijus priklausomoms imtims arba Mano ir Vitnio Vilkoksono kriterijus. Reikšmingumo lygmuo – 0,05. Kriterijų galiai apskaičiuoti taikyta *GPower* (*Dusseldorf University*, Vokietija, 3.1.9.2 versija) programa.

3.2. Restauracijų ant dantų implantų tikslumo vertinimas

3.2.1. Restauracijų ant dantų implantų tikimo vertinimas

Šešiems pacientams pagamintos 24 dalinės fiksuotos cirkonio oksido restauracijos ant dviejų implantų: dviejų (n = 7), trijų (n = 11) ir keturių (n = 6) vienetų. Keturiolika restauracijų buvo viršutiniame žandikaulyje, o dešimt – apatiniame, visos buvo galinių dantų srityje.

Kiekvienu atveju pagaminta po dvi cirkonio oksido restauracijas: po vieną iš analoginių atspaudų (C grupė) ir po vieną iš skaitmeninių atspaudų (D grupė), skenavimui naudojant *Trios* 3 IOS (3*Shape*, Danija), iš viso – 48 restauracijos. Restauracijų dizainas susideda iš dviejų cilindrų, sujungtų sija, kad nesiremtų į gretimus ir antagonuojančius dantis, būtų minimalaus diametro ties dantenomis ir neapsunkintų protezo fiksavimo burnoje. Darbiniai gipsiniai modeliai pagaminti pagal analoginius atspaudus,

patikrintas jų tinkamumas, modeliai nuskenuoti laboratoriniu skeneriu D800 (3*Shape*, Danija). Išfrezavus 24 cirkonio oksido restauracijas, patyręs dantų technikas sucementavo jas su beheksėmis originaliomis titaninėmis bazėmis (*AnyOne, Megagen*), prisuktomis prie implantų analogų. Taip suformuota C tiriamųjų grupė. D duomenų grupei suformuoti implantų padėtys nuskenuotos intraoraliniu skeneriu burnoje, naudojant *Trios* 3 IOS ir originalius skenavimo kūnus. Taikant tuos pačius parametrus, kaip ir C grupėje, išfrezuotos dar 24 cirkonio oksido restauracijos, tačiau jos sucementuotos su beheksėmis titaninėmis bazėmis, netaikant modelio stebėjimo mikroskopu. Tiek C, tiek D grupių restauracijos po cementavimo kruopščiai nuvalytos garais ir alkoholiniu tirpalu.

C ir D grupių restauracijos pritvirtintos prie darbinio modelio atsitiktine tvarka skalpeliu pažymėtuose keturiuose taškuose: meziobukaliai (MB), distobukaliai (DB), meziolingvaliai (ML), distolingvaliai (DL). Matuota skenuojančiu elektroniniu mikroskopu (SEM) (*Hitachi* TM-1000, *Hitachi High-Technologies Corporation*, Japonija) padidinus 150 kartų. Prisukus mezialiai esančio implanto protezinį varžtelį 35 Ncm jėga, o distaliai esančio implanto varžtelio neprisukus visai, buvo laikoma, kad pirmasis varžtelis yra pasyvus. Tris kartus išmatuotas atstumas visuose MB, DB, ML, DL taškuose nuo viršutinio Ti bazės krašto iki viršutinio implanto analogo krašto ties mezialiniu implantu ($D_{pasyvus}$). Distalinio implanto protezinis varžtelis prisuktas 20 Ncm jėga. Laikyta, kad jis yra nepasyvus. Išmatuotas atstumas nuo Ti bazės viršutinio krašto iki implanto analogo viršutinio krašto tuose pačiuose taškuose ($D_{nepasyvus}$). Iš viso atlikti 576 matavimai, trys atmesti dėl SEM vaizdų netikslumų. Atstumų tarp pasyvaus ir nepasyvaus implanto skirtumas ($D_{netikslumas}$) apskaičiuotas pagal formulę:

$$D_{netikslumas} = D_{nepasyvus} - D_{pasyvuus}.$$

$D_{netikslumas}$ skirtumai C ir D grupėse vėliau panaudoti siekiant įvertinti asociacijas su atstumo tarp skenavimo kūnų ir kampo tarp implantų matavimais, todėl naujas parametras $\Delta D_{netikslumas}$ apskaičiuotas pagal formulę:

$$\Delta D_{netikslumas} = D_{netikslumas}\,(\text{C grupė}) - D_{netikslumas}\,(\text{D grupė}).$$

Cemento tarpas C ir D grupių restauracijose ($D_{cementas}$) išmatuotas kaip trumpiausias atstumas nuo žemiausio cirkonio oksido restauracijos krašto iki Ti bazės viršutinio krašto po tris kartus MB, DB, ML, DL mezialinio ir distalinio implantų analogų taškuose SEM padidinus 1 000 kartų, iš viso atlikti 576 matavimai. $D_{cemento}$ skirtumai C ir D grupėse vėliau panaudoti

vertinant asociacijas su atstumo tarp skenavimo kūnų ir kampo tarp implantų matavimais, todėl naujas parametras $\Delta D_{cemento}$ apskaičiuotas pagal formulę:

$$\Delta D_{cemento} = D_{cemento}\,(\text{C grupė}) - D_{cemento}\,(\text{D grupė}).$$

Statistinei analizei naudota R programa (*Lucent Technologies,* Naujoji Zelandija, 2.3–2 versija). Norint išsiaiškinti, ar duomenys pasiskirstę pagal normalųjį skirstinį, atliktas Šapiro ir Vilko testas. Kadangi duomenys nebuvo pasiskirstę pagal normalųjį skirstinį, duomenų analizei taikyti Vilkoksono rangų sumų priklausomoms imtims ir Frydmano rangų sumų kriterijai. Spirmeno koreliacijos kriterijus taikytas asociacijoms tarp C ir D grupių $D_{netikslumas}$, $\Delta D_{netikslumas}$, $D_{cemento}$ ir $\Delta D_{cemento}$ duomenų ir vidutiniam atstumui tarp skenavimo kūnų bei kampui tarp implantų įvertinti. Reikšmingumo lygmuo – 0,05. Kriterijų galiai apskaičiuoti taikyta *GPower* (*Dusseldorf University,* Vokietija, 3.1.9.2 versija) programa.

3.2.2. Restauracijų ant dantų implantų pasyvumo vertinimas

Restauracijų (C (n = 24) ir D (n = 24) grupės) ir darbinių gipsinių modelių iš restauracijų ant dantų implantų tinkamumo vertinimo tyrimo medžiaga panaudota restauracijų pasyvumo analizei. Papildomai paruošti kontroliniai modeliai, burnoje sujungus atspaudines detales su šviesoje kietėjančia akriline plastmase. Pakartotinai nuėmus ir uždėjus konstrukciją ant implantų ir patikrinus jos tikslumą, prie šios konstrukcijos pritvirtinti implantų analogai. Kontroliniai modeliai pagaminti pagal tą pačią metodiką, kaip ir darbiniai modeliai.

C ir D grupių restauracijų pasyvumas vertintas burnoje, ant darbinių ir ant kontrolinių modelių. Atliktas balansavimo testas – spaudžiant pirštais vieną kraštą, tikrinta, ar tiltinė konstrukcija balansuoja; vėliau vieno varžto Šefildo testas – prisukus vieną varžtelį, stebėta, ar likusi restauracijos dalis pasikelia. Paprasta restauracijos konstrukcija užtikrino, kad ši konstrukcija nesiremtų nei į gretimus, nei į antagonuojančius dantis ar restauracijas ir dantenas. Burnoje, ant darbinio ir kontrolinio modelių, kiekvienos restauracijos pasyvumas matuotas vertinant protezinio varžtelio rotacijos kampą veržiant nuo 5 Ncm iki 35 Ncm, esant pasyviai situacijai ($SR_{pasyvus}$), kai antras varžtelis iš tiltinės restauracijos nepritvirtinamas, ir nepasyviai situacijai ($SR_{nepasyvus}$), kai vienas iš dviejų tilto varžtelių jau fiksuotas 15 Ncm jėga. Varžtelio rotacijos kampas išmatuotas prie protezinio dinamometro pritvirtinus goniometrą (*Saehan, Saehan Corporation, Bongamgongdan*, Korėja), o varžtelio pasipriešinimas apskaičiuotas pagal formulę:

$$SR = SR_{pasyvus} - SR_{nepasyvus}$$

Atlikta po 96 matavimus burnoje ir ant darbinių modelių, o ant kontrolinių modelių – 40. Apskaičiuotas vidutinis varžtelio rotacijos kampas titaninę bazę be restauracijos prisukant prie darbinio modelio nuo 5 Ncm iki 35 Ncm jėga dešimt kartų ir matuojant rotacijos kampą (87±5°), jis panaudotas kaip atskaitos taškas toliau lyginant duomenis.

Statistinei analizei naudota R programa (*Lucent Technologies,* Naujoji Zelandija, 2.3–2 versija). Siekiant išsiaiškinti, ar duomenys pasiskirstę pagal normalųjį skirstinį, atliktas Šapiro ir Vilko testas. Kadangi dauguma duomenų nebuvo pasiskirstę pagal normalųjį skirstinį, taikyti neparametriniai kriterijai. Vilkoksono rangų sumų kriterijus priklausomoms imtims naudotas norint palyginti C ir D grupių matavimus burnoje, ant darbinio ir kontrolinio modelių. Spirmeno koreliacijos kriterijus taikytas siekiant nustatyti asociacijas tarp varžtelio pasipriešinimo parametro ir atstumo tarp skenavimo kūnų bei kampo tarp implantų matavimų. Reikšmingumo lygmuo – 0,05. Kriterijų galiai apskaičiuoti taikyta *GPower* (*Dusseldorf University*, Vokietija, 3.1.9.2 versija) programa.

4. TIKSLUMO VERTINIMAS *IN VITRO* IR *IN VIVO*

Šiame tyrime dalyvavo aštuoni pacientai, turintys bent vieną bedantį žandikaulį ir keturis integruotus implantus (10 bedančių žandikaulių, 40 implantų). Kiekvienam pacientui paimti analoginiai implantų atspaudai vinil-polisiloksanine atspaudine mase (*Express,* 3M ESPE, JAV) ir pagamintos prisukamos titaninės sijos su skylutėmis: dvi antrųjų kandžių ir dvi antrųjų premoliarų srityse. Jose savaime kietėjančia akriline plastmase (*Pattern resin,* GC, Japonija) fiksuoti keturi skenavimo kūnai (CARES RC *Mono scan body, Straumann*, Šveicarija), statmeni sijos paviršiui. Sijos pritvirtintos pacientų burnose ir skenuotos *Trios* 3 (3*Shape*, Danija) intraoraliniu skeneriu 8 kartus, suformuota IOS duomenų grupė. Vėliau, atsargiai išėmus sijas iš burnos, jos fiksuotos prie darbinių modelių ir dar po 8 kartus skenuotos ant darbinių modelių, suformuota MIOS duomenų grupė. Vėliau darbiniai modeliai su sijomis skenuoti laboratoriniu skeneriu D800 (3*Shape,* Danija) po 8 kartus ir suformuota RS duomenų grupė. Taigi kiekvienas lankas skenuotas po 24 kartus, iš viso atlikta 240 skenavimų.

Duomenys analizuoti ir lyginti atvirkštinės inžinerijos programa *Geomagic Control* X 2018 (3D *Systems Corporation,* JAV), tikslumas vertintas kaip tikrumo ir preciziškumo kombinacija. Matuota atstumai ir kampai tarp skenavimo kūnų bei skenavimo kūnų paviršiaus sutapimas, lyginti IOS, MIOS ir RS grupių duomenys. Statistinei analizei naudota *MatLab* programa (*The MathWorks, Inc.*, JAV). Siekiant nustatyti, ar duomenys pasiskirstę pagal normalųjį skirstinį, atliktas Šapiro ir Vilko testas. Gautiems duomenims lyginti taikytas Stjudento t kriterijus priklausomoms imtims arba Mano ir Vitnio Vilkoksono kriterijus. Reikšmingumo lygmuo – 0,05. Kriterijų galiai apskaičiuoti taikyta *GPower* (*Dusseldorf University*, Vokietija, 3.1.9.2 versija) programa.

Toliau pateikiami pagrindiniai kiekvienos tyrimo dalies rezultatai.

4.1. Tikslumo vertinimas *in vitro*

Dalinai bedančių modelių tikrumo (angl. *trueness*) rezultatai varijuoja tarp skirtingų skenerių ir parametrų. Nors papildomi atskaitos taškai ant modelių pagerino visų penkių intraoralinių skenerių tikrumo rezultatus, tačiau statistiškai reikšmingų skirtumų tarp modelių, nenaudojant papildomų atskaitos taškų ir juos naudojant, rasta tik *Medit* i500 IOS matuojant visus parametrus ir *Primescan* atliekant kampo matavimus ($p < 0,05$) (žr. 1 lentelę).

1 lentelė. Tikrumo rodiklio rezultatai dalinai bedančiuose modeliuose, matuojant atstumą, kampą ir vertikalų poslinkį tarp skenavimo kūnų.

	Atstumas	Kampas	Vertikalus poslinkis
	Vidurkis±SD, µm	Vidurkis±SD°	Vidurkis±SD, µm
CS	190,76±172,57	–0,03±0,52	–33,68±115,13
CS_ds	117,70±232,28	0,44±0,49	–14,99±45,00
Me	**392,07±314,88**	**0,21±0,13**	**107,16±103,47**
Me_ds	**–12,17±34,55**	**–0,25±0,19**	**–69,12±45,20**
PS	–25,13±20,77	**0,22±0,04**	40,26±12,08
PS_ds	–17,45±16,11	**0,18±0,04**	36,73±10,82
T3	–46,74±15,37	–0,04±0,15	–75,60±50,41
T3_ds	–31,99±18,00	0,02±0,18	–59,48±44,86
T4	–33,36±18,10	–0,11±0,14	–107,97±47,06
T4_ds	–34,39±13,01	–0,15±0,13	–86,91±42,05

SD – standartinis nuokrypis, CS – Carestream 3600 IOS, Me – Medit i500 IOS, PS – Primescan IOS, T3 – Trios 3 IOS, T4 – Trios 4 IOS, DS – papildomas atskaitos taškas. Paryškinti statistiškai reikšmingi skirtumai tarp skenavimų, naudojant papildomus atskaitos taškus ir jų nenaudojant.

Geriausi preciziškumo (angl. *precision*) rezultatai gauti skaičiuojant *Trios* 3 IOS atstumo (12,82±7,18 µm), *Primescan* kampo (0,03±0,03°) ir vertikalaus poslinkio parametrus (9,04±7,43 µm). Vis dėlto nenustatyta statistiškai reikšmingų skirtumų tarp skenavimų, naudojant papildomus atskaitos taškus ir jų nenaudojant, tarp skirtingų IOS, išskyrus *Medit* i500, atliekant atstumo ir vertikalaus poslinkio matavimus, ir CS3600 IOS, skaičiuojant vertikalaus poslinkio parametrus (žr. 2 lentelę).

2 lentelė. Preciziškumo rodiklio rezultatai dalinai bedančiuose modeliuose, matuojant atstumą, kampą ir vertikalų poslinkį tarp skenavimo kūnų.

	Atstumas	Kampas	Vertikalus poslinkis
	Vidurkis±SD	Vidurkis±SD	Vidurkis±SD
CS	143,39±83,28	0,41±0,28	**90,62±63,37**
CS_ds	200,48±96,42	0,35±0,33	**37,06±21,33**
Me	**238,48±189,63**	0,10±0,08	**81,76±57,25**
Me_ds	**26,49±20,34**	0,14±0,11	**35,53±24,95**
PS	17,49±9,57	0,03±0,03	9,04±7,43
PS_ds	12,88±8,66	0,03±0,02	8,30±6,37
T3	12,82±7,18	0,13±0,07	37,69±31,03
T3_ds	15,47±7,63	0,14±0,10	36,59±22,50
T4	15,33±8,14	0,10±0,09	39,71±21,50
T4_ds	10,96±5,84	0,10±0,07	32,35±24,61

SD – standartinis nuokrypis, CS – Carestream 3600 IOS, Me – Medit i500 IOS, PS – Primescan IOS, T3 – Trios 3 IOS, T4 – Trios 4 IOS, DS – papildomas atskaitos taškas. Paryškinti statistiškai reikšmingi skirtumai tarp skenavimų, naudojant papildomus atskaitos taškus ir jų nenaudojant.

Skenuojant visiškai bedančių žandikaulių modelius, papildomi atskaitos taškai nepagerino nei tikrumo, nei preciziškumo rezultatų, tačiau pastebėta, kad, ilgėjant atstumui tarp matuojamų atkarpų, paklaidų apimtis didėja. Vis dėlto *Primescan* ir *Trios* 4 IOS rezultatai buvo geriausi, atliekant visų atkarpų atstumo, kampo ir vertikalaus poslinkio matavimus (žr. 3–4 lenteles).

3 lentelė. Tikrumo rodiklio rezultatai visiškai bedančiuose modeliuose, matuojant atstumą, kampą ir vertikalų poslinkį tarp skenavimo kūnų.

	Atstumas_1	Atstumas_2	Atstumas_3	Kampas_1	Kampas_2	Kampas_3	Vertikalus poslinkis_1	Vertikalus poslinkis_2	Vertikalus poslinkis_3
	Vidurkis±SD, µm	Vidurkis±SD, µm	Vidurkis±SD, µm	Vidurkis±SD °	Vidurkis±SD °	Vidurkis±SD °	Vidurkis±SD, µm	Vidurkis±SD, µm	Vidurkis±SD, µm
CS	97,72±68,74	35,29±84,17	–39,30±64,46	–0,32±0,15	**0,52±0,10**	**–0,05±0,09**	**–124,25±95,87**	**–87,22±33,39**	**–3,58±37,20**
CS_ds	88,45±43,81	40,36±41,22	–37,14±53,84	–0,48±0,29	**0,08±0,16**	**–0,31±0,14**	**141,71±111,73**	**51,44±27,16**	**–55,00±33,17**
Me	12,78±19,59	10,50±19,79	**–17,07±59,74**	**–0,44±0,38**	**0,30±0,25**	**0,18±0,18**	**93,02±111,00**	**46,07±58,91**	**–163,85±40,73**
Me_ds	8,54±35,75	10,51±45,46	**150,82±43,69**	**0,60±0,58**	**0,46±0,07**	**–0,25±0,55**	**–259,15±129,62**	**–43,70±33,40**	**–61,32±76,66**
PS_	–24,93±8,01	–42,84±7,24	–46,05±4,32	–0,32±0,08	0,21±0,08	–0,56±0,08	–11,70±17,69	–25,80±12,63	**27,79±12,66**
PS_ds	–22,85±9,55	–45,72±13,36	–48,81±18,60	–0,28±0,07	0,22±0,05	–0,52±0,07	–21,50±21,33	–31,47±8,64	**40,81±10,85**
T3	**–12,17±11,50**	**–41,49±19,95**	–93,21±33,46	–0,08±0,13	**0,49±0,13**	–0,38±0,15	**–175,86±47,37**	**–92,45±25,78**	**31,20±34,71**
T3_ds	**–32,76±23,38**	**–85,10±34,78**	–130,77±73,46	–0,21±0,14	**0,08±0,17**	–0,22±0,34	**11,37±32,27**	**1,01±35,49**	**–88,33±64,70**
T4	**–24,51±8,39**	**–42,39±7,53**	**–45,02±14,20**	–0,29±0,08	**0,19±0,09**	**–0,54±0,08**	**–14,01±30,65**	**–24,85±13,05**	**28,57±13,20**
T4_ds	**–1,80±16,34**	**13,59±15,72**	**22,15±16,34**	–0,27±0,09	**–0,04±0,10**	**–0,15±0,10**	**103,05±47,33**	**59,80±34,74**	**–153,68±22,73**

SD – standartinis nuokrypis, CS – Carestream 3600 IOS, Me – Medit i500 IOS, PS – Primescan IOS, T3 – Trios 3 IOS, T4 – Trios 4 IOS, DS – papildomas atskaitos taškas. Paryškinti statistiškai reikšmingi skirtumai tarp skenavimų, naudojant papildomus atskaitos taškus ir jų nenaudojant.

4 lentelė. Preciziškumo rodiklio rezultatai visiškai bedančiuose modeliuose, matuojant atstumą, kampą ir vertikalų poslinkį tarp skenavimo kūnų.

	Atstumas_1	Atstumas_2	Atstumas_3	Kampas_1	Kampas_2	Kampas_3	Vertikalus poslinkis_1	Vertikalus poslinkis_2	Vertikalus poslinkis_3
	Vidurkis±SD	Vidurkis±SD	Vidurkis±SD	Vidurkis±SD	Vidurkis±SD	Vidurkis±SD	Vidurkis±SD	Vidurkis±SD	Vidurkis±SD
CS	55,57±35,97	**68,56±43,15**	46,80±41,49	**0,11±0,09**	0,08±0,06	0,07±0,05	78,64±48,15	26,38±18,48	26,94±23,81
CS_ds	36,99±19,98	**32,09±23,55**	44,68±26,07	**0,25±0,12**	0,13±0,09	0,11±0,06	94,45±50,70	21,34±15,01	25,34±19,66
Me	14,44±12,21	13,73±13,50	48,31±31,23	0,31±0,17	**0,22±0,09**	**0,14±0,10**	88,78±59,69	46,82±32,15	32,69±21,71
Me_ds	28,73±16,97	33,53±26,79	33,26±22,93	0,47±0,26	**0,06±0,04**	**0,41±0,32**	103,72±62,39	25,44±18,41	60,18±39,11
PS	6,47±4,20	5,49±4,35	3,63±1,80	0,06±0,04	0,06±0,04	0,06±0,04	13,06±10,99	10,22±6,60	10,56±6,04
PS_ds	7,71±5,00	10,75±7,08	15,27±9,32	0,05±0,03	0,04±0,03	0,06±0,03	18,68±8,20	7,37±3,79	8,08±6,73
T3	**8,41±7,25**	15,14±11,97	**27,81±16,13**	0,11±0,07	0,10±0,08	**0,12±0,07**	35,35±28,95	20,46±14,13	25,66±21,76
T3_ds	**19,53±11,08**	25,36±22,25	**64,73±27,22**	0,10±0,09	0,12±0,11	**0,28±0,16**	28,17±11,60	27,81±19,74	51,55±35,12
T4	**6,73±4,40**	5,81±4,34	9,89±9,58	0,07±0,04	0,07±0,05	0,07±0,04	22,06±19,96	**10,12±7,42**	10,92±6,34
T4_ds	**13,54±7,96**	11,61±9,87	12,99±8,92	0,08±0,05	0,08±0,05	0,08±0,05	38,96±23,55	**26,01±21,34**	18,18±12,21

SD – standartinis nuokrypis, CS – *Carestream* 3600 IOS, Me – *Medit* i500 IOS, PS – *Primescan* IOS, T3 – *Trios* 3 IOS, T4 – *Trios* 4 IOS, DS – papildomas atskaitos taškas. Paryškinti statistiškai reikšmingi skirtumai tarp skenavimų, naudojant papildomus atskaitos taškus ir jų nenaudojant.

4.2. Tikslumo vertinimas *in vivo*

4.2.1. Implantų atspaudų tikslumo vertinimas

A. Implantų analoginių ir skaitmeninių atspaudų palyginimas, naudojant *Trios* intraoralinį skenerį

Skaitmeninių ir analoginių atspaudų matavimai statistiškai reikšmingai skyrėsi matuojant atstumą tarp skenavimo kūnų, kampą tarp implantų ir skenuojant kūnų paviršiaus sutapimą, tačiau skirtumų tarp mezialiai ir distaliai esančių skenavimo kūnų paviršiaus sutapimo nenustatyta (žr. 5 lentelę).

5 lentelė. Atstumo tarp skenavimo kūnų, kampo tarp implantų, rotacijos, vertikalaus poslinkio, skenavimo kūnų paviršiaus sutapimo prie mezialinio ir distalinio implantų palyginimas.

Parametras	Analoginis atspaudas		Skaitmeninis atspaudas		Skirtu-mų vidurkis (SD)	*p* reikš-mė	Vilkokso-no ran-gų sumų kriterijaus galia
	vidurkis (SD)	mediana	vidurkis (SD)	mediana			
Atstumas tarp skenavimo kūnų	14,28 (6,75) mm	14,99	14,33 (6,77) mm	15,00	73,7 (75) µm	0,00	6 %
Kampas	14,17 (9,54)°	10,16	14,38 (9,8)°	10,74	0,42 (0,3)°	0,00	10 %
Rotacija	33,58 (23,19)°	28,40	33,27 (22,61)°	29,07	0,72 (0,55)°	0,098	8 %
Vertikalus poslinkis	1,58 (2,15) mm	0,85	1,57° (2,2) mm	0,83	98,9 (96,33) µm	0,63	6 %
M implanto paviršiaus sutapimas	14,27 (21,5) µm	14,32	31,8 (25,6) µm	19,68	–	0,00	100 %
D implanto paviršiaus sutapimas	14,65 (19,7) µm	14,32	30,68 (28,7) µm	22,67	–	0,00	100 %

Intraoralinis skeneris – *Trios,* SD – standartinis nuokrypis.

Statistiškai reikšmingos Spirmeno kriterijaus koreliacijos atskleidė, kad atstumas tarp skenavimo kūnų ir kampas tarp implantų teigiamai koreliuoja su

atstumo tarp skenavimo kūnų, kampo tarp implantų ir vertikalaus poslinkio matavimų skirtumais tarp *Trios* ir D800 grupių (koreliacija varijuoja nuo silpnos iki vidutinio stiprumo). Tiesinės regresijos modelis parodė, jog visos tirtos asociacijos yra statistiškai reikšmingos ($p < 0,05$), išskyrus vidutinio atstumo tarp skenavimo kūnų ir kampo tarp skenavimo kūnų matavimų skirtumus (žr. 6 lentelę).

6 lentelė. Tiesinės regresijos modelio rezultatai.

Priklausomi kintamieji	Nepriklausomi kintamieji					
	Vidutinis atstumas tarp skenavimo kūnų			Vidutinis kampas tarp implantų		
	Spirmeno koeficientas	Tiesinės regresijos modelis		Spirmeno koeficientas	Tiesinės regresijos modelis	
		p reikšmė	Modelio galia		*p* reikšmė	Modelio galia
Atstumas tarp skenavimo kūnų	0,19	0,35	27 %	0,3	0,02	91 %
Kampas	0,08 (NS)	0,02	93 %	0,53	0,0	100 %
Vertikalus poslinkis	0,53	0,0	99,9 %	0,52	0,0	100 %

NS – statistiškai nereikšminga koreliacija. Rezultatai atskleidžia, kaip vidutinis atstumas tarp skenavimo kūnų ir kampas tarp implantų koreliuoja su atstumo tarp skenavimo kūnų, kampo ir vertikalaus poslinkio skirtumais (Trios IOS).

B. Implantų analoginių ir skaitmeninių atspaudų palyginimas, naudojant *Trios* 3 intraoralinį skenerį

Statistiškai reikšmingų skirtumų tarp Trios 3 ir D800 nustatyta atlikus visų parametrų, išskyrus kampo ($p < 0,05$), matavimus. Skaitmeninių atspaudų grupėje statistiškai reikšmingai skyrėsi mezialinio ir distalinio skenavimo kūnų paviršiaus sutapimas, o CII grupėje statistiškai reikšmingų skirtumų nenustatyta (žr. 7 lentelę).

7 lentelė. Atstumo tarp skenavimo kūnų, kampo tarp implantų, rotacijos, vertikalaus poslinkio, skenavimo kūnų paviršiaus sutapimo prie mezialinio ir distalinio implantų palyginimas.

Parametras	Analoginis atspaudas		Skaitmeninis atspaudas		Skirtumų vidurkis (SD)	*p* reikšmė	Vilkoksono rangų kriterijaus galia
	Vidurkis (SD)	Media-na	Vidurkis (SD)	Media-na			
Atstumas tarp skenavimo kūnų	15,80 (5,65) mm	16,19	15,83 (5,67) mm	16,16	70,8 (59) µm	<0,001	5 %
Kampas	9,99 (5,57)°	9,37	9,97 (5,65)°	9,66	0,37 (0,3)º	0,79	5 %
Rotacija	35,65 (23,45)°	34,48	35,05 (23,42)°	34,8	2,0 (1,37)º	0,013	6,4 %
Vertikalus poslinkis	1,54 (1,91) mm	1,2	1,57 (1,92) mm	1,1	82,2 (61,7) µm	0,001	5,8 %
M implanto paviršiaus sutapimas	14,19 (3,22) µm	14,28	34,14 (36,69) µm	29,28	–	<0,001	98 %
D implanto paviršiaus sutapimas	14,19 (2,29) µm	14,72	34,24 (14,64) µm	33,52	–	<0,001	100 %

Intraoralinis skeneris – *Trios 3*, SD – standartinis nuokrypis.

Remiantis Spirmeno koreliacijos kriterijaus duomenimis, atstumo tarp skenavimo kūnų koreliacija su matuotais parametrų skirtumais statistiškai nereikšminga. Kampo tarp implantų matavimai statistiškai patikimai koreliuoja su atstumo tarp skenavimo kūnų, kampo tarp implantų ir vertikalaus poslinkio matavimų skirtumais tarp CII ir DII grupių, tačiau koreliacija silpna. Tiesinės regresijos kriterijaus rezultatai atskleidė, jog kampo tarp implantų asociacijos su visais matuotais parametrų skirtumais yra statistiškai reikšmingos ($p < 0,05$) (žr. 8 lentelę).

8 lentelė. Tiesinės regresijos modelio rezultatai

Priklausomi kintamieji	Nepriklausomi kintamieji					
	Vidutinis atstumas tarp skenavimo kūnų			Vidutinis kampas tarp implantų		
	Spirmeno koefi-cientas	Tiesinės regresijos modelis		Spirmeno koefi-cientas	Tiesinės regresijos modelis	
		p reikšmė	Modelio galia		*p* reikšmė	Modelio galia
Atstumas tarp skenavimo kūnų	–0,036 (NS)	0,078	19,8 %	0,24	<0,001	64 %
Kampas	0,13 (NS)	0,08	19,6 %	0,35	0,013	35,1 %
Vertikalus poslinkis	0,11 (NS)	0,219	8,3 %	0,36	0,0006	33,1 %

NS – statistiškai nereikšminga koreliacija. Rezultatai atskleidžia, kaip vidutinis atstumas tarp skenavimo kūnų ir kampas tarp implantų koreliuoja su atstumo tarp skenavimo kūnų, kampo ir vertikalaus poslinkio skirtumais (Trios 3 IOS).

4.2.2. Restauracijų ant dantų implantų tikslumo vertinimas

4.2.2.1. Restauracijų ant dantų implantų tikimo vertinimas

Remiantis Vilkoksono kriterijumi, $D_{netikslumas}$ D grupėje buvo didesnis negu C grupėje ($p < 0,05$) (žr. 9 lentelę). Be to, $D_{netikslumas}$ matavimai tarp C ir D grupių statistiškai reikšmingai skyrėsi visuose matuotuose paviršiuose ($p < 0,05$) (žr. 10 lentelę). Cemento tarpo matavimai C grupėje buvo didesni negu D grupėje, tačiau, remiantis Frydmano kriterijumi, $D_{cemento}$ matavimai tarp skirtingų paviršių statistiškai reikšmingai nesiskyrė ($p = 0,785$) (žr. 11 lentelę). Lyginant $\Delta D_{netikslumas}$ matavimus tarp viršutinio ir apatinio žandikaulio restauracijų, statistiškai reikšmingų skirtumų ($p = 0,575$) nenustatyta, kaip ir tarp skirtingo ilgio restauracijų matavimų ($p = 0,47$). Lyginant $\Delta D_{cemento}$ matavimus tarp viršutinio ir apatinio žandikaulių restauracijų, nustatytas statistiškai reikšmingas skirtumas ($p = 0,0005$), bet tarp skirtingo ilgio restauracijų skirtumų nerasta ($p = 0,052$) (žr. 12 lentelę).

9 lentelė. $D_{netikslumas}$ ir $D_{cemento}$ medianos ir tarpkvartiliniai skirtumai [IQR] cirkonio oksido fiksuotose restauracijose ant dviejų implantų C ir D grupėse.

	C grupė	D grupė	Vilkoksono rangų sumų kriterijaus *p* reikšmė
$D_{netikslumas}$ [IQR] (µm)	59,00 [60,00]	78,00 [88,00]	0,00
$D_{cemento}$ [IQR] (µm)	38,90 [23,20]	34,90 [25,70]	0,00

10 lentelė. $D_{netikslumas}$ MB, ML, DB, DL paviršių matavimų palyginimas C ir D grupėse.

Matavimo vieta	$D_{netikslumas}$		Vilkoksono rangų sumų kriterijaus *p* reikšmė	Frydmano rangų sumų kriterijaus *p* reikšmė
	C grupė	D grupė		
	Mediana [IQR] (µm)	Mediana [IQR] (µm)		
MB	51,50 [55,25]	65,00 [67,50]	0,00	0,01
ML	62,00 [58,50]	96,00 [93,00]	0,00	
DB	67,00 [61,75]	78,00 [73,75]	0,00	
DL	68,00 [72,00]	71,00 [101,25]	0,01	

[IQR] – tarpkvartilinis skirtumas.

11 lentelė. $D_{cemento}$ MB, ML, DB, DL paviršių matavimų palyginimas C ir D grupėse.

Matavimo vieta	$D_{cemento}$		Vilkoksono rangų sumų kriterijaus *p* reikšmė	Frydmano rangų sumų kriterijaus *p* reikšmė
	C grupė	D grupė		
	Mediana [IQR] (µm)	Mediana [IQR] (µm)		
MB	36,40 [20,70]	40,05 [29,48]	0,51	0,79
ML	40,00 [23,50]	35,30 [26,80]	0,00	
DB	41,85 [21,50]	35,8 [23,68]	0,00	
DL	35,65 [26,28]	31,75 [22,50]	0,00	

[IQR] – tarpkvartilinis skirtumas.

12 lentelė. $\Delta D_{netikslumo}$ ir $\Delta D_{cemento}$ matavimų palyginimas pogrupiuose: viršutiniame ir apatiniame žandikauliuose; esant dviejų, trijų ir keturių vienetų tiltinėms konstrukcijoms.

Pogrupiai	$\Delta D_{netikslumo}$ Mediana [IQR] (μm)	Vilkokso-no rangų sumų kriterijaus *p* reikšmė	Frydmano rangų sumų kriterijaus *p* reikšmė	$\Delta D_{cemento}$ Mediana [IQR] (μm)	Vilkokso-no rangų sumų kriterijaus *p* reikšmė	Frydmano rangų sumų kriterijaus *p* reikšmė
Viršutinis žandikaulis	44,00 [64,00]	0,58	–	18,00 [17,60]	0,00	–
Apatinis žandikaulis	42,50 [66,00]			13,70 [19,60]		
Dviejų vnt.	36,50 [47,25]	–	0,47	14,70 [21,09]	–	0,05
Trijų vnt.	53,00 [72,00]			17,60 [17,70]		
Keturių vnt.	42,50 [81,00]			14,65 [19,27]		

[IQR] – tarpkvartilinis skirtumas.

4.2.2.2. Restauracijų ant dantų implantų pasyvumo vertinimas

Protezinio varžtelio rotacijos kampai skirtingose situacijose pateikiami 13 lentelėje. C grupės restauracijų SR (16,25±15,52°), matuojant burnoje, buvo didesnis negu D grupės (13,85±10,78°), bet skirtumas statistiškai nereikšmingas (p = 0,557). SR parametrą matuojant ant darbinio modelio, C grupės vertės buvo mažesnės negu D grupės, skirtumas statistiškai reikšmingas. Bendrasis SR rodmuo jį matuojant burnoje buvo šiek tiek didesnis negu matuojant ant darbinio modelio, tačiau reikšmingų skirtumų nenustatyta (žr. 14 lentelę).

13 lentelė. Protezinio varžtelio rotacijos kampai (nuo 5 Ncm iki 35 Ncm) pasyvioje (P) ir nepasyvioje (NP) situacijose.

Intraoraliai				Darbinis modelis				Kontrolinis modelis			
C grupė		D grupė		C grupė		D grupė		C grupė		D grupė	
P	NP	P	NP	P	NP	P	NP	P	NP	P	NP
88± 17°	102± 25°	84± 15°	95± 15°	84± 13°	86± 20°	83± 15°	85± 17°	87± 14°	90± 16°	85± 13°	87± 14°

14 lentelė. Protezinio varžtelio pasipriešinimo matavimai (SR) skirtingose grupėse.

Kintamasis	Vidurkis±SD	Mediana [IQR]
C grupės SR, matuotas intraoraliai	16,25±15,52°	10 (10)°
D grupės SR, matuotas intraoraliai	13,85±10,78°	10 (10)°
C grupės SR, matuotas ant darbinio modelio	6,04±7,43°	5 (10)°
D grupės SR, matuotas ant darbinio modelio	13,12±13,86°	10 (15)°
C grupės SR, matuotas ant darbinio modelio	12,5±9,79°	10 (10)°
D grupės SR, matuotas ant darbinio modelio	5,5±5,35°	5 (10)°
C grupės SR (bendrasis rodmuo)	12,7±13,98°	10 (15)°
D grupės SR (bendrasis rodmuo)	13,22±10,28°	10 (15)°
Intraoraliai matuotas SR (bendrasis rodmuo)	13,22±13,06°	10 (15)°
Darbinio modelio SR (bendrasis rodmuo)	12,08±11,79°	10 (15)°
Kontrolinio modelio SR (bendrasis rodmuo)	9,75±8,5°	5 (8,75)°

SD – standartinis nuokrypis, IQR – tarpkvartilinis skirtumas.

D grupės restauracijų, kai kampas tarp implantų didesnis negu 10 laipsnių, SR matavimai burnoje buvo statistiškai reikšmingai didesni negu D grupės restauracijų, kurių kampas tarpas tarp implantų mažesnis negu 10 laipsnių ($p = 0,037$) (žr. 15 lentelę). Atstumo tarp skenavimo kūnų, kampo tarp implantų ir SR matavimų įvairiose situacijose statistiškai reikšmingų koreliacijų nenustatyta.

15 lentelė. Varžtelio pasipriešinimo (SR) palyginimas tarp pogrupių, kai kampas tarp implantų didesnis arba mažesnis negu 10 laipsnių.

Palyginimų pogrupiai	Vilkoksono rangų sumų kriterijaus *p* reikšmė
Intraoraliai SR C grupė >10° *vs*. Intraoraliai SR C grupė <10°	0,227
Intraoraliai SR D grupė >10° *vs*. Intraoraliai SR D grupė <10°	0,037
Darbinio modelio SR C grupė >10° *vs*. Darbinio modelio SR grupė C <10°	0,169
Darbinio modelio SR D grupė >10° *vs*. Darbinio modelio SR D grupė <10°	0,336
Kontrolinio modelio SR C grupė >10° vs. Kontrolinio modelio SR C grupė <10°	0,156
Kontrolinio modelio SR D grupė >10° *vs*. Kontrolinio modelio SR D grupė <10°	0,103

Intraoraliai SR bendrasis >10° *vs.* Intraoraliai SR bendrasis <10°	0,288
Darbinio modelio SR bendrasis >10° *vs.* Darbinio modelio SR bendrasis <10°	0,145
Kontrolinio modelio SR bendrasis >10° *vs.* Kontrolinio modelio SR bendrasis <10°	0,73

4.3. Tikslumo vertinimas *in vitro* ir *in vivo*

Didėjant atstumui tarp skenavimo kūnų, atstumo matavimų preciziškumas prastėjo. Statistiškai reikšmingų skirtumų tarp IOS ir MIOS grupių nustatyta matuojant didžiausią atkarpą. Atstumo matavimų preciziškumas skenuojant *in vitro* buvo geresnis negu *in vivo* sąlygomis. Matuojant atstumą, tikrumo rodiklis tarp skenavimų intraoraliai ir ekstraoraliai buvo panašus, tačiau, didėjant atkarpų ilgiams, paklaidų daugėjo.

Matuojant kampą tarp implantų, preciziškumo ir tikrumo rodikliai skenuojant *in vitro* buvo geresni negu *in vivo* sąlygomis, tačiau paklaidų daugėjo tik didėjant kampui tarp implantų. Vis dėlto statistiškai reikšmingų skirtumų tarp IOS ir MIOS grupių nustatyta tik matuojant ilgiausias atkarpas.

Vertinant skenavimo kūnų paviršiaus sutapimo laipsnį, preciziškumas tarp IOS ir MIOS grupių statistiškai reikšmingai nesiskyrė (skirtingai negu tikrumo atveju). Skenuojant ekstaoraliai, paviršiaus sutapimo parametro tikrumas reikšmingai skyrėsi nuo matavimų intraoraliai.

5. DISKUSIJA

Papildomų atskaitos taškų naudojimas skenuojant intraoraliniu skeneriu mokslinėje literatūroje aprašytas kaip metodas, gerinantis skaitmeninio atspaudo kokybę[20]. Atliekant pirmąją disertacijoje pristatomo tyrimo dalį, bedančiuose ir dalinai bedančiuose spausdintuose modeliuose kaip papildomi atskaitos taškai naudotos stiklojonomerinio cemento tabletės. Papildomi atskaitos taškai pagerino dalinai bedančių žandikaulių modelių tikrumo ir preciziškumo rodiklius, matuojant atstumą, kampą ir vertikalų poslinkį tarp skenavimo kūnų. Vis dėlto statistiškai reikšmingų skirtumų tarp skenavimų, kai papildomi atskaitos taškai buvo naudojami arba nenaudojami, nenustatyta ($p > 0,05$). Visiškai bedančių žandikaulių modelių tikrumo ir preciziškumo rodikliams papildomi atskaitos taškai teigiamos įtakos neturėjo, tačiau pastebėta, kad, ilgėjant atstumui tarp skenavimo kūnų, skenavimo paklaidų daugėja matuojant visus vertintus parametrus.

Lyginant analoginių ir skaitmeninių atspaudų tikslumą, restauracijų ant implantų horizontalioms ir kampo matavimų paklaidoms pasirinkti kliniškai reikšmingi atskaitos rodikliai 100 µm ir 0,4°[60]. Atliekant tyrimą, kai skaitmeniniams atspaudams naudotas *Trios* IOS, vidutinis atstumas tarp skenavimo kūnų (73,7±75 µm) ir vertikalaus poslinkio rodikliai (98,9±96,33 µm) buvo mažesni negu 100 µm. Atsižvelgus į pakankamai didelius standartinius nuokrypius, galima teigti, kad šie rodikliai viršija pasirinktus atskaitos slenksčius ir gali turėti klinikinės reikšmės kaip ir kampo tarp implantų matavimai (0,42±0,3°).

Tyrimo dalyje, kurioje naudotas *Trios* 3 IOS, statistiškai reikšmingų skirtumų nustatyta matuojant analoginių ir skaitmeninių atspaudų atstumus tarp skenavimo kūnų (70,8±59 µm) ir vertikalaus poslinkio (82,2±61,7 µm). Kampo matavimų (0,37±0,3º), kaip ir kitų išmatuotų parametrų, skirtumai neviršijo atskaitos rodiklių ir gali būti laikomi kliniškai mažai reikšmingais. Gauti duomenys patvirtina ir kitų mokslinių studijų rezultatus, liudijančius, kad implantų skaitmeniniai atspaudai gali būti patikima alternatyva analoginiams[17, 37]. Minėtina, kad atliekant tyrimą nustatyti skirtumai buvo netgi mažesni negu minimi kituose tyrimuose[12].

Implanto atramos rotacinis netikslumas klinikinėje praktikoje dažnai sukelia restauracijos tikimo problemų, todėl, atliekant tyrimą, vertinta skenavimo kūno rotacija[78]. Tyrimo dalyje, kurioje naudotas *Trios* IOS, vidutinis skirtumas tarp skaitmeninių ir analoginių atspaudų buvo 0,72±0,55°, o naudojant *Trios* 3 IOS – 2,0±1,37º, bet statistiškai reikšmingų skirtumų nustatyta tik vertinant *Trios* 3 intraoralinio skenerio duomenis. Klinikinė minėtų skirtumų reikšmė, deja, negali būti patikimai interpretuojama, nes

tiltinėms konstrukcijoms naudotos beheksės titaninės bazės. Kita vertus, situacijose, kai komponentai be rotacijos elementų nenaudotini, rotacinis detalių paslankumas gali turėti neigiamos įtakos visos restauracijos tikimui[79].

Lyginant skenavimo kūnų paviršiaus sutapimo laipsnio matavimus tarp mezialinio ir distalinio skenavimo kūno iš skaitmeninių atspaudų *Trios* ir *Trios* 3 IOS, statistiškai reikšmingų skirtumų nė vienoje tyrimo dalyje nenustatyta. Vis dėlto mokslinėje literatūroje teigiama, jog skenavimo vieta neigiamai veikia skenavimo tikslumą, nes, esant ilgai bedantei zonai tarp implantų, kyla vaizdų susiejimo problemų[15, 16, 53]. Šis aspektas, atliekant eksperimentus su minėtais skeneriais, galėjo turėti įtakos skenavimo netikslumams, nes tyrime su *Trios* IOS 24 restauracijos iš 27, o tyrime su *Trios* 3 IOS visos 24 restauracijos buvo gaminamos galinių dantų srityje. Laboratorinio skenerio vaizduose skenavimo kūnų paviršiaus sutapimo laipsnis buvo du kartus geresnis negu naudojant intraoralinius skenerius. Šie duomenys turi klinikinės reikšmės, nes, atsiradus paklaidai, pozicionuojant skaitmeninį analogą pagal netinkamą skenavimo kūno padėtį, galutinė restauracija taip pat bus netiksli.

Tiesinės regresijos kriterijaus rezultatai atskleidė, jog vidutinio atstumo tarp skenavimo kūnų asociacijos su atstumo bei kampo tarp skenavimo kūnų matavimų skirtumais yra statistiškai nereikšmingos nei *Trios*, nei *Trios* 3 grupėse. Vertikalaus poslinkio matavimų skirtumams įtakos turėjo vidutinis atstumas tarp skenavimo kūnų, tačiau tik *Trios* grupėje. Vis dėlto kampas tarp implantų reikšmingai paveikė visus vertintus parametrus, nors Spirmeno koreliacijos buvo santykinai silpnos (0,24–0,52). Flugge ir bendraautoriai bei Papaspyridakos ir bendraautoriai teigia, jog didėjantis kampas ir atstumas tarp implantų neigiamai veikia intraoralinių skenerių tikslumą[50, 80], tačiau kiti tyrėjai pateikia priešingų rezultatų[37, 81].

SEM matavimų analizė atskleidė, jog $D_{netikslumas}$ mediana D grupėje (78 μm) reikšmingai skyrėsi nuo C grupės (59 μm). Kadangi 150 μm kraštinio tikslumo paklaidos riba laikoma klinikiniu atskaitos tašku[64], 19 μm $D_{netikslumas}$ skirtumas tarp C ir D grupių gali būti laikomas kliniškai mažai reikšmingu. Vis dėlto reikia atsižvelgti į maksimalias $D_{netikslumas}$ vertes C ir D grupėse (181 ir 250 μm), nes kraštinio tikslumo riba viršijama. Matavimai atlikti su kelis kartus patikrintu darbiniu modeliu, tačiau pagal šiuos matavimus visiškai tiksliai interpretuoti klinikinio vaizdo negalime. Dėl šios priežasties būtini tolesni tyrimai *in vivo*, kuriuose būtų pasirinktas patikimas tikslesnio vertinimo atskaitos taškas.

Lyginant $D_{netikslumas}$ matavimus skirtingose grupėse ir matavimo vietose, nustatyta statistiškai reikšmingų skirtumų. Daugiau negu 34 μm aukštesnės $D_{netikslumas}$ vertės rastos D grupėje, vertinant matavimų skirtumus skirtingose

vietose. Nevienodai tikslus restauracijos kraštas didina bakterijų kaupimosi galimybę prie implantų ir gali sukelti aplinkinių audinių uždegimą[88, 89], tačiau klinikinėje praktikoje aptikti tokias mažas paklaidas beveik neįmanoma.

Vertinant restauracijų ant implantų pasyvumą, SR burnoje, ant darbinio ir kontrolinio modelio koreliacija su atstumu bei kampu tarp skenavimo kūnų buvo statistiškai nereikšminga, todėl galima teigti, jog šie veiksniai restauracijų ant implantų pasyvumui įtakos neturi. Panašūs rezultatai pateikiami ir mokslinėje literatūroje[105]. Kalbamosios tyrimo dalies trūkumas yra tai, kad, esant skirtingiems implanto ir atramos jungties tipams, SR matavimų reikšmės gali skirtis. Šiame tyrime naudota 11° vidinė implanto ir atramos jungtis, kuri yra mažiau atspari veržimo jėgai, palyginti su išorinio tipo jungtimis[100, 105]. Be to, SR matavimai gali skirtis ir naudojant protezavimo komponentus su antirotaciniu elementu ar be jo.

Kalbamojo tyrimo metu naudota protezinė terkšlė buvo papildyta goniometru. Šios priemonės naudojimas odontologijoje nėra plačiai aprašytas. Vienos goniometro padalos vertė yra 5 laipsniai, o tai galėjo paveikti matavimų tikslumą. Kaip alternatyva mokslinėje literatūroje aprašytas *OsseoCare* (*Nobel Biocare*) matavimo prietaisas varžtelio pasipriešinimui įvertinti, tačiau šiuo prietaisu galima tik kokybinė, o ne kiekybinė varžtelio pasipriešinimo analizė[107].

Nuolat tobulėjant skaitmeninėms technologijoms, daugėja aukštos vertės tikslumo vertinimo tyrimų, ypač klinikinėmis sąlygomis. Intraoralinių skenerių programinės įrangos ir optinių prietaisų atnaujinimai gerina skenavimo tikrumą ir preciziškumą[29, 51], didėja skenavimo greitis, duomenų analizė[109], papildomai įdiegiama naujų funkcijų, tokių kaip ėduonies detektoriai, 3D judesių registravimas. Reikia daugiau tyrimų, norint išsiaiškinti, kaip šios naujovės pagerina viso skaitmeninio restauracijų gamybos kelio tikslumą.

6. IŠVADOS

1. Skenuojant bedančius ir dalinai bedančius modelius, iš penkių naudotų skenerių mažiausiai tikslūs buvo *Medit* i500 ir CS3600 intraoraliniai skeneriai. *Primescan, Trios* 3, *Trios* 4 skenerių tikslumas buvo panašus, tačiau statistiškai reikšmingai geresnis negu *Medit* i500 ir CS3600 skenerių.

2. Papildomų atskaitos taškų naudojimas dalinai bedančiuose modeliuose pagerino skenavimo tikslumą, tačiau statistiškai reikšmingi skirtumai nustatyti tik skenuojant *Medit* i500 intraoraliniu skeneriu. Visiškai bedančiuose modeliuose papildomi atskaitos taškai teigiamą poveikį turėjo daugiausia skenavimo tikrumui, bet nepagerino preciziškumo.

3. Pagal pasirinktus matavimo parametrus analoginiai atspaudai klinikinėmis sąlygomis buvo tikslesni negu skaitmeniniai. *Trios* 3 skeneris skenavo tiksliau negu *Trios*. Naudojant *Trios* 3, skenavimo kūnų poziciniai netikslumai kliniškai buvo mažai reikšmingi.

4. Atstumas ir kampas tarp implantų neigiamai veikė *Trios* skenerio tikslumą, o *Trios* 3 skenerio tikslumui reikšmingai neigiamą įtaką darė tik kampas tarp implantų.

5. Analoginiu būdu pagamintų tiltinių restauracijų ant dviejų implantų tinkamumas buvo statistiškai reikšmingai geresnis negu pagamintų skaitmeniniu būdu, tačiau rasti skirtumai yra maži ir, tikėtina, kliniškai nereikšmingi.

6. Analoginiu būdu pagamintų tiltinių restauracijų ant dviejų implantų cemento tarpelis statistiškai reikšmingai didesnis negu skaitmeniniu būdu be fizinio darbinio modelio gamintų restauracijų.

7. Matuojant burnoje, analoginiu ir skaitmeniniu būdu gamintų restauracijų protezinio varžtelio pasipriešinimo matavimų duomenys statistiškai reikšmingai nesiskyrė, tačiau statistiškai reikšmingų skirtumų nustatyta matuojant protezinio varžtelio pasipriešinimą ant darbinio ir kontrolinio modelių.

8. Bedantį žandikaulį restauracijai ant implantų skenuojant intraoraliniu skeneriu laboratorinėmis ir klinikinėmis sąlygomis, skenavimo tikrumas ir preciziškumas nesiskyrė.

7. PRAKTINĖS REKOMENDACIJOS

1. Papildomų atskaitos taškų naudojimas bedantėse zonose, skenuojant ilgoms tiltinėms konstrukcijoms ant implantų, gali pagerinti atspaudo tikslumą. Visiškai bedančiuose žandikauliuose papildomi atskaitos taškai pagerina tikrumo rodiklį, tačiau neturi įtakos preciziškumui.

2. Implantų tarpusavio pasvirimo kampas daugiau negu 10 laipsnių neigiamai veikia skaitmeniniu būdu gamintų prisukamų restauracijų ant implantų pasyvumą, todėl taikant skaitmeninį protokolą reikia atkreipti didesnį dėmesį į implantų pasvirimo kampą.

3. Skaitmeninis protezų ant implantų gamybos būdas yra patikima alternatyva analoginiam gamybos būdui, gaminant tiltines fiksuotas restauracijas ant implantų nuo 2 iki 4 vienetų.

4. Restauracijų pasyvumo vertinimo metodikos nėra objektyvios, todėl klinikinėje praktikoje turėtų būti naudojamos jų kombinacijos bei toliau stengiamasi jas kuo labiau objektyvizuoti.

List of Publications

1. Rutkunas V., Geciauskaite A., Jegelevicius D., Vaitiekūnas M. Accuracy of digital implant impressions with intraoral scanners. A systematic review. Eur J of Oral Implant 2017;10 Suppl 1:101-120.
2. Gedrimiene A., Adaskevicius R., Rutkunas V. Accuracy of digital and conventional dental implant impressions for fixed partial dentures: A comparative clinical study. J Adv Prosthodont 2019;11:271–9. https://doi.org/10.4047/jap.2019.11.5.271.
3. Rutkunas V., Larsson C., Vult von Steyern P., Mangano F., Gedrimiene A. Clinical and laboratory passive fit assessment of implant-supported zirconia restorations fabricated using conventional and digital workflow. Clin Implant Dent Relat Res 2020;22:237–45. https://doi.org/10.1111/cid.12885.

Paper I

Accuracy of digital and conventional dental implant impressions for fixed partial dentures: A comparative clinical study

***Gedrimiene A.**, Adaskevicius R., Rutkunas V.*

J Adv Prosthodont 2019;11:271–9.

Accuracy of digital and conventional dental implant impressions for fixed partial dentures: A comparative clinical study

Agne Gedrimiene[1]*, Rimas Adaskevicius[2], Vygandas Rutkunas[1]

[1]Department of Prosthodontics, Institute of Odontology, Faculty of Medicine, Vilnius University, Lithuania
[2]Department of Electrical Power Systems, Faculty of Electrical and Electronics Engineering, Kaunas University of Technology, Lithuania

PURPOSE. The newest technologies for digital implant impression (DII) taking are developing rapidly and showing acceptable clinical results. However, scientific literature is lacking data from clinical studies about the accuracy of DII. The aim of this study was to compare digital and conventional dental implant impressions (CII) in a clinical environment. **MATERIALS AND METHODS.** Twenty-four fixed zirconia restorations supported by 2 implants were fabricated using conventional open-tray impression technique with splinted transfers (CII group) and scan with Trios 3 IOS (3Shape) (DII group). After multiple verification procedures, master models were scanned using laboratory scanner D800 (3Shape). 3D models from conventional and digital workflow were imported to reverse engineering software and superimposed with high resolution 3D CAD models of scan bodies. Distance between center points, angulation, rotation, vertical shift, and surface mismatch of the scan bodies were measured and compared between conventional and digital impressions. **RESULTS.** Statistically significant differences were found for: a) inter-implant distance, b) rotation, c) vertical shift, and d) surface mismatch differences, comparing DII and CII groups for mesial and distal implant scan bodies ($P \leq .05$). **CONCLUSION.** Recorded linear differences between digital and conventional impressions were of limited clinical significance with two implant-supported restorations. ***[J Adv Prosthodont 2019;11:271-9]***

KEYWORDS: Digital impression; Dental implant; Impression accuracy

INTRODUCTION

Digital implant impressions (DII) with intraoral scanners (IOS) are a relatively novel, but continuously improving technique. Their popularity is increasing because of various patient-related (increased comfort due to avoidance of impression tray and materials) and dentist-orientated (time and cost savings, digital data storage and analysis, etc.) aspects.[1] IOS have supplemented the traditional prosthodontic approach and contributed to the concept of "virtual patient".

Conventional implant impressions (CII) have been a standard procedure for fixed prosthodontics for a long time. The workflow associated with CII has limitations that affect the efficiency. Selection of tray and impression material, impression technique, time consumption, impression disinfection, transportation, and storage issues are the main reasons for considering alternative impression techniques in fixed prosthodontics.[2] DII were proposed as a possible alternative to the conventional workflow a few decades ago.[3]

The newest technologies of IOS hardware and software are developing rapidly and showing acceptable clinical results for tooth-supported crowns.[4] A recent systematic review reported deviations in digital implant impressions of less than 100 μm in mainly *in vitro* studies.[5] *In vitro* studies allow using true reference data. However, the equipment for obtaining reference data cannot be used in a clinical study and digital impressions generally can be compared only to the conventional ones. *In vitro* studies do not fully represent the clinical situation, as there are many variables that could affect the accuracy of DII intraorally.

Corresponding author:
Agne Gedrimiene
Institute of Odontology, Faculty of Medicine, Vilnius University
Žalgirio g. 115, Vilnius, LT-08217, Lithuania
Tel. +37063653731: e-mail, geciauskaite.agne@gmail.com
Received July 14, 2019 / Last Revision October 11, 2019 / Accepted October 29, 2019

As there are plenty of randomized clinical studies of the accuracy of digital impressions on sound teeth[6], scientific literature is lacking data from clinical studies about the accuracy of digital impressions for implant-supported restorations.[7-10] The aim of this study was to evaluate and compare the digital and conventional dental implant impressions in the clinical setting.

MATERIALS AND METHODS

Twenty-four fixed partial restorations supported by 2 AnyOne implants in six patients (Megagen, Daegu, Korea) were included. All implants were placed in the posterior area of the mouth. Two-unit (n = 7), three-unit (n = 11), and four-unit (n = 6) zirconia restorations were fabricated. The average inter-implant distance was 15.82 ± 5.66 mm. Clinical study was approved by the Vilnius Regional Ethics Committee for Biomedical Research (No 158 200-16-861-370).

Two different types of implant impressions were performed for each case in random order. A conventional open-tray impression technique with splinted transfers using vinyl-polysiloxane (Express, 3M, Mapplewood, MN, USA) was made (CII group). A splinting procedure of the impression copings and their verification of passive-fit was applied.[11] A digital impression was taken using original scan bodies torqued to the implants at 15 Ncm and a Trios 3 IOS (3Shape; version 1.3.4.2) (DII group). The scanning technique making less than 1,000 images per arch was completed under manufacturer's recommendations. In the maxilla, the scanning started from occlusal surface moving to buccal and palatal surfaces, while in the mandible, the lingual and buccal surfaces were captured after scanning the occlusal surfaces (Fig. 1). Standard tessellation language (STL) files were used for comparisons.

Master models were fabricated from conventional impressions with type IV plaster (FujiRock, GC, Tokyo, Japan) under the manufacturer's instructions and allowed to set at room temperature for 24 hours. A verification jig was used to assess the accuracy of the position of the implant analogues in the master model. Passive fit evaluation techniques, such as finger pressure and Sheffield and screw-resistance tests,[12] were used during the verification procedure. After verification of the master model, same scan bodies at the same implant locations and in the same rotational positions were attached to the implant analogues using 15 Ncm torque. Scanning of master models was completed using a D800 (3Shape, Copenhagen, Denmark) laboratory scanner and Dental System software (version 2.9.9.3). After exportation of the STL files, the 3D models were compared with the 3D models obtained from the DII procedure. Implant-supported zirconia restorations were fabricated from the conventional impressions. During all steps of the manufacture and final delivery of the restoration, passive fit was additionally evaluated using the same techniques as were used with the verification jig. As all the restorations were clinically acceptable, master models were additionally confirmed as accurate. Also they were regarded as the best available reference, due to the multiple verification procedures of the master model and final restorations.

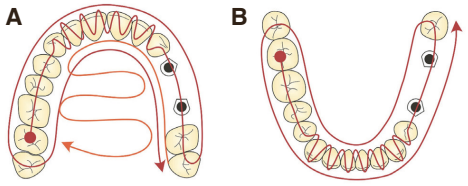

Fig. 1. Scanning sequence with IOS: (A) upper jaw, (B) lower jaw.

The high resolution and high accuracy 3D Computer-Aided Design (CAD) models were imported into Rapidform 2006 (INUS Technology Inc., Seoul, Korea) reverse engineering software. 3D models produced from data captured by the IOS and laboratory scanner were compared with 3D CAD models of scan bodies. Each imported 3D model was checked for the presence of any non-manifold, redundant, crossing, and unstable faces in the imported shell. The positions of reference points were imported for calculations by using data analysis software in Matlab R2014b (The MathWorks, Inc., Santa Clara, CA, USA).

Each 3D model had its own position in space and its own rotation. For the alignment of 3D models, a coarse alignment was applied, and then a fine alignment was performed using iterative closest point (ICP). The coarse alignment approximates the rigid transformation between models. This is a manual step in which a researcher must select three corresponding 3D points on the captured image and original 3D model of the scan body (Fig. 2A). Each pair of corresponding points is represented by a small square in different color.

The fine alignment algorithm is an iterative procedure minimizing the mean square error (MSE) between points of the first model surface and the closest points, respectively, on the other surface. The algorithm represents the geometric transformation that best aligns the original model and the closest points, respectively, on the scan body surface.

The alignment procedure was repeated with other models of the scan bodies.

In the next steps, all processing and measurements were performed using only the high precision 3D CAD models of the scan body. To identify the scan body axis, the section plane was created on the scan body shell. This section plane is perpendicular to the cylinder part direction and a reference vector normal to this reference plane is the axis of the scan body. The center point of the scan body is at the intersection between this axis and the top plane, which can be found by picking three reference points on the top surface of the scan body model (Fig. 2B). Similar method of hori-

zontal plane detection was discussed by Flügge *et al.*,[13] but they did not use original 3D CAD files of the scan body for data analysis. In case the 3D model of scan body was developed from solid model, the top plane could be described as one flat polygon. So, in this study, it is necessary only to define the position of this plane, passing through points $P_1(x_1,y_1,z_1)$, $P_2(x_2,y_2,z_2)$, and $P_3(x_3,y_3,z_3)$:

$$A \cdot x + B \cdot y + C \cdot z + D = 0 \tag{1}$$

where

$$\begin{aligned} A &= \begin{vmatrix} y_2 - y_1 & z_2 - z_1 \\ y_3 - y_1 & z_3 - z_1 \end{vmatrix} \\ B &= \begin{vmatrix} x_2 - x_1 & z_2 - z_1 \\ x_3 - x_1 & z_3 - z_1 \end{vmatrix} \\ C &= \begin{vmatrix} x_2 - y_1 & y_2 - y_1 \\ x_3 - y_1 & y_3 - y_1 \end{vmatrix} \\ D &= -\begin{vmatrix} x_1 & y_1 & z_1 \\ x_2 & y_2 & z_2 \\ x_3 & y_3 & z_3 \end{vmatrix} \end{aligned} \tag{2}$$

The Euclidean distance between center points P_1 (x_1,y_1,z_1) and P_2 (x_2,y_2,z_2) of two scan bodies was measured as the length of the straight line that connects these two points (Fig. 2C) and can be expressed as:

$$d = \sqrt{(x_2 - x_1)^2 + (y_2 - y_1)^2 + (z_2 - z_1)^2} \tag{3}$$

The angulation of scan bodies was measured as the angle between two vectors representing the axes of scan bodies in 3D space (Fig. 2D). The angle between the two lines u and v was calculated using the expression:

$$\theta = \cos^{-1}\left(\frac{\vec{u}\cdot\vec{v}}{|\vec{u}|\cdot|\vec{v}|}\right) \tag{4}$$

where $\vec{u}$ and $\vec{v}$ are direction vectors of the lines u and v.

For the evaluation of the rotation between two scan bodies, the vertical edges of the scan body can be used. For the identification of the vector representing the top edge, the parameters of the side front plane and top plane of a flat surface of the scan body were calculated by picking three points on each wall. The result of the intersection of two selected front and top planes is the edge vector (Fig. 2E). The angle between the top edges of two scan body models was calculated using formula (4). This angle is the rotation of one scan body in relation to the other one (Fig. 2F).

The shortest distance between a center point of one scan body and the top plane of another scan body was calculated as:

$$d = \frac{A\cdot x + B\cdot y + C\cdot z + D}{\sqrt{A^2 + B^2 + C^2}} \tag{5}$$

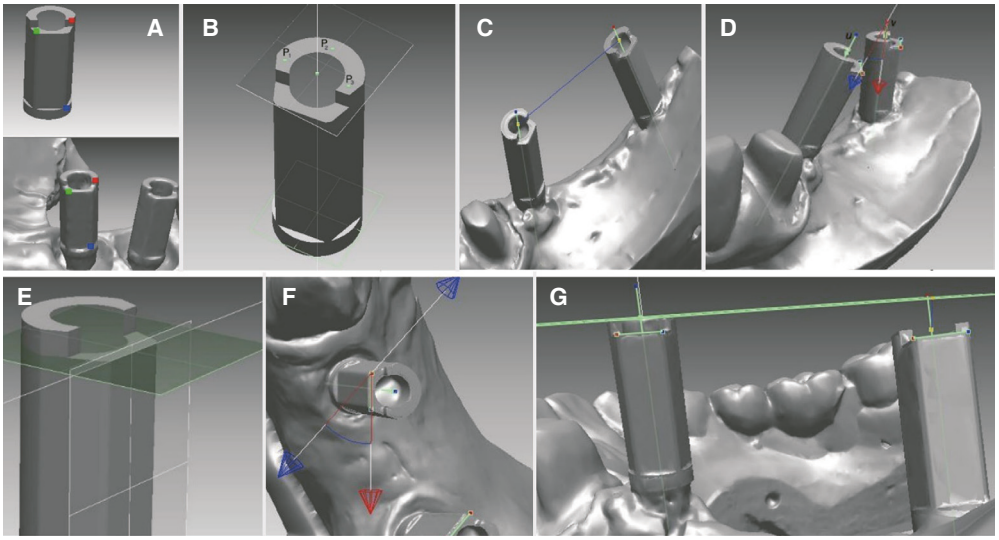

Fig. 2. (A) 3D computer models obtained using different scanning techniques. For coarse alignment, three corresponding points on the surface of each model are marked. (B) The center point of the scan body is at the intersection between its axis and top plane. (C) The Euclidean distance between the center points of two scan bodies. (D) The angulation of scan bodies. (E) Detecting the edge of the scan body. (F) The rotation of one scan body in relation to the other one. (G) The vertical shift of the scan body.

where *A*, *B*, *C*, and *D* are coefficients of the top plane of the scan body and *x*, *y*, and *z* are coordinates of the center point of another scan body. This was evaluated as the vertical shift of the scan body (Fig. 2G).

To evaluate the mismatch between the original model and the 3D model of the scan body, average distances between these given surfaces were measured. The Euclidean distance was calculated for each pair of corresponding points obtained by ICP algorithm. Five measurements for each parameter were done for each case.

To compare variables of conventional and digital groups, the average values and standard deviations of all parameters examined were calculated. New parameters of average distance between scan bodies and angulation were calculated by the formula (D800 data + Trios3 data)/2. They were used in order to evaluate the effect of the distance between scan bodies and angulation on the differences measured between conventional and digital impressions.

R software, (Lucent Technologies, Auckland, New Zealand), package 2.3 - version 2, was used for statistical analysis. Shapiro-Wilk test of normality revealed that not all data were distributed normally, and therefore the Wilcoxon signed rank test for paired data was applied for the comparison of medians. Association between measured differences and distance between the scan bodies or angulation between implants was evaluated using the Spearman correlation coefficient and linear regression models. Power of statistical criteria was calculated using GPower (Dusseldorf University, Dusseldorf, Germany) version 3.1.9.2 software. Statistical significance was set at $P < .05$.

RESULTS

Mean differences between CII and DII groups for distance between the scan bodies were found to be 70.8 ± 59 μm. Mean of differences for angulation was 0.37 ± 0.3°; for the rotation - 2.0 ± 1.37° and for vertical shift - 82.2 ± 61.7 μm. Except for the angulation variable, differences were statistically significant between all digital and conventional impression measurements (Table 1). Surface mismatch measurements comparing DII and CII were 34.14 ± 36.69 μm and 14.19 ± 3.22 μm for the mesial implant scan body and 34.24 ± 14.64 μm and 14.19 ± 2.29 μm for the distal implant scan body. Surface mismatch between mesially and distally located scan bodies in the DII group was significantly different, contrary to the CII group, where no differences were detected.

Distance between the scan bodies did not significantly correlate with any measured differences in distance between scan bodies, angulation, or vertical shift according to Spearmen correlation coefficients. Angulation between implants was significantly correlated with detected distance between scan bodies, angulation, and vertical shift differences, but the correlation was weak (Table 2). According to lin-

Table 1. Differences between digital and conventional workflow

Variable	Conventional impression		Digital impression		Mean of differences ± SD	*P* value	Wilcoxon signed rank test power
	Mean ± SD	Median	Mean ± SD	Median			
Distance between scanbodies	15.80 ± 5.65 mm	16.19	15.83 ± 5.67 mm	16.16	70.8 ± 59 μm	< .001	5%
Angulation	9.99 ± 5.57°	9.37	9.97 ± 5.65°	9.66	0.37 ± 0.3 °	.79	5%
Rotation	35.65 ± 23.45°	34.48	35.05 ± 23.42°	34.8	2.0 ± 1.37 °	.013	6.4%
Vertical shift	1.54 ± 1.91 mm	1.2	1.57 ± 1.92 mm	1.1	82.2 ± 61.7 μm	.001	5.8%
Mismatch M implant	14.19 ± 3.22 μm	14.28	34.14 ± 36.69 μm	29.28	-	< .001	98%
Mismatch D implant	14.19 ± 2.29 μm	14.72	34.24 ± 14.64 μm	33.52	-	< .001	100%

Table 2. Results of linear regression model (NS - not significant correlation)

Dependent variables (Differences between DII and CII)	Independent variables					
	Actual mean of distance between scanbodies			Actual mean of inter implant angulation		
	Spearmen coefficient	Linear regression model		Spearmen coefficient	Linear regression model	
		P value	Model power		*P* value	Model power
Distance between scanbodies	-0.036 (NS)	.078	19.8%	0.24	< .001	64%
Angulation	0.13 (NS)	.08	19.6%	0.35	.013	35.1%
Vertical shift	0.11 (NS)	.219	8.3%	0.36	.0006	33.1%

ear regression results, association of inter-implant angulation with measured differences between DII and CII was statistically significant in all variables ($P < .05$).

Means and standard deviations of all measured parameters are presented in Fig. 3, Fig. 4, Fig. 5, and Fig. 6. Differences of 100 µm for linear and 0.4° for angular variables were taken as tentative threshold values.[10]

DISCUSSION

DII are reported in the literature to be a viable alternative to conventional techniques, but these statements are based mostly on *in vitro* study results and subjective clinical experience.[5,14] Despite the growing opportunities of new technologies, like replicating mucosal tissue at the formed pontic area

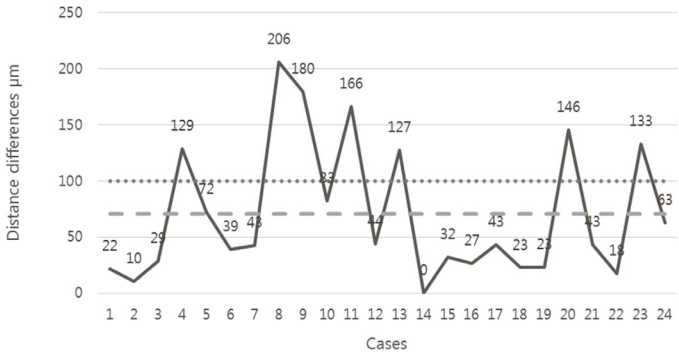

Fig. 3. Differences of distance between scan body measurements of conventional and digital impressions (mean 70.8 ± 59 µm). The dotted line represents the tentative clinical threshold of 100 µm misfit, and the dashed line represents the mean of the differences measured.

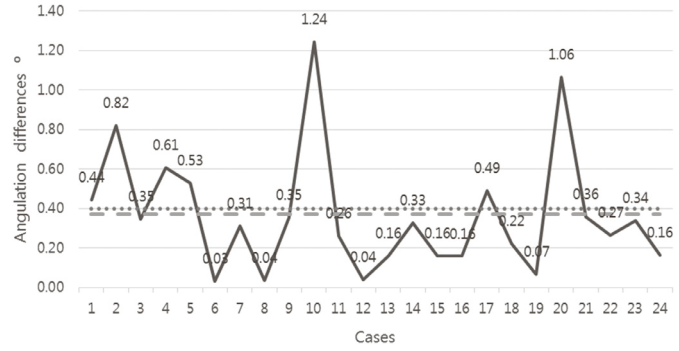

Fig. 4. Differences in angulation between the measurements of digital and conventional impressions (mean 0.37 ± 0.3°). The dotted line represents the tentative clinical threshold of angular misfit 0.4°, and the dashed line represents the mean of differences measured.

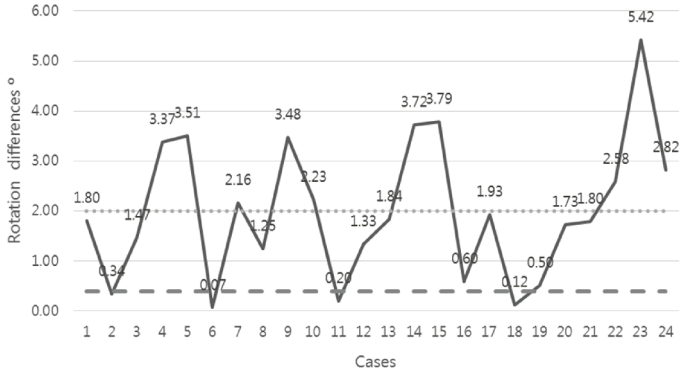

Fig. 5. Differences in rotation between the measurements of digital and conventional impressions (mean 2.0 ± 1.37°). The dashed line represents the tentative clinical threshold of angular misfit 0.4°, and the dotted line represents the mean of the differences measured.

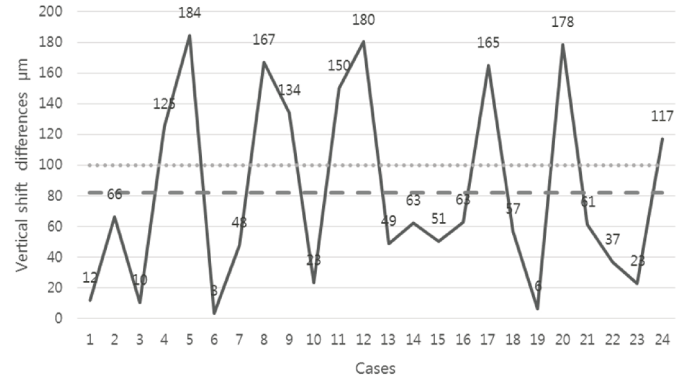

Fig. 6. Differences in vertical shift between digital and conventional groups (mean 82.2 ± 61.7 µm). The dotted line represents the tentative clinical threshold of 100 µm misfit, and the dashed line represents the mean of the differences measured.

and emerging profile of the peri implant tissue[15] or recording movements of patient's mandible, a fully digital workflow is not yet possible for every clinical situation. Digital and conventional impression techniques can both be recommended for single-unit fixed dental prostheses. Nevertheless, the digital workflow for short-span implant-supported restorations is less documented. Accurate conventional impressions and bite registrations are still needed for full-arch and complex cases.[16]

Besides the impression technique, master model fabrication, milling process, type of restoration material, and other factors can influence the final fit of the restoration.[16-19] Misfit is regarded as a potential risk factor for both cement- and screw-retained restorations. However, no widely accepted clinical threshold of marginal misfit has been determined, and values vary from 10 to 150 µm in the litera-

ture.[20,21] According to Katsoulis *et al.*,[22] there is a biological and mechanical tolerance to the misfit of restorations on implants, and therefore no threshold for maximum gap size or strain levels (screw, framework, implant-bone complex) can be defined. Clinical methods used to assess misfit (visual, tactile, and radiographic) are not sensitive enough to verify a gap of less than 50 μm, and misfit greater than 150 μm can easily be diagnosed without any sophisticated methods. Furthermore, bone strains caused by non-passive implant prosthesis can decrease because of bone adaptation when implants are loaded statically and dynamically.[23]

Few *in vivo* studies evaluating the accuracy of digital implant impressions and restorations on implants have been published in the literature.[5] The majority of studies are *in vitro* because it is possible to obtain true reference positions of scan bodies or implants using industrial measuring equipment. Applying industrial-grade reference scanner in clinical study is one of the approaches, but can only be performed in the anterior region of the maxilla under special conditions.[24] In this study, all restorations were in the posterior region, so this technique could not be adapted. Another approach was applied in the study by Alsharbaty *et al.*,[9] in which 36 patients with two implant-supported restorations were included. The accuracy of three impression techniques (DII using a Trios IOS, open-tray, and closed-tray CII) was evaluated by comparing them to reference models fabricated from splinted impression copings. Reference models were measured by a coordinate measuring machine. Conventional implant impressions made by the pick-up technique were found to be the most accurate. The accuracy of digital impressions showed the poorest results, and they were rendered clinically unacceptable to fabricate well-fitting restorations on implants. Angular mean deviation was found to be 6.77 ± 0.91°; mean linear displacement was 360 ± 46 μm, and deviation of 3D distance was 220 ± 30 μm. However, this method of obtaining reference data in the clinical study still has to be validated.[9]

Since there are no reliable techniques to obtain a true reference in the clinical circumstances, master models fabricated from the conventional impressions were used as the best available reference in this study. Also, validation of master model was employed according to strict protocol. Fit assessment of the final restoration also served as additional criteria to confirm the accuracy of conventional impressions. In this way, digital impression accuracy was compared to the conventional one. However, considering general practice, more variability in the accuracy of conventional implant impressions could be expected.

The clinically relevant threshold for the distortions of impressions and restorations is still unknown. Based on the recent study, the threshold for horizontal/vertical misfit and angulation errors of two implant-supported restorations were taken as 100 μm and 0.4°, respectively.[10] Statistically significant differences between scan bodies' distances were found between the conventional and digital groups; the resulting mean (70.8 ± 59 μm) was below 100 μm. Vertical shift differences were lower than 100 μm (82.2 ± 61.7 μm), and statistically significant difference was found between CII and DII. Mean angulation differences were below 0.4 ° (0.37 ± 0.3°). Considering these thresholds, the measured means can be regarded as having minimal clinical relevance. These results are in line with *in vitro* studies concluding that DII can be as accurate as conventional impressions.[14,15] Resulting differences were much lower, as in the study by Alsharbaty *et al.*[9] However, considering high standard deviation of the detected differences, maximum values could be of potential clinical significance.

Since rotational misfit of dental implant abutments can affect the fitting of implant superstructures,[25,26] the rotation of scan bodies was evaluated. Mean rotation difference was found to be 2.0 ± 1.37°, and statistically significant difference was detected between DII and CII. Hence, the abutments without anti-rotational features are commonly recommended for multiple-unit implant-supported restorations. However, in cases in which titanium bases without antirotational features are not available with a certain implant system, minor changes in the rotational position of abutments can negatively influence the fitting of the prosthesis.[17]

Surface mismatch was more pronounced when the scan bodies were scanned with the IOS than with the laboratory scanner. Differences between Trios3 and D800 were statistically significant for both mesial and distal scan bodies. Surface mismatch when scanned with the IOS was approximately two times higher than in the case of the laboratory scanner. This type of error can lead to discrepancies when the 3D position of the scan body's CAD model is being defined and contributes to the final amount of misfit. The entire workflow can therefore be affected in this way.

Analysis of linear regression models showed that the actual mean of distance between scan bodies did not significantly correlate with distance between scan bodies, angulation, and vertical shift differences detected in both groups. However, angulation between scan bodies significantly ($P < .05$) affected the differences of all parameters assessed, although Spearmen correlation coefficients were weak, ranging from 0.24 to 0.36. Flügge *et al.* and Papaspyridakos *et al.* have reported that increasing angulation and distance between scan bodies negatively affected scanning precision.[27,28] However, other authors have claimed the opposite.[29,30] Limited values for inter-implant distance and angulation causing clinically significant errors should be defined for the different IOS in the future.

The accuracy of digital implant impressions can be negatively influenced by additional factors as well: the repositioning accuracy of prosthetic components, construction and shape of the scan bodies, scanning area, scanning sequence, and others.[31-33] Machining accuracy of prosthetic components[34] and different types of implant-abutment connections could have an impact on the results, when the accuracy and precision of the impression techniques are evaluated. The implant system used in the study employs an 11° internal hex connection. Therefore, the results with implants having other types of connections or different

geometries of prosthetic components could be different.

Due to constant improvements in digital technologies, the scientific field is rapidly filled with new information validating digital impression procedures. Since the potential of IOS clinical applications is also increasing, further studies will be needed before digital impressions are able to fully substitute conventional ones.

CONCLUSION

Considering limitations, some conclusions can be drawn. Firstly, recorded linear differences between digital and conventional impressions are of limited clinical significance in two implant-supported restorations of up to four units. Secondly, the angulation between implants affected distance between scan bodies, angulation, and vertical shift differences in the scan body position resulting from digital and conventional workflow. Moreover, scan body surface mismatch was higher for the intraoral scanner group. However, methods to obtain true reference data in the clinical studies should be validated and would need further research.

ORCID

Vygandas Rutkunas *https://orcid.org/0000-0002-5096-2086*
Agne Gedrimiene *https://orcid.org/0000-0003-3377-9447*
Rimas Adaskevicius *https://orcid.org/0000-0003-2385-8854*

REFERENCES

1. Joda T, Katsoulis J, Brägger U. Clinical fitting and adjustment time for implant-supported crowns comparing digital and conventional workflows. Clin Implant Dent Relat Res 2016;18:946-54.
2. Baig MR. Accuracy of impressions of multiple implants in the edentulous arch: a systematic review. Int J Oral Maxillofac Implants 2014;29:869-80.
3. Mormann WH, Brandestini M, Lutz F, Barbakow F, Gotsch T. CAD-CAM ceramic inlays and onlays: a case report after 3 years in place. J Am Dent Assoc 1990;120:517-20.
4. Zarauz C, Valverde A, Martinez-Rus F, Hassan B, Pradies G. Clinical evaluation comparing the fit of all-ceramic crowns obtained from silicone and digital intraoral impressions. Clin Oral Investig 2016;20:799-806.
5. Rutkūnas V, Gečiauskaitė A, Jegelevičius D, Vaitiekūnas M. Accuracy of digital implant impressions with intraoral scanners. A systematic review. Eur J Oral Implantol 2017;10:101-120.
6. Biagioni A, Ferrari M, Pecciarini M. A systematic review about randomized clinical trials on digital impressions on sound teeth. J Osseointegration 2019;11:2-6.
7. Flügge T, van der Meer WJ, Gonzalez BG, Vach K, Wismeijer D, Wang P. The accuracy of different dental impression techniques for implant-supported dental prostheses: A systematic review and meta-analysis. Clin Oral Implants Res 2018;29:374-92.
8. Cappare P, Sannino G, Minoli M, Montemezzi P, Ferrini F. Conventional versus digital impressions for full arch screw-retained maxillary rehabilitations: A randomized clinical trial. Int J Environ Res Public Health 2019;16:829.
9. Alsharbaty MHM, Alikhasi M, Zarrati S, Shamshiri AR. A clinical comparative study of 3-dimensional accuracy between digital and conventional implant impression techniques. J Prosthodont 2019;28:e902-8.
10. Andriessen FS, Rijkens DR, van der Meer WJ, Wismeijer DW. Applicability and accuracy of an intraoral scanner for scanning multiple implants in edentulous mandibles: a pilot study. J Prosthet Dent 2014;111:186-94.
11. Rutkunas V, Ignatovic J. A technique to splint and verify the accuracy of implant impression copings with light-polymerizing acrylic resin. J Prosthet Dent 2014;111:254-6.
12. Abduo J, Bennani V, Waddell N, Lyons K, Swain M. Assessing the fit of implant fixed prostheses: a critical review. Int J Oral Maxillofac Implants 2010;25:506-15.
13. Flügge TV, Att W, Metzger MC, Nelson K. Precision of dental implant digitization using intraoral scanners. Int J Prosthodont 2016;29:277-83.
14. Gherlone EF, Ferrini F, Crespi R, Gastaldi G, Capparé P. Digital impressions for fabrication of definitive "all-on-four" restorations. Implant Dent 2015;24:125-9.
15. Venezia P, Torsello F, Cavalcanti R, Casiello E, Chiapasco M. Digital registration of peri-implant transmucosal portion and pontic area in the esthetic zone. J Osseointegration 2017;9:312-6.
16. Abduo J. Fit of CAD/CAM implant frameworks: a comprehensive review. J Oral Implantol 2014;40:758-66.
17. Beuer F, Schweiger J, Edelhoff D. Digital dentistry: an overview of recent developments for CAD/CAM generated restorations. Br Dent J 2008;204:505-11.
18. Kohorst P, Brinkmann H, Li J, Borchers L, Stiesch M. Marginal accuracy of four-unit zirconia fixed dental prostheses fabricated using different computer-aided design/computer-aided manufacturing systems. Eur J Oral Sci 2009;117:319-25.
19. Papaspyridakos P, Chen CJ, Gallucci GO, Doukoudakis A, Weber HP, Chronopoulos V. Accuracy of implant impressions for partially and completely edentulous patients: a systematic review. Int J Oral Maxillofac Implants 2014;29:836-45.
20. Brånemark PI. Osseointegration and its experimental background. J Prosthet Dent 1983;50:399-410.
21. Jemt T. Failures and complications in 391 consecutively inserted fixed prostheses supported by Brånemark implants in edentulous jaws: a study of treatment from the time of prosthesis placement to the first annual checkup. Int J Oral Maxillofac Implants 1991;6:270-6.
22. Katsoulis J, Takeichi T, Sol Gaviria A, Peter L, Katsoulis K. Misfit of implant prostheses and its impact on clinical outcomes. Definition, assessment and a systematic review of the literature. Eur J Oral Implantol 2017;10:121-38.
23. Karl M, Taylor TD. Bone adaptation induced by non-passively fitting implant superstructures: A randomized clinical trial. Int J Oral Maxillofac Implants 2016;31:369-75.
24. Nedelcu R, Olsson P, Nyström I, Rydén J, Thor A. Accuracy

and precision of 3 intraoral scanners and accuracy of conventional impressions: A novel in vivo analysis method. J Dent 2018;69:110-8.
25. Semper W, Kraft S, Mehrhof J, Nelson K. Impact of abutment rotation and angulation on marginal fit: theoretical considerations. Int J Oral Maxillofac Implants 2010;25:752-8.
26. Alikhasi M, Monzavi A, Bassir SH, Naini RB, Khosronedjad N, Keshavarz S. A comparison of precision of fit, rotational freedom, and torque loss with copy-milled zirconia and prefabricated titanium abutments. Int J Oral Maxillofac Implants 2013;28:996-1002.
27. Flügge TV, Att W, Metzger MC, Nelson K. Precision of dental implant digitization using intraoral scanners. Int J Prosthodont 2016;29:277-83.
28. Papaspyridakos P, Benic GI, Hogsett VL, White GS, Lal K, Gallucci GO. Accuracy of implant casts generated with splinted and non-splinted impression techniques for edentulous patients: an optical scanning study. Clin Oral Implants Res 2012;23:676-81.
29. Tan MY, Yee SHX, Wong KM, Tan YH, Tan KBC. Comparison of three-dimensional accuracy of digital and conventional implant impressions: Effect of interimplant distance in an edentulous arch. Int J Oral Maxillofac Implants 2019;34:366-80.
30. Gintaute A. Accuracy of computerized and conventional impression-making procedures of straight and tilted dental implants [Internet]. Freiburg; Albert-Ludwig Universitat; 2015. Available from: https://freidok.uni-freiburg.de/dnb/download/10655
31. Giménez B, Özcan M, Martínez-Rus F, Pradíes G. Accuracy of a digital impression system based on active triangulation technology with blue light for implants: Effect of clinically relevant parameters. Implant Dent 2015;24:498-504.
32. Gimenez-Gonzalez B, Hassan B, Özcan M, Pradíes G. An in vitro study of factors influencing the performance of digital intraoral impressions operating on active wavefront sampling technology with multiple implants in the edentulous maxilla. J Prosthodont 2017;26:650-5.
33. Müller P, Ender A, Joda T, Katsoulis J. Impact of digital intraoral scan strategies on the impression accuracy using the TRIOS Pod scanner. Quintessence Int 2016;47:343-9.
34. Stimmelmayr M, Güth JF, Erdelt K, Edelhoff D, Beuer F. Digital evaluation of the reproducibility of implant scanbody fit-an in vitro study. Clin Oral Investig 2012;16:851-6.

Paper II

Accuracy of digital implant impressions with intraoral scanners. A systematic review

*V. Rutkūnas, **A. Gečiauskaitė**, D. Jegelevičius, M. Vaitiekūnas*

Eur J of Oral Implant 2017;10 Suppl 1:101-120.

Vygandas Rutkūnas, Agnė Gečiauskaitė, Darius Jegelevičius, Mantas Vaitiekūnas

Accuracy of digital implant impressions with intraoral scanners. A systematic review

Vygandas Rutkūnas
Associate Professor, Department of Prosthodontics, Institute of Odontology, Faculty of Medicine, Vilnius University, Lithuania

Agnė Gečiauskaitė
PhD student, Department of Prosthodontics, Institute of Odontology, Faculty of Medicine, Vilnius University, Lithuania

Darius Jegelevičius
Head of Laboratory, Biomedical Engineering Institute, Kaunas University of Technology, Lithuania
Associate Professor, Department of Electronics Engineering, Kaunas University of Technology, Lithuania

Mantas Vaitiekūnas
PhD student, Biomedical Engineering Institute, Kaunas University of Technology, Lithuania

Correspondence to:
Assoc Prof Vygandas Rutkūnas DDS, PhD, Dip Prost
Department of Prosthodontics
Institute of Odontology
Faculty of Medicine
Vilnius University
Žalgirio str. 115, LT-08217
Vilnius, Lithuania
Email: vygandasr@gmail.com

Key words *accuracy, CAD/CAM, dental implant, digital, impression, intraoral scanner, systematic review*

Aim: The use of intraoral scanners (IOS) for making digital implant impressions is increasing. However, there is a lack of evidence on the accuracy of IOS compared with conventional techniques. Therefore, the aim of this systematic review was to collect evidence on the accuracy of digital implant impression techniques, as well as to identify the main factors influencing the accuracy outcomes.
Materials and methods: Two reviewers searched electronic databases in November, 2016. Controlled vocabulary, free-text terms, and defined inclusion and exclusion criteria were used. Publications in English language evaluating the accuracy outcomes of digital implant impressions were identified. Pooled data were analysed qualitatively and pertinent data extracted.
Results: In total, 16 studies fulfilled the inclusion criteria: one *in vivo* and 15 *in vitro* studies. The clinical study concluded that angular and distance errors were too large to be acceptable clinically. Less accurate findings were reported by several *in vitro* studies as well. However, all *in vitro* studies investigating the accuracy of newer generation IOS indicated equal or even better results compared with the conventional techniques. Data related to the influence of distance and angulation between implants, depth of placement, type of scanner, scanning strategy, characteristics of scanbody and reference scanner, operator experience, etc were analysed and summarised. Linear deviations (means) of IOS used in *in vitro* studies ranged from 6 to 337 μm. Recent studies indicated small angle deviations (0.07–0.3°) with digital impressions. Some studies reported that digital implant impression accuracy was influenced by implant angulation, distance between the implants, implant placement depth and operator experience.
Conclusions: According to the results of this systematic review and based on mainly *in vitro* studies, digital implant impressions offer a valid alternative to conventional impressions for single- and multi-unit implant-supported restorations. Further *in vivo* studies are needed to substantiate the use of currently available IOS, identify factors potentially affecting accuracy and define clinical indications for specific type of IOS. Data on Data on accuracy OF digital records, as well as accuracy of printed or milled models for implant-supported restorations, are of high relevance and are still lacking.

Conflict-of-interest and funding statement: *The authors state there is no conflict of interest.*

■ Introduction

Oral implants have improved the care of partially and completely edentulous patients for several decades. Although implant-supported dental prostheses have proved to be a reliable long-term solution[1,2], many biological and technical challenges still remain[3,4]. Digital technologies have revolutionised clinical prosthodontics, extending diagnostic, treatment and follow-up possibilities[5,6]. They have improved

conventional prosthetic approaches and enabled completely new treatment workflows, as well as introducing the concept of the "virtual patient"[7].

Accuracy is a key aspect in function and aesthetics of indirect restorations. The fit of implant-supported dental restorations has been discussed extensively in the literature[8]. In contrast to natural teeth, osseointegrated implants are not able to compensate for small inaccuracies of the prostheses, as they are virtually immobile[9]. Their sensory discrimination is more limited than for teeth[10]. The demand for accurately fitting implant-supported prostheses is further increased with the use of screw-retained restorations or when stiff and prone to cracking materials (e.g. materials (e.g. ceramics) are used to splint multiple implants with fixed partial dentures (FPD). Due to a build-up of errors in each clinical and laboratory step, a certain degree of inaccuracy is unavoidable. Many techniques have been proposed to evaluate the passive fit of restorations, however, none of them can be relied on solely[8]. Consequently, various methods to improve the fit of the multiple implant-supported restorations has been suggested[11,12,13]. Non-passively fitting restorations could potentially be related to mechanical complications: loss of retention, screw loosening, fracture of framework or veneering material[14,15]. However, consensus on the clinically acceptable level of misfit has not yet been reached. Several authors have proposed different recommendations for clinically acceptable misfit ranging from 10 μm to 150 μm[16]. It has even been suggested that for maintaining osseointegration of endosseous implants, passivity of fit of multi-unit restorations seems not to be as critical as previously thought[17]. Since the definition of the passive fit is still hypothetical and the level of clinically acceptable misfit has not been determined, clinicians should always strive to achieve the most accurate fit possible for implant-supported FPDs.

While modern CAM technologies technologies are capable of achieving a precise fit exceeding that of casting techniques, they still rely on the accuracy of impressions, definitive models and bite registrations[18]. Many previous studies reported on the accuracy of different conventional implant impression (CII) techniques, addressing the influence of number of implants, angulation, implant placement depth, type of implant-abutment connection, direct or indirect technique, and splinting of impression copings[19,20]. As a result, several systematic reviews have addressed the accuracy of conventional implant impression techniques[21-26]. Recently published studies preferred direct to indirect impressions and splinted over non-splinted techniques, especially with increased number of implants[21,27,28]. Implant angulation of 20 to 25 degrees negatively affected the multiple implant impression accuracy[24]. Results reported for internal connection implants were less consistent, in contrast to reports on external connection implants[29]. Even with procedural diligence, conventional impression techniques involve process-related risks, uncontrolled variables, expensive laboratory and chairside time, material expense, and patient discomfort[30].

Digital impressions were proposed as viable alternative to make impressions for tooth- and implant-supported restorations. The number of digital intraoral scanners (IOS) on the market is increasing, and new improved hardware and software versions are released continuously. IOS can capture the images as digital photographs or video. They eliminate tray selection, dispensing, setting and volumetric changes of impression materials, disinfection and transporting to dental laboratory, gypsum pouring and cast preparation for articulation[28].

As defined by ISO-5725-1:1994, accuracy of IOS consists of trueness and precision. Trueness describes the deviation of scans from the true dimensions of the object, while precision describes how much separate scans of the same object differ from each other.

IOS usage for teeth-supported restorations has more documentation than use with implant-supported prostheses. According to a recent systematic review, tooth-supported single-unit crowns fabricated using the digital impression technique presented statistically similar marginal discrepancies compared with those obtained with the conventional impression technique[31]. However, there is less evidence available on the accuracy of digital impressions for implant-supported restorations, especially FPDs[24]. In fact, a systematic review, addressing the accuracy of different implant impression techniques concluded that insufficient data exists on digital impression techniques and that the further studies are needed[28]. Recently, a number of articles addressing the accuracy of digital implant impressions (DII) have been published.

Table 1 Search strategy for MEDLINE/PubMed.

Search terms	Number of records returned
MeSH terms:	
"Dental Impression Technique"[Mesh]) AND "Dental Implants"[Mesh]	657
"Dental Impression Technique"[Mesh]) AND "Dimensional Measurement Accuracy"[Mesh]	59
"Dental Implants"[Mesh]) AND "Printing, Three-Dimensional"[Mesh]	23
"Dental Implant-Abutment Design"[Mesh]) AND "Dental Impression Technique"[Mesh]	136
"Dental Impression Materials"[Mesh] AND "Dental Implants"[Mesh]	398
Free-text:	
Implant AND intraoral scanner	37
Implant position AND digital	163
Implant AND impression	1007
Implant impression AND accuracy	233
Implant impression AND optical	44
Implant impression AND digital	104

Therefore, the aim of this review was to collect available evidence and evaluate accuracy outcomes of DII techniques. Additionally, different variables influencing accuracy of DII were identified when possible.

■ Materials and methods

This systematic review was conducted following PRISMA (Preferred Reporting for Systematic Reviews and Meta-Analyses) guidelines.

■ Focused question

What are the accuracy outcomes of digital implant impression techniques?

■ Inclusion and exclusion criteria

PICOS (patient, intervention, comparison, outcomes, study design) criteria were used for inclusion and exclusion of studies:

- Patients: partially or completely edentulous dental arch or replica with implants.
- Intervention: taking single-unit or multi-unit conventional and digital, or only digital implant impressions with commercially available IOS, using scanbodies.
- Comparison: accuracy of DII (or model produced from DII) compared to the reference model (or the model produced from CII).
- Outcomes: quantitative measurement of accuracy (linear, angular).
- Study design: *in vivo* and *in vitro* experimental studies.

Studies with clearly explained impression accuracy assessment methodology were included in the systematic review. Case reports, expert opinions, technical or clinical reports, incomplete publications, and review articles were excluded. However, potentially relevant information from these publications was also considered, though these publications were not included into the systematic review. Studies comparing outcomes of restorations fabricated from digital and conventional impressions were not included, as the restoration the fabrication process alone can considerably influence accuracy.

■ Search strategy and data collection

An electronic search was performed using selected databases: MEDLINE/PubMed, Cochrane Central Register of Controlled Trials (CENTRAL), Web of Science, AMED (Ovid). Only English language publications were Included. Published and early-view online articles were identified. The latest search was conducted on November 10, 2016. A detailed search strategy was prepared including free-text and MeSH (Medical Subject Headings) terms for each database search. Search strategy for MEDLINE/PubMed is presented in Table 1. Additionally, a hand search was performed reviewing references of potentially

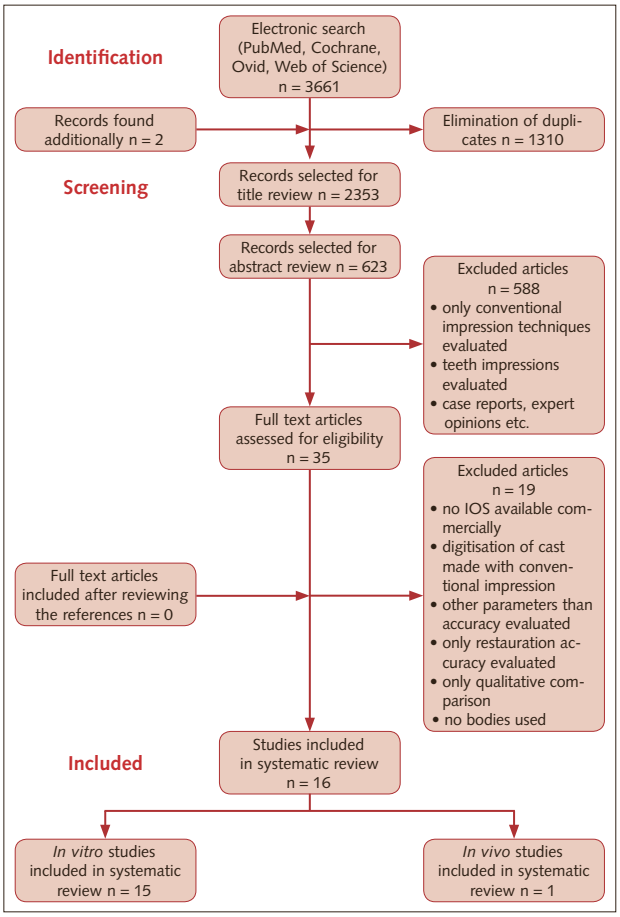

Fig 1 Study selection process.

pertinent papers, review papers as well as content of the following journals: Journal of Dental Research, Clinical Implant Dentistry and Related Research, Clinical Oral Implants Research, European Journal of Oral Implantology, Implant Dentistry, International Journal of Oral and Maxillofacial Surgery, Journal of Cranio-Maxillo-Facial Surgery, Journal of Oral Implantology, Journal of Dentistry, Clinical Oral Investigations, and Journal of Oral Rehabilitation.

Identified publications were imported into the reference manager program (Zotero, Fairfax, VA, USA) and duplicates were removed electronically. Titles of the publications were screened by two calibrated reviewers (VR and AG). Abstracts of remaining publications were then screened. In cases when information provided in the abstract was insufficient, full-text articles were reviewed. Selected records were obtained for the full-text review. Based on inclusion and exclusion criteria, publications were selected for the systematic review. References of these publications were additionally searched for the other relevant publications. Following data, when possible, was extracted using the electronic spreadsheet: anatomic location, implant type, distance and angulation between implants, depth of placement, impression level, implant-abutment connection type, type of the scanner (powder/no powder), scanning strategy, characteristics of scanbody and reference scanner, operator experience, accuracy measurement methodology. Disagreements regarding record screening, title, abstract or full-text review, and data extraction were solved by discussion, leading to the consensus between all authors. In order to reduce the risk of bias, PRISMA guidelines were followed.

RESULTS

Included studies

The initial search resulted in 3661 records. After removing duplicates and adding records identified through other sources (one of them a PhD thesis published online), 2353 records were selected for title review. The subsequent selection at the title level yielded 623 titles. Screening of the abstracts revealed 35 publications. Of the 35 articles selected for the full-text review, 16 publications were finally included (Fig 1). Articles that were not included in this systematic review and the reasons for exclusion are shown in Table 2.

Characteristics of the included studies

Of the 16 included studies, one study was an *in vivo* study and 15 others were *in vitro* studies.

The majority of studies evaluated the accuracy of iTero IOS (n = 8), then True Definition (n = 5), Trios (n = 3), Lava COS (n = 3), Trios Color (n = 2), Cerec Bluecam (n = 2), ZFX Intrascan (n = 2), Cerec Omnicam (n = 1), 3D Progress (n = 1), CS3500

Table 2 Excluded studies and reasons for exclusion.

Studies	Reason for exclusion
Ortorp et al[62] 2005; Bergin et al[63] 2013	No commercially available scanner. Limited clinical applications.
Eliasson et al[64] 2012; Howell et al6[5] 2013	Conventional impressions from digitally coded healing abutments taken. No digital impression technique with intraoral scanner was used.
Lee et al[66] 2013; Lee et al[67] 2013; Wismeijer et al[68] 2014; Calesini et al[69] 2014; Joda et al[53] 2015; Schepke et al[70] 2015; Joda et al[52] 2015; Joda et al[71] 2016	Accuracy of digital implant impression techniques was not evaluated.
Aktas et al[72] 2014; Abdel-Azim et al[73] 2014; Karl et al[74] 2012	Accuracy of different impression techniques was not evaluated. Fit of the prosthesis produced from conventional and digital impressions was evaluated *in vitro*.
Gherlone et al[75] 2015; Lee et al[76] 2015; Gherlone et al[77] 2016	Clinical study. No evaluation of digital implant impression accuracy.
Ajioka et al[38] 2016	No scanbodies used for the experiment.

(n = 1) and Planmeca Planscan (n = 1). Eight studies indicated the version of the IOS software[32–37,39,40], while the other eight studies did not[41–48]. Eight of the included studies evaluated accuracy of DII in the maxilla[33–35,42–45,40] and the other eight related to the mandible[32,36,37,41,46–48,39]. Six studies investigated situations with partially edentulous arch (from 1 to 3 implant-supported single- and multi-unit restorations)[41,44–46,37,40], and 10 looked at completely edentulous situations with two to six implants[32–36,42,43,47,48,40]. Data obtained from DII was compared with data from the reference model in 12 studies[33–35,41–44,48,40,36,47,39], with data from conventional models in four studies[36,47,39,32]. The majority of studies evaluated trueness of DII as a measure of accuracy. Precision was evaluated by five studies[41,44,45,48,40]. Three studies compared the accuracy of milled models fabricated from DII with reference or conventional models[44–46]. Distance (3D or in specific plane) and angle deviations were estimated in the included studies. Detailed characteristics and main findings of the included studies are listed in Tables 3 and 4.

Table 3 Characteristics and main findings of included *in vivo* study.

Article	No. of implants, positions	No. of patients, restorations	Implant angulation, average distance	Implant characteristics	Impression level	Scanned object, strategy	Type of intraoral scanner	Reference	Accuracy evaluation	Conclusion
Andriessen et al[32] 2014	2, regio #33 and #43	25, 25	No data	Standard SLA-active RN (Straumann, Basel, Switzerland), 4.1/12 mm; Internal connection	Implant level	RN Scanbody (Straumann); Hand-tightened; 5 scans (occlusal, 45 degrees buccal, 45 degrees lingual, mesioproximal, and distoproximal)	iTero (Cadent Inc); Software version 3.5.0; No powder	Master model, scanned with Lava Scan STscanner (3M ESPE, Seefeld, Germany)	Linear and angular. Measurement of the mid-centre line of the 2 scan abutments, showed a distance mean error of 226.0 mm compared with the reference scan. Distance error was smaller than 100 µm in 5 of the 21 scans. The mean absolute angulation error was 2.582 degrees. An angulation error <0.4 degrees was recorded in 3 of the 21 scans.	Digital impression accuracy is not adequate

Table 4 Characteristics and main findings of included *in vitro* studies.

Article	No. of implants. positions	Angulation	Placement depth (mm)	Implant manufacturer. connection	CII technique	DII technique: IOS; use of powder; scanning strategy	Number of impressions	Scanbody. torque value Ncm
Single-unit digital implant impressions								
Lee et al[45] 2015	1. #25	No data	No data	Bone Level. Regular Crossfit. (Straumann); Internal connection	CT. IL	iTero (Align Technology. Israel). no data on version; NP; No data on strategy	30	Scanbody (Straumann); No data on torque value
Koch et al[44] 2016	1. #25	No data	No data	Bone Level. Regular Crossfit (Straumann); Internal connection	Not used	iTero (Align Technology). no data on version; NP; No data on strategy	30	Scanbody (Straumann); No data on torque value
Multi-unit digital implant impressions								
Lin et al[46] 2015	2. #35 and #37. distance of 10 mm		1 mm coronal	RN. Standard Plus (Straumann); Internal connection	OT. NSp. IL	iTero (Align Technology). no data on version; NP; No data on strategy	40	Two-piece scanbody (Straumann); 15 Ncm
		0° divergency						
		15° divergency						
		30° divergency						
		45° divergency						
Papaspyridakos et al[47] 2015	5. interforaminal region	The medial 3implants - parallel; distal left - 10°. distal right - 15°.	No data	Bone Level Regular Crossfit (Straumann); Internal connection	OT 1)IL. Sp 2) IL. NSp 3) AL. Sp 4) AL. NSp	Trios (3Shape). No data on version; NP; No data on strategy	10	Scanbody (Straumann). No data on torque value
Vandeweghe et al[48] 2016	6. #36. #34. #32. #42. #44. #46	Parallel	No data	IBT. Southern Implants (Irene. South Africa); External connection	Not used	Lava COS (3M ESPE). no data on version; P; No data on strategy	10	PEEK. (Proscan Zonhoven Belgium); 10 Ncm preload
						3M True Definition (3M ESPE). no data on version; P; No data on strategy		
						Cerec Omincam (Sirona). no data on version; NP; No data on strategy		
						Trios (3Shape). no data on version; NP; No data on strategy		

VPS – polyvinylsiloxane; PE – polyether; CII – conventional implant impression; DII – digital implant impression; IOS – intraoral scanner; CMM – coordinate measuring machine; CT – closed tray; OT – open tray; IL – implant level; AL – abutment level; Sp – splinted; NSp – non-splinted; S – significant; NS – non-significant; BL – bone level; TL - tissue level; Absd - absolute angular distortion; P – powdered; NP – non-powdered.

<table>
<tr><th>Reference scanner</th><th>Accuracy evaluation. results</th><th>Conclusions</th></tr>
<tr><td colspan="3"></td></tr>
<tr><td>Lava Scan ST (3M ESPE)</td><td>Comparison (linear): models produced from DII (milled model) and CII (gypsum model). compared to reference model
Horizontal CII 34 ± 9 mm. DII 11 ± 13 mm (NS)
Vertical CII -88 ± 44 mm. DII 93 ± 61 mm (S)</td><td>Vertical position of the implant in milled models was more coronal than in the plaster model. Cause of vertical position errors is commented to be processing errors of the analogue placement.</td></tr>
<tr><td>Lava Scan ST (3M ESPE)</td><td>Comparison: mean volumetric deviations at 5 selected points between DII model (digitized milled model) at implant surface and reference model
DII vs reference model -6 ± 40μm
DII vs milled model from DII 19 ± 162μm
DII model (milled) vs reference model 14 ± 170μm</td><td>Cumulative errors were found in the line of workflow. Software. scanner. and milling error (standard deviations. respectively: ±1. ±21. and ±98 μm) were shown to propagate throughout the digital workflow to the milled model (100 μm).</td></tr>
<tr><td colspan="3"></td></tr>
<tr><td>Cagenix scanner (Cagenix Inc)</td><td>Differences between models produced from DII (digitised milled models) and CII (digitised impression models) (comparison of CII/DII models with reference model is not included in the table)
Linear differences | Angular differences
221 ± 35μm (S) | 0.986 ± 0.218° (S)
260 ± 35 μm (S) | 1.551 ± 0.218° (S)
159 ± 36 μm (S) | 0.004 ± 0.218° (NS)
75 ± 36 μm (NS) | 0.438 ± 0.218° (NS)</td><td>Models made from CII were more accurate than made from DII. Divergence between the two implants significantly affected the accuracy. In 0° and 15° groups. the digital pathway resulted in less accurate models compared with the conventionally created ones. DII produced more accurate definitive models when the two implants diverged more.</td></tr>
<tr><td>IScan D103i (Imetric)</td><td>Comparison of 3D deviations (μm) of scanbodies on models produced from DII (digital model) and CII (digitised stone model) as compared to reference model (Interquartile range is shown in parenthesis).
Implant number | IL - Sp | IL - NSp | DII | AL - Sp | AL - NSp
1 | 5.79 (5.69–5.94) | 21.89 (21.84–21.98) | 23.39 (23.27–23.47) | 33.10 (32.93–33.24) | 14.59 (14.52–14.76)
3 | 9.16 (8.99–9.28) | 13.00 (12.84–13.21) | 15.27 (15.18–15.53) | 14.31 (13.98–14.49) | 1.27 (1.19–1.37)
4 | 4.70 (4.54–4.81) | 13.39 (12.97–13.46) | 7.60 (7.54–7.67) | 12.04 (11.86–12.13) | 6.91 (6.69–6.96)
5 | 12.52 (12.44–12.67) | 131.75 (131.6–132.1) | 29.02 (28.78–29.15) | 8.86 (8.81–9.01) | 9.63 (9.37–9.78)</td><td>The accuracy of DII was not different than the implant-level. splinted CII and more accurate than the implant-level. non-splinted impressions.
The accuracy of implant impressions was not affected by the implant angulation up to 15°</td></tr>
<tr><td>104i scanner (Imetric)</td><td>Comparison: 3D deviations comparing DII (digital model) and reference model
Trueness | Precision
112 ± 25 μm | 66 ± 25 μm
35 ± 12 μm | 30 ± 11 μm
61 ± 23 μm | 59 ± 24 μm
28 ± 7 μm | 33 ± 12 μm
Non-significant difference between 3M True Definition and Trios for trueness and precision.</td><td>Significant differences in accuracy between the different scanners were found. Lava COS scanner did not achieve the necessary level of accuracy to be used for large-span implant-supported reconstructions. Other scanners demonstrated an acceptable level of trueness and precision for this indication.</td></tr>
</table>

Article	No. of implants. positions	Angulation	Placement depth (mm)	Implant manufacturer. connection	CII technique	DII technique: IOS; use of powder; scanning strategy	Number of impressions	Scanbody. torque value Ncm
Flügge et al[41] 2016	Model 1: 2. #36. #35 Model 2: 5. #36. #35. #33 and #45. #47	Non parallel	No data	Bone Level and Tissue Level (Straumann); Internal connection	Not used	iTero (Align Technology). no data on version; NP; No data on strategy Trios (3Shape). no data on version. NP; No data on strategy True Definition (3M ESPE). no data on version;P; No data on strategy	10	Bone Level and Tissue Level scanbody (Straumann) No data on torque value
Gimenez et al[43] 2016	6. #17. #15. #12. #22. #25. #27	#17. #12. #22. #27 - 0° #15 - 30° distally. #25 - 30° mesially	#17. #27. #15. #25- 0 mm #12 - 4 mm #22 - 2 mm	Certain 4. 1/11 mm. (Biomet 3i. Palm Beach Gardens. FL. USA); Internal connection	Not used	True Definition (3M ESPE); no data on version; P	4 operators. 5 DII each	PEEK (Createch Medical S.L.); No data on torque value
Gimenez et al[42] 2015	6. #17. #15. #12. #22. #25. #27	#17. #12. #22. #27 - 0° #15 - 30° distally. #25 - 30° mesially	#17. #27. #15. #25- 0 mm #12 - 4 mm #22 - 2 mm	Certain 4. 1/11 mm. (Biomet 3i); Internal connection	Not used	Lava COS (3M ESPE); Version 0.3.0.2; P	4 operators. 5 DII each	PEEK (Createch Medical S.L.); No data on torque value
Gimenez et al[35] 2015	6. #17. #15. #12. #22. #25. #27	#17. #12. #22. #27 - 0° #15 - 30° distally. #25 - 30° mesially	#17. #27. #15. #25- 0 mm #12 - 4 mm #22 - 2 mm	Certain 4. 1/11 mm. (Biomet 3i); Internal connection	Not used	3D Progress (MHT); no data on version; NP ZFX Intrascan (ZFX); no data on version; NP	4 operators. 5 DII each	PEEK (Createch Medical S.L.); No data on torque value
Gimenez et alAM[34] 2015	6. #17. #15. #12. #22. #25. #27	#17. #12. #22. #27 - 0° #15 - 30° distally. #25 - 30° mesially	#17. #27. #15. #25- 0 mm #12 - 4 mm #22 - 2 mm	Certain 4. 1/11 mm (Biomet 3i); Internal connection	Not used	CEREC AC Bluecam (Sirona); Version 4.0; P	4 operators. 5 DII each	PEEK (Createch Medical S.L.); No data on torque value

VPS – polyvinylsiloxane; PE – polyether; CII – conventional implant impression; DII – digital implant impression; IOS – intraoral scanner; CMM – coordinate measuring machine; CT – closed tray; OT – open tray; IL – implant level; AL – abutment level; Sp – splinted; NSp – non-splinted; S – significant; NS – non-significant; BL – bone level; TL - tissue level; Absd - absolute angular distortion; P – powdered; NP – non-powdered.

Reference scanner	Accuracy evaluation. results					Conclusions
D250 (3Shape)	Measurement location	Comparison: DII (digital model) distances and angles between two neighboring scanbodies (only statistically significant (p<0.05) data)				A smaller variation of the distance measurements was observed for the intraoral scanners True Definition and Trios. and a higher variation was seen for the iTero. Scanning precision worsened with increasing distance and angulation between scanbodies. Differences of mean distances between scanbodies comparing to dental lab scanning system (D250. 3Shape) were less than 40 µm.
		Mean distance (mm) and standard deviation (µm)		**Mean angle and standard deviation**		
		iTero	**True Definition**	**iTero**	**True Definition**	
	#35 - #36	6.669 (28)	6.647 (4)	8.06° (0.18)	8.20° (0.04)	
	#35 - #36 (model 2)			8.19° (0.24)	8.12° (0.10)	
	#35 - #45	40.608 (28)	40.566 (44)	17.47° (0.21)	17.33° (0.09)	
	#36 - #47	50.479 (64)	50.405 (60)	23.09° (0.20)	23.28° (0.15)	
CMM Crista Apex (Mitutoyo)	Comparison: DII (digital model) vs reference model					Accuracy is clinically acceptable. Scanbody visibility. observer experience. and scanning area affect accuracy.
		Distance		**Angulation**		
	First quadrant	7.6 ± 17.6 µm (S)		0.21 ± 0.17° (S)		
	Second quadrant	-10.3 ± 39.2 µm (S)		0.28 ± 0.16° (S)		
CMM Crista Apex (Mitutoyo)	Comparison: DII (digital model) vs reference model					Experienced operators delivered more accurate DII. Angulated implants and the deeply placed implants did not decrease the accuracy in digital impressions.
	Group			Mean (SD)		
	Experienced			-30.8 ± 25.9 µm		
	Inexperienced			13.3 ± 51.2 µm		
	Angulated			-20.2 ± 21.9 µm		
	Parallel			-37.9 ± 26.2 µm		
	Deep implant			-34.3 ± 18.7 µm		
	Gingival margin level			-28.5 ± 29.8 µm		
CMM Crista Apex (Mitutoyo)	Comparison: DII (digital model) vs reference model					The 3D progress IOS performed significantly better in the first quadrant. ZFX Intrascan in the second quadrant. Tested scanners not suitable for multi-implant impressions.
	Group	ZFX Intrascan		3D Progress		
	Experienced	-179 ± 601 µm		249 ± 702 µm		
	Inexperienced	-101 ± 705 µm		224 ± 930 µm		
	Angulated	-125 ± 596 µm		257 ± 776 µm		
	Parallel	-150 ± 693 µm		224 ± 854 µm		
	Deep implant (2 mm)	-150 ± 397 µm		87 ± 403 µm		
	Gingival margin level	-133 ± 782 µm		337 ± 997 µm		
CMM Crista Apex (Mitutoyo)	Comparison: DII (digital model) vs reference model					Tested scanner is clinically acceptable. The experience of the operator affected the accuracy. Angulation and location of the camera affect scanner results. The error increased from the first to the last implant scanned.
	Group			Mean (SD)		
	Experienced			-85.4 ± 98.9 µm		
	Inexperienced			-47.3 ± 75.7 µm		
	Angulated			-72.7 ± 81.7 µm		
	Parallel			-84.3 ± 99.9 µm		
	0 mm implant depth			-89.47 ± 105.59 µm		
	2 mm implant depth			-22.46 ± 30.92 µm		
	4 mm implant depth			-107.25 ± 68.65 µm		
	First quadrant			-17 ± 26.3 µm		
	Second quadrant			-116 ± 103 µm		

Article	No. of implants. positions	Angulation	Placement depth (mm)	Implant manufacturer. connection	CII technique	DII technique: IOS; use of powder; scanning strategy	Number of impressions	Scanbody. torque value Ncm
Gimenez et alAM[33] 2014	6. #17. #15. #12. #22. #25. #27	#17. #12. #22. #27 - 0° #15 - 30° distally. #25 - 30° mesially	#17. #27. #15. #25- 0 mm #12 - 4 mm #22 - 2 mm	Certain 4. 1/11 mm (Biomet 3i); Internal connection	Not used	iTero (Align Technology); Version 4.5.0.1.5.1; NP	4 operators. 5 DII each	PEEK (Createch Medical S.L.); No data on torque value
van der Meer et al[37] 2012	3. #36. #41. #46	-	Gingival level	No information	Not used	CEREC Bluecam. (Sirona); Version 3.85 P iTero. (Align Technology); Version 3.5.0 NP Lava COS (3M ESPE); Version 2.1 P	n = 10	PEEK (Createch Medical S.L.); No data on torque value
Mangano et al[40] 2016	Model 1: 3. #21. #24. #26; Model 2: 6. #16. #14. #11. #21. #24. #26	No data	No data	BTK implants (Dueville. Vicenza. Italy)	Not used	Trios Color (3Shape); Version 2014 – 1. 1.3.3.1. NP CS 3500 (CarestreamHealth. Rochester. NY. US); Version 2016-4. 2.1.4.10. NP ZFX Intrascan (MHT); Version 0.9 RC33 2.8. NP Planmeca PlanScan (E4D Technologies. LLC. Richardson. TX. USA); Version 5 – 2015. NP	n = 5	PEEK; No data on torque value
Chew et al[39] 2016	2. #44. #45	Parallel	No data	Tissue and Bone Level Standard Plus (Straumann)	OT	Trios Color (3Shape); Version 3.1.4 NP iTero (Align Technology); Version HD 2.9; NP True Definition (3M ESPE); no data on version. P	n = 5	Core Scanbody 2077 RC and 2088 WN (Core 3D centres); Handtightened

Reference scanner	Accuracy evaluation. results						Conclusions
CMM Crista Apex (Mitutoyo)	Comparison: DII (digital model) vs reference model						Angulated implants did not decrease digital impression accuracy. Impressions of implants placed at a depth of 0 mm?? were less accurate then deeper placed ones.
	Implant depth		Mean error and standard deviation				
	0 mm		-23.1 ± 149.485 µm				
	2 mm		-16.2 ± 34.569 µm				
	4 mm		-27.9 ± 61.643 µm				
	First quadrant		-28 ± 153 µm				
	Second quadrant		-15 ± 30 µm				
Contact scanner Leitz (PMM 12106)	Comparison: DII (digital model) vs reference model						The Lava COS resulted in the smallest mean distance errors in full arch impressions. Lava COS had smallest angulation errors between cylinder 1–2 and the largest errors between cylinder 1–3. Although the absolute difference with the best mean value (iTero) was very small.
	Absolute errors in distance between cylinders						
	CEREC Bluecam		**iTero**		**Lava COS**		
	1-2	1-3	1-2	1-3	1-2	1-3	
	79.6 ± 77.1 µm	81.6 ± 52.5 µm	70.5 ± 56.3 µm	61.1 ± 53.9 µm	14.6 ± 12.7 µm	23.5 ± 14.2 µm	
	Absolute errors in angle between cylinders						
	CEREC		**iTero**		**Lava COS**		
	1-2	1-3	1-2	1-3	1-2	1-3	
	0.6303 ± 0.5499°	0.4378 ± 0.3211°	0.3451 ± 0.3382°	0.4192 ± 0.1667°	0.2049 ± 0.0440°	0.4722 ± 0.1436°	
IScan D104I (Imetric3D GmbH)	Comparison: DII (digital model) vs reference model						No significant differences were found between partial and total edentulous models. CS 3500 intraoral scanner had the best result in terms of trueness and precision.
	Scanner	**Model 1**		**Model 2**		**Significance**	
	Mean trueness						
	Trios Color	72.2 ± 19.5 µm		71.6 ± 26.7 µm		NS	
	CS 3500	47.8 ± 7.3 µm		63.2 ± 7.5 µm		S	
	ZFX Intrascan	117.0 ± 28.6 µm		103.0 ± 26.9 µm		S	
	Planscan	233.4 ± 62.6 µm		253.4 ± 13.6 µm		S	
	Mean precision						
	Trios Color	51.0 ± 18.5 µm		67.0 ± 32.2 µm		S	
	CS 3500	40.8 ± 6.4 µm		55.2 ± 10.4 µm		S	
	ZFX Intrascan	126.2 ± 21.2 µm		112.4 ± 22.6 µm		S	
	Planscan	219.8 ± 59.1 µm		204.2 ± 22.7 µm		S	
CMM (Model Global Silver Edition. Brown and Sharpe)	Comparison: DII (digital model) vs reference model						Between BL and TL groups BLCNV had the lowest global linear distortion. which was statistically significant. All TL groups were not significantly different. There were no significant differences in absolute angular distortions among all test groups.
	Test group		**Global linear distortion**		**Absolute angular distortion**		
					AbsdΘ	**AbsdΘ**	
	BLCII		35 ± 6 µm		0.058 ± 0.031°	0.09 ± 0.082°	
	BLTrios Color		64 ± 10 µm		0.105 ± 0.058°	0.206 ± 0.044°	
	BLiTero		62 ± 18 µm		0.191 ± 0.124°	0.154 ± 0.113°	
	BLTrue Definition		63 ± 17 µm		0.315 ± 0.138°	0.226 ± 0.143°	
	TLCII		49 ± 10 µm		0.186 ± 0.161°	0.196 ± 0.147°	
	TLTrios Color		58 ± 11 µm		0.089 ± 0.039°	0.066 ± 0.033°	
	TLiTero		66 ± 34 µm		0.203 ± 0.094°	0.160 ± 0.121°	
	TLTrue Definition		64 ± 16 µm		0.206 ± 0.115°	0.195 ± 0.140°	

Article	No. of implants. positions	Angulation	Placement depth (mm)	Implant manufacturer. connection	CII technique	DII technique: IOS; use of powder; scanning strategy	Number of impressions	Scanbody. torque value Ncm
Gintaute AM[36] 2015	4. #34. #32. #42. #44	Parallel	No data	Osseotite 2 Certain Implants (Biomet 3i); Internal connection	OT. Sp. IL	True Definition Scanner (3M ESPE); Version 4.0.3.1. P		PEEK (Createch Medical S.L.); No data on torque value
		2 anterior - parallel. 2 posterior - 40-45°						

VPS – polyvinylsiloxane; PE – polyether; CII – conventional implant impression; DII – digital implant impression; IOS – intraoral scanner; CMM – coordinate measuring machine; CT – closed tray; OT – open tray; IL – implant level; AL – abutment level; Sp – splinted; NSp – non-splinted; S – significant; NS – non-significant; BL – bone level; TL - tissue level; Absd - absolute angular distortion; P – powdered; NP – non-powdered.

The *In vivo* study evaluated accuracy of multi-unit DII (two implant-supported bar in the edentulous mandible) in 25 patients. The scanning procedure was done with iTero IOS, after detaching the bars, using a defined scanning strategy. Definitive casts, which had been used for the fabrication of bars, served as reference casts. Authors presumed that the maximum acceptable horizontal misfit and angulation errors, considering two implant-supported restoration, should not exceed 100 µm and 0.4° respectively[32].

Of 15 included *in vitro* studies, two evaluated accuracy of single-unit and 13 evaluated the multi-unit DII. As for multi-unit DII, three studies used models with two implants[46,49,39], two had three implants[50,40], one was with 4 implants[36], two were with five implants[47,49], and seven used models with six implants[33–35,42,43,48,40]. Five of the studies evaluating the accuracy of full-arch DII from six implants, used the identical model[33–35,42,43]. Five studies evaluated the influence of operator experience and implant placement depth[33–35,42,43], nine evaluated implant angulation[33–36,41–43,46,47], eleven the distance between the implants[33–37,41–43,39–40], and one looked at the influence of scanning protocol[42].

Main findings

The majority of included studies indicated the importance of error accumulation process throughout the digital workflow. Lack of reference points, scanbody design, scanned surface characteristics, sensor size, scanning strategy, software and some other factors were considered to affect accuracy. The factors potentially influencing the DII accuracy are summarised in Figure 2.

A workflow to produce indirect restoration in the laboratory starts from the time of impression. Therefore, accuracy of the impression is one of the most important aspects. If inaccuracies build up this could lead to misfits and strains in the final restoration. As the threshold for a clinically acceptable misfit is not defined clearly, it is difficult to judge the accuracy of DII, reported in the included studies, as clinically acceptable or not. In the literature, misfit of the implant-supported restoration of 100 µm or less is often considered as clinically acceptable[51]. However, level of the acceptable misfit could relate to the extent of the implant-supported restoration[14]. Different IOS utilising various data acquisition principles were investigated in the included studies. A summary of separate accuracy measurements collected from included studies is presented in Figures 3 and 4.

In vivo study

According to the results of only one *in vivo* study included, due to a poor reference points caused by the mucosa of edentulous sites with little variation

Reference scanner	Accuracy evaluation. results			Conclusions
CMM Crista Apex (Mitutoyo)	Comparison: DII (digital model) and CII (digitised VPS and PE models) vs reference model			Digital and conventional impression-making approaches (with polyether and VPS materials) are applicable for straight and tilted dental implants.
		Distance deviation	**Angulation deviation**	
	Model 1			
	DII	9.46 ± 16.04 μm (NS)	0.17 ± 0.14° (S DII vs PE); S DII vs VPS)	
	VPS	12.74 ± 12.5 μm (NS)	0.07 ± 0.1°	
	PE	12.22 ± 16.93 μm (NS)	0.08 ± 0.07°	
	Model 2			
	DII	35.78 ± 24.22 μm (S DII vs VPS)	0.22 ± 0.19°. (NS DII vs VPS)	
	VPS	4.87 ± 21.34 μm	0.04 ± 0.04°. (S)	
	PE	19.78 ± 21 μm	0.16 ± 0.1 6° (S)	

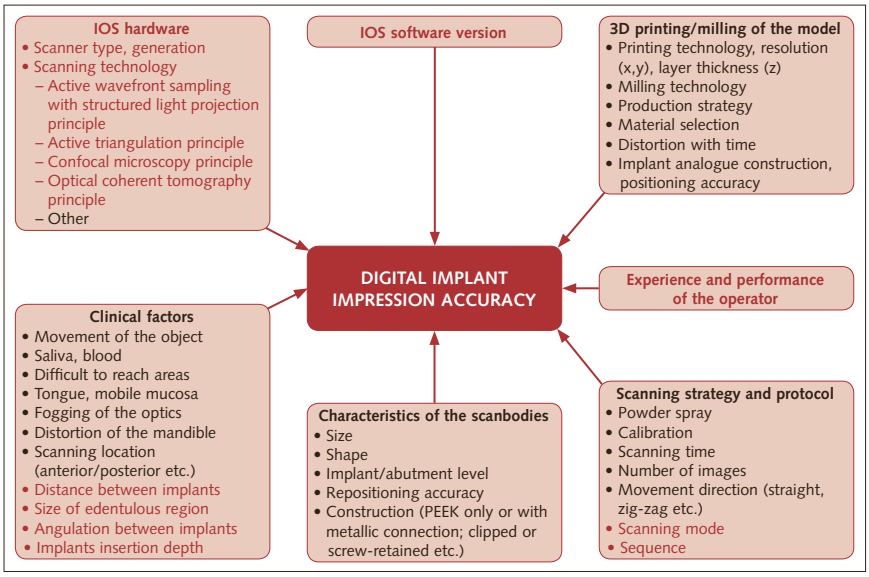

Fig 2 Main factors potentially affecting accuracy of digital implant impressions (DII). Items presented in red were investigated in the included studies.

in texture and height, digital impressions of four patients were impossible to perform[32]. Only in five cases were no optical irregularities of the IOS scans noticed. It was concluded that mean angular and distance errors were too large to be clinically acceptable.

In vitro studies

Two studies comparing models made from DII and CII for single-unit implant crowns reported different results. One study indicated significant change in the vertical position (93 μm) of the implant analogue in milled models[45], while in another the mean error was comparatively small, but with a larger

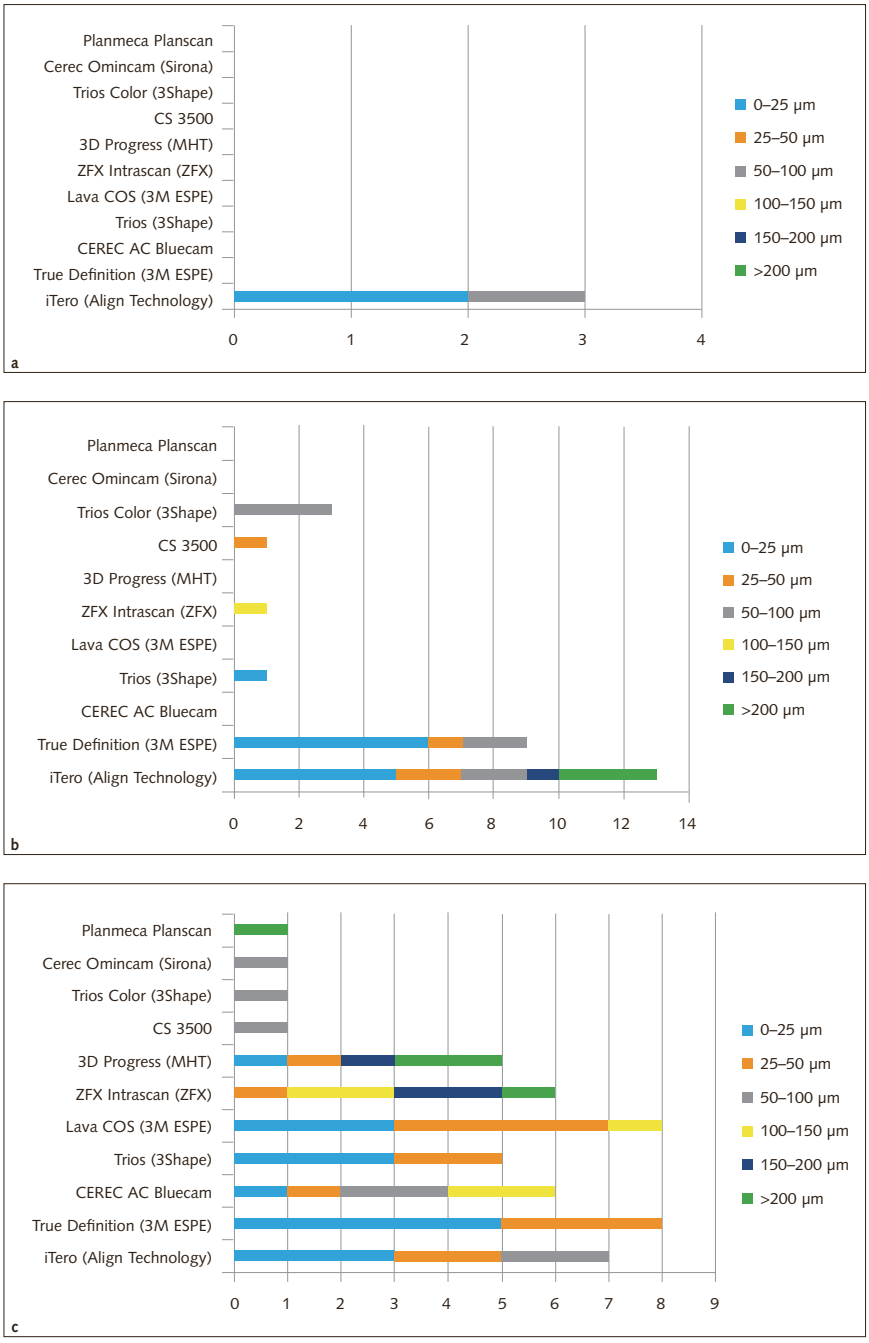

Fig 3 Digital implant impressions for: a) single-unit cases, b) FPD cases, c) fixed full-arch cases. Number of results reporting different linear absolute mean error intervals with certain IOS.

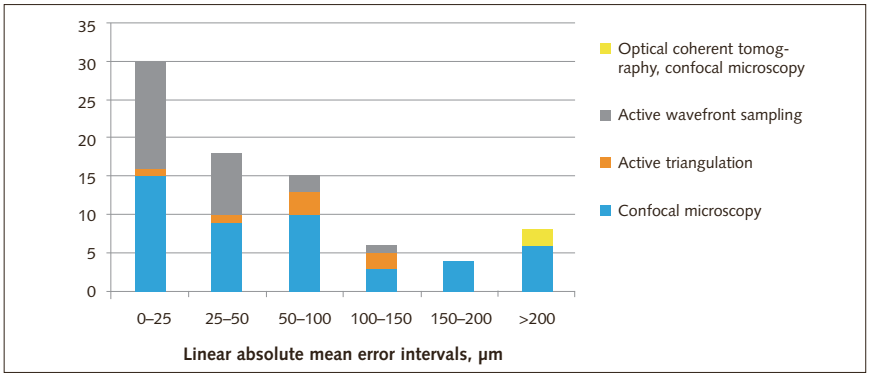

Fig 4 Number of results reporting linear absolute mean error intervals with different scanning technologies.

standard deviation: 14 ± 170 µm[45]. These results could not be considered as clinically acceptable, however reported deviations are the net result of inaccuracies introduced during digital impression taking, milling of the model, and positioning of the implant analogue. One of these studies also compared deviations between DII and the reference model (isolated assessment of only DII accuracy), and the difference was considerably smaller – -6 ± 40 µm[46]. Analysis of the accumulated errors in the digital workflow showed that the largest source of inaccuracy was the milling process (contributed SD is ± 98 µm) followed by the DII (contributed SD is ± 21 µm)[44]. Therefore, other factors besides DII could be responsible for less consistent results reported in these studies.

Thirteen studies investigated the accuracy of DII for multi-unit implant-supported restorations. Mean errors of several IOS used in five of these studies was higher than 100 µm[34,35,46,40,48].

The results diverged with older generation IOS used in the included studies (Lava COS, iTero, Cerec Bluecam, 3D Progress, ZfX Intrascan), as there were studies reporting deviations above[34,35,46,48] and below[33,37,42] 100 µm.

Different results could be explained by methodological differences as well. One of the studies reporting adequate results used less clinically relevant full-arch models, with between distantly oriented scanbodies, dentate segments, avoiding simulation of edentulous areas[37]. Remaining teeth in between the implants could help as reference areas, facilitating stitching of the images and, possibly, improving the accuracy. In contrast, a study utilising the single-implant model reported higher mean errors with iTero IOS for single-unit implant situation, as measurements were done on the model milled from polyurethane material based on DII data. Thus, error accumulation during fabrication of the model was inevitable[46].

All studies analysing IOS of the newer generation (Trios, Color, True Definition, Cerec Omnicam, CS3500) reported deviations of less than100 µm[36,43,47,48,40]. Interesting to note, was that all of these studies employed full-arch models with four to six implants. However, the accuracy of Planscan IOS was significantly less –253,4 ± 13,6 µm for the full-arch situation[40].

One study investigated only precision of DII with three different IOS[41]. It was concluded that the precision of IOS tested (iTero, Trios, True Definition) was significantly different, and decreased with increasing distances between the scanbodies.

Some of the included studies explored the influence of angulated implants on the accuracy of DII[33–36,42,43,46,47]. Reference models in these studies had implants angulated from 10°[47] to 45°[36]. The clinically acceptable threshold for the angle deviations generated during impression procedure is not defined in the literature. However, based on simple trigonometrical calculations (and assuming that the maximal lateral apex movement of 50 µm is acceptable), one study[32] suggested that up to 0.4° angle deviation between implants could be acceptable, with total length of the implant of 14.8 mm. The majority of *in vitro* studies included in this systematic review

used shorter implants for the reference models. In the case of shorter implants, larger inter-implant angle deviation can possibly be accepted, as this angle can be defined by the formula: 2× arctan (0,05/L implant length in mm). Two studies have reported higher deviations in angulation (up to 1.6°)[37,46], while recent studies using newer generation of IOS indicated much smaller angle deviations (0.07 to 0.3°)[36,43,39].

The depth of implant placement as a factor was also considered in the included studies. Supragingival[46], equigingival[33–35,37,42,43] and 2 to 4 mm subgingival[33–35,42,43] implant positions were used.

In summary, the included studies reported that DII accuracy was influenced by implant angulation[46], distance between the implants[43], implant placement depth[33,43], and scanning mode[42]. Most studies investigating impact of operator experience concluded that this aspect was of significant importance[33,34,42,43].

Studies comparing accuracy of newer generation IOS (True Definition, Trios) with conventional impressions for partial- and full-arch implant-supported dental restorations, indicated that the accuracy of DII did not significantly differ from CII and could serve as a viable alternative[36,47,39]. Accuracy of implant-level, non-splinted CII was reported as being even less accurate compared with DII[47].

■ Discussion

To our knowledge, this is the first systematic review addressing DII accuracy. Results of this review are important, as intraoral implants and IOS are both used extensively in practitioners' clinical practice. IOS offers many new diagnostic and treatment workflows. Originally aimed at making the optical impression from the teeth, IOS has now become multifunctional instruments, which are able to measure the shade and work as intraoral cameras etc. Keeping the patient data unchanged for a long time, sharing it with treatment team members, following-up the patient condition objectively, integrating IOS data with data from CBCT, laboratory scanner, face scanner and photos, are among the few options IOS can offer today.

The number of publications related to the various uses of IOS is rapidly increasing. Patient- and dentist-centred and efficiency outcomes are also being investigated[52,53]. However, one of the main goals is to improve the accuracy of the digital workflow and to achieve aesthetic and functional restorations with minimal effort.

Digital workflow is still susceptible to errors, which can come from the digital impression and CAD/CAM software, as well as production (subtractive or additive) processes. Although manufacturing techniques have become very accurate, they still depend on the accuracy of the impression and master model. IOS are an integral part of the digital workflow; therefore accuracy is an essential requirement.

As the evidence on accuracy of DII is lacking, a thorough search was conducted in order to identify relevant publications. Strict criteria were applied for the studies, with accuracy measuring methodology described in detail. Despite the growing popularity of IOS devices, only one *in vivo* and 15 *in vitro* studies evaluating the accuracy of DII were identified.

While the *in vivo* study showed that accuracy of DII is not adequate for clinical applications, the majority of *in vitro* studies showed less than 100 µm deviations. This could also indicate significantly different conditions for *in vitro* and *in vivo* environments.

The only *in vivo* study used an older generation scanner. According to the *in vitro* results, newer versions of the scanners performed considerably better. Accuracy of these scanners was evaluated with partial- and full-arch models containing from two to six implants. A study comparing DII (obtained by True Definition and Trios) with a reference model containing six implants, reported values for trueness and precision ranging from 28 µm to 35 µm[48]. DII (True Definition) from four parallel mandibular implants did not statistically significantly differ from CII, however with distal implants tilted, statistically significant differences were detected[36]. As absolute values of these differences were approximately 30 µm, it can be concluded these differences could be of limited clinical significance. Based on this, IOS seem to become a reliable alternative to conventional impressions for the selected indications. However, results of this review should be interpreted with caution, as there are several limiting factors. Only one *in vivo* study satisfied inclusion criteria[32]. iTero IOS was used for DII and stitching problems leading to the

deformed image of the scan abutment, as described by the authors. The information is lacking if the accuracy of definitive models was rechecked by again fitting the bar to the model, as the true reference is difficult to obtain in *in vivo* studies, and this remains one of the challenges for the clinical evaluations. Hypothetically, trueness of the DII data could be better, but still deviate from the potentially less accurate model fabricated from the conventional impression. Moreover, at the time of this systematic review, a new version of the scanner used in this *in vivo* study became available, claiming much faster and more accurate scanning in colour. As the older version of the scanner and software were used, the findings of the study are therefore less relevant today.

In vivo use of IOS could be compromised by many aspects: movements of the object, saliva, fogging of the optics, and other patient-, operator- and device-related limiting factors. Scanning location can be important, as distant regions could be difficult to reach in a real clinical situation. Length of the edentulous ridge, lack of attached gingiva, tongue and cheek mobility could also negatively affect the ability to stitch the images. Scanning strategy and mode were also proved important aspects[42,55]. A recent study showed that intraoral scanning was less precise than model scanning[54].

Comparison of the results of the *in vitro* studies could also be limited by disparities in study design, the models and techniques used. IOS can utilise several different technologies: confocal microscopy, optical coherence tomography, active and passive stereovision/triangulation, phase-shift principles, accordion fringe interferometry, etc[36]. Different IOS systems with different software versions compromise the comparisons further. Moreover, no studies have been published with other new IOS systems – DWIOS, Condor, CS3600, Aadva, Trios 3 and many others. In this regard, there is a big difference between DII and CII, as the principles of conventional impression taking do not change that dramatically with time, and features of the products from different companies are relatively less different compared with IOS.

Accuracy of DII can also be affected by other factors. Characteristics of the scanbodies could be another source of errors. Shorter and less visible scanbodies can negatively influence the accuracy[56]. It was recommended that longer scanbodies should be used with deep-placed implants[43]. One of the studies included in the systematic review used longer scanbodies, which could also contribute to better-measured accuracy[47]. Sharp angles of the scanbodies could negatively influence scan accuracy. One study was excluded from the review, as healing abutments instead of scanbodies were used, making the results of this study less relevant[38].

Spraying of the scanbodies with powder is still needed for some of the IOS to reduce the reflections and aid the stitching of the images. Powdering could potentially influence the accuracy of scanning through homogeneity and thickness of spray. It was reported that experienced clinicians achieved greater homogeneity and thinner coatings[57]. Therefore it is recommended to use only light dusting on the surfaces to be scanned. As powder could be inhaled by the patient and clinician or swallowed by patient, more information is needed about the effect of it on human health[58].

Similarly, as with conventional impressions, type of the implant-abutment connection can influence the accuracy. External implant – abutment connection was reported to provide more consistent accuracy for CII[25]. Only one of the included studies investigated DII accuracy with external connection implants[48].

A potential effect of embedment relaxation and manufacturing tolerances should be taken into consideration when selecting prosthetic components[59]. Repositioning accuracy of scanbodies could have an effect on the accuracy of the DII. It was reported that the ability of repositioning of the scanbody is better on lab analogues than on original implants[60]. However, other authors suggested that the precision of implant scanbody scanning was not significantly influenced by detachment and repositioning of the scanbody[56]. Not all the studies standardised the use of the scanbodies (eg, tightening ranged from finger tightening to 15 Ncm) and this could act as an additional variable. Also, it could be hypothesised, that scanbodies with metallic base should have better repositioning accuracy as compared with fully plastic scanbodies.

Three studies evaluated accuracy of milled models obtained from DII[44–46]. It appeared that milling and positioning of implant analogues resulted in bigger deviations as compared with reference model. None of these studies described milling parameters they have used to fabricate the models. Also, information

about implant analogues dedicated for milled models was lacking. No publication was identified, utilising 3D printing to fabricate the model from DII data. As models are necessary for layered restorations, occlusal adjustments etc., more research is needed to define milling and printing parameters in order to avoid inaccuracies and increase applications of IOS.

Despite good accuracy results reported by *in vitro* studies, digital workflow based on DII is still lacking some reliable conventional solutions – use of verification jigs to validate the master model, easy and reliable recording of the emergence profile, validated techniques to record static and dynamic occlusal relationships, etc. Recent studies also identify the significance of inaccuracies of occlusal contacts of stereolithographic models fabricated, based on data from IOS[61].

Although scientific literature is struggling to keep up with the newest IOS developments, due to positive clinical experience, constantly increasing opportunities with digital workflow and marketing, its use in clinical practice is growing fast. Further IOS improvements need to be done in order to replace conventional techniques and increase the potential of digital workflow, especially in partially and fully edentulous patients.

Conclusions

1. Within the limitations of this systematic review (one *in vivo* and 15 *in vitro* studies identified), it can be concluded that digital implant impressions offer a valid alternative to conventional impressions for single- and multi-unit implant-supported restorations;
2. *In vivo* studies investigating the accuracy of newest available IOS are needed to further define their clinical indications;
3. Factors potentially affecting accuracy of digital implant impressions should be more extensively described and investigated in clinical studies;
4. Due to the constant changes in IOS hardware and software, reliable methodology, representing less forgiving *in vivo* situations should be defined to timely evaluate and compare trueness and precision of modern IOSs, and to provide clinical guidelines;
5. Digital implant impression techniques still have to be improved in order to fully substitute conventional ones;
6. Further studies are needed to investigate the accuracy of digital interocclusal records and master model production methods (milling, 3D printing) to ensure clinically acceptable results.

Funding

No funding was received for conducting this systematic review.

References

1. Pjetursson BE, Thoma D, Jung R, Zwahlen M, Zembic A. A systematic review of the survival and complication rates of implant-supported fixed dental prostheses (FDPs) after a mean observation period of at least 5 years. Clin Oral Implants Res 2012;23:22–38.
2. Srinivasan M, Meyer S, Mombelli A, Müller F. Dental implants in the elderly population: a systematic review and meta-analysis. Clin Oral Implants Res 2016. Epub ahead of print.
3. Lemos CAA, de Souza Batista VE, Almeida DA de F, Santiago Júnior JF, Verri FR, Pellizzer EP. Evaluation of cement-retained versus screw-retained implant-supported restorations for marginal bone loss: A systematic review and meta-analysis. J Prosthet Dent 2016;115:419–427.
4. Papaspyridakos P, Chen CJ, Chuang SK, Weber HP, Gallucci GO. A systematic review of biologic and technical complications with fixed implant rehabilitations for edentulous patients. Int J Oral Maxillofac Implants 2012;27:102–110.
5. Fasbinder DJ. Computerized technology for restorative dentistry. Am J Dent 2013;26:115–120.
6. Clinical Applications of Digital Dental Technology. Radi Masri (Editor), Carl F. Driscoll (Editor);May 2015, Wiley-Blackwell.
7. Joda T, Brägger U, Gallucci G. Systematic literature review of digital three-dimensional superimposition techniques to create virtual dental patients. Int J Oral Maxillofac Implants 2015;30:330–337.
8. Abduo J, Lyons K, Bennani V, Waddell N, Swain M. Fit of screw-retained fixed implant frameworks fabricated by different methods: a systematic review. Int J Prosthodont 201;24:207–220.
9. Boldt J, Knapp W, Proff P, Rottner K, Richter EJ. Measurement of tooth and implant mobility under physiological loading conditions. Ann Anat 2012;194:185–189.
10. Hsieh WW, Luke A, Alster J, Weiner S. Sensory discrimination of teeth and implant-supported restorations. Int J Oral Maxillofac Implants. 2010;25:146–152.
11. Wee AG, Aquilino SA, Schneider RL. Strategies to achieve fit in implant prosthodontics: a review of the literature. Int J Prosthodont 1999;12:167–178.
12. Manzella C, Bignardi C, Burello V, Carossa S, Schierano G. Method to improve passive fit of frameworks on implant-supported prostheses: An in vitro study. J Prosthet Dent 2016;116:52–58.
13. Rutkunas V, Ignatovic J. A technique to splint and verify the accuracy of implant impression copings with light-polymerizing acrylic resin. J Prosthet Dent 2014;111:254–256.

14. Mericske-Stern R, Worni A. Optimal number of oral implants for fixed reconstructions: a review of the literature. Eur J Oral Implantol 2014;7:S133-153.
15. Schwarz MS. Mechanical complications of dental implants. Clin Oral Implants Res 2000;11:156–158.
16. Jemt T. Failures and complications in 391 consecutively inserted fixed prostheses supported by Brånemark implants in edentulous jaws: a study of treatment from the time of prosthesis placement to the first annual checkup. Int J Oral Maxillofac Implants 1991;6:270–276.
17. Karl M, Taylor TD. Bone Adaptation Induced by Non-Passively Fitting Implant Superstructures: A Randomized Clinical Trial. Int J Oral Maxillofac Implants 2016;31:369–375.
18. Abduo J. Fit of CAD/CAM implant frameworks: a comprehensive review. J Oral Implantol 2014;40:758–766.
19. Rutkunas V, Sveikata K, Savickas R. Effects of implant angulation, material selection, and impression technique on impression accuracy: a preliminary laboratory study. Int J Prosthodont 2012;25:512–515.
20. Siadat H, Alikhasi M, Beyabanaki E, Rahimian S. Comparison of Different Impression Techniques When Using the All-on-Four Implant Treatment Protocol. Int J Prosthodont. 2016;29:265–270.
21. Lee H, So JS, Hochstedler JL, Ercoli C. The accuracy of implant impressions: A systematic review. J Prosthet Dent 2008;100:285–291.
22. Papaspyridakos P, Chen CJ, Gallucci GO, Doukoudakis A, Weber HP, Chronopoulos V. Accuracy of implant impressions for partially and completely edentulous patients: a systematic review. Int J Oral Maxillofac Implants 2014;29:836–845.
23. Baig MR. Accuracy of impressions of multiple implants in the edentulous arch: a systematic review. Int J Oral Maxillofac Implants 2014;29:869–880.
24. Baig MR. Multi-unit implant impression accuracy: A review of the literature. Quintessence Int 1985. 2014;45:39–51.
25. Kim J-H, Kim KR, Kim S. Critical appraisal of implant impression accuracies: A systematic review. J Prosthet Dent 2015;114:185–192.
26. Moreira AHJ, Rodrigues NF, Pinho ACM, Fonseca JC, Vilaça JL. Accuracy Comparison of Implant Impression Techniques: A Systematic Review. Clin Implant Dent Relat Res 2015;17:e751–764.
27. Kim J-H, Kim KR, Kim S. Critical appraisal of implant impression accuracies: A systematic review. J Prosthet Dent 2015;114:185–192.
28. Papaspyridakos P, Chen C-J, Gallucci GO, Doukoudakis A, Weber H-P, Chronopoulos V. Accuracy of implant impressions for partially and completely edentulous patients: a systematic review. Int J Oral Maxillofac Implants 2014;29:836–845.
29. Kim JH, Kim KR, Kim S. Critical appraisal of implant impression accuracies: A systematic review. J Prosthet Dent 2015;114:185–192.
30. Bergin JM, Rubenstein JE, Mancl L, Brudvik JS, Raigrodski AJ. An in vitro comparison of photogrammetric and conventional complete-arch implant impression techniques. J Prosthet Dent 2013;110:243–251.
31. Chochlidakis KM, Papaspyridakos P, Geminiani A, Chen CJ, Feng IJ, Ercoli C. Digital versus conventional impressions for fixed prosthodontics: A systematic review and meta-analysis. J Prosthet Dent 2016;116:184–190.e12.
32. Andriessen FS, Rijkens DR, van der Meer WJ, Wismeijer DW. Applicability and accuracy of an intraoral scanner for scanning multiple implants in edentulous mandibles: a pilot study. J Prosthet Dent 2014;111:186–194.
33. Giménez B, Özcan M, Martínez-Rus F, Pradíes G. Accuracy of a digital impression system based on parallel confocal laser technology for implants with consideration of operator experience and implant angulation and depth. Int J Oral Maxillofac Implants 2014;29:853–862.
34. Giménez B, Özcan M, Martínez-Rus F, Pradíes G. Accuracy of a Digital Impression System Based on Active Triangulation Technology With Blue Light for Implants: Effect of Clinically Relevant Parameters. Implant Dent 2015;24: 498–504.
35. Giménez B, Pradíes G, Martínez-Rus F, Özcan M. Accuracy of two digital implant impression systems based on confocal microscopy with variations in customized software and clinical parameters. Int J Oral Maxillofac Implants 2015; 30:56–64.
36. Gintaute, Aiste. Accuracy of computerized and conventional impression-making procedures of straight and tilted dental implants [Internet]. [Freiburg]: Albert-Ludwigs-Universität; 2015. Available from: https://freidok.uni-freiburg.de/dnb/download/10655
37. van der Meer WJ, Andriessen FS, Wismeijer D, Ren Y. Application of intra-oral dental scanners in the digital workflow of implantology. PloS One 2012;7:e43312.
38. Ajioka H, Kihara H, Odaira C, Kobayashi T, Kondo H. Examination of the Position Accuracy of Implant Abutments Reproduced by Intra-Oral Optical Impression. PloS One 2016;11:e0164048.
39. Chew AA, Esguerra RJ, Teoh KH, Wong KM, Ng SD, Tan KB. Three-Dimensional Accuracy of Digital Implant Impressions: Effects of Different Scanners and Implant Level. Int J Oral Maxillofac Implants 2017;32:70–80.
40. Mangano FG, Veronesi G, Hauschild U, Mijiritsky E, Mangano C. Trueness and Precision of Four Intraoral Scanners in Oral Implantology: A Comparative in Vitro Study. PloS One 2016;11:e0163107.
41. Flügge TV, Att W, Metzger MC, Nelson K. Precision of Dental Implant Digitization Using Intraoral Scanners. Int J Prosthodont 2016;29:277–283.
42. Gimenez BD, Ozcan MD, Martinez-Rus FD, Pradies GD. Accuracy of a Digital Impression System Based on Active Wavefront Sampling Technology for Implants Considering Operator Experience, Implant Angulation, and Depth. Clin Implant Dent Relat Res 2015;17:e54–64.
43. Gimenez-Gonzalez B, Hassan B, Özcan M, Pradíes G. An In Vitro Study of Factors Influencing the Performance of Digital Intraoral Impressions Operating on Active Wavefront Sampling Technology with Multiple Implants in the Edentulous Maxilla. J Prosthodont 2016. Epub ahead of print.
44. Koch GK, Gallucci GO, Lee SJ. Accuracy in the digital workflow: From data acquisition to the digitally milled cast. J Prosthet Dent 2016;115:749–754.
45. Lee SJ, Betensky RA, Gianneschi GE, Gallucci GO. Accuracy of digital versus conventional implant impressions. Clin Oral Implants Res 2015;26:715–9.
46. Lin WS, Harris BT, Elathamna EN, Abdel-Azim T, Morton D. Effect of implant divergence on the accuracy of definitive casts created from traditional and digital implant-level impressions: an in vitro comparative study. Int J Oral Maxillofac Implants 2015;30:102–109.
47. Papaspyridakos P, Gallucci GO, Chen C-J, Hanssen S, Naert I, Vandenberghe B. Digital versus conventional implant impressions for edentulous patients: accuracy outcomes. Clin Oral Implants Res 2016;27:465–472.
48. Vandeweghe S, Vervack V, Dierens M, De Bruyn H. Accuracy of digital impressions of multiple dental implants: an in vitro study. Clin Oral Implants Res 2017;28:648–653.
49. Flugge TV, Att W, Metzger MC, Nelson K. Precision of Dental Implant Digitization Using Intraoral Scanners. Int J Prosthodont 2016;29:277–283.
50. van der Meer WJ, Andriessen FS, Wismeijer D, Ren Y. Application of intra-oral dental scanners in the digital workflow of implantology. PloS One 2012;7:e43312.

51. Katsoulis J, Mericske-Stern R, Rotkina L, Zbären C, Enkling N, Blatz MB. Precision of fit of implant-supported screw-retained 10-unit computer-aided-designed and computer-aided-manufactured frameworks made from zirconium dioxide and titanium: an in vitro study. Clin Oral Implants Res 2014;25:165–174.
52. Joda T, Brägger U. Digital vs. conventional implant prosthetic workflows: a cost/time analysis. Clin Oral Implants Res 2015;26:1430–1435.
53. Joda T, Brägger U. Patient-centered outcomes comparing digital and conventional implant impression procedures: a randomized crossover trial. Clin Oral Implants Res 2016;27:e185–e189.
54. Flügge TV, Schlager S, Nelson K, Nahles S, Metzger MC. Precision of intraoral digital dental impressions with iTero and extraoral digitization with the iTero and a model scanner. Am J Orthod Dentofacial Orthop 2013;144:471–478.
55. Müller P, Ender A, Joda T, Katsoulis J. Impact of digital intraoral scan strategies on the impression accuracy using the TRIOS Pod scanner. Quintessence Int 2016;47:343–349.
56. Fluegge T, Att W, Metzger M, Nelson K. A Novel Method to Evaluate Precision of Optical Implant Impressions with Commercial Scan Bodies-An Experimental Approach. J Prosthodont 2015;26:34-41.
57. Dehurtevent M, Robberecht L, Béhin P. Influence of dentist experience with scan spray systems used in direct CAD/CAM impressions. J Prosthet Dent 2015;113:17–21.
58. Patzelt SBM, Vonau S, Stampf S, Att W. Assessing the feasibility and accuracy of digitizing edentulous jaws. J Am Dent Assoc 2013;144:914–920.
59. Yilmaz B, Gilbert AB, Seidt JD, McGlumphy EA, Clelland NL. Displacement of Implant Abutments Following Initial and Repeated Torqueing. Int J Oral Maxillofac Implants 2015;30:1011–1018.
60. Stimmelmayr M, Güth J-F, Erdelt K, Edelhoff D, Beuer F. Digital evaluation of the reproducibility of implant scanbody fit--an in vitro study. Clin Oral Investig 2012;16:851–856.
61. Wilding RJ, Adams LP, Lewin A. Absence of association between a preferred chewing side and its area of functional occlusal contact in the human dentition. Arch Oral Biol 1992;37:423–428.
62. Ortorp A, Jemt T, Bäck T. Photogrammetry and conventional impressions for recording implant positions: a comparative laboratory study. Clin Implant Dent Relat Res 2005;7:43–50.
63. Bergin JM, Rubenstein JE, Mancl L, Brudvik JS, Raigrodski AJ. An in vitro comparison of photogrammetric and conventional complete-arch implant impression techniques. J Prosthet Dent 2013;110:243–251.
64. Eliasson A, Ortorp A. The accuracy of an implant impression technique using digitally coded healing abutments. Clin Implant Dent Relat Res 2012;14:e30-38.
65. Howell KJ, McGlumphy EA, Drago C, Knapik G. Comparison of the accuracy of Biomet 3i Encode Robocast Technology and conventional implant impression techniques. Int J Oral 2013;28:228–240.
66. Lee SJ, Gallucci GO. Digital vs. conventional implant impressions: efficiency outcomes. Clin Oral Implants Res 2013;24:111–115.
67. Lee SJD, MacArthur RXID, Gallucci GOD. An evaluation of student and clinician perception of digital and conventional implant impressions. J Prosthet Dent 2013;110:420–423.
68. Wismeijer D, Mans R, van Genuchten M, Reijers HA. Patients' preferences when comparing analogue implant impressions using a polyether impression material versus digital impressions (Intraoral Scan) of dental implants. Clin Oral Implants Res 2014;25:1113–1118.
69. Calesini G, Zarone F, Sorrentino R, Micarelli C, Fabianelli A, Papacchini F, Gherlone E. Effect of 2 impression techniques on the dimensional accuracy of working implant prosthesis models: an in vitro study. J Craniofac Surg 2014;25:822–827.
70. Schepke UD, Meijer HJAD, Kerdijk W, Cune MSD. Digital versus analog complete-arch impressions for single-unit premolar implant crowns: Operating time and patient preference. J Prosthet Dent 2015;114:403–406.
71. Joda T, Lenherr P, Dedem P, Kovaltschuk I, Bragger U, Zitzmann NU. Time efficiency, difficulty, and operator's preference comparing digital and conventional implant impressions: a randomized controlled trial. Clin Oral Implants Res 2016, Epub ahead of print.
72. Aktas G, Özcan N, Aydin DH, Şahin E, Akça K. Effect of digitizing techniques on the fit of implant-retained crowns with different antirotational abutment features. J Prosthet Dent 2014;111:367–372.
73. Abdel-Azim T, Zandinejad A, Elathamna E, Lin W, Morton D. The influence of digital fabrication options on the accuracy of dental implant-based single units and complete-arch frameworks. Int J Oral Maxillofac Implants 2014;29:1281–1288.
74. Karl M, Graef F, Schubinski P, Taylor T. Effect of intraoral scanning on the passivity of fit of implant-supported fixed dental prostheses. Quintessence Int 2012;43:555–562.
75. Gherlone EF, Ferrini F, Crespi R, Gastaldi G, Capparé P. Digital impressions for fabrication of definitive "all-on-four" restorations. Implant Dent 2015;24:125–129.
76. Lee CY, Wong N, Ganz SD, Mursic J, Suzuki JB. Use of an Intraoral Laser Scanner During the Prosthetic Phase of Implant Dentistry: A Pilot Study. J Oral Implantol 2015;41:e126-132.
77. Gherlone E, Capparé P, Vinci R, Ferrini F, Gastaldi G, Crespi R. Conventional Versus Digital Impressions for "All-on-Four" Restorations. Int J Oral Maxillofac Implants 2016;31:324–330.

NOTES

Vilnius University Press
9 Saulėtekio Ave., Building III, LT-10222 Vilnius
Email: info@leidykla.vu.lt, www.leidykla.vu.lt
Print run copies 20